



<https://theses.gla.ac.uk/>

Theses Digitisation:

<https://www.gla.ac.uk/myglasgow/research/enlighten/theses/digitisation/>

This is a digitised version of the original print thesis.

Copyright and moral rights for this work are retained by the author

A copy can be downloaded for personal non-commercial research or study, without prior permission or charge

This work cannot be reproduced or quoted extensively from without first obtaining permission in writing from the author

The content must not be changed in any way or sold commercially in any format or medium without the formal permission of the author

When referring to this work, full bibliographic details including the author, title, awarding institution and date of the thesis must be given

Enlighten: Theses

<https://theses.gla.ac.uk/>  
[research-enlighten@glasgow.ac.uk](mailto:research-enlighten@glasgow.ac.uk)

**The role of SPI-1 and SPI-2 type three secretion  
systems in persistent *Salmonella enterica* serovar  
Pullorum infections of chicken**

**By Lucy Chappell**

**Thesis submitted for the degree of Doctor of Philosophy  
in the Faculty of Veterinary Medicine, University of Glasgow**

**Division of Infection and Immunity, University of Glasgow**

**Institute for Animal Health**

**July 2007**

© 2007 Lucy Chappell

ProQuest Number: 10390742

All rights reserved

INFORMATION TO ALL USERS

The quality of this reproduction is dependent upon the quality of the copy submitted.

In the unlikely event that the author did not send a complete manuscript and there are missing pages, these will be noted. Also, if material had to be removed, a note will indicate the deletion.



ProQuest 10390742

Published by ProQuest LLC (2017). Copyright of the Dissertation is held by the Author.

All rights reserved.

This work is protected against unauthorized copying under Title 17, United States Code  
Microform Edition © ProQuest LLC.

ProQuest LLC.  
789 East Eisenhower Parkway  
P.O. Box 1346  
Ann Arbor, MI 48106 – 1346

GLASGOW  
UNIVERSITY  
LIBRARY:

## Abstract

*Salmonella enterica* serovar Pullorum causes a septicaemic, persistent, systemic disease of poultry known as Pullorum Disease (PD). PD causes high mortality in young birds with those that survive becoming carriers of the disease. Transmission between birds in the same generation is predominantly faecal-oral, with birds in subsequent generations becoming infected via vertical transmission. Groups of virulence genes on the *Salmonella* genome cluster in areas known as pathogenicity islands. A range of *in vitro* and *in vivo* techniques were used to assess the role of *Salmonella* pathogenicity islands 1 and 2 (SPI-1 and SPI-2) in the establishment and persistence of serovar Pullorum infection in the chicken. The results collectively suggest that serovar Pullorum does not promote the induction of a pro-inflammatory immune response in the gut, but virulence factors encoded by SPI-1 lead to up-regulation of  $\text{IL-1}\beta$ , IL-6, CXCL1 and CXCL2 to recruit phagocytes to the site of infection. Thereby, although not required for full-virulence, SPI-1 enables faster dissemination of serovar Pullorum to systemic sites. At systemic sites away from the gut, SPI-1 is responsible for down-regulation of the antimicrobial peptides avian  $\beta$ -defensins 1, 3 and 5, and of CXCL1. SPI-2 is responsible for maintaining sustainable intracellular numbers within macrophages, inhibiting nitric oxide synthesis and down-regulating IL-6 expression. SPI-1 and SPI-2 both contribute to the virulence of serovar Pullorum, enabling the establishment of a more rapid and stealthy infection in the chicken.

## Contents

<b>Abstract</b>	2
<b>Contents</b>	3
<b>List of Figures and Tables</b>	7
<b>Acknowledgement</b>	14
<b>Author's Declaration</b>	15
<b>Chapter 1: Introduction</b>	16
1.1 <i>Salmonella enterica</i>	16
1.2 Pullorum Disease	19
1.3 Early stages of <i>Salmonella enterica</i> infection and the role of <i>Salmonella</i> Pathogenicity Island 1	22
1.4 Systemic <i>Salmonella enterica</i> infection and the role of <i>Salmonella</i> Pathogenicity Island 2	33
1.5 Immune responses to <i>S. enterica</i> infection	40
1.6 Aims and objectives of the study	46
<b>Chapter 2: Materials and Methods</b>	51
2.1 Molecular techniques	51
2.1.1 Polymerase Chain Reaction (PCR)	51
2.1.1.1 Standard PCR	51
2.1.1.2 PCR for $\lambda$ -Red Mutagenesis	51
2.1.1.3 Agarose gel electrophoresis	52
2.1.2 Purification of PCR product	52
2.1.2.1 PCR product direct purification	52
2.1.2.2 Gel purification of PCR products	53
2.1.3 Plasmid DNA preparation	54
2.1.4 RNA extraction	55
2.1.4.1 Collection and homogenisation of samples from cells	55
2.1.4.2 Collection and homogenisation of samples from tissues	55
2.1.4.3 RNA extraction from homogenised lysate	56
2.1.5 Real-Time Quantitative RT-PCR	57
2.2 Microbiological techniques	62
2.2.1 Bacterial strains	62

2.2.2	Competent cells	63
2.2.3	Agglutination assays	64
2.3	Immunological techniques	65
2.3.1	Cells	65
2.3.1.1	Chick Kidney Cells	65
2.3.1.2	IID11 cells	65
2.3.1.3	Isolation of blood-derived monocytes	66
2.3.2	Monoclonal antibody purification	67
2.3.2.1	Monoclonal antibody purification using protein G	67
2.3.2.1	BCA protein assay	68
2.3.3	Detection of surface antigen by flow cytometry	68
2.3.4	Staining for confocal microscopy	69
2.3.4.1	Phagocytosis assay	69
2.3.4.2	Staining cells for confocal microscopy	70
2.3.4.3	Confocal microscopy	70
2.3.5	Transmission Electron Microscopy	72
2.3.6	Cell stimulation	73
2.3.7	Gentamicin protection assay	73
2.3.8	Griess assay	74
2.3.9	Superoxide anion assay	74
	<b>Chapter 3: Generation of bone marrow-derived macrophages</b>	76
3.1	Introduction	76
3.2	Methods	81
3.2.1	Bone marrow-derived macrophages	81
3.2.1.1	Complete Media	81
3.2.1.2	Generation of bone marrow-derived macrophages	81
3.2.2	Data Analysis	83
3.3	Results	83
3.3.1	Physical appearance	83
3.3.2	Cell surface markers and the physical capacity of the cell	86
3.3.2.1	Flow cytometry	86
3.3.2.2	Confocal imaging	92
3.3.3	Secretory products	95

3.3.3.1 Cytokines and chemokines	95
3.3.3.2 Metabolites	103
3.4 Discussion	110
<b>Chapter 4: Bacterial mutant construction</b>	118
4.1 Introduction	118
4.1.1 Molecular Koch's postulates	119
4.1.2 Genes for $\lambda$ Red mutagenesis	122
4.2 Methods	130
4.2.1 $\lambda$ -Red mutagenesis	130
4.3 Results	133
4.4 Discussion	133
<b>Chapter 5: Modelling the role of the SPI-1 TTSS and the SPI-2 TTSS in infection with <i>Salmonella enterica</i> serovar Pullorum <i>in vitro</i></b>	137
5.1 Introduction	137
5.2 Methods	140
5.2.1 Bacterial strains	140
5.2.2 Data analysis	140
5.3 Results	140
5.3.1 The effect of SPI-1 TTSS on invasion of CKC with serovar Pullorum	140
5.3.2 The effect of SPI-2 TTSS on invasion of CKC with serovar Pullorum	146
5.3.3 The effect of SPI-1 TTSS on invasion of HD11 cells with serovar Pullorum	152
5.3.4 The effect of SPI-2 TTSS on invasion of HD11 cells with serovar Pullorum	158
5.3.5 The effect of SPI-2 TTSS on invasion of and persistence in bone marrow-derived macrophages with serovar Pullorum	164
5.4 Discussion	176



<b>Chapter 6: The role of the SPI-1 TTSS in early-stage infection with <i>Salmonella enterica</i> serovar Pullorum <i>in vivo</i></b>	185
6.1 Introduction	185
6.2 Methods	187
6.2.1 Animal Experiment	187
6.2.2 Post-mortem analysis	187
6.2.3 Data Analysis	188
6.3 Results	188
6.3.1 Bacteriology	188
6.3.2 Pathological observations made post mortem	191
6.3.3 Pro-inflammatory cytokine mRNA expression	191
6.3.4 Pro-inflammatory chemokine mRNA expression	195
6.3.5 Avian $\beta$ -defensin mRNA expression	199
6.4 Discussion	207
<b>Chapter 7: General Discussion</b>	216
7.1 The initial invasion event during Pullorum Disease	217
7.2 Persistence within macrophages during Pullorum Disease	219
7.3 Avian $\beta$ -defensins in Pullorum Disease	221
7.4 Areas of future work	221
7.4.1 Work involving primary macrophages	221
7.4.2 Determining the roles of virulence factors during infection with serovar Pullorum	222
7.4.3 The mechanisms of infection of the reproductive tract and subsequent transovarian transmission of serovar Pullorum	223
7.5 Final conclusions	224
<b>References</b>	225

## List of Figures and Tables

Figures and tables are listed below in the order which they appear in the text.

### Chapter one

Figure 1.1: Diagrammatic representation of the needle-complex structure of a type three secretion system (TTSS).

Figure 1.2: Genetic organization of SPI-1.

Figure 1.3: Salmonella SPI-1-mediated cell entry.

Figure 1.4: Genetic organization of SPI-2.

Table 1.1: Nomenclature of avian  $\beta$ -defensins

### Chapter two

Table 2.1: Primers and Probes for Real-Time qRT-PCR

Table 2.2: Antibodies and stains used for confocal microscopy and flow cytometry

### Chapter three

Figure 3.1: Typical TEM images of bone marrow-derived macrophages.

Figure 3.2: Typical TEM images of peripheral blood mononuclear cells.

Figure 3.3: Typical TEM images of HD11 cells.

Figure 3.4: Typical confocal images of bone marrow-derived macrophages to show ultrastructure.

Figure 3.5: Typical flow cytometry results from bone marrow-derived macrophage cells.

Table 3.3.1: Flow cytometry results of bone marrow-derived macrophages stained with antibodies for KUL01 and MHC class II in the FL-1 channel and with propidium iodide in the FL2 channel.

Figure 3.6: Typical confocal images of bone marrow-derived macrophages.

Figure 3.7: Typical confocal images of HD11 cells and CKC.

Figure 3.8: IL-1 $\beta$  (A), IL-6 (B) and IL-18 (C) mRNA expression levels in bone marrow-derived macrophages 5 days *ex vivo* following stimulation with either rchIFN- $\gamma$ , *E. coli* LPS, *E. coli* LPS + rchIFN- $\gamma$  or no stimulation, compared with the mRNA expression profiles for PBMC and HD11 cells.

Figure 3.9: CXCLi1 (A) and CXCLi2 (B) mRNA expression levels in bone marrow-derived macrophages 5 days *ex vivo* following stimulation with either rchIFN- $\gamma$ , *E. coli* LPS, *E. coli* LPS + rchIFN- $\gamma$  or no stimulation, compared with the mRNA expression profiles for PBMC and HD11 cells.

Figure 3.10: IL-1 $\beta$  (A), IL-6 (B) and IL-18 (C) mRNA expression levels in bone marrow-derived macrophages 7 days *ex vivo* following stimulation with either rchIFN- $\gamma$ , *E. coli* LPS, *E. coli* LPS + rchIFN- $\gamma$  or no stimulation, compared with the mRNA expression profiles for PBMC and HD11 cells.

Figure 3.11: CXCLi1 (A) and CXCLi2 (B) mRNA expression levels in bone marrow-derived macrophages 7 days *ex vivo* following stimulation with either rchIFN- $\gamma$ , *E. coli* LPS, *E. coli* LPS + rchIFN- $\gamma$  or no stimulation, compared with the mRNA expression profiles for PBMC and HD11 cells.

Figure 3.12: Griess assay to determine Nitric Oxide production by bone marrow-derived macrophages during stimulation with either *E. coli* LPS, rchIFN- $\gamma$  or *E. coli* LPS+rchIFN- $\gamma$ .

Table 3.3.2: Nitrite concentrations ( $\mu\text{M}$ ) by bone marrow-derived macrophages determined by Griess assay following stimulation with either *E. coli* LPS, rhIFN- $\gamma$  or *E. coli* LPS+rhIFN- $\gamma$ .

Table 3.3.3: P values for significantly different data from the experiment shown in Figure 3.12 and Table 3.3.2.

Figure 3.13: Superoxide anion production by bone marrow-derived macrophages during stimulation with rhIFN- $\gamma$ .

## **Chapter four**

Figure 4.1: *avrA* alignment viewer from *coli*BASE.

Figure 4.2: *sopE2* alignment viewer from *coli*BASE.

Figure 4.3: *mgtB* alignment viewer from *coli*BASE.

Figure 4.4: *sitE* alignment viewer from *coli*BASE.

Figure 4.5: *sitE'* alignment viewer from *coli*BASE.

Table 4.1: Primers for  $\lambda$  Red mutagenesis.

## **Chapter five**

Figure 5.1: Intracellular bacterial counts from CKC following infection with 100  $\mu\text{l/ml}$  of a late log phase  $10^8$  cfu/ml culture of either *Salmonella enterica* serovar Pullorum, serovar Pullorum *spaS*- or serovar Enteritidis.

Figure 5.2: Nitric oxide production by CKC following infection with 100  $\mu\text{l/ml}$  of a late log phase  $10^8$  cfu/ml culture of either *Salmonella enterica* serovar Pullorum, serovar Pullorum *spaS*- or serovar Enteritidis.

Figure 5.3: IL-1 $\beta$  (A), IL-6 (B), CXCLi1 (C) and CXCLi2 (D) mRNA expression levels in CKC following infection with 100  $\mu\text{l/ml}$  of a late log phase  $10^8$  cfu/ml culture of

either *Salmonella enterica* serovar Pullorum, serovar Pullorum *spaS*-, serovar Enteritidis or mock-infected control.

Figure 5.4: Intracellular bacterial counts from CKC following infection with 100  $\mu$ l/ml of a late log phase  $10^8$  cfu/ml culture of either *Salmonella enterica* serovar Pullorum, serovar Pullorum *ssaU*- or serovar Enteritidis.

Figure 5.5: Nitric oxide production by CKC following infection with 100  $\mu$ l/ml of a late log phase  $10^8$  cfu/ml culture of either *Salmonella enterica* serovar Pullorum, serovar Pullorum *ssaU*- or serovar Enteritidis.

Figure 5.6: IL-1 $\beta$  (A), IL-6 (B), CXCLi1 (C) and CXCLi2 (D) mRNA expression levels of CKC following infection with 100  $\mu$ l/ml of a late log phase  $10^8$  cfu/ml culture of either *Salmonella enterica* serovar Pullorum, serovar Pullorum *ssaU*-, serovar Enteritidis or mock-infected control.

Figure 5.7: Intracellular bacterial counts from HD11 cells following infection with 100  $\mu$ l/ml of a late log phase  $10^8$  cfu/ml culture of either *Salmonella enterica* serovar Pullorum, serovar Pullorum *spaS*- or serovar Enteritidis.

Figure 5.8: Nitric oxide production of HD11 cells following infection with 100  $\mu$ l/ml of a late log phase  $10^8$  cfu/ml culture of either *Salmonella enterica* serovar Pullorum, serovar Pullorum *spaS*- or serovar Enteritidis.

Figure 5.9: IL-1 $\beta$  (A), IL-6 (B), CXCLi1 (C) and CXCLi2 (D) mRNA expression levels of HD11 cells following infection with 100  $\mu$ l/ml of a late log phase  $10^8$  cfu/ml culture of either *Salmonella enterica* serovar Pullorum, serovar Pullorum *spaS*-, serovar Enteritidis or mock-infected control.

Figure 5.10: Intracellular bacterial counts from HD11 cells following infection with 100  $\mu$ l/ml of a late log phase  $10^8$  cfu/ml culture of either *Salmonella enterica* serovar Pullorum, serovar Pullorum *ssaU*- or serovar Enteritidis.

Figure 5.11: Nitric oxide production by HD11 cells following infection with 100  $\mu$ l/ml of a late log phase  $10^8$  cfu/ml culture of either *Salmonella enterica* serovar Pullorum, serovar Pullorum *ssaU*- or serovar Enteritidis.

Figure 5.12: IL-1 $\beta$  (A), IL-6 (B), CXCLi1 (C) and CXCLi2 (D) mRNA expression levels in HD11 cells following infection with 100  $\mu$ l/ml of a late log phase  $10^8$  cfu/ml culture of either *Salmonella enterica* serovar Pullorum, serovar Pullorum *ssaU*-, serovar Enteritidis or mock-infected control.

Figure 5.13: Intracellular bacterial counts from chicken bone marrow-derived macrophages following infection with 100  $\mu$ l/ml of a late log phase  $10^8$  cfu/ml culture of either *Salmonella enterica* serovar Pullorum, serovar Pullorum *ssaU*- or serovar Enteritidis.

Figure 5.14: Nitric oxide production by chicken bone marrow-derived macrophages following infection with 100  $\mu$ l/ml of a late log phase  $10^8$  cfu/ml culture of either *Salmonella enterica* serovar Pullorum, serovar Pullorum *ssaU*- or serovar Enteritidis.

Figure 5.15: IL-1 $\beta$  (A), IL-6 (B), CXCLi1 (C) and CXCLi2 (D) mRNA expression levels in chicken bone marrow-derived macrophages following infection with 100  $\mu$ l/ml of a late log phase  $10^8$  cfu/ml culture of either *Salmonella enterica* serovar Pullorum, serovar Pullorum *ssaU*-, serovar Enteritidis or mock-infected control.

Figure 5.16: Intracellular bacterial counts from chicken bone marrow-derived macrophages following infection with 100  $\mu$ l/ml of a late log phase  $10^8$  cfu/ml culture of (i) either *Salmonella enterica* serovar Pullorum, serovar Pullorum *ssaU*- or serovar Enteritidis, and (ii) comparison of the gradients of the time course for serovar Pullorum and serovar Pullorum *ssaU*- .

Figure 5.17: Nitric oxide production by chicken bone marrow-derived macrophages following infection with 100  $\mu$ l/ml of a late log phase  $10^8$  cfu/ml culture of either *Salmonella enterica* serovar Pullorum, serovar Pullorum *ssaU*- or serovar Enteritidis.

Figure 5.18: IL-1 $\beta$  (A), IL-6 (B), CXCLi1 (C) and CXCLi2 (D) mRNA expression levels in chicken bone marrow-derived macrophages following infection with 100  $\mu$ l/ml of a late log phase  $10^8$  cfu/ml culture of either *Salmonella enterica* serovar Pullorum, serovar Pullorum *ssaU*-, serovar Enteritidis or mock-infected control.

## Chapter six

Figure 6.1: Bacterial counts (expressed as log cfu/ml) from dilutions of caecal contents (A) and homogenised liver (B) obtained post-mortem from line 7<sub>2</sub> birds at 10, 24 and 48 hours post-infection with a 0.1 ml broth culture of  $10^8$  cfu of either *Salmonella enterica* serovar Pullorum, serovar Pullorum *spaS*- or serovar Enteritidis.

Figure 6.2: IL-1 $\beta$  mRNA levels of ileal (A), caecal tonsil (B) and splenic (C) tissues obtained post-mortem from line 7<sub>2</sub> birds 10, 24 and 48 hpi with a 0.1 ml broth culture of  $10^8$  cfu of either *Salmonella enterica* serovar Pullorum, serovar Pullorum *spaS*- or serovar Enteritidis.

Figure 6.3: IL-6 mRNA levels of ileal (A), caecal tonsil (B) and splenic (C) tissues obtained post-mortem from line 7<sub>2</sub> birds 10, 24 and 48 hpi with a 0.1 ml broth culture of  $10^8$  cfu of either *Salmonella enterica* serovar Pullorum, serovar Pullorum *spaS*- or serovar Enteritidis.

Figure 6.4: CXCLi1 mRNA levels of ileal (A), caecal tonsil (B) and splenic (C) tissues obtained post-mortem from line 7<sub>2</sub> birds 10, 24 and 48 hpi with a 0.1 ml broth culture of  $10^8$  cfu of either *Salmonella enterica* serovar Pullorum, serovar Pullorum *spaS*- or serovar Enteritidis.

Figure 6.5: CXCL12 mRNA levels of ileal (A), caecal tonsil (B) and splenic (C) tissues obtained post-mortem from line 7<sub>2</sub> birds 10, 24 and 48 hpi with a 0.1 ml broth culture of 10<sup>8</sup> cfu of either *Salmonella enterica* serovar Pullorum, serovar Pullorum *spaS*- or serovar Enteritidis.

Figure 6.6: AvBD1 mRNA levels of ileal (A), caecal tonsil (B) and splenic (C) tissues obtained post-mortem from line 7<sub>2</sub> birds 10, 24 and 48 hpi with a 0.1 ml broth culture of 10<sup>8</sup> cfu of either *Salmonella enterica* serovar Pullorum, serovar Pullorum *spaS*- or serovar Enteritidis.

Figure 6.7: AvBD2 mRNA levels of ileal (A), caecal tonsil (B) and splenic (C) tissues obtained post-mortem from line 7<sub>2</sub> birds 10, 24 and 48 hpi with a 0.1 ml broth culture of 10<sup>8</sup> cfu of either *Salmonella enterica* serovar Pullorum, serovar Pullorum *spaS*- or serovar Enteritidis.

Figure 6.8: AvBD3 mRNA levels of ileal (A), caecal tonsil (B) and splenic (C) tissues obtained post-mortem from line 7<sub>2</sub> birds 10, 24 and 48 hpi with a 0.1 ml broth culture of 10<sup>8</sup> cfu of either *Salmonella enterica* serovar Pullorum, serovar Pullorum *spaS*- or serovar Enteritidis.

Figure 6.9: AvBD5 mRNA levels of ileal (A), caecal tonsil (B) and splenic (C) tissues obtained post-mortem from line 7<sub>2</sub> birds 10, 24 and 48 hpi with a 0.1 ml broth culture of 10<sup>8</sup> cfu of either *Salmonella enterica* serovar Pullorum, serovar Pullorum *spaS*- or serovar Enteritidis.

Figure 6.10: AvBD14 mRNA levels of ileal (A), caecal tonsil (B) and splenic (C) tissues obtained post-mortem from line 7<sub>2</sub> birds 10, 24 and 48 hpi with a 0.1 ml broth culture of 10<sup>8</sup> cfu of either *Salmonella enterica* serovar Pullorum, serovar Pullorum *spaS*- or serovar Enteritidis.



## Acknowledgement

This project was proposed by Dr Paul Wigley following ideas which came from research he undertook on *Salmonella enterica* serovar Pullorum. Funding for the research as a PhD project and the bursary came from the Institute for Animal Health. Supervision was by Dr Paul Wigley, Dr Mike Jones and Professor Paul Barrow within the Avian Enterics Research Group and Dr Pete Kaiser within the Avian Genomics Research Group at the Institute for Animal Health. Registration for the degree of PhD was with the University of Glasgow, and supervision was provided by Professor Mark Roberts. I would like to thank all my supervisors for their guidance, help, advice and support throughout my PhD research, especially Pete for taking me on at such a late stage. I would also like to thank members (past and present) of the Avian Enterics Research Group and the Avian Genomics Research Group at the Institute for Animal Health. In particular I would like to thank Annelise Soulier for providing the TaqMan primers and probes for avian  $\beta$ -defensins; Dr Zhiguang Wu for her advice about flow cytometry; Lisa Rothwell for technical advice on a range of subjects; and Pippa Hawes for her help with confocal and TEM images.

Finally, I would like thank my friends and family for all the love and support they have given me during my PhD. Thanks to John for putting up with me; thanks to Fiona for understanding; and thanks to Mum, Dad, Sophie and Jessica for believing in me.

**Author's Declaration**

I hereby declare that I am the sole author of this thesis and the work of which the thesis is a record. No portion of work contained in this thesis has been submitted in support of any application for any other degree or qualification of this or any other University or Institute of learning.

Lucy Chappell

## Chapter 1: General Introduction

### 1.1 *Salmonella enterica*

*Salmonella enterica* encompasses a large number of disease-causing serovars which can be loosely split into two main groups. The first group includes the serovars Typhimurium and Enteritidis, which cause gastrointestinal diseases in a wide range of hosts. Infections with serovars from this group either remain restricted to the gastrointestinal tract for the duration, or in some circumstances will become systemic. For example, the serovars Typhimurium and Enteritidis cause a systemic infection when infecting young animals, but usually remain in the gastrointestinal tract when infecting mature animals. Systemic infections follow a successful intestinal colonisation, which is sustained throughout the infection course. The second group of serovars cause host-restricted, chronic, typhoid-like diseases. This group includes serovar Typhi in humans, serovar Dublin in cattle and serovars Gallinarum and Pullorum, which both cause systemic disease in chicken. During infection with serovars from this group, bacteria move out of the intestine and spread systemically. An example of the aetiological difference between these groups can be found by comparing bacterial numbers in the chicken during infection with serovar Typhimurium and with serovar Pullorum. During infection with serovar Typhimurium, bacterial numbers in the caeca and in the intestines remain at a constant level over the course of the infection, demonstrating effective intestinal colonisation (Henderson *et al.*, 1999). During infection with serovar Pullorum bacterial numbers in the caeca and intestines fall rapidly over the course of the infection as the bacteria migrate to more systemic sites (Henderson *et al.*, 1999).

The most common route of infection for *S. enterica* is faecal-oral. Serovar Typhimurium (Henderson *et al.*, 1999; Mitrucker and Kaufman, 2000), serovar

Gallinarum (Lowry *et al.*, 1999; Henderson *et al.*, 1999; Barrow *et al.*, 2000) and serovar Pullorum (Henderson *et al.*, 1999) favour associations with, and therefore most likely entry through, the gut-associated lymphoid tissue (GALT). In mammals, *S. enterica* can exit the gut lumen through cells within the intestinal mucosa, such as M cells (Wallis and Galyov, 2000). The processes involved in this are discussed in detail later in the Chapter. However, this may not be the case for the avian-specific serovars Pullorum or Gallinarum, where the caecal tonsil and bursa of Fabricius have been proposed as routes of entry from the intestine (Henderson *et al.*, 1999). The caecal tonsils are the largest lymphoid aggregate in the avian gut and are found at the junction between the caeca (two blind-ended sections of intestine situated at the anterior section of the ileum) and the ileum. Caeca have a very low flow rate, on average emptying twice a day. They are therefore a favourable site of colonisation for many avian intestinal pathogens. The bursa of Fabricius is a primary and secondary lymphoid organ; the site of B cell maturation in birds. It is situated dorsal to the cloaca, so is easily accessible to bacteria in the gastrointestinal tract.

A further route of infection may be through the process of retrograde peristalsis, which causes the movement of material from the cloacal opening back towards the colon. This results in an influx of bacteria to the distal intestine from the cloacal opening. By this route, it is possible that bacteria in the external environment may bypass the digestive process.

Although the exact mechanisms for the systemic spread of *S. enterica* are not fully understood, phagocytic cells have been considered as possible vehicles for systemic transport in mammals from mucosal sites such as Peyer's patches to mesenteric lymph nodes and other organs (Rescigno *et al.*, 2001; Cheminay *et al.*, 2002). Early dissemination is thought to be via CD18-expressing phagocytes in mammals (Vazquez-

Torres *et al.*, 1999). The cell surface antigen CD18 mediates leukocyte transmigration and congenic CD18-deficient mice are resistant to systemic dissemination (to sites such as the liver and spleen) of serovar Typhimurium following oral infection in mice (Vazquez-Torres *et al.*, 1999). During avian infection with serovar Pullorum, macrophages are also thought to be responsible for transporting the bacteria systemically (Wigley *et al.*, 2001). Following oral infections, confocal microscopy was used to show gfp-expressing serovar Pullorum bacteria localised within macrophages in the spleen (Wigley *et al.*, 2001).

Following spread to systemic organs, the bacteria may select specific subsets of macrophages to use for persistence. During infection with serovar Typhimurium, the vast majority of bacteria reside within macrophages located within the red pulp and marginal zones of the murine spleen (Salcedo *et al.*, 2001). A low proportion of serovar Typhimurium invade marginal metallophilic macrophages and a relatively high proportion invade phagocytic marginal zone macrophages (Salcedo *et al.*, 2001). The phagocytic ability of macrophages in the spleen varies, and is considerably lower for marginal metallophilic macrophages than for phagocytic marginal zone macrophages (Kraal, 1992; Hughs *et al.*, 1995). Levels of bacterial uptake may therefore result from the phagocytic ability of the cells rather than the invasive potential of serovar Typhimurium (Salcedo *et al.*, 2001). *Salmonella* can persist for long periods of time, residing within macrophages, often after all visible symptoms of the disease have ceased.

Serovar Enteritidis is one of the most common *S. enterica* serovars affecting the human population in the UK and is therefore of serious public health concern (data from the Health Protection Agency). One of the main causes of *Salmonella* infection in the human population is contact with contaminated food, which is mainly of animal origin.

A big risk factor is the ability of serovar Enteritidis to contaminate eggs often without causing serious illness in the chicken, meaning it can remain undetected in a flock. In the UK, incidence of human infection with serovar Enteritidis has been steadily falling in recent years and this has mainly been attributed to industry control programs, including the vaccination of chicken flocks but the importation of eggs from foreign countries where these control programs are not in place still poses a significant risk (data from the Health Protection Agency and Food Standards Agency).

## 1.2 Pullorum Disease

Pullorum Disease (PD) is caused by infection with *Salmonella enterica* serovar Pullorum. It is a septicaemic, persistent, systemic disease of poultry. PD causes high mortality in young birds with those that survive becoming carriers of the disease. Transmission, as with other *S. enterica* serovars, is initially faecal-oral and so affects birds in the same generation, but systemic disease can lead to infection of the reproductive tract in sexually mature adult birds and consequently vertical transovarian transmission to subsequent generations (Snoyenbos, 1991).

*Salmonella enterica* serovar Pullorum is a rod-shaped facultative intracellular Gram-negative bacterium. The slender serovar Pullorum rods are between 1.0-2.5  $\mu\text{m}$  in length and between 0.3-1.5  $\mu\text{m}$  in width (Shivaprasad, 2000). Serovar Pullorum forms homogeneous small, discrete, greyish-white colonies and can be grown on *Salmonella*-selective media such as Brilliant Green agar (Shivaprasad, 2000). Serovar Pullorum is very similar to serovar Gallinarum at the chromosomal level (Olsen *et al.*, 1996) and both are part of serogroup D according to the Kauffman-White scheme. The Kauffman-White scheme is a classification system which differentiates serological varieties of *Salmonella* from each other by determining the surface antigens of the bacterium.

Separation of serotypes is on the basis of antigenic polymorphisms in O (somatic), Vi (capsular), and H (flagellar) antigens. The somatic O group antigens are the polysaccharide side-chains associated with lipopolysaccharide (LPS) which is the main constituent of the outer membrane of Gram-negative bacteria. Although the core structure of this molecule (lipid A) remains largely conserved in all *Salmonella*, the polysaccharide side chains are highly polymorphic because the *rfb* region, containing enzymes necessary for the biosynthesis of LPS, is polymorphic (Liu *et al.*, 1991). The different antigens are numbered sequentially and each serotype is given an antigenic formula and classified into a group. Both serovar Pullorum and serovar Gallinarum possess the LPS O antigens 1, 9 and 12, with the antigenic formula for serovar Pullorum being 1, 9, 12<sub>1</sub>, 12<sub>2</sub> and 12<sub>3</sub>. Most antigenic variation in serovar Pullorum strains involves antigen 12, with differing amounts of the minor somatic antigens 12<sub>2</sub> and 12<sub>3</sub> depending on the strain.

PD was first described by Rettgerin in 1900, and was originally known as “bacillary white diarrhoea” due to the symptom of white diarrhoea which is associated with the infection. PD is historically a disease of chicks and poults with the highest mortality rates occurring between 2 and 3 weeks of age. Both mortality and morbidity due to PD are highly variable and dependent on various factors including age, strain and the general health of the birds infected. Although morbidity is generally higher than mortality following infection, mortality rates can vary greatly between 0 and 100%. In cases when death does occur, this is usually between 5 and 10 days after initial exposure. The main clinical signs of PD have been described previously (Beaudette, 1930; Beaudette, 1933; Evans *et al.*, 1955; Ferguson *et al.*, 1961; Johnson *et al.*, 1992; Mayahi *et al.*, 1995; Salem *et al.*, 1992). They include anorexia, depression, dehydration and white diarrhoea. Non-clinical signs may include a reduction in feed consumption, a

droopy appearance and ruffled feathers. During acute cases of infection, the liver, spleen, kidneys and heart may become congested and enlarged with visible white necrotic foci. Ulceration in the caeca and the small intestine is often accompanied by a generalised vascularisation and infiltration of a mixed population of inflammatory cells (Shivaprasad, 2000). In adult layers, lesions can also be observed on the ovaries. Birds which survive the initial infection with serovar Pullorum will often become sub-clinical carriers of the bacterium. After primary infection, the birds appear to recover. At this stage the bacteria persist within macrophages within the liver and spleen at almost undetectable levels. In females, once sexual maturity is reached, bacterial numbers increase greatly and there is a subsequent colonisation of the reproductive tract. This does not happen in males and the bacteria remain at a low level for the duration of the infection (Wigley *et al.*, 2005). The increase in bacterial numbers in female birds coincides with a non-specific suppression of cellular responses which occurs at the onset of laying (Wigley *et al.*, 2005). This suppression is thought to enable serovar Pullorum to infect the reproductive tract, resulting in transmission to eggs (Wigley *et al.*, 2005).

PD causes high morbidity, mortality and reduced fecundity in infected commercial flocks, resulting in a massive loss of revenue. Serovar Pullorum can survive for a long time within a favourable environment outside the host (Snoeyenbos, 1991) and therefore once a PD outbreak occurs it is easily transmitted to other flocks. This can be by infected feed, or through farm workers or veterinarians who do not take appropriate measures to avoid transport of the bacteria from place to place. The full economic losses attributed to PD can therefore be very high. General good-practice disease management procedures have eradicated PD from commercial poultry in much of the developed world (e.g. Western Europe, USA, Canada, Australia and Japan),



although PD is still common and poses a problem in areas of the world which have developing poultry industries (e.g. Mexico, Central and South America, Africa and the Indian sub-continent). Commercial flocks in the US and in northern Europe still suffer from occasional outbreaks which may indicate a reservoir for the bacteria in wild and non-commercial birds (Shivaprasad, 2000). PD may become a more important issue due to the increasing popularity of free-range farming techniques, where biosecurity is hard to maintain and birds can come into contact with wild reservoirs of the disease.

Although the presence of PD in commercial flocks in the US and northern Europe remains very limited, it can still be found in small non-commercial flocks (Erbeck *et al.*, 1993; van Buskirk, 1987; Shivaprasad, 2000). The separation of commercial and non-commercial flocks is usually effective in preventing the spread of PD between these two populations (Shivaprasad, 2000). A series of outbreaks in the USA, which occurred in a completely integrated broiler operation across 5 states between 1990 and 1991, can be used as an example of the extent of the cost that PD can have for the poultry industry (Johnson *et al.*, 1992; Salem *et al.*, 1992). The outbreak, which eventually involved 19 breeder flocks and over 260 grower facilities, was traced back to an infected grandparent line and resulted in the eradication of the grandparent, parent and grower birds (Johnson *et al.*, 1992). Although the exact economic cost of this outbreak is unknown, it was considerable as it led to the replacement of all the bird lines eradicated and loss of profits during the outbreak (Johnson *et al.*, 1992; Salem *et al.*, 1992).

### **1.3 Early stages of *Salmonella enterica* infection and the role of *Salmonella***

#### **Pathogenicity Island 1**

Comparisons of a range of genomic sequences of Gram-negative bacteria have suggested that *Salmonella* originally evolved as a pathogen through the acquisition of

large clusters of virulence genes (Baumler *et al.*, 1998; Groisman and Oehman, 1997). These virulence genes are often grouped together on the genome in areas known as pathogenicity islands. Two of the best described of these pathogenicity islands are *Salmonella* Pathogenicity Island 1 (SPI-1), and *Salmonella* Pathogenicity Island 2 (SPI-2), which are homologous to pathogenicity islands described in other gram-negative bacteria, such as *Escherichia coli* and *Yersinia pestis*. These two pathogenicity islands appear to be important in both the establishment and persistence of *Salmonella* infections.

Type three secretion systems (TTSS) are found in many different species of Gram-negative pathogenic bacteria, and their machinery spans the cell wall or membrane, facilitating the transfer of effector proteins out of the bacterial cell and into a target cell. A diagrammatic representation of the structure of a TTSS is shown in Figure 1.1. The *Salmonella* TTSS which facilitates entry into the host/target cell is encoded by a locus approximately 40 kb in length encoded on SPI-1, at centisome 63 of the chromosome. The SPI-1 TTSS consists both of structural proteins to form a needle-like delivery system, and secreted proteins which are delivered through the TTSS into the target cell.

Components of the SPI-1 TTSS needle-like delivery system apparatus include inner membrane proteins (InvA, SpaP, SpaQ, SpaR and SpaS), outer membrane proteins (InvG, PrgH and PrgK), proteins involved in energy transduction (InvC), chaperones (InvI, SicA), regulatory proteins (InvF, HilA, OrgA, InvE), and two other proteins associated with invasion (InvH and IacP) (Suárez and Rüssmann, 1998). Proteins secreted by the SPI-1 TTSS can be split into two groups; those which are directly involved in the secretion process (InvJ, SpaO, SipD) and those which have a putative effector function in the target host cell (SipA, SipB, SipC, SptP, AvrA) (Suárez and

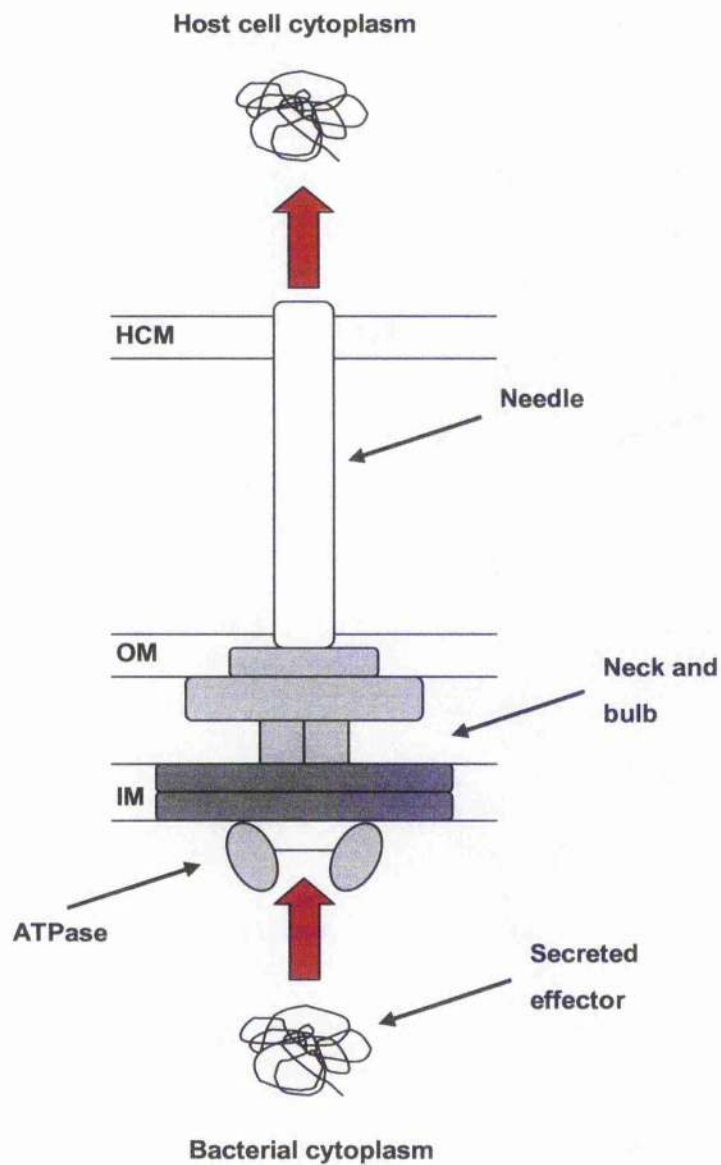


**Figure 1.1: Diagrammatic representation of the needle-complex structure of a type three secretion system (TTSS).** Host cell membrane (HCM), bacterial outer membrane (OM), bacterial inner membrane (IM).

Rüssmann, 1998). The genetic organisation of the SPI-1 locus is shown in Figure 1.2. The SPI-1 contributes to, but is not essential for, full virulence in serovar Pullorum infections (Wigley *et al.*, 2002). Jones *et al.* (2001) found that SPI-1 function had no effect on the virulence of serovar Gallinarum *in vitro*, and had little or no effect *in vivo*. A more recent study has demonstrated a more important role for SPI-1 in the virulence of serovar Gallinarum *in vivo* (Shah *et al.*, 2005). These differences could be due to the differences in the age and breed of chicken used for the experimental infections (Shah *et al.*, 2005). It is therefore most likely that although SPI-1 contributes to the virulence of serovar Gallinarum infection, the age and genetic makeup of the chicken may also contribute to any effect (Shah *et al.*, 2005).

When *S. enterica* exit the gut in mammals they invade through M cells, which have not yet been described in the chicken. M cells function as antigen-sampling cells and consequently are often used by pathogens as a port of entry into the surrounding intestinal tissue. The invasion of enterocytes and M cells results in the extrusion of damaged and infected epithelial cells into the intestinal lumen (Wallis and Galyov, 2000). This extrusion leads to villus blunting and consequently the loss of absorptive surfaces, coupled with a polymorphonuclear cell (PMN) influx into the intestinal mucosa (Wallis and Galyov, 2000). Therefore, when *S. enterica* serovars exit the host gut this typically results in a host inflammatory response which can cause a significant amount of damage to the intestinal epithelia. Interestingly, during infection with serovar Pullorum there is relatively little inflammation in the intestines, whereas there is considerable inflammation observed during infection with other *S. enterica* serovars (Henderson *et al.*, 1999). Histological investigation has shown that during infection with serovar Typhimurium there is a marked PMN infiltration into the intestinal epithelia, but that this is only mild during infection with serovar Pullorum (Henderson

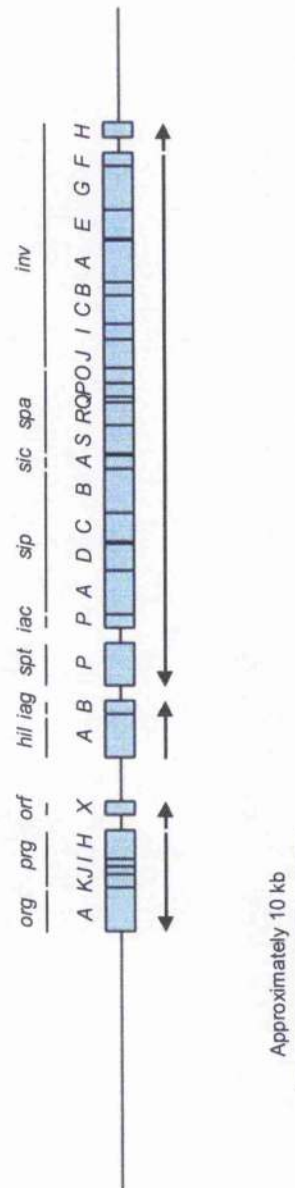


**Figure 1.2: Genetic organization of SPI-1.** Invasion region at centisome 63 in the *Salmonella* chromosome. Vertical arrows indicate the boundaries of the pathogenicity island. Horizontal arrows indicate the direction of transcription of the corresponding open reading frames (adapted from Collazo and Galán, 1997).

*et al.*, 1999). Serovar Pullorum is more sensitive to PMN killing compared to serovar Typhimurium (Henderson *et al.*, 1999) and this apparent reduced inflammation could therefore be a mechanism used by the bacteria to reduce the chance of elimination by the host immune response, in order to spread systemically (Shivaprasad, 2000).

Although early stages in the infection of different *S. enterica* serovars are thought to be fairly distinct (Weinstein *et al.*, 1998), there has been a lack of research into infection with serovar Pullorum.

The uptake of *S. enterica* into non-phagocytic enterocytes and M cells has been termed "passive entry" and follows a cascade of host cell signalling events, resulting in the manipulation and subversion of cellular membrane ruffles, which contain macropinocytotic machinery necessary for mediating pinocytotic processes (Francis *et al.*, 1993). Thus, *S. enterica* exploits the necessary process of pinocytosis through membrane ruffling in order to enter the cell by direct stimulation of this membrane ruffling process (Francis *et al.*, 1993). It is not just the exploitation of membrane ruffles that enable the entry of these bacteria into non-phagocytic cells. The movement of bacteria into non-phagocytic cells by macropinocytosis utilises the nucleation of host cell polymerisation of actin and the bundling of actin filaments into cables (Hayward and Koronakis, 1999). Recent studies, reviewed by Zhou and Galán (2001), describe *Salmonella*-induced reversible actin cytoskeleton rearrangements that take place as a result of the delivery of SPI-1 effector proteins into the host cell. These cytoskeletal rearrangements are seemingly the result of two co-ordinated steps. Firstly, the stimulation of signal transduction in the host indirectly promotes the rearrangement of actin and secondly there is direct modulation of the actin dynamics (Figure 1.3) (Zhou and Galán, 2001). The initial stimulation of the actin cytoskeleton is with the SPI-1 effectors SopE (a guanyl-nucleotide-exchange factor) and SopB (an inositol

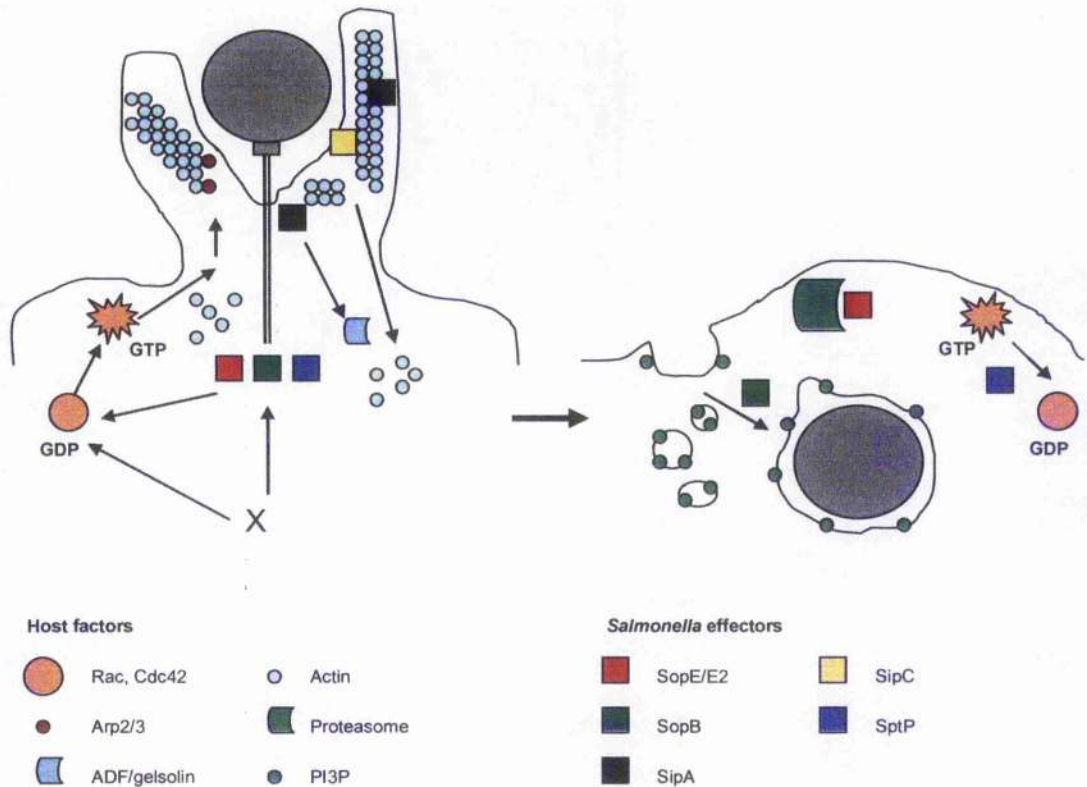


**Figure 1.3: *Salmonella* SPI-1-mediated cell entry.** Multiple host and bacterial effectors function in concert to promote entry. **(a)** Upon contact, *Salmonella* delivers multiple effectors into the host cell. SopE/E2 and SopB induce RhoGTPase activation (Cdc42 and Rac) leading to actin remodeling, presumably by way of the host-encoded actin nucleation machinery (Arp2/3). *Salmonella* effectors also engage actin directly. SipA promotes F-actin polymerization and bundling. Moreover, it prevents F-actin disassembly by inhibiting host ADF/cofilin and gelsolin. SipC also nucleates actin polymerization. **(b)** Coincident with internalization, SopB generates phosphatidylinositol 3 phosphate (PI3P) decorated, fusogenic macropinosomes and *Salmonella* containing vacuoles (SCVs), which can coalesce to create a spacious phagosome for *Salmonella* to reside. The rapid degradation of SopE by way of the host proteasome coupled to the prolonged stability of SptP halts RhoGTPase-induced actin remodeling. The mechanisms to counter SipA- and SipC-induced actin remodeling remain unclear (adapted from Patel and Galán, 2005).

polyphosphate phosphatase), which stimulate the host cell GTPases cdc42 and Rac to carry out this rearrangement (Galán and Zhou, 2000). The SPI-1 actin-binding protein SipC (Hayward and Koronakis, 1999) is enhanced by the protein effector SipA (McGhie *et al.*, 2001) and directly modulates the actin dynamics of the host cell in order to enable bacterial uptake. It does this by lowering the critical concentration of G-actin, by stabilising F-actin at the site of bacterial entry, and by increasing the binding activities of T-plastin (Galán and Zhou, 2000). These cell-altering activities are relatively short-lived. The SPI-1 T1SS secreted effector SptP directly reverses these rearrangements by acting as a GTPase-activating protein (GAP) for both cdc42 and Rac, returning the cell to its original state (Fu and Galán, 1999). It is possible that this activity could be utilised by serovar Pullorum to exit the gut by stealth, as damaged cells release signals to induce the initiation of immune responses. Therefore, returning the cells to their original state may be a way of minimising this. The exploitation of membrane ruffles as a mode of non-phagocytic cell entry may not be the only mechanism of invasion employed by *Salmonella*. Jepson *et al.* (2001) suggested the involvement of the SPI-1 secreted effector protein SipA in promoting the invasion of *S. enterica* by a mechanism other than membrane ruffling. Serovar Typhimurium *sipA* mutants failed to invade cells, or invaded at a very slow rate, following the spread of membrane ruffles on the host cell (Jepson *et al.*, 2001). The SPI-1 gene *invA* is important in the initial intestinal invasion event, as serovar Typhimurium bacteria containing mutations in this gene displayed a decreased ability in mice to colonise Peyer's patches, the ileal wall, and the spleen compared to wild-type bacteria (Galán and Curtiss, 1989). The protein InvA is a membrane-bound protein with seven hydrophobic transmembrane domains and a hydrophilic carboxyterminal domain which is thought to be located within the cytoplasm (Ginocchio *et al.*, 1994).



In mammals, a SPI-1 TTSS-independent method of traversing the epithelial cell lining of the gut involves bacterial up-take by dendritic cells (DC) (Rescigno *et al.*, 2001). DC are able to project dendrites through the epithelial lining into the intestinal lumen, internalize luminal bacteria and then transport the organisms to the basolateral side of the epithelium (Rescigno *et al.*, 2001). If transported by DC across the gut epithelium, serovar Typhimurium quickly exits DC by inducing cell death to enter macrophages, which are its preferred cell type (van der Velden *et al.*, 2003). This is probably due to the fact that although serovar Typhimurium is able to survive within murine DC, the intracellular environment does not appear to support replication, as numbers of intracellular serovar Typhimurium remained as a static, non-dividing population over the course of infection of a population of murine bone marrow-derived DC (Jantsch *et al.*, 2003).

The recruitment of inflammatory cells to the gut is thought to be a key factor in determination of virulence, underlying the development of *Salmonella*-induced enteritis (McCormick *et al.*, 1995). During infections with serovar Typhimurium, the secretion of SPI-1 TTSS effector proteins induces the activation of mitogen-activated protein (MAP) kinase signalling pathways in the host cell (Hobbie *et al.*, 1997). This MAP kinase activation then activates the transcription factors NF $\kappa$ B and AP-1, and consequently results in the expression of pro-inflammatory cytokines (Hobbie *et al.*, 1997). During serovar Typhimurium infection in the human intestine, a trans-epithelial migration of PMN rapidly follows the attachment of the bacteria to the epithelial apical membrane (McCormick *et al.*, 1993). No such influx of PMN is observed following serovar Pullorum infection in the intestine or in the caeca (Henderson *et al.*, 1999). McCormick *et al.* (1993) demonstrated that serovar Typhimurium could signal through intact epithelium to recruit sub-epithelial PMN to migrate across the epithelia. Only

those *S. enterica* serovars that caused enteritis were able to elicit this trans-epithelial migration of PMN (McCormick *et al.*, 1995). This provides a link between PMN migration and the intestinal inflammation which contributes to enteritis. In the intestine, the mechanism by which serovar Typhimurium elicits trans-epithelial migration and influx of PMN cells is by stimulating epithelial cells to release chemoattractants such as the chemokine IL-8 (Lee *et al.*, 2000). The internalisation of bacteria is not required for the release of these chemoattractants, which is via the protein kinase C-dependent signalling pathway (Lee *et al.*, 2000). SipA is thought to be involved in activating this signalling pathway (Lee *et al.*, 2000).

As the influx of PMN is not apparent during serovar Pullorum infection (Henderson *et al.*, 1999), it is unlikely that SipA, if present in the serovar Pullorum genome, is being transcribed effectively. Infection with serovar Typhimurium causes a marked pro-inflammatory response in the intestines of day-old chicks (Withanage *et al.*, 2004), indicating an up-regulation of pro-inflammatory mediators. Transcription of IL-6 is up-regulated approximately 10-fold in chick kidney cells (a gut epithelial cell model) in response to infection with serovar Typhimurium (Kaiser *et al.*, 2000). In comparison, levels of transcription of this pro-inflammatory cytokine following infection with serovar Gallinarum are not up-regulated and there is an active down-regulation of IL-1 $\beta$  and IL-2 mRNA (Kaiser *et al.*, 2000). This indicates modulation of the immune response by serovar Gallinarum, which like serovar Pullorum causes a chronic typhoid-like disease in chicken. The down-regulation of pro-inflammatory cytokines following infection with serovar Pullorum has been demonstrated *in vitro* in avian cells (Lazzerine, Barrow, Wigley and Kaiser, unpublished results). It is possible that this is one of the mechanisms employed by serovar Pullorum to enable initial establishment of an infection and avoid clearance by the immune system.

It is widely thought that the SPI-1 TTSS apparatus and its effectors are only used during the initial invasion event by *S. enterica* in the gut, but recent evidence suggests otherwise. The *invA* gene is essential for successful intracellular replication of serovar Typhimurium in non-phagocytic cells, with vacuoles containing *invA* mutant bacteria exhibiting abnormal maturation (Steele-Mortimer *et al.*, 2002). No such role has yet been determined for *invA* in *Salmonella* internalised within phagocyte vacuoles, and it is here that *S. enterica* bacterial persistence takes place (Steele-Mortimer *et al.*, 2002).

The transport system SitABCD is encoded in the SPI-1 but is not part of the TTSS. SitABCD is important in the acquisition of iron for the bacteria, and is therefore thought to be required for the full virulence of serovar Typhimurium (Janakiraman and Slauch, 2000). Transcription of the *sitABCD* operon is induced in iron-deficient environmental conditions, and in the mouse these conditions are specifically encountered following intestinal epithelial invasion (Janakiraman and Slauch, 2000). SitA is a periplasmic binding protein, SitB an ATP-binding protein and SitC and SitD are integral membrane proteins (Zhou *et al.*, 1999). In mice, infections with serovar Typhimurium bacterial *sit* mutants are significantly attenuated, indicating an important role for this gene locus in virulence (Janakiraman and Slauch, 2000). Although this transport system is encoded on the SPI-1, its functions are primarily in iron-restricted environments, which are typically during intracellular stages. This would suggest that SPI-1 genes can be transcribed concurrently with SPI-2 genes, as SPI-2 is implicated in intramacrophage survival. This implies an overlap between the operational stages of SPI-1 and SPI-2 gene products, and their ability to be transcribed at the same time.

## 1.4 Systemic *Salmonella enterica* infection and the role of *Salmonella* Pathogenicity

### Island 2

A second 40 kb pathogenicity island region, known as SPI-2, lies at centisome 30.7 of the *Salmonella* chromosome (Ochman *et al.*, 1996; Shea *et al.*, 1996). SPI-2 encodes a second TTSS and a two-component regulatory system (Ochman *et al.*, 1996; Shea *et al.*, 1996). Loci within the SPI-2 region are annotated as *ssa*, for genes encoding the secretion system apparatus; *ssr*, for genes encoding secretion system regulators; *sse*, for genes encoding secretion system chaperones; and *sse*, for genes encoding secretion system effectors (Hensel *et al.*, 1997a). The majority of *ssa* genes are located in a 25 kb segment beginning at the 31 centisome boundary (Hensel *et al.*, 1997b). These 13 structural genes found at the boundary comprise the *ssaK/U* operon and *ssaJ* (Hensel *et al.*, 1997a). Two chaperones, (*ssaA* and *ssaB*) and seven effector proteins (*ssaA-G*) are located upstream of *ssaJ* (Cirillo *et al.*, 1998; Hensel *et al.*, 1998). *SsaC* encodes an additional TTSS structural protein and is located in a region approximately 8 kb upstream from *ssaJ* (Hensel *et al.*, 1998; orf 11 in Shea *et al.*, 1996; *spiA* in Ochman *et al.*, 1996). The two component regulatory system *ssrAB* is also located in this region (Hensel *et al.*, 1998; orf 12 in Shea *et al.*, 1996; *spiR* in Ochman *et al.*, 1996). Figure 1.4 shows the genetic organisation of the SPI-2 locus. Induction of SPI-2 gene expression is modulated by the global regulatory system PhoPQ and is dependent on SsrAB (Deiwick *et al.*, 1999). The SPI-2 TTSS is thought to aid intramacrophage *S. enterica* survival (Ochman *et al.*, 1996; Cirillo *et al.*, 1998; Hensel *et al.*, 1998; Valdivia and Falkow, 1997).

Macrophages play vital roles in both the innate and adaptive immune response. In mammals they originate from myelomonocytic stem cells in the bone marrow, which then form pro-monocytes before differentiating into monocytes. It is

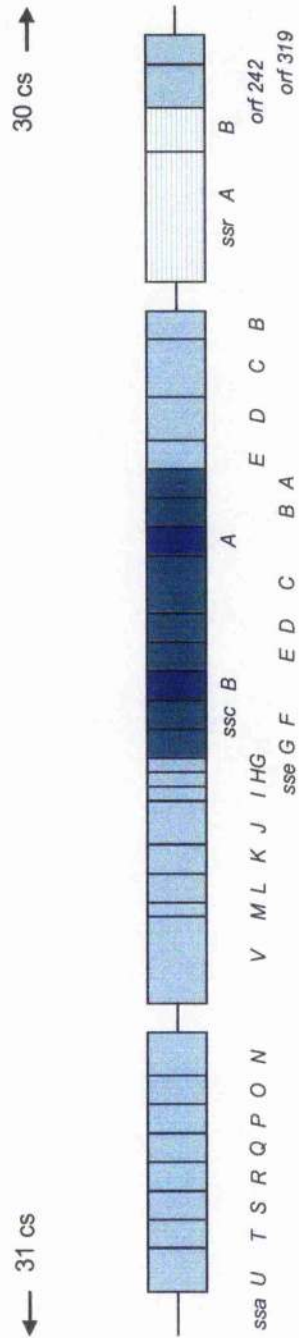


**Figure 1.4: Genetic organization of SPI-2.** Genes encoding the type III secretion system apparatus (*ssa*, open arrows), putative effector proteins (*sse*, filled arrows), specific chaperones (*ssc*, shaded arrows) and the two-component regulatory system (*ssr*, hatched arrows) of SPI2 are indicated (adapted from Deiwick *et al.*, 1999).

likely that they differentiate through a similar route in avian species. Monocytes make up approximately 10% of the white blood cells in avian blood, and upon leaving the blood they can differentiate into phagocytic macrophages. Macrophages are involved in the clearance and destruction of both intracellular and extracellular pathogens, through a process of recognition then phagocytosis. The processing of sampled self and non-self antigens encountered during scavenging is followed by expression of peptides from these antigens through the Major Histocompatibility Complex (MHC). Two main types of MHC molecules exist. MHC class I molecules bind peptides derived from cytosolic proteins. Present on most nucleated cells, they are recognised by  $CD8^+$  T cells (cytotoxic T cells). MHC class II molecules bind peptides from endocytosed proteins. They are only expressed on antigen presenting cells (APC) and are recognised by  $CD4^+$  T cells (T helper cells). When non-self internalised peptides are presented,  $CD4^+$  T cells then activate the macrophage by producing  $IFN-\gamma$ . Macrophages can also be activated by coming into contact with endotoxins. In addition to their ability to phagocytose and kill microorganisms and to present antigen to T cells, activated macrophages also secrete a range of pro-inflammatory cytokines and chemokines.

Several different mechanisms contributing to intramacrophage survival have already been recognised and associated with effector genes found in the SPI-2 TTSS of *S. enterica* serovars. Entrance to the macrophage is via endocytosis into a *Salmonella*-containing vacuole (SCV) within the cell. When a phagocyte (such as a macrophage) ingests a microbe, it first encloses the microbe within a phagosome and then alters the microenvironment of the phagosome by fusion with a lysosome. If successful, this fusion then enables killing of the microbe by both oxygen-dependent (such as superoxide and nitric oxide) and oxygen-independent mechanisms (such as acid phosphatase).

SPI-2 gene expression occurs in the SCV, where the pH is between 4 and 5, and therefore a trigger factor for the expression of SPI-2 is likely to be the environmental pH (Beuzón *et al.*, 1999). Interestingly, the SPI-2 TTSS-secreted effector protein SseB is only secreted below pH 5.0 (Beuzón *et al.*, 1999). Environmental regulation of serovar Typhimurium SPI-2 gene expression is induced by  $Mg^{2+}$  deprivation and phosphate starvation, which are both conditions in the SCV (Deiwick *et al.*, 1999). The environmental signals for induction of expression of SPI-2 genes may therefore be a combination of several factors rather than just a single cue. This could be a fail-safe mechanism employed by the bacteria, to ensure the activation of the SPI-2 genes in the event of a defect in any one of the receptors for environmental cues. This highlights the importance of the functionality of the SPI-2 to the bacteria and, during infection with serovar Pullorum, the full functionality of the SPI-2 TTSS is essential for virulence and persistence (Wigley *et al.*, 2002).

Many different pathogenic organisms opt for intracellular stages in their lifecycle to evade the immune response and avoid detection. Different pathogens have solved the problem of survival within the phagosome in different ways. One way is to escape the phagosome and live free within in the cytoplasm (*c.f. Trypanosoma, Leishmania* and *Listeria*). *S. enterica* remain within the SCV and employ several mechanisms to enable survival following the targeting of bactericidal events to the SCV. These events include the intraphagosomal production of reactive oxygen species (ROS), the acidification of the SCV, and the fusion of the phagosome with lysosomes for the delivery of hydrolytic enzymes to the SCV (Gallois *et al.*, 2001). One mechanism used by serovar Typhimurium is the exclusion of the NADPH oxidase membrane component flavocytochrome *b558* from the membrane of the phagosome (Gallois *et al.*, 2001). This prevents the assembly of the NADPH oxidase complex, and

consequently prevents the production of superoxide anion by the phagosome (Gallois *et al.*, 2001). This process of exclusion appears to be SPI-2-dependent during serovar Typhimurium infection of murine macrophages (Gallois *et al.*, 2001). Phagosomes containing SPI-2 null mutants, unlike those containing the wild-type, were able to correctly assemble the NADPH oxidase and thereby generate ROS (Gallois *et al.*, 2001). It has been suggested that SPI-2 also interferes with the trafficking of oxidase-containing vesicles to the phagosome, thus abrogating the assembly of NADPH oxidase (Vazquez-Torres *et al.*, 2000). Reactive nitrogen intermediates (RNI), synthesised by inducible nitric oxide synthase (iNOS), are also involved in antimicrobial processes directed towards the SCV. Immunofluorescence microscopy of murine macrophages has demonstrated efficient localisation of iNOS in the SCV during infections with serovar Typhimurium mutants lacking a functional SPI-2 TTSS, compared to an inability during infection with wild-type bacteria to localise iNOS in the SCV (Chakravorty *et al.*, 2002). Once in the macrophage, the bacteria can then replicate using the host cell as a hiding place (Fields *et al.*, 1986; Leung and Finlay, 1991).

*In vitro* investigations into serovar Typhimurium-induced cytokine production in murine macrophages measured increased levels of IL-12, a pro-inflammatory cytokine which is produced in response to intracellular pathogens (Svensson *et al.*, 2001). IL-6, which promotes growth of antibody-producing B cells, and TNF- $\alpha$ , which stimulates the recruitment of monocytes and neutrophils to the site of infection, were also up-regulated (Svensson *et al.*, 2001). Surface expression of MHC class I, MHC class II, CD86 (a co-stimulator for T cell stimulation) and CD54 (also known as ICAM-1 and important in cell-cell adhesion) was also up-regulated (Svensson *et al.*, 2001). Initially, the up-regulation of these molecules would seem to be an attempt to mediate an anti-*Salmonella* immune response. This is not obviously beneficial to bacterial persistence,



but one explanation could be that recruitment of monocytes to the site of infection may facilitate further infection of these cells.

*Salmonella* replicate inside the SCV, as the ability to survive and replicate in macrophages is essential for virulence (Fields *et al.*, 1986; Leung and Finlay, 1991). *Salmonella* that do not replicate in cultured cell lines are avirulent in animals (Fields *et al.*, 1986; Leung and Finlay, 1991). In infections with serovar Typhimurium this replication is SPI-2 TTSS-dependent (Ochman *et al.*, 1996; Cirillo *et al.*, 1998; Hensel *et al.*, 1998). Following replication, the bacteria need to escape the cell and invade new cells. One way in which they do this is by initiating apoptosis of the cell in which they reside. The initiation of apoptosis at different stages of serovar Typhimurium infection takes place at different rates (van der Velden *et al.*, 2000). Rapid induction of macrophage apoptosis during the initial invasion event in the gut is dependent upon SPI-1 and specifically the secreted effector molecule SipB (van der Velden *et al.*, 2000). SipB activates the cysteine protease caspase-1, which causes both apoptosis and the release of pro-inflammatory cytokines in mammalian cells (Monack *et al.*, 2000). Experiments using mice lacking functional caspase-1 have shown that although *Salmonella* are able to breach the initial M cell barrier in the gut, there is a decrease in the number of apoptotic cells, intracellular bacteria, and a decrease in the recruitment of PMN cells to Peyer's patches compared to infection of intact mice (Monack *et al.*, 2000). Caspase-1, a pro-apoptotic and pro-inflammatory mediator, is therefore essential for the colonisation of the intestine and ultimately plays an important role in the causation of systemic disease (Monack *et al.*, 2000). Collier-Hyams *et al.* (2002) described another SPI-1 secreted effector that induces rapid apoptosis, but this time in epithelial cells. AvrA, which is homologous to the *Yersinia* protein YopJ, also induces apoptosis in target cells (Collier-Hyams *et al.*, 2002). Both proteins inhibit the

activation of the transcription factor NF- $\kappa$ B but they appear to take effect at different points in the associated signalling pathway, with YopJ being a potent inhibitor of I $\kappa$ B- $\alpha$  whilst AvrA is not (Collier-Hyams *et al.*, 2002).

The rapid induction of apoptosis in macrophages within the gut-associated lymphoid tissue (GALT) may be due to the fact that the apoptosis event serves to attract additional macrophages to the site of inflammation, thereby facilitating the infection of a higher number of host cells (van der Velden *et al.*, 2000). During infection with serovar Typhimurium, the SPI-1-dependent rapid killing mechanism becomes repressed upon full internalisation within macrophages (van der Velden *et al.*, 2000). A delayed rate of apoptosis of the infected macrophages, dependent on *ompR* and SPI-2, then takes effect (van der Velden *et al.*, 2000). This delay provides the time needed for serovar Typhimurium to proliferate within the SCV before the apoptotic event, enabling the systemic spread of the infection (van der Velden *et al.*, 2000). Delayed apoptosis in infected macrophages is also partly mediated by caspase-1 and is activated by virulence proteins secreted from the SPI-2 TTSS, although it is not yet clear which proteins are responsible (Monack *et al.*, 2001).

The relative importance of SPI-1 and SPI-2 in the virulence of serovar Gallinarum in avian infections has been assessed through the use of bacterial mutants (Jones *et al.*, 2001). The SPI-1 TTSS null mutant had decreased invasive capacity for avian cells *in vitro*, but was still able to effectively infect and persist in macrophages, which would indicate that the SPI-1 TTSS has little effect on the virulence of serovar Gallinarum (Jones *et al.*, 2001). Functionality of the SPI-2 TTSS was required, however, for the virulence of serovar Gallinarum, as although SPI-2 TTSS null mutants were able to invade non-phagocytic cells, they were unable to persist in macrophages (Jones *et al.*, 2001). This suggests the SPI-2 TTSS is essential for the virulence of

serovar Gallinarum infections in chicken, whereas the SPI-1 TTSS is not (Jones *et al.*, 2001). The roles of the SPI-1 and SPI-2 have also been investigated for serovar Typhimurium infection in chicken (Jones *et al.*, 2007). Interestingly the SPI-1 TTSS was shown to be involved in both gastrointestinal and systemic colonisation during serovar Typhimurium infection of chicken, but was not essential for either of these processes (Jones *et al.*, 2007). The SPI-2 TTSS, though, was required for establishment of successful systemic infection and played a significant role in the establishment of gastrointestinal colonisation (Jones *et al.*, 2007). Therefore the roles played by SPI-1 and SPI-2, and their relative contribution to the virulence of the infection, may vary between different serovars.

### **1.5 Immune responses to *S. enterica* infection**

Host immune responses to *S. enterica* are important to consider when investigating virulence, which is the relative ability of the bacterium to cause disease. The host immune response to *S. enterica* infection must be either overcome or utilised by the bacteria in order to establish a successful infection.

Cytokines provide insight into the host immune response, indicating cell activation, suppression and clonal expansion. In mammals cytokine-specific ELISAs are used to determine levels in samples. Unfortunately in avian species few of these specific ELISAs exist, and so real-time detection of quantitative Reverse Transcriptase-PCR (real-time qRT-PCR) is widely used to quantify cytokine mRNA expression levels in samples. It is important to consider, though, that mRNA levels do not necessarily accurately represent levels of protein.

During serovar Pullorum infection, very little pathological physical evidence of a pro-inflammatory immune response is observed in the chicken (Henderson *et al.*,

1999). This is in contrast to extensive pathology observed during infection with other *S. enterica* serovars (Henderson *et al.*, 1999). This project aims to investigate the contribution of SPI-1 and SPI-2 to the virulence of serovar Pullorum. Since the inflammatory response to serovar Pullorum appears unusually low compared to that observed for other related serovars, the contribution of these pathogenicity islands to any regulation of the pro-inflammatory immune response is of interest.

The cytokine IL-1 $\beta$  is a key mediator of host inflammatory responses in innate immunity. It is secreted by many different cell types and acts on a range of target cells. In mammals, IL-1 $\beta$  is part of the IL-1 gene family which also includes IL-1 $\alpha$ , the IL-1 receptor antagonist (IL-1ra), IL-18 and six other cytokines (IL-1F5 -10). In avian species, only chIL-1 $\beta$  (Weining *et al.*, 1998) and chIL-18 (Schneider *et al.*, 2000) have been identified to date. Prior to the sequencing of chIL-1 $\beta$ , Hayari *et al.* (1982) demonstrated an IL-1-like activity in the supernatants of LPS-stimulated chicken splenocytes. Weining *et al.* (1998) cloned and sequenced chIL-1 $\beta$ , describing it as a K60-inducing cytokine. K60, now known as CXCLi1, is a chicken IL-8-like pro-inflammatory chemokine. Induction of the chemokine IL-8 (CXCL8) is one of the many pro-inflammatory functions of IL-1 $\beta$  and this has been demonstrated in human cells where IL-1 $\beta$  induced synthesis of IL-8 (Mukaida *et al.*, 1990). In adult chickens intravenous injections of chIL-1 $\beta$  induce a rapid increase in serum corticosterone levels (Weining *et al.* 1998). Serum corticosterone is an immune-activating steroid which helps to prepare the host to fight infection, in mammals it is often produced during intestinal diseases.

*In vitro* infection of chick kidney cells (a gut epithelial cell model) with serovar Typhimurium has little effect on IL-1 $\beta$  mRNA expression, but during infection with serovars Enteritidis and Gallinarum, IL-1 $\beta$  mRNA expression was down-regulated

(Kaiser *et al.*, 2000). When newly-hatched chicks were infected with serovar Typhimurium, there was significant up-regulation of IL-1 $\beta$  in the intestinal tissues, which accompanied extensive inflammatory pathology in these tissues (Withanage *et al.*, 2004).

IL-6 is a pleiotropic cytokine, produced by a variety of cells, which plays a major role in regulating immune responses, in acute phase reactions and in haematopoiesis (Kishimoto *et al.*, 1995). IL-6 induces myeloid precursor differentiation, and consequently it was previously described as macrophage granulocyte inducer type 2 (Shabo *et al.*, 1998). IL-6 also switches the differentiation of monocytes from DC to macrophages (Chomarat *et al.*, 2000). It has been suggested that IL-6 may modulate the Th1/Th2 response by actively inhibiting Th1 differentiation (Diehl *et al.*, 2000). Mice deficient in IL-6 develop normally but are unable to control infections with vaccinia virus and *Listeria monocytogenes*, as they have a severely impaired acute-phase response (Kopf *et al.*, 1994). IL-6 is essential for the regulation of the immune process but overproduction of IL-6 leads to inflammation and auto-immune diseases in humans, such as rheumatoid arthritis and Crohn's disease.

The infection of chick kidney cells with either serovar Typhimurium or serovar Enteritidis *in vitro* up-regulates IL-6 mRNA expression levels, but this response is not evident following infection with serovar Gallinarum (Kaiser *et al.*, 2000). Infection of PBMC (peripheral blood mononuclear cells) with serovar Enteritidis, however, down-regulates IL-6 mRNA expression (Kaiser *et al.*, 2006).

In most mammals there is a single gene encoding the pro-inflammatory chemokine IL-8. At the equivalent locus in the chicken there are two genes, which share similar identity to mammalian IL-8. These genes, previously known as K60 and IL-8, are now known as CXCLi1 and CXCLi2 respectively (Kaiser *et al.*, 2005). CXCLi1 and

CXCLi2 share 48% and 50% homology with human CXCL8 (IL-8) (Sick *et al.*, 2000; Kaiser *et al.*, 1999), but their functions differ. CXCLi1 preferentially chemo-attracts heterophils (the avian equivalent of neutrophils) and CXCLi2 mainly functions to chemo-attract monocytes (Poh, Pease, Young, Bunstead and Kaiser unpublished results). It is therefore important to measure the activity of both CXCLi1 and CXCLi2 when investigating infection as this can give an insight into the types of cells that are recruited as part of a pro-inflammatory response. CXCLi1 and CXCLi2 are both up-regulated in the intestines and liver of newly-hatched chicks infected with serovar Typhimurium (Withanage *et al.*, 2004). During infection of PBMC with serovar Enteritidis there is a down-regulation of CXCLi2 expression (Kaiser *et al.*, 2006).

Antimicrobial peptides have broad spectrum microbicidal activities, and in mammals are expressed by a wide variety of cells. One group of antimicrobial peptides are the defensins. In mammals there are two main types of defensin:  $\alpha$ -defensins and  $\beta$ -defensins. A third type of defensin, the  $\theta$ -defensins, are found in the rhesus macaque. In avian species, the only family of defensins identified are  $\beta$ -defensins. They are characterised by a conserved six cysteine residue motif, forming three disulphide bridges (Sugiarto and Yu, 2004). The exact mechanism of action of these peptides is unknown but they are thought to cause disruption in membrane integrity, resulting in cell death (Kagan *et al.*, 1990). Avian antimicrobial peptides were first described by both the terms "gallinacin" and " $\beta$ -defensin" and due to inconsistency in nomenclature arising between different research groups, a new system has now been proposed and they are now known as avian  $\beta$ -defensins (abbreviated to AvBD) (Lynn *et al.*, 2007). To date 14 avian  $\beta$ -defensin molecules have been described in the literature and they are now numbered AvBD1-14 (Table 1.1) (Evans *et al.*, 1994; Harwig *et al.*, 1994; Zhao *et al.*, 2004; Lynn *et al.*, 2004; Xiao *et al.*, 2004, Lynn *et al.*, 2007).

New gene/protein name	Lynn/Higgs et al. definition	Xiao et al. definition	RefSeq <sup>a</sup> definition	RefSeq <sup>a</sup> accession no.
Avian $\beta$ -defensin 1 (AvBD1)	Gallinacin 1 (GAL1)	Gallinacin 1 (GAL1)	Gallinacin 1 (GAL1)	NM_204993
Avian $\beta$ -defensin 2 (AvBD2)	Gallinacin 2 (GAL2)	Gallinacin 2 (GAL2)	Gallinacin 2 (GAL2)	NM_204992
Avian $\beta$ -defensin 3 (AvBD3)	Gallinacin 3 (GAL3)	Gallinacin 3 (GAL3)	Beta-defensin prepropeptide (GAL3)	NM_204650
Avian $\beta$ -defensin 4 (AvBD4)	Gallinacin 7 prepropeptide (GAL7)	Beta-defensin 4 (GAL4)	GAL 4 (GAL4)	NM_001001610
Avian $\beta$ -defensin 5 (AvBD5)	Gallinacin 9 prepropeptide (GAL9)	Beta-defensin 5 (GAL5)	GAL 5 (GAL5)	NM_001001608
Avian $\beta$ -defensin 6 (AvBD6)	Gallinacin 4 prepropeptide (GAL4)	Beta-defensin 6 (GAL6)	GAL 6 (GAL6)	NM_001001193
Avian $\beta$ -defensin 7 (AvBD7)	Gallinacin 5 prepropeptide (GAL5)	Beta-defensin 7 (GAL7)	GAL 7 (GAL7)	NM_001001194
Avian $\beta$ -defensin 8 (AvBD8)	Gallinacin 12 prepropeptide (GAL12)	Beta-defensin 8 (GAL8)	GAL 8 (GAL8)	NM_001001781
Avian $\beta$ -defensin 9 (AvBD9)	Gallinacin 6 prepropeptide (GAL6)	Beta-defensin 9 (GAL9)	GAL 9 (GAL9)	NM_001001611
Avian $\beta$ -defensin 10 (AvBD10)	Gallinacin 8 prepropeptide (GAL8)	Beta-defensin 10 (GAL10)	GAL 10 (GAL10)	NM_001001609
Avian $\beta$ -defensin 11 (AvBD11)		Beta-defensin 11 (GAL11)	Gallicin 11 (GAL11)	NM_001001779
Avian $\beta$ -defensin 12 (AvBD12)	Gallinacin 10 prepropeptide (GAL10)	Beta-defensin 12 (GAL12)	Beta-defensin 12 (GAL12)	NM_001001607
Avian $\beta$ -defensin 13 (AvBD13)	Gallinacin 11 prepropeptide (GAL11)	Beta-defensin 13 (GAL13)	Beta-defensin 13 (GAL13)	NM_001001780
Avian $\beta$ -defensin 14 (AvBD14) <sup>b</sup>				

<sup>a</sup> NCBI RefSeq database (<http://www.ncbi.nlm.nih.gov/RefSeq/>).

<sup>b</sup> Avian  $\beta$ -defensin 14 has recently been deposited in the GenBank database as gallinacin 14 (GAL14) (AM402954).

**Table 1.1: Nomenclature of avian  $\beta$ -defensins (adapted from Lynn et al., 2007)**

Transgenic mice expressing human enteric defensin 5 have complete protection against normally lethal doses of serovar Typhimurium (Salzman *et al.*, 2003). Also, mice deficient in matrilysin, the protein responsible for the activation of enteric defensins, are more susceptible to serovar Typhimurium infection (Wilson *et al.*, 1999). AvBD1 and AvBD2 were first isolated from chicken heterophils and both elicit a potent antimicrobial action against serovar Enteritidis *in vitro* (Evans *et al.*, 1995; Harwig *et al.*, 1994). AvBD3 has been isolated from chicken epithelial tissues including the tongue and the large intestine (Zhao *et al.*, 2001), and AvBD9 has been isolated in relatively high levels from the oesophagus and the crop, with moderate levels found in the rest of the gastro-intestinal tract (van Dijk *et al.*, 2007). A recent analysis of the distribution of AvBD4, AvBD5 and AvBD6 through chicken epithelial tissue has shown that AvBD4 is ubiquitous in its distribution, whereas AvBD5 and AvBD6 are specific to epithelial tissues including the ovary (AvBD5 and AvBD6), trachea (AvBD6), and lung (AvBD5) (Milona *et al.*, 2007). Furthermore, there is an up-regulation of AvBD4 in the liver in response to infection with serovar Enteritidis (Milona *et al.*, 2007). Expression of AvBD5 and AvBD6 is not induced *in vivo* during infection with serovar Enteritidis, but *in vitro* assays demonstrate that AvBD4, AvBD5 and AvBD6 all have antimicrobial activity against serovars Enteritidis and Typhimurium (Milona *et al.*, 2007).

Inducible nitric oxide synthase (iNOS) is a free radical-generating system found in a variety of cells, but most commonly described in macrophages, that has potent antimicrobial functions. Inducible NOS is a cytosolic enzyme absent in resting cells but induced following stimulation. In macrophages, iNOS can be induced in IFN- $\gamma$  primed cells in response to LPS. In non-immune cells, iNOS production follows stimulation through the JAK/STAT signalling pathway. The enzyme functions by catalysing the conversion of arginine to citrulline in order to produce nitric oxide (NO). NO has many



roles and functions. It is a potent endogenous vasodilator, is involved in neurotransmission, inflammation, thrombosis, immunity, and in the control of cell growth and cell death (Bredt and Snyder, 1994; Dawson and Dawson, 1995). It can therefore be a useful indicator of induction of an inflammatory immune response. When produced in acidic phagosomes, NO combines with hydrogen peroxide or superoxide anion to produce highly reactive peroxynitrite radicals, which have a potent antimicrobial function. This makes NO important in controlling intracellular infections. Measuring the NO produced by a cell can give an indication of both the immune response to, and the ability of a cell to clear, intracellular pathogens. NO levels can be measured in cell culture supernatants using the Griess assay. Nitrite is a stable breakdown product of NO and can be measured using a diazotization reaction originally described by Griess in 1879. Pathogens may interfere with iNOS induction in order to ensure successful intracellular survival. Immunofluorescence microscopy has demonstrated that serovar Typhimurium without a functional SPI-2 can effectively co-localise iNOS, but wild-type bacteria are unable to do this (Chakravorty *et al.*, 2002). This suggests that the SPI-2 system interferes with the localization of iNOS during intracellular infections (Chakravorty *et al.*, 2002).

### **1.6 Aims and objectives of the study**

The overall aim of this research was to investigate the role of SPI-1 and SPI-2 in persistent *Salmonella enterica* serovar Pullorum infection in the chicken. There are several different stages of disease during infection with serovar Pullorum, including the initial exit of the bacteria from the gut, the move to systemic sites, low-level bacterial persistence within systemic sites, followed by a rapid increase in bacterial numbers at the onset of sexual maturity in female birds and subsequent colonisation of the

reproductive tract. The mechanisms leading to this colonisation are not known, but it results in vertical transovarian transmission to subsequent generations (Snoeyenbos, 1991). Previous work has implicated SPI-1 and SPI-2 TTSS as being important in the earlier stages of infection. The SPI-1 TTSS is involved in, but not essential for, the establishment of a systemic infection (Wigley *et al.*, 2002). SPI-1 TTSS-attenuated serovar Pullorum mutants were reduced in virulence in orally infected day-old chicks when compared to wild-type bacteria (Wigley *et al.*, 2002). The study also demonstrated that the SPI-2 TTSS was essential for virulence by serovar Pullorum (Wigley *et al.*, 2002). SPI-2 TTSS-attenuated mutants showed no reduction in invasiveness, but were fully attenuated for virulence as they could not establish successful systemic infection and were rapidly cleared from systemic sites (Wigley *et al.*, 2002). This project will therefore concentrate on the early stages of infection, i.e. the initial invasion event in the gut, the movement of the bacteria to systemic sites and the establishment of persistence at these sites. Previous studies have concentrated on whether or not SPI-1 and SPI-2 TTSS contribute to virulence and not on the actual virulence mechanisms. The effect of serovar Pullorum infection on the host immune response has therefore not yet been investigated. As serovar Pullorum interacts so closely with the host, virulence will be determined in part by the host immune response. This study will therefore investigate the effect of SPI-1 and SPI-2 TTSS on the host immune response in order to determine some of the bacterial virulence mechanisms. Due to the lack of an obvious visual pro-inflammatory immune response following infection with serovar Pullorum, in contrast to infection with other *S. enterica* serovars (Henderson *et al.*, 1999), it is likely that the bacteria modulate the host immune response. This study aims to determine the involvement of SPI-1 and SPI-2 TTSS in immune modulation by the bacteria. To do this, the project will use both *in vivo* and *in*

*vitro* infection models. The hypothesis is that serovar Pullorum actively down-regulate the pro-inflammatory host immune response during infection to aid in establishment and persistence. To investigate this hypothesis, comparisons will be made with responses to serovar Enteritidis.

An important consideration when investigating the role of pathogenicity islands is the use of suitable bacterial mutants *in vitro* and *in vivo*. Although a bacterial mutant in both the SPI-1 TTSS (Jones *et al.*, 1998; Wigley *et al.*, 2002) and SPI-2 TTSS (Jones *et al.*, 2001; Wigley *et al.*, 2001) already exists, these constructs were engineered via an insertion mutation and were not deemed to be sufficiently stable for long-term *in vivo* work. An initial aim of the project will therefore be to construct stable bacterial mutants in a range of selected genes using the  $\lambda$ -Red mutagenesis technique, which has not been previously used with serovar Pullorum.

Using *in vitro* techniques to determine virulence has the advantage of concentrating on specific cell types and therefore separates out the different responses of these cells to infection. The movement of bacteria out of the gut during serovar Pullorum infection of the chicken occurs through areas of organised gut-associated lymphoid tissue (GALT) (Henderson *et al.*, 1999). It is difficult to accurately replicate these areas of GALT *in vitro*, and therefore the most appropriate cell model to use is that of intestinal epithelial cells. No chicken intestinal epithelial cell line has yet been developed and so an alternative must be used. Chick kidney cells (CKC) contain a high proportion of epithelial cells, relatively few phagocytic cells, and are readily invaded by a range of *S. enterica* serovars (Barrow and Lovell, 1989). CKC have been used in previous studies to model different aspects of the *Salmonella* invasion event, and consequently are now accepted as the best available model for chicken gut epithelial cells (Kaiser *et al.*, 2000; Wigley *et al.*, 2002). A different cell type is needed to model

persistence. Macrophages are sites of persistence during systemic serovar Pullorum infection (Wigley *et al.*, 2001) and they are therefore the most useful cell type for study when modelling this event. Although a chicken macrophage-like cell line, HD11, is already widely available for use (Beug *et al.*, 1979), previous attempts to use this cell line to model serovar Pullorum persistence have been unsuccessful (Paul Wigley, personal communication). This could be due to the fact that once the cells are infected they cannot be kept for a long-enough period of time in culture to observe the phenotype. One of the aims of the project will therefore be to develop a new appropriate cell model for use in persistence assays. Development of this cell model will require characterisation of the cells, a secondary aim of the project. The main aim of the *in vitro* studies will be to determine the effect of the SPI-1 and SPI-2 TTSS during infection of CKC and macrophages with serovar Pullorum. The hypotheses are that there will be a SPI-1-mediated down-regulation in pro-inflammatory cytokine production during infection of CKC and that there will be a SPI-2-mediated down-regulation in both pro-inflammatory cytokine production and in NO synthesis during infection of macrophages with serovar Pullorum. Also, that functionality of the SPI-2 is necessary for long-term persistence in macrophages.

Although *in vitro* assays enable the dissection of the host immune response, with regards to the specific cells involved in the infection, they do not give a true picture of what is happening during infection. The immune response of an organism is very intricate, involving a complex network of interactions between different components of the immune system. The ability to carry out experimental infections *in vivo* gives a valuable overview of the interactions between pathogen and host. The main aim of the *in vivo* research in this project will be to investigate the chicken immune response during early-stage serovar Pullorum infection, to test the hypothesis that SPI-1 enables a

quicker and quieter establishment of systemic infection, by reducing the pro-inflammatory immune response and thereby reducing host-mediated pathogenesis in the gut.

The project, therefore, will use a range of techniques to establish the role of the SPI-1 and SPI-2 TTSS in persistent systemic infection in the chicken with serovar Pullorum. This should enable a better understanding of the mechanisms by which serovar Pullorum bacteria seemingly avoid detection and clearance by the host during infection.

## Chapter 2: Materials and Methods

### 2.1 Molecular techniques

#### 2.1.1 Polymerase Chain Reaction (PCR)

##### 2.1.1.1 Standard colony PCR

Polymerase chain reactions (PCR) to amplify specific DNA sequences were performed in standard 50  $\mu$ l reactions. A small number of live bacteria, less than half of a bacterial colony, were used to provide template DNA for the reaction, which was estimated as approximately 40 ng DNA using a spectrometer. The reaction also contained 1 x PCR Buffer (Invitrogen), 1.5 mM MgCl<sub>2</sub> (Invitrogen), 0.2 mM dNTPs (Invitrogen), 0.2  $\mu$ M of each Primer (Sigma-Genosys) and 1 unit of *Taq* Polymerase.

Typical cycle conditions were:

Denaturation	95°C	10 min	1 cycle
Denaturation	95°C	30 sec	} 25 cycles
Annealing	50°C*	30 sec	
Extension	72°C	30 sec	
Extension	72°C	10 min	1 cycle

(\* The annealing temperature was varied according to the melting temperature of the primers used).

The reactions were performed using an Eppendorf Mastercycler PCR machine.

##### 2.1.1.2 PCR for $\lambda$ -Red Mutagenesis

PCR for the  $\lambda$ -Red mutagenesis technique was also performed in a standard 50  $\mu$ l reaction containing 40 ng template DNA, 1 x PCR Buffer (Invitrogen), 2 mM MgCl<sub>2</sub>

(Invitrogen), 0.2 mM dNTPs (Invitrogen), 0.3  $\mu$ M of each Primer (Sigma-Genosys) and 1 unit of *Taq* Polymerase. Typical cycle conditions were:

Denaturation	95°C	1 min	1 cycle
Denaturation	95°C	30 sec	} 29 cycles
Annealing	55°C*	30 sec	
Extension	72°C	1 min	
Extension	72°C	5 min	1 cycle

(\* The annealing temperature was varied according to the melting temperature of the primers used).

The reactions were performed using an Eppendorf Mastercycler PCR machine.

### 2.1.1.3 Agarose gel electrophoresis

To determine the success of the PCR and to visualise the size of the product, 2  $\mu$ l loading buffer (Invitrogen) were added to 10  $\mu$ l of PCR product. The product was then loaded onto a 0.8% agarose gel containing ethidium bromide (1  $\mu$ g/ml) and electrophoresed in 1 x Tris-borate-EDTA (TBE) buffer (Sigma) for approximately 1 h at 100 V. The addition of ethidium bromide enabled visualisation of the DNA following electrophoresis using an ultraviolet transilluminator connected to a camera and a monitor.

## 2.1.2 Purification of PCR product

### 2.1.2.1 PCR product direct purification

The QIAquick PCR Purification Kit (Qiagen) was used for PCR product purification as per the manufacturer's instructions. Five volumes of buffer PB were added to 1 volume of the PCR sample, mixed, then placed onto a QIAquick spin column

in a 2 ml collection tube and centrifuged for 1 min at 13,000 x g. The addition of buffer PB to the PCR product resulted in a high salt concentration which enabled binding of the DNA to the silica-membrane, whilst non-DNA contaminants passed through the column. The flow-through was discarded and the column placed back into the same collection tube. The bound DNA was then washed by the addition of 0.75 ml of buffer PE to the column followed by centrifugation for 1 min at 13,000 x g to remove any impurities. Again, the flow-through was discarded and the column placed back into the same collection tube and centrifuged for a further minute at 13,000 x g. The column was placed into a clean microcentrifuge tube and the DNA then eluted by centrifugation at 13,000 x g for 1 min in an appropriate amount of H<sub>2</sub>O (Sigma).

#### **2.1.2.2 Gel purification of PCR products**

After electrophoresis through an agarose gel (section 2.1.1.3), fragments of interest were excised and purified using the QIAquick Gel Purification Kit (Qiagen) as per the manufacturer's instructions. The excised gel fragments were weighed in clear microcentrifuge tubes and 3 volumes of buffer QG were added per 1 volume of gel. The gel fragment was incubated with buffer QG at 50°C for 10 min to dissolve the fragment, vortexing every 2-3 min to mix. The dissolved gel fragment in buffer QG was then placed onto a QIAquick spin column in a 2 ml collection tube and centrifuged for 1 min at 13,000 x g. The addition of buffer QG to the PCR product resulted in a high salt concentration which enabled binding of the DNA to the silica-membrane, whilst non-DNA contaminants passed through the column. The flow-through was discarded and the column placed back into the same collection tube. The bound DNA was then washed by the addition of 0.75 ml of buffer PE to the column followed by centrifugation for 1 min at 13,000 x g to remove any impurities. Again, the flow-through was discarded and the



column placed back into the same collection tube and centrifuged for a further minute at 13,000 x g. The column was placed into a clean microcentrifuge tube and the DNA then eluted by centrifugation at 13,000 x g for 1 min in an appropriate amount of H<sub>2</sub>O (Sigma).

### 2.1.3 Plasmid DNA preparation

Qiagen Plasmid Midi Kits (Qiagen) were used to purify plasmid DNA. Qiagen plasmid purification protocols are based on a modified alkaline lysis procedure followed by the binding of plasmid DNA to Qiagen anion-exchange resin under appropriate low-salt and pH conditions. The plasmids in lab *E. coli*  $\lambda$ -pir strains were cultured overnight in 100 ml selective LB medium at an appropriate temperature (i.e. 37°C for non-temperature-sensitive plasmids or below 30°C for temperature-sensitive plasmids) with vigorous shaking (300 rpm). The bacterial cells were harvested by centrifugation at 6,000 x g for 15 minutes at 4°C, and the resulting pellet re-suspended in 4 ml of buffer P1. Then 4 ml of buffer P2 were added to the re-suspended cells and mixed thoroughly by inverting the sealed tube 6 times. The mixture was then incubated at room temperature for 5 min. Chilled buffer P3 (4 ml) was then added to the lysate, which was mixed thoroughly by inverting 6 times. The lysate was then incubated on ice for 15 min, then centrifuged at 20,000 x g for 30 min at 4°C, and the supernatant containing the plasmid DNA removed. The supernatant was then centrifuged again at 20,000 x g for 15 min at 4°C to remove suspended and particulate material from the lysate and the supernatant removed immediately. This centrifugation prevents the application of particulate material to the Qiagen-tip 100 which could block the flow. The Qiagen-tip 100 contains an anion-exchange resin which binds plasmid DNA under low-salt and pH conditions. To equilibrate the Qiagen-tip 100, 4 ml of buffer QBT were run through the

column by gravitational flow. The supernatant was then added to the column and allowed to run through by gravitational flow. RNA, proteins and low molecular weight impurities were removed by medium-salt washes of 2 x 10 ml buffer QC. Plasmid DNA was eluted in the high-salt buffer QF. The DNA was concentrated, desalted by precipitation in 0.7 volumes of isopropanol and pelleted by centrifugation at 15,000 x g for 30 min at 4°C. The supernatant was carefully removed from the DNA pellet, which was then washed by adding 2 ml of room temperature 70% ethanol, and centrifugation at 15,000 x g for 10 min. The supernatant was carefully removed from the DNA pellet, which was then left to air-dry for 10 min. The pellet was then re-suspended in 100  $\mu$ l H<sub>2</sub>O (Sigma).

#### **2.1.4 RNA extraction**

##### **2.1.4.1 Collection and homogenisation of samples from cells**

RNA was extracted from cells using the RNeasy Kit (Qiagen), following the manufacturer's protocol. The supernatants were removed from cell monolayers and cells were then lysed by the addition of 350  $\mu$ l RLT buffer. RLT buffer contains the highly denaturing chemical guanidine isothiocyanate, which acts by immediately inactivating RNases and lysing the cells. Samples were homogenised by centrifugation at 13,000 x g for 2 min through a QIAshredder (Qiagen).

##### **2.1.4.2 Collection and homogenisation of samples from tissues**

Tissues (below 30 mg in weight) were removed from birds and placed directly into cryovials containing 500  $\mu$ l RNAlater (Qiagen). The cryovials were stored overnight at 4°C to enable effective penetration of the tissues with RNAlater, then transferred to -20°C for storage until processing. To extract the RNA, the tissue was

removed from the *RNAlater* and weighed to ensure its weight was below 30 mg, then transferred into a cryovial containing 600  $\mu$ l RLT buffer and a sterile 3mm stainless steel bead. The sample was then disrupted and homogenised in a Retsch MM300 bead mill. The lysate was then centrifuged for 3 min at 13,000 x g and the supernatant carefully removed and transferred to a new tube.

#### **2.1.4.3 RNA extraction from homogenised lysate**

To extract the RNA from the homogenised lysates of samples, 70% ethanol (1 volume) was added to the homogenised lysate and mixed. The lysate was then transferred to an RNeasy spin column in a 2 ml collection tube, and centrifuged at 8,000 x g for 15 sec. The RNA binds to the silica-based membrane of the RNeasy column, made possible by the addition of ethanol to the lysate which provides the appropriate binding conditions. The flow-through was discarded. Buffer RW1 (700  $\mu$ l) was added to the column and it was then centrifuged at 8,000 x g. The flow-through was discarded and the column transferred to a new collection tube. The column was washed by the addition of 2 x 500  $\mu$ l of buffer RPE with centrifugation for 15 sec at 8,000 x g for the first wash, and centrifugation for 2 min at 8,000 x g for the second wash, discarding the flow-through. The collection tube was discarded and replaced with a new tube to collect residual fluid by centrifugation at 13,000 x g for 1 min. RNA was eluted into a fresh tube following the addition of 30  $\mu$ l DEPC- $H_2O$  for preparations from cells or 50  $\mu$ l for preparations from tissues to the column, then centrifugation at 8,000 x g for 1 min. Samples were stored in the short-term at -20°C, and at -80°C in the long-term.

### 2.1.5 Real-Time Quantitative RT-PCR

To quantify levels of cytokine and avian  $\beta$ -defensin mRNA in cell and tissue samples from assays, real-time quantitative RT-PCR (qRT-PCR) was used. The TaqMan assay uses specially designed reagents with a sequence detection system to quantify mRNA expression through a PCR-based assay. Laser scanning technology within the sequence detection system excites fluorescent dyes in the TaqMan probes, and Real-Time sequence detection software allows the visualization of increases in detectable fluorescence. TaqMan probes are designed to the target sequence of RNA, with a quencher dye at the 3' end and a fluorescent reporter dye at the 5' end. When the probe is intact, the close proximity of the quencher to the reporter suppresses the reporter's fluorescence. During the PCR, forward and reverse primers hybridize to the target sequence within the sample RNA, and the TaqMan probe then hybridizes to the target sequence within the PCR product. Taq polymerase then displaces the 5' end of the probe, before cleaving it with its 5'-3' nuclease activity during the extension phase of the PCR. This cleavage event separates the reporter and quencher dyes, resulting in an increase in the detectable fluorescence of the reporter dye. This change in detectable fluorescence is directly proportional to the increase in PCR product. Detectable fluorescence is determined at each of the 40 cycles of the PCR cycle. An endogenous control (housekeeper gene) is used to normalise the quantitation of the mRNA target for differences in the amounts of total RNA added to each reaction. This method is widely used for quantitatively measuring levels of specific cytokine mRNA in samples. RNA was purified from the samples and real-time qRT-PCR performed using the Reverse Transcriptase qPCR™ Master Mix kit (Eurogentec). Experiments were performed in parallel to detect both gene-specific as well as 28S rRNA-specific amplification. The

detection of the housekeeping gene 28S rRNA allows for the normalisation of RNA amounts in each sample.

The primer and probe sequences for the cytokines and 28S were provided by Dr Pete Kaiser (IAH), and the primer and probe sequences for the avian  $\beta$ -defensins were provided by Annelise Soulier (IAH). These are shown in Table 2.1. The probes were labelled with 5-carboxyfluorescein (FAM) at the 5' end and the quencher N,N,N,N'-tetramethyl-6-carboxyrhodamine (TAMRA) at the 3' end. Although a DNase digestion step was not performed during RNA extraction, the silica-based columns provided in the RNeasy kit are designed to preferentially bind to RNA, thus minimising contamination from genomic DNA. As an additional measure taken to minimise false positives from DNA contamination, either one of the primers or the probe used for each message had been designed spanning an intron/exon boundary. To maximise specificity, both the primers and probe were designed to be 18-30 bases long, with 30-80% GC content. Mis-priming of the probe was minimised by ensuring that there were less than 4 contiguous Gs. The  $T_m$  of the primers was 58-60°C, whilst the  $T_m$  of the probe was 68-70°C. A 5' G was avoided in the probe as this quenches the fluorophore. The 3' end of the primer was designed as close as possible to the probe to keep 5' nuclease activity at an optimum.

Real-time qRT-PCR measures the accumulation of PCR product during the experimental phase of the reaction through the detection of the reporter dye. Whilst the probe is intact, the quencher dye is located in close proximity and so absorbs the emission from the reporter dye. During the extension phase of the PCR reaction, the 5'-nuclease activity of the *rTth* DNA polymerase hydrolyses the probe and in doing so separates the quencher from the reporter. Results are expressed as threshold cycle values ( $C_t$ ), when the increase in fluorescence emission, subtracted from background

RNA Target	Probe/Primer Sequence (5'-3')	Optimal primer concentration ( $\mu$ M)
28s	Probe (FAM)-AGGACCGCTACGGACCTCCACCA-(TAMRA) Forward GGCGAAGCCAGAGGAACT Reverse GACGACCGATTTGCACGTC	0.6
IL-1 $\beta$	Probe (FAM)-CCACACTGCAGCTGGAGGAAGCC-(TAMRA) Forward GCTCTACATGTCGTGTGTGATGAG Reverse TGTCGATGTCCCGCATGA	0.4
IL-6	Probe (FAM)-AGGAGAAATGCCTGACGAAGCTCTCCA-(TAMRA) Forward GCTCGCCGGCTTCGA Reverse GGTAGGCTGAAAGCGGAACAG	0.2
IL-18	Probe (FAM)-CCGCGCCTTCAGCAGGGATG-(TAMRA) Forward AGGTGAAATCTGGCAGTGAAT Reverse ACCTGGACGCTGAATGCAA	0.8
CXCL1	Probe (FAM)-TGGCTCTTCTCCTGATCTCAATG-(TAMRA) Forward GCACTGGCATCGGAGTTCA Reverse TCGCTGAACGTGCTTGAGCCATACCTT	0.4
CXCL2	Probe (FAM)-GCCCTCCTCCTGGTTTCAG-(TAMRA) Forward TGGCACCGCAGCTCATT Reverse TCTTTACCAGCGTCTACCTTGCGACA	0.6
AvBD1	Probe (FAM)-ATCCTGCAGCACCCCTGGGCCA-(TAMRA) Forward TGCTCCTCCCCTTCATCCT Reverse GAAAACAATCTGACTTCCTTCTAGAG	1.0
AvBD2	Probe (FAM)-CCAGGTTTCTCCAGGTTGTCTTCGC-(TAMRA) Forward CCTGCTTTTCTCTCTCCTCTTCCT Reverse CCCTCCTTTACAGAAGAGCATGT	1.0
AvBD3	Probe (FAM)-TGGCAGTTTCTGCAGCACCCCTG-(TAMRA) Forward CATCCCCTTCTTCTCTTGTTC Reverse CACGACAGAATCCTCCTTATTCT	0.8
AvBD5	Probe (FAM)-CAGCCCTGGTTCTGCCCGGA-(TAMRA) Forward AGATCCTGCCTCTCCTTTTGC Reverse CCCACGGCGCTCACAGT	0.6
AvBD14	Probe (FAM)-CCCAGGCTGCACCAGAGTCGGA-(TAMRA) Forward CTGTTTCTTGTCTCCTGGCAGTA Reverse CTTCATCTCCGACATGTGACAGT	0.6

**Table 2.1: Primers and Probes for Real-Time qRT-PCR**

signal, passes a significant threshold. Amplification and detection of specific products was performed using the ABI PRISM™ 7700 Sequence Detection System, with the following cycle profile: 1 cycle of 50°C for 2 min, 60°C for 30 min (reverse transcription step) and 95°C for 5 min (hot start), and 40 cycles of 94°C for 20 sec (denaturation step) and 59°C for 1 min (annealing and extension).

Experimental primer concentrations had been optimised previously and were supplied by Dr Pete Kaiser (IAH) and Annelise Soulier (IAH). These are shown in Table 2.1.

Each RT-PCR reaction (25  $\mu$ l) was set up as described below:

2 X Master mix (Eurogentec qRT-PCR kit)	12.50 $\mu$ l
Enzyme (Eurogentec qRT-PCR kit)	0.125 $\mu$ l
Forward primer	0.50 $\mu$ l
Reverse primer	0.50 $\mu$ l
DEPC-H <sub>2</sub> O	5.875 $\mu$ l
Total RNA	5.00 $\mu$ l

To generate standard curves for the cytokine, avian  $\beta$ -defensin and 28S rRNA-specific reactions, total RNA extracted from *E. coli* LPS-stimulated HD11 cells was serially diluted in sterile DEPC-H<sub>2</sub>O and dilutions made from 10<sup>-1</sup> to 10<sup>-5</sup>. Each experiment contained three no-template controls, test samples in triplicate and a log<sub>10</sub> dilution series (standard curve) in triplicate.

The threshold  $\Delta R_n$  (change in the reporter dye) was determined as the lowest fluorescence detected above background that was on the exponential phase of the standard curve, and this factor was kept constant throughout the experiment. Baseline values were set to those cycles in which there would be insufficient product for

detection and were also kept constant throughout the experiment. Any product detected during these cycles was considered as background and subtracted from measurements.

Results are calculated as described in Moody *et al.* (2000) and in Kaiser *et al.* (2000). Results are expressed in terms of the cycle threshold value ( $C_t$ ), which is the cycle at which the change in the reporter dye ( $\Delta R_n$ ) passes a significant threshold. Cycle threshold values are expressed subtracted from 40 which is the negative end point of the assay. Therefore, higher values represent higher levels of cytokine mRNA. To control for variation in sampling and RNA preparation, the  $C_t$  values for cytokine-specific product for each sample were standardized using the  $C_t$  value of 28S rRNA product for the same sample from the reaction run simultaneously. To normalize RNA levels between samples within an experiment, the mean  $C_t$  value for 28S rRNA-specific product was calculated by pooling values from all samples in that experiment. Tube to tube variations in 28S rRNA  $C_t$  values, about the experimental mean, were calculated. The slope of the 28S rRNA  $\log_{10}$  dilution series regression line was used to calculate differences in input total RNA. Using the slopes of the respective cytokine  $\log_{10}$  dilution series regression lines, the difference in input total RNA, as represented by the 28S rRNA, was then used to adjust cytokine-specific  $C_t$  values.

In summary, to calculate the corrected  $C_t$  values ( $D_{it}$ ), a normalisation factor ( $N_i$ ) was added to the sample mean ( $C_{it}$ ). The normalisation factor was calculated by dividing the sample slope ( $S$ ) by the 28S slope ( $S'$ ) and multiplying this by the value obtained from the mean of the 28S  $C_t$  values ( $C_{it}'$ ) for the associated samples subtracted from the median of the 28S  $C_t$  values ( $D_i'$ ) for the associated samples. The equations are shown below:

$$D_{it} = C_{it} + N_i$$

$$\text{where } N_i = \frac{S}{S'} (D_i' - C_{it}')$$



## 2.2 Microbiological techniques

### 2.2.1 Bacterial strains

A spontaneous nalidixic acid-resistant (Nal<sup>r</sup>) mutant of *S. enterica* serovar Pullorum 449/87 was provided by Professor Paul Barrow and was grown from stocks maintained at -70°C in Luria Bertani (LB) broth supplemented with 30% v/v glycerol. This strain was originally from the Veterinary Laboratories Association, where it had been isolated from a case of Pullorum Disease which had occurred in free-range birds, and has been previously well characterised (Berchieri *et al.*, 2001; Wigley *et al.*, 2001). The strain containing a mutation in *spaS*, a structural component of the SPI-1 TTSS, was provided by Mike Jones and had been generated by conjugation of the suicide plasmid pSS1 (Jones *et al.*, 1998) into serovar Pullorum 449/87 Nal<sup>r</sup> to make an insertion mutant. This mutant is referred to in the text as *spaS*<sup>-</sup>. The strain containing a mutation in *ssaU*, a structural component of the SPI-2 TTSS, was also provided by Mike Jones and had been generated by the conjugation of the suicide plasmid pSS2 (Jones *et al.*, 2001) into serovar Pullorum 449/87 Nal<sup>r</sup> to make an insertion mutant. This mutant is referred to in the text as *ssaU*<sup>-</sup>. A spontaneous nalidixic acid-resistant (Nal<sup>r</sup>) mutant of *S. enterica* serovar Enteritidis 125109 was provided by Professor Paul Barrow, and was grown from stocks maintained at -70°C in LB broth supplemented with 30% v/v glycerol. This strain was isolated from a poultry farm that had been identified as the cause of a human outbreak by the Public Health Laboratory in Colindale, and has previously been well characterised (Barrow 1991; Barrow and Lovell, 1991; Barrow *et al.*, 1991; Halavatkar and Barrow, 1993; Berchieri *et al.*, 2001). The bacteria were streaked aseptically onto LB agar using an inoculating loop and incubated overnight at 37°C. To obtain single colonies, the overnight growth was

touched with a sterile inoculating loop and re-streaked in three stages onto fresh LB agar, incubating overnight at 37°C.

Before use, bacteria were grown to a late log phase of growth, by inoculating LB broth with a single colony and culturing for 16 h at 37°C in an orbital shaking incubator at 160 rpm, then using this culture to re-inoculate a fresh LB culture at 1/1000. This culture was then grown for a further 4 h in the same conditions, until the optical density (OD) of the culture was either 0.25 for serovar Pullorum or 0.4 for serovar Enteritidis, at which point the bacterial concentration of the culture was  $1 \times 10^8$  cells/ml.

### 2.2.2 Competent cells

Competent cells were made by aseptically inoculating 10 ml of LB with the required bacterial culture, then growing overnight (16 h) in an orbital shaking incubator at 37°C, 160 rpm. This overnight culture (1 ml) was used to aseptically inoculate 100 ml of LB, which was then grown for 4 h under the same conditions to obtain cells at the late log growth phase. The culture was then put on ice at 4°C for 10 min to halt growth. The culture was then split into two 50 ml polypropylene tubes (Falcon), and the cells were pelleted by centrifuging the culture at 3,500 x g for 15 min at 4°C. The supernatant was then removed and the cells in each polypropylene tube re-suspended in 50 ml Super-Q water. The cells were then centrifuged at 2,000 x g for 12 min at 4°C and the supernatant removed from each cell pellet. The cells were re-suspended in 50 ml Super-Q water per polypropylene tube and centrifuged at 2,000 x g for 12 min at 4°C. The supernatant was removed from each cell pellet and the cells re-suspended in 2 ml of sterile 10% glycerol. The cells were centrifuged at 2,000 x g for 12 min at 4°C and the glycerol supernatant poured off the pellet. Due to the viscosity of glycerol, a small

amount (approximately 500  $\mu$ l) was left in each polypropylene tube and the cells were re-suspended in this. The competent cells were immediately stored at  $-80^{\circ}\text{C}$  until use.

### 2.2.3 Agglutination assays

Slide agglutination assays can be used to determine if a bacterial colony has an intact (smooth) or damaged (rough) LPS coat. They can also be used to determine the antigenic identification of the colony. O surface antigens are somatic antigens from the external part of cell wall LPS, and the different antigenic groups are used for characterisation under the Kaufman-White serotyping scheme, as described in Chapter 1. The *Salmonella enterica* serovars are part of the D group and serovar Pullorum can be identified using the O9 surface antigen of this group. To determine whether the LPS structure is intact, an inoculation loop-full of sterile PBS was put onto a glass slide. Approximately half a cfu (colony forming unit) of the bacterial colony to be tested was transferred from an LB agar plate to the glass slide aseptically using an inoculation loop, and mixed well with the PBS. A loop-full of acriflavin (1 g/500 ml) was added to the suspension on the glass slide and mixed well. If the suspension remained opaque then the bacterial colony was deemed smooth. If agglutination was observed in the suspension, then the bacterial colony was deemed rough. If the colony was smooth, the antigenic identity of the bacterial colony was then determined by the addition of an inoculation loop-full of O9 antisera. If agglutination was observed in the suspension, then the bacterial colony was positively identified as *S. enterica* serovar Pullorum. A negative control was performed using O27 antisera, to which serovar Pullorum would be negative, to demonstrate the specificity of agglutination.

## **2.3 Immunological techniques**

### **2.3.1 Cells**

#### **2.3.1.1 Chick Kidney Cells**

Chick Kidney Cells (CKC) were prepared as described in Barrow and Lovell (1989) by the IAH Compton Microbiological Services. After isolation, cells were seeded at  $5 \times 10^6$  cells/ml in 24-well plates in EMEM (Eagle's modified Eagle's medium) containing 12.5% heat-inactivated newborn bovine serum, 10% tryptose phosphate broth (TPB), 1% HEPES and 0.1% penicillin and streptomycin (from a stock at 10,000 units/ml). After seeding, cells were incubated at 37°C, 5% CO<sub>2</sub> for 48 h before use. Two hours prior to use, the monolayer was washed to remove all traces of antibiotics and the cell culture media was replaced with pre-warmed DMEM (Dulbecco's modified Eagle's medium) containing 12.5% heat-inactivated foetal bovine serum and 10% TPB, adjusted to pH 7.0.

#### **2.3.1.2 HD11 cells**

HD11 cells (Beug *et al.*, 1979) are maintained by the IAH Compton Microbiological Services. Cells were initially seeded in 24-well plates at  $3 \times 10^5$  cells/ml in RPMI 1640 containing 2.5% foetal bovine serum, 2.5% chicken serum (Sigma) and 10% TPB. After seeding, cells were incubated at 37°C, 5% CO<sub>2</sub> for 48 h before use. Two hours prior to use, the monolayer was washed to remove all traces of antibiotics and the cell culture media was replaced with RPMI 1640 containing 2.5% heat-inactivated foetal bovine serum.

### 2.3.1.3 Isolation of blood-derived monocytes

Birds were killed then bled by cardiac puncture and the blood collected via a needle into syringes containing heparin to prevent clotting. The blood was diluted with an equal volume of PBS and 5-10 ml were carefully overlaid onto 5 ml room-temperature Histopaque 1083 (Sigma) in a 15 ml polypropylene tube (Falcon). The tube was then centrifuged at 1,200 x g for 40 min without braking. After centrifugation, the peripheral blood mononuclear cells (PBMC), which form a buffy coat at the interface between the red blood cells and serum, were removed and transferred to a new polypropylene tube (Falcon). The volume was made up to 10 ml with PBS and the cells pelleted by centrifugation at 1,200 x g for 10 min. The cells were then washed three times in ice-cold PBS by centrifugation at 1,200 x g for 5 min at 4°C and re-suspended at a concentration of  $5 \times 10^6$  cells/ml in complete media. For approximately 100 ml complete media, 93 ml RPMI 1640 containing L-glutamine (Sigma) were supplemented with 5 ml chick serum (Sigma), 2 ml HEPES, 100  $\mu$ l gentamicin (IAH media stock at 50 mg/ml), 100  $\mu$ l penicillin and streptomycin stock (IAH media stock at 10,000 units/ml) and 200  $\mu$ l nystatin (IAH media stock at 10,000 units/ml). The cell concentration was determined and cell viability was assessed by mixing equal volumes of cell culture and Trypan blue, then counting viable cells using a Neubauer haemocytometer. Live cells have the ability to exclude the dye Trypan blue whereas dead or dying cells do not. The cells were cultured in 24-well flat-bottomed plates at 37°C, 5% CO<sub>2</sub>. After overnight incubation, the medium was gently agitated to dislodge non-adherent cells. The supernatant containing the non-adherent cells (lymphocytes and granulocytes) was removed and replaced with fresh, pre-warmed complete media. Cells were incubated for a further 48 h before use, replacing the supernatant with fresh complete media daily, to remove contaminating thrombocytes.

## **2.3.2 Monoclonal antibody purification**

### **2.3.2.1 Monoclonal antibody purification using protein G**

Monoclonal antibody 2G11 (to chicken MHC class II) was obtained as technomouse fluid from Jim Kaufman (IAH). This was gently passed through a 0.45  $\mu\text{m}$  filter to remove debris. Protein G sepharose fast flow beads (5 ml, Amersham) were centrifuged at 300 x g for 5 min at 4°C. The supernatant was then removed and the beads re-suspended in 10 ml starting buffer (20 mM sodium phosphate pH 7.0). The bead solution was added to a C10 chromatography column (GE Healthcare Life Sciences), to hold the beads which were used to bind the antibody, coupled with an AC10 adaptor (GE Healthcare Life Sciences). The column was washed with 50 ml starting buffer. The monoclonal antibody preparation was then loaded onto the column and left to flow through so the antibody could bind to the beads. The column was then washed with 50 ml starting buffer. The bound antibody was eluted with 20 ml glycine elution buffer (0.1 M glycine pH 2.7) and collected in 1 ml fractions. The fractions were collected directly into eppendorf tubes containing 60  $\mu\text{l}$  neutralising buffer (1 M Tris-HCl pH 9.0) to neutralise the pH of the eluted antibody solution. The protein concentrations of the fractions were then calculated in order to determine which fractions contained the highest levels of antibody, using the BCA assay kit (Perbio Science) according to the manufacturer's instructions (described below). The fractions with the highest protein (antibody) concentration were aliquotted into smaller volumes and stored at -20°C until use. The column was stripped by passing 20 ml of stripping buffer (6 M guanidine hydrochloride) through it.

### 2.3.2.1 BCA protein assay

Protein concentrations from samples were determined using the BCA™ assay kit (Perbio Science) according to the manufacturer's instructions. A standard curve was prepared in a 96-well plate by performing a serial dilution of 2 mg/ml BSA (25  $\mu$ l per well). The BCA™ working reagent was made by adding 50 parts BCA™ reagent A to 1 part BCA™ reagent B. Experimental samples were added to the 96-well plate in 25  $\mu$ l volumes. BCA™ working reagent (200  $\mu$ l) was added to every well and mixed thoroughly. The plate was then incubated at 37°C for 30 min protected from light. The plate was then cooled to room temperature and the absorbance was measured in a plate reader at 562 nm. The protein concentration of the experimental samples was determined using the standard curve.

### 2.3.3. Detection of surface antigen by flow cytometry

Bone marrow-derived cells were stained for surface antigens by flow cytometry using KUL01 and 2G11 mAbs. In preparation for flow cytometry, bone marrow-derived cells were grown in low-adherence plates (Corning) as described in Chapter 3. Once cells were ready for use, 100  $\mu$ l of cell suspension at  $1 \times 10^7$  cells/ml were added to a round-bottomed 96-well plate. The plate was centrifuged at 350 x g for 1 min and the supernatant briskly flicked off. The cell pellets were washed in FACS buffer (PBS containing 10 mg/ml BSA and 0.2% sodium azide) by centrifugation at 350 x g for 1 min, then the supernatant briskly flicked off. To stain surface antigen, cells were mixed and incubated with 100  $\mu$ l of the appropriate concentration for each mAb for 15 min at room temperature, protected from light. For concentrations of mAbs and stains used see Table 2.2. Following staining, the cells were washed three times using FACS buffer by centrifugation at 350 x g for 1 min, then briskly flicking the supernatant off the plate.

To determine viability of the cell population, 50  $\mu$ l propidium iodide (PI) was used, as viable cells exclude this stain. When staining with PI, the cells were stained for 5 min on ice, protected from light, followed by washing as previously, prior to analysis. Cells (100  $\mu$ l) from each well were added to plastic FACS tubes containing 500  $\mu$ l PBS and kept on ice until analysis. The fluorescence of 10,000 cells in each sample was measured on the fluorescence-activated cell sorter FACScan (Becton Dickinson) using CELLquest™ software (Becton Dickinson). The instrument settings were set up as follows, saved and used for all repetitions of the assay. To capture the maximum amount of cells, the voltage of the FSC and the SSC photomultiplier tubes were adjusted using the unstained cells, until the bulk of the cells appeared in the lower left quadrant of a FSC vs SSC dot plot. A “spill over” of one colour from one channel into another can happen if the fluorochrome used is too bright or has a broad spectrum. To minimise this, the compensation was adjusted using histograms for all the channels used (FL1, FL2, FL3 and FL4). The data were analysed using FCS Express version 2 flow cytometry analysis software (De Novo software).

### **2.3.4 Staining for confocal microscopy**

#### **2.3.4.1 Phagocytosis assay**

To demonstrate the phagocytic ability of primary cells, fluorescent beads were added to the culture and visualised via confocal imaging. The beads used were Fluoresbrite™ Carboxylate Microspheres, with a diameter of 0.50  $\mu$  and Yellow-Green (YG) in colour (Polysciences Inc.). The manufacturer’s instructions were followed (Polysciences Inc., data sheet 430). The beads were supplied at a concentration of  $1.8 \times 10^8$  particles/ml and prior to the assay were first opsonised using normal serum to facilitate phagocytic activity. To opsonise, 1 ml of beads was incubated with 500  $\mu$ l



foetal calf serum (Sigma) and 500  $\mu$ l PBS at 37°C for 30 min. Once opsonised, 10  $\mu$ l of the beads (at  $9.0 \times 10^7$  cells/ml) were added to 100  $\mu$ l primary cells on a monolayer in complete media (at  $5 \times 10^6$  cells/ml) and incubated at 37°C for 1 h. The phagocytosis reaction was stopped after 1 h by the addition of ice-cold PBS to the cells and mixing by pipetting. The cell monolayer was washed three times in ice-cold PBS to remove all adherent, non-phagocytosed beads.

#### **2.3.4.2 Staining cells for confocal microscopy**

Primary cells grown on a monolayer on glass coverslips in 24-wellplates were stained with various antibodies and stains to identify both ultrastructure and cell surface antigens (see Table 2.2). To reduce background staining a 15 min incubation step at room temperature with 5% foetal calf serum (Sigma) in PBS was performed. Staining was by incubation with the required antibody (see Table 2.2 for concentration used) for 15 min at room temperature protected from light. If necessary, this was followed by incubation with a secondary antibody. This was followed by washing the cell monolayer three times in PBS to remove excess antibody/stain. Staining of the cells to visualise ultrastructure was performed at IAH Pirbright by Pippa Hawes. Cells used for this purpose were first fixed for 1 h in 4% paraformaldehyde in PBS. The fixative was then removed and replaced with PBS. The cells were kept in PBS on ice for transport to IAH Pirbright, where the cell monolayers were treated with 0.1% Triton-X 100 in PBS for 15 min to permeabilise cells then stained for confocal analysis as described above.

#### **2.3.4.3. Confocal microscopy**

Once all staining had been completed, the glass coverslips were removed from the 24-well plate using forceps and dipped into deionised water. The coverslip was then

Antibody/Stain	Antigen recognised or target for stain	Working concentration	Source/reference
KUL01 (murine mAb)	Unknown but a chicken macrophage marker	Confocal 1/5000 Flow cytometry 1/100	Southern Biotech
2G11 (murine mAb)	Chicken MHC class II	Confocal 1/1000	Dr Jim Kaufman, IAH
Phalloidin conjugated to Alexafluor 568	Actin	Confocal 1/25	Invitrogen
Tubulin (murine mAb)	Tubulin	Confocal 1/1000	Sigma
ERP60 (rabbit Ab)	Luminal Endoplasmic Reticulum	Confocal 1/200	Dr Paul Monaghan, IAH
DAPI	Nucleus	Confocal 1/10000	Sigma
TRITC (rabbit Ab)	Murine Ig	Confocal 1/10000	Molecular Probes
FITC (rabbit Ab)	Murine Ig	Flow cytometry 1/20	Molecular Probes
Nile Red	Lipid Bilayer	Confocal 1/500	Molecular Probes
CC14 (murine mAb)	Bovine CD1	Flow cytometry 1/5	Machugh <i>et al.</i> , 1988
Propidium Iodide	Dead/dying cells	Flow cytometry 50 $\mu$ l of 25 $\mu$ g/ml solution	Sigma

**Table 2.2: Antibodies and stains used for confocal microscopy and flow cytometry**

mounted onto glass slides using aqueous Vectorshield mount (Vector Laboratories), sealing with nail varnish. The cells were examined under a Leica Sp2 microscope with 405, 488, 568 and 633 lasers at 63x using emersion oil. LCS Lite Leica confocal software was used to analyse the images.

### **2.3.5 Transmission Electron Microscopy (TEM)**

The cells were grown on a monolayer on 13 mm diameter Thermanox EM coverslips (Science Services UK). The cells were fixed with EM fixative, which was prepared as follows in the fume-hood. To make 0.2 M EM buffer, 50 ml solution A (2.722 g sodium dihydrogen orthophosphate in 100 ml distilled water) were added to 32 ml solution B (8 g sodium hydroxide in 100 ml distilled water). The pH was checked and adjusted to pH 7.2, and the solution diluted to 0.05 M in distilled water. EM fixative was then made with 92 ml 0.05 M buffer plus 8 ml of 25% gluteraldehyde and 1.71 g sucrose. The supernatant was carefully removed from the cell monolayer and the cells were washed three times in PBS. Cells were then fixed in EM fixative and transported immediately in the fixative to IAH Pirbright for processing and TEM imaging, carried out by Pippa Hawes. Processing of the cells at IAH Pirbright was as follows. The cells were incubated at room temperature in the EM fixative for approximately 2 h. The EM fixative was then removed from the monolayer and replaced by 1% osmium tetroxide, incubating at room temperature for 2 h. The 1% osmium tetroxide was then removed and the cell monolayers dehydrated in an ethanol series (70% ethanol for 45 min, 90% ethanol for 15 min, 100% ethanol for 2 x 15 min). The coverslips were then transferred into polythene cups and washed in propylene oxide (a transitional fluid) for 15 min to prepare them for the embedding process. The samples were infiltrated with a 1:1 mix of propylene oxide and epoxy resin for 30 min at room temperature on a rotator. The 1:1

mix was removed from the coverslips and replaced with 100% epoxy resin. The cell samples on the coverslips were infiltrated for 1 h on a rotator. The coverslips were transferred into fresh polythene cups containing fresh resin and polymerised at 60°C for approximately 20 h. The Thermanox backing was then removed from the blocks leaving the cells embedded in the resin. The resin blocks were then incubated at 60°C for a further 24 h. Images of the cells embedded in the resin blocks were taken using a Tietz F214 2k x 2k digital camera (Gauting, Germany) attached to a FEI Technai 12 Microscope (Eindhoven, Netherlands).

### **2.3.6 Cell stimulation**

For assays requiring the stimulation of cells, either 1  $\mu\text{g/ml}$  *E. coli* LPS (Sigma), 1/1000 rhIFN- $\gamma$  (from Dr Pete Kaiser, IAH Compton) or both were added to the culture for 24 h at 37°C, 5% CO<sub>2</sub>.

### **2.3.7 Gentamicin protection assay**

Bacterial cultures were added to the cells at 100  $\mu\text{l/ml}$  of cells and allowed to invade for 1 h at 37°C, 5% CO<sub>2</sub>. A negative control of LB was also added to appropriate cells for comparison. After 1 h, the supernatant was removed and replaced with the appropriate media, according to the cell type, containing 100  $\mu\text{g/ml}$  gentamicin. The cells were then incubated for a further 1 h to kill all extracellular bacteria. The supernatant was then removed and replaced with the appropriate media for the cell culture, containing 50  $\mu\text{g/ml}$  gentamicin, for the duration of the experiment. To determine the nitric oxide response to the bacteria at each time-point, the cell supernatant was harvested for use in Griess assays. For RNA isolation, RLT buffer containing  $\beta$ -mercaptoethanol (Sigma) was then added to the cell monolayer and the

lysate containing the mRNA from the cells was then harvested and stored at -20°C until RNA isolation. To determine intracellular bacterial numbers at each time-point, cells were lysed for 10 min at 37°C, 5% CO<sub>2</sub> with 1% Triton X-100 in PBS, and dilutions of the lysate plated aseptically onto plain LB agar.

### **2.3.8. Griess assay**

The Griess assay is used to determine the nitrite concentration in supernatants from cell stimulation assays. A 100  $\mu$ M nitrite solution was prepared in the buffer used for the original cell stimulation assay (i.e. complete media). A nitrite standard curve was constructed by performing a serial dilution in triplicate using 3 columns of a 96-well plate (50  $\mu$ l per well). Cell supernatant (50  $\mu$ l) from each experimental sample was then added to the plate in triplicate. Room-temperature sulfanilamide (50  $\mu$ l of a 1 g/100 ml in 2.5% phosphoric acid solution) was added to the standard curve and experimental samples, then the plate was incubated for 10 min at room temperature protected from light. Room temperature naphthylethylenediamide (50  $\mu$ l of a 0.3 g/100 ml in 2.5% phosphoric acid solution) was added to the standard curve and experimental samples then the plate was incubated for 10 min at room temperature protected from light. Absorbance was measured in a plate reader at 550 nm. The nitrite concentration of the experimental samples was calculated using the nitrite standard curve.

### **2.3.9 Superoxide anion assay**

Cells were grown on a monolayer at  $5 \times 10^6$  cells/ml in a 96-well plate and either left un-stimulated or stimulated with 1/1000 rhIFN- $\gamma$  for 24 h. The supernatant was removed from the cell monolayers and the cells were washed with phenol red-free Hanks Buffered Saline Solution (HBSS) (Sigma). The cell monolayers were split into

two groups (each containing stimulated and non-stimulated cells), A and B. To group A, 75  $\mu$ l phenol red-free HBSS and 25  $\mu$ l ferricytochrome C (2.7 mg/ml cytochrome C in phenol red-free HBSS) were added. To group B, 50  $\mu$ l phenol red-free HBSS, 25  $\mu$ l ferricytochrome C and 25  $\mu$ l SOD (superoxide dismutase, 1 mg/ml) were added. A cell-free control was also added to both groups. Then 10  $\mu$ l PMA (10  $\mu$ g/ml phorbol 12-myristate 13-acetate in DMSO) were added to all wells, and the plate incubated for 1 h at room temperature protected from light. Supernatant (200  $\mu$ l) from each well was transferred into the corresponding well in a new U-bottomed 96-well plate, to reduce interference from particulate cellular matter when reading the plate. Absorbance of the plate was read at 550 nm in a plate reader. Sodium dithionite (10  $\mu$ l of 1 mg/ml) was added to all wells on the plate and the absorbance read again at 550 nm using a plate reader.

The amount of  $O_2^-$  was then calculated from the absorbance values as follows. The total amount of ferricytochrome C reduction (% dithionite reduced) was determined by expressing the first absorbance reading as a percentage of the absorbance reading obtained after dithionite treatment of the samples. The absorbance values of the SOD-treated samples were subtracted from the corresponding experimental samples (i.e. experimental-SOD).

The equation used to calculate the nmol  $O_2^-$  released is as follows:

$$\text{nmol } O_2^- \text{ released} = (\text{experimental} - \text{SOD}) \times \% \text{ dithionite reduced} \times 10.9 \text{ nmol}$$

(N.B. 10.9 nmol is the amount of ferricytochrome C added to the reaction.)

## Chapter 3: Generation of bone marrow-derived macrophages

### 3.1 Introduction

Macrophages are a heterogeneous population of bone marrow-derived mononuclear cells. This heterogeneity reflects the diverse functions of these cells. They are potent innate effector cells with antimicrobial activities, and are integral in both processing and presenting antigen to lymphocytes. Macrophages also function as regulatory cells influencing both localised and systemic responses by the secretion of immunomodulatory cytokines and metabolites. Together, these functions help to clear and protect against invading pathogens whilst minimising damage to the host.

The bone marrow is the site of production of all circulating blood cells through a process called haematopoiesis. Progenitor cells within the marrow are stimulated to differentiate down specific pathways by cytokines. Macrophages originate from a monocytic lineage, and the production of these cells from myeloid progenitors is driven by cytokines produced within the bone marrow. The main cytokine responsible for driving this differentiation is GM-CSF (granulocyte-macrophage colony stimulating factor); a haematopoietin which stimulates the growth and differentiation of myelomonocytic stem cells. Once the cells have differentiated, they move to the blood where they circulate as monocytes until they enter tissue, when they become macrophages.

The activation of macrophages can be divided into two stages. The first stage transforms naïve cells from a “responsive” to a “primed” state, which decreases the amount of secondary signal required for terminal activation. The model signal used *in vitro* to prime the macrophage is IFN- $\gamma$ . IFN- $\gamma$  alters macrophage gene expression (Hamilton and Adams, 1987; Tannenbaum *et al.*, 1988). The second stage of

macrophage activation results in terminal activation of the cell, and the model signal for this is LPS. Although priming with IFN- $\gamma$  reduces the amount of LPS needed to activate macrophages, prolonged exposure to LPS abolished the need for this priming (Johnston *et al.*, 1987).

Macrophages are often referred to as sampling cells, due to their phagocytic ability, which is a function of all sub-sets of these cells. The extent of the phagocytic ability may vary between sub-sets of cells and this serves a variety of purposes. Macrophages sample antigen through phagocytosis from their environment as they travel through tissue. Once phagocytosed, these antigens are processed and broken down into polypeptides, then presented to lymphocytes via the MHC. Another function of phagocytosis is the internalisation of micro-organisms for destruction within phagolysosomal vacuoles. This is again followed by the subsequent processing and presentation of polypeptides from the antigen to lymphocytes. Phagocytosis is also used for the programmed elimination of dead or dying cells. Macrophages can do this effectively as they have an ability to distinguish self from non-self and also to distinguish infected or dying from viable host cells. Phagocytosis can be described as "specific", which involves uptake of antigen via the Fc immunoglobulin receptor or the C3 complement receptor, or "non-specific", which involves all other forms of recognised antigen uptake.

Because macrophages are antigen presenting cells, their responses to bacterial infection are central to the complex interactions between *Salmonella* and the host. Extra-intestinal dissemination of serovar Typhimurium to systemic sites in the mouse is via CD18-expressing tissue macrophages (Vazquez-Torrez *et al.*, 1999) and is a site of persistence (Alpuche-Aranda *et al.*, 1994) and of replication (Buchmeier and Heffron, 1989; Richter-Dahlfours *et al.*, 1997; Salcedo *et al.*, 2001). Once inside the



macrophage, serovar Typhimurium can influence both the expression of cell surface molecules and the production of cytokines (Svensson *et al.*, 2001). Wigley *et al.* (2001) demonstrated that splenic macrophages were a site of long-term persistence during serovar Pullorum infection in the chicken using experimental *in vivo* infections and confocal microscopy. The study of the avian macrophage is therefore important when considering immune modulation and persistence of serovar Pullorum in infections of poultry.

Although macrophages play a key role in the host response to disease, comparatively little has been done to investigate their role in avian species and consequently methods for the isolation of primary macrophages are not as advanced and well described as for mammalian macrophages. One routine method used to obtain high numbers of murine primary cells is the isolation of peritoneal macrophages, but this method in the chicken yields relatively low numbers of cells (Rose and Hesketh, 1974). Other methods used by avian immunologists to obtain primary macrophages include the isolation of bone marrow macrophages (Peck *et al.*, 1982), peripheral blood monocytes (Vanio *et al.*, 1983; Wigley *et al.*, 2002), bursal-derived macrophages (Peck *et al.*, 1982), thymic-derived macrophages (Peck *et al.*, 1982) and splenic macrophages (Peck *et al.*, 1982; Wigley *et al.*, 2001). Although these methods do indeed generate macrophages, yields are low, and often not sufficient for use in extensive bacterial invasion assays. This Chapter describes the development of a protocol for the isolation of large quantities of primary macrophages from the chicken for use in subsequent serovar Pullorum invasion and persistence assays.

One of the most widely used sources for macrophage isolation is the blood. The isolation and culture of primary monocytes from blood is possible because the monocyte/macrophage cells are “sticky” and readily adhere to the plastic surface of

culture vessels to form a monolayer. After approximately 48 hours, all dead or non-adherent cells (i.e. contaminating thrombocytes, erythrocytes, etc.) can be easily removed by gentle washing of the monolayer. Another, more rapid, method of removing unwanted cell types is by prior centrifugation of the blood over a Histopaque 1086 gradient. Histopaque 1086 has a density of 1.086, and consists of ficoll and sodium diatrizoate. During the centrifugation process, the ficoll aggregates the erythrocytes and granulocytes causing them to sediment at the bottom of the tube, whilst the mononuclear cells separate as a band at the plasma/Histopaque interface, where they can then be harvested and washed before culture. However this method gives low yields of cells. This is partly due to the difficulty of obtaining large amounts of blood from the chicken. Another reason is that monocytes/macrophages cannot clonally expand in culture, and as the numbers of circulating monocytes in the blood is very low (approximately 10% of the total immune cells) few cells can be harvested even with the most careful isolation technique. Another primary macrophage isolation method, that would avoid these problems and produce a very high yield, would be to isolate myelomonocytic stem cells and subsequently differentiate them to the monocyte lineage (as one progenitor will yield many monocyte/macrophage cells). This method relies on the stimulation of the progenitor cell with GM-CSF to produce monocyte/macrophage cells, and the lack of stimulation of other types of progenitor cell.

The culture and stimulation of pluripotent stem cells with GM-CSF from the bone marrow to produce cells of the monocyte/macrophage lineage has the potential to produce a very large population of cells, much greater than would be possible using the method described by Peck *et al.* (1982) to isolate macrophages direct from the marrow. Routinely used methods to obtain bone marrow-derived macrophages from mice use GM-CSF to drive the differentiation of progenitor cells. The previous unavailability of

chicken GM-CSF hampered the development of a similar method for use with chicken bone marrow cells. The sequencing of the chicken T2 cytokine gene cluster by Avery *et al.* (2004) identified the GM-CSF gene and recombinant bioactive chicken GM-CSF was expressed. The availability of rchGM-CSF should enable the derivation of a protocol to generate chicken bone marrow-derived macrophages based on that used to generate macrophages in mice.

It is very hard to conclusively prove that the cells obtained through any purification or culture method are macrophages, as avian macrophages are not well described in the literature and may be quite different to their mammalian counterparts. Therefore, a range of methods must be employed to gather evidence to suggest that the cells are indeed macrophages. The physical appearance of the cells can be assessed by their general appearance under the microscope and whether they adhere to substrate. Adhering to substrate separates the cells from lymphocytes, which do not stick, and the length of time they adhere for can separate them from thrombocytes, heterophils and DC, which lift off the monolayer after 48 hours. Very few cell surface markers have been described for avian macrophage-like cells and many of the antibodies that recognise these are not commercially available. KUL01 (Mast *et al.*, 1998) is an antibody which recognises an unknown non-specific chicken macrophage cell surface marker. Chicken MHC class II is recognised by the antibody 2GII (from Dr Jim Kaufman, IAH), but is not specific to macrophages so cannot be used to differentiate the cells from other antigen presenting cells. The phagocytic ability (physical capacity) of the cells can be investigated using fluorescently labelled latex beads. The production of secretory products and metabolites known to be produced by macrophages are chemical properties which can be investigated (e.g. IL-1 $\beta$  mRNA, nitric oxide, superoxide anion).

The combination of evidence from all these different sources should prove, beyond reasonable doubt, the cell lineage.

## **3.2 Methods**

### **3.2.1 Bone marrow-derived macrophages**

#### **3.2.1.1 Complete Media**

Complete media for bone marrow-derived macrophages was made as follows. For approximately 100 ml of complete media; 93 ml RPMI 1640 (Sigma); 5 ml heat-inactivated chicken serum (Sigma); 2 ml HEPES (IAH Media stock); 100  $\mu$ l gentamicin (50 mg/ml, Sigma); 100  $\mu$ l penicillin and streptomycin stock (10,000 units/ml, IAH media stock); 200  $\mu$ l nystatin (10,000 units/ml, IAH media stock); recombinant chicken GM-CSF added at a concentration of 1/100 unless otherwise specified.

#### **3.2.1.2 Generation of bone marrow-derived macrophages**

The following protocol was developed and adapted from a protocol to isolate murine bone marrow-derived macrophages taken from "Isolation of murine bone marrow-derived macrophages" Current Protocols in Immunology, Supplement 11, 14.1.3.

Femurs were removed post-mortem from out-bred Rhode Island Red (RIR) chickens of a minimum age of 4 weeks. The ends of the bones were carefully cut using sterile surgical bone-cutters and the marrow flushed out with approximately 20 ml pre-warmed RPMI 1640 (this was adjusted slightly according to the size of the femur to remove the optimum amount of bone marrow). The resulting marrow was then centrifuged at 500 x g for 10 min at room temperature and the supernatant discarded. The cells were re-suspended in 2 ml of pre-warmed RPMI 1640 and counted using a

haemocytometer, determining the viability of the cells by Trypan Blue exclusion, and the volume adjusted to  $5 \times 10^6$  cells/ml in pre-warmed complete media (in some of the assays described in this Chapter, cells were initially seeded at both  $2.5 \times 10^6$  cells/ml and  $5 \times 10^6$  cells/ml for comparison). The cells were cultured *ex vivo* in one of two ways, either on a monolayer or if required in suspension, on Low-adherence plates (Corning). The cells that were grown on a monolayer were seeded into 24-well cell culture plates (Invitrogen) and incubated at  $37^\circ\text{C}$ , 5%  $\text{CO}_2$  for seven days (in some of the assays described in this Chapter, cells were grown for both five and seven days *ex vivo* for comparison), changing the media every 48/72 h. To change the media, cell supernatants were gently removed with a pipette and replaced with fresh, pre-warmed complete media. The cells that were seeded into the Low-adherence plates were incubated at  $37^\circ\text{C}$ , 5%  $\text{CO}_2$  for seven days (in some of the assays described in this Chapter, cells were grown for both five and seven days *ex vivo* for comparison), changing the media every 48/72 h. To change the media of the cell suspension, the cells were harvested from the Low-adherence plates and centrifuged at  $500 \times g$  for 10 min at room temperature, discarding the supernatant and re-suspending the cells in fresh pre-warmed complete. On day six (or day seven when using the cells for flow cytometry), the cell suspension was carefully layered over room temperature Histopaque 1083, then centrifuged at  $1,200 \times g$  for 40 min. Cells were then collected from the interface and washed twice in PBS to remove any transferred histopaque. The cell concentration was then adjusted to  $5 \times 10^6$  cells/ml in pre-warmed media. The cells were incubated for a further 24 h at  $37^\circ\text{C}$ , 5%  $\text{CO}_2$  (except for cells used for flow cytometry which were used immediately) before use.

### 3.2.2 Data Analysis

Experiments were performed in on three separate occasions and for each experiment each parameter was repeated in triplicate. For real-time qRT-PCR, just one of the repeated parameters was taken from each experiment (giving  $n=3$ ) for the analysis.

Where appropriate, differences were analysed using Analysis of Variance and the two-tailed t-test, and were carried out using the Minitab for Windows version 14 statistical package (Minitab Ltd., Coventry, West Midlands, UK). Values of  $P \leq 0.05$  were taken as significant.

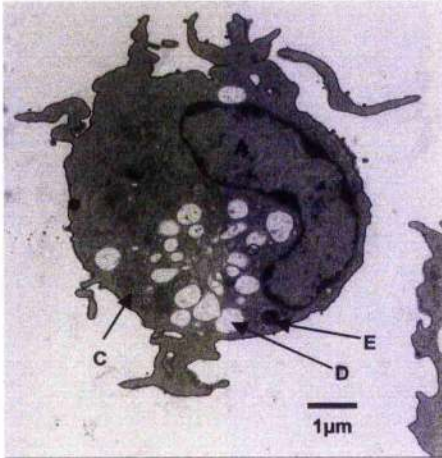
## 3.3 Results

### 3.3.1 Physical appearance

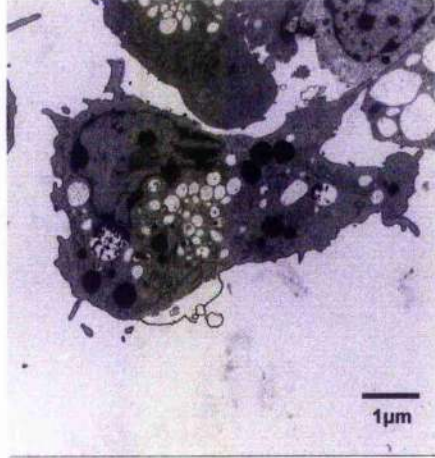
Figure 3.1 shows typical transmission electron microscope (TEM) images of bone marrow-derived macrophages grown to day 7 with 1/100 rhGM-CSF *ex vivo*. The images show that the nucleus was bifurcated and located to one side of the cell. The organelles of the cell were generally visible and centrally located and they included the endoplasmic reticulum, mitochondria, vacuoles and vesicles which appear to contain granules. The cells contained a large amount of vacuoles, the number of which increased with the size of the cell. The processes of the cells are visible in images 1 and 2 of the figure.

Figure 3.2 shows typical TEM images of PBMC. The nuclei of the cells were again bifurcated, and located to one side of the cell. The organelles of the cell were again generally centrally located, including endoplasmic reticulum, mitochondria and vacuoles. The vesicles containing granules were clearly visible in higher numbers throughout the cells compared to numbers observed in the bone marrow-derived macrophages (Figure 3.1), and appeared to contain varying amounts of granules.

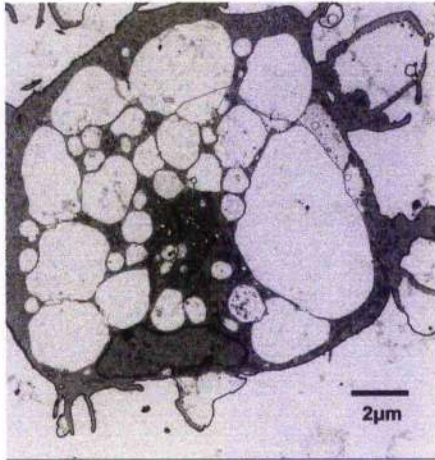
1



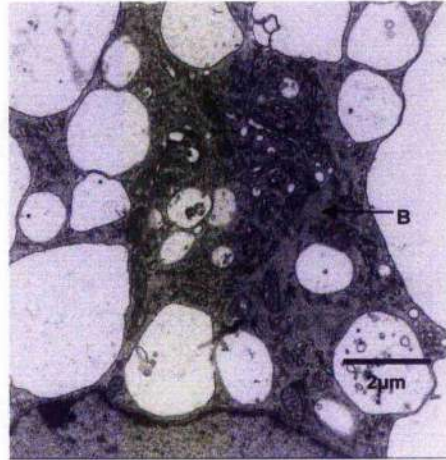
2



3



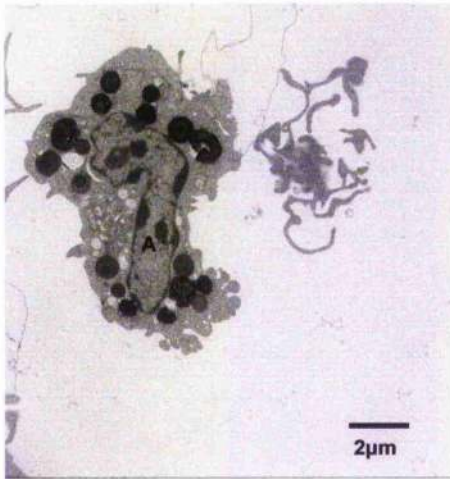
4



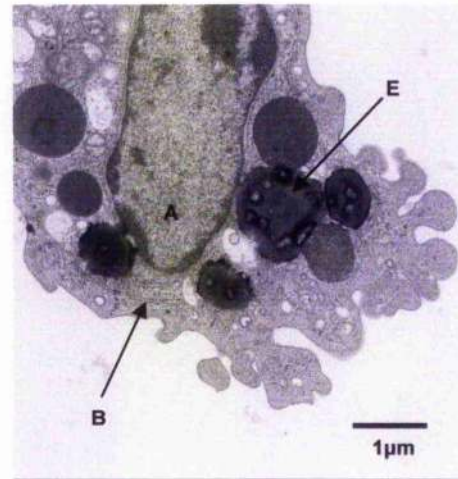
- A: Nucleus**  
**B: Endoplasmic Reticulum**  
**C: Mitochondria**  
**D: Vacuole**  
**E: Vesicle containing granules**

**Figure 3.1: Typical TEM images of bone marrow-derived macrophages.**

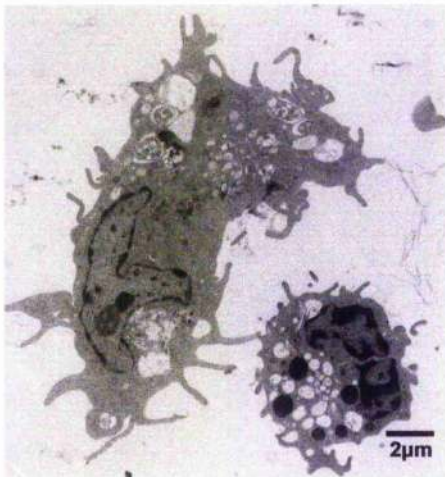
1



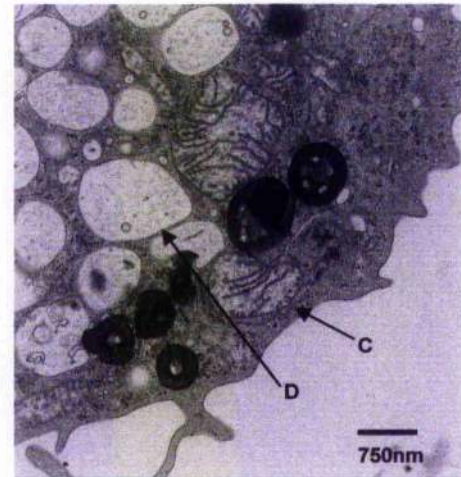
2



3



4



- A: Nucleus**  
**B: Endoplasmic Reticulum**  
**C: Mitochondria**  
**D: Vacuole**  
**E: Vesicle containing granules**

**Figure 3.2: Typical TEM images of peripheral blood mononuclear cells.**



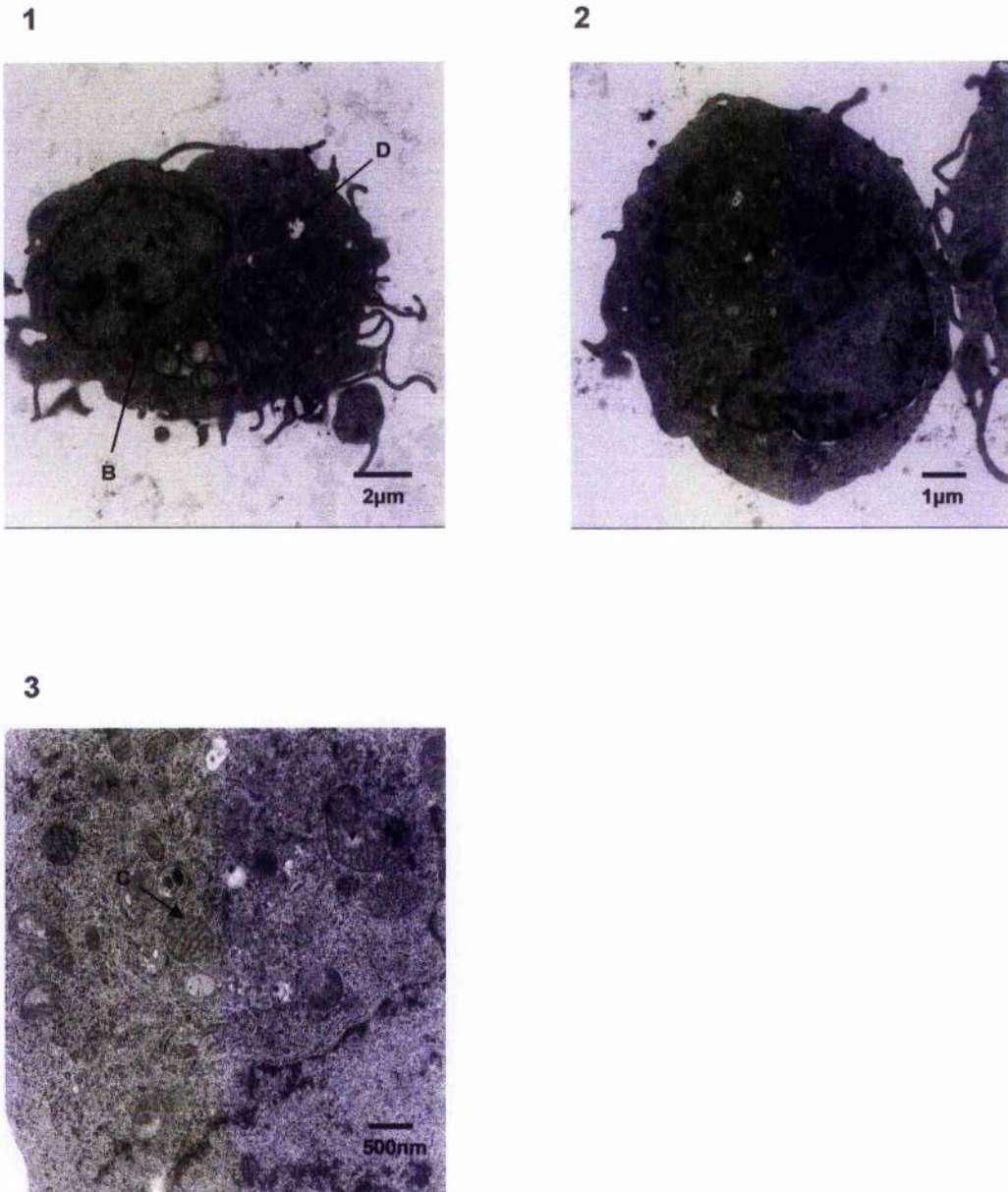
Figure 3.3 shows typical TEM images of HD11 cells. The nuclei of the cells were bifurcated and located to one side of the cell as with the bone marrow-derived macrophages and PBMC. Although the organelles of the cell were centrally located, they appeared to be much more densely packed into the cell compared to those in bone marrow-derived macrophages and PBMC. The overall shape of the cells was rounder than the bone marrow-derived macrophages and the PBMC.

Figure 3.4 shows typical confocal images of bone marrow-derived macrophages to demonstrate ultrastructure. The nuclei of the cells shown in Figure 3.4A were DAPI-stained (blue) and the actin of the cells was stained with phalloidin (red). The DAPI stain shows that the nuclei were located to one side of the cells, and the phalloidin stain shows that actin was present throughout the cells, with an increased staining intensity towards the edges of the cell. The nuclei of the cells in Figure 3.4B were DAPI-stained (blue), the  $\alpha$ -tubulin of the cells were stained with Tubulin (red) and the endoplasmic reticulum was stained with ERP60 (green). The nuclei of the cells were again visibly located to one side, the  $\alpha$ -tubulin appeared to be relatively centrally located within the cells and the endoplasmic reticulum was visible as a network throughout the cell. There were two main types of cells visible, the first encompassing smaller, rounder cells, and the second encompassing larger cells with more processes.

### **3.3.2 Cell surface markers and the physical capacity of the cell**

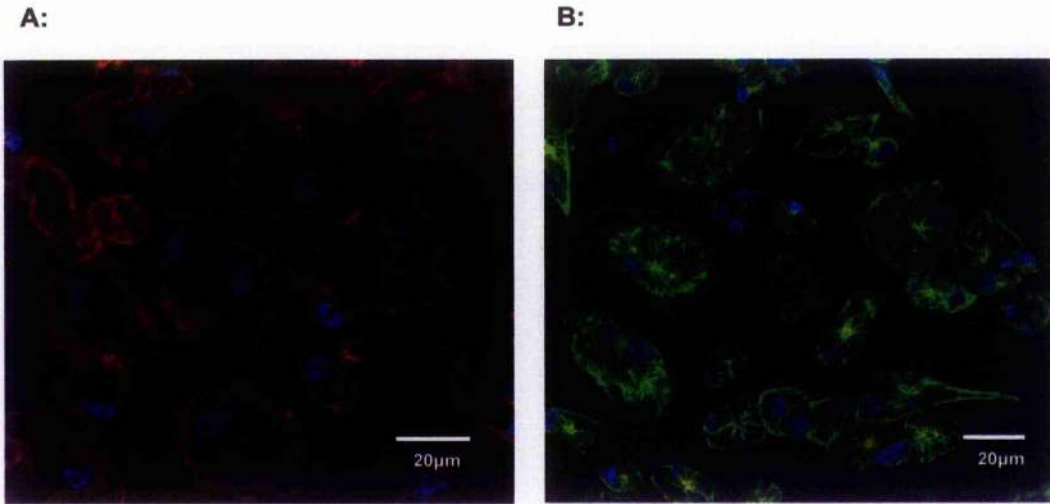
#### **3.3.2.1 Flow cytometry**

Figure 3.5 shows typical results taken from flow cytometry assays to investigate the surface expression of KUL01 and MHC class II on bone marrow-derived macrophages cultured in 1/100 rhGM-CSF till 7 days *ex vivo*. The controls for the assay are shown in Figure 3.5A, B, C and D. The negative control (un-stained cells)



**A: Nucleus**  
**B: Endoplasmic Reticulum**  
**C: Mitochondria**  
**D: Vacuole**

**Figure 3.3: Typical TEM images of HD11 cells.**



**Figure 3.4: Typical confocal images of bone marrow-derived macrophages to show ultrastructure.** The images show staining for actin (A), and staining for tubulin and endoplasmic reticulum (B). The nuclei of the cells are stained and shown in blue (DAPI - Sigma). Actin staining is shown in red (Phalloidin Ab conjugated to Alexafluor 568- Invitrogen) in image A. Tubulin staining is shown in red (Tubulin - Sigma) and endoplasmic reticulum staining is shown in green (ERP60 - IAH Pirbright) in image B.

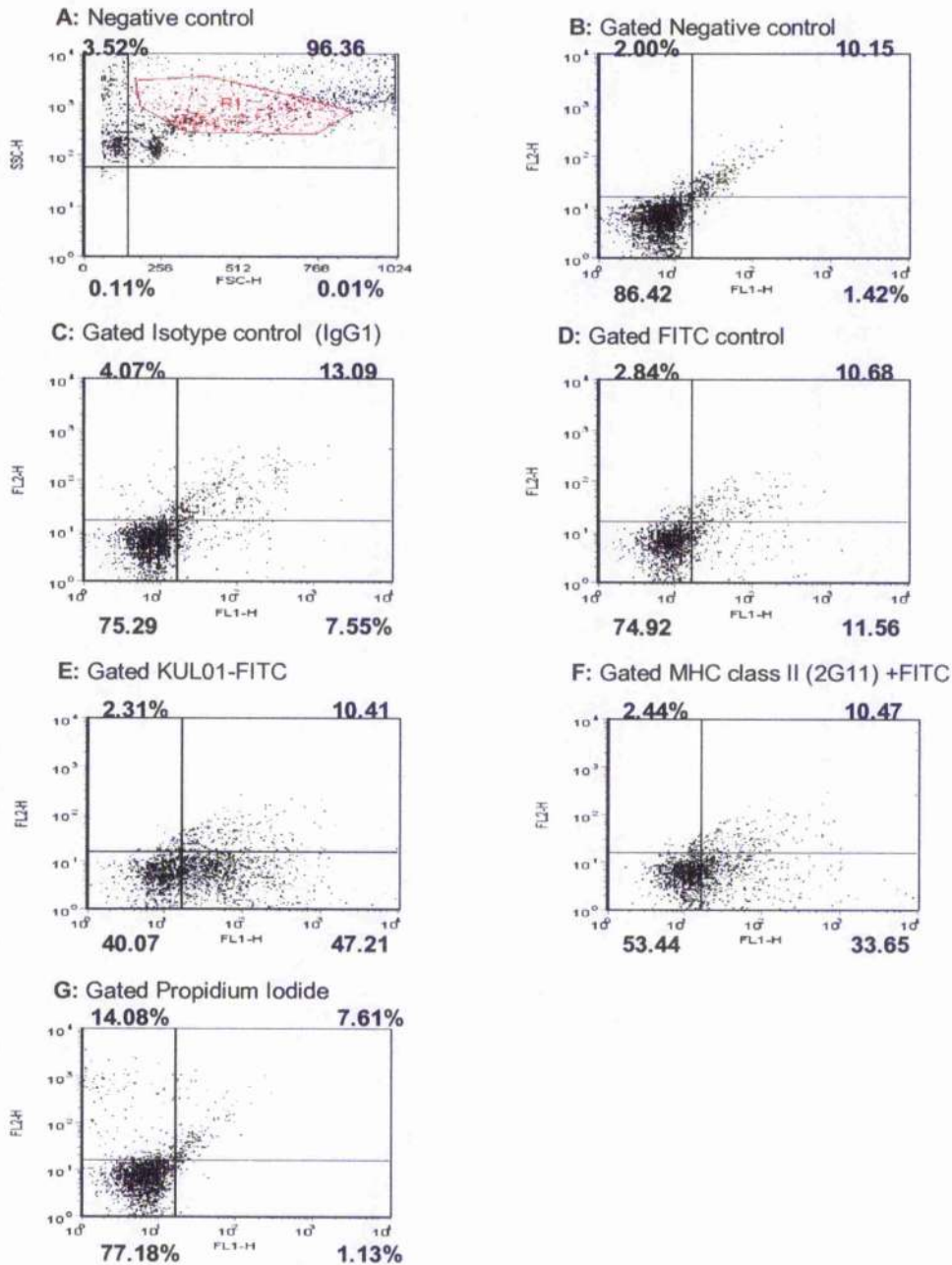


**Figure 3.5: Typical flow cytometry results from bone marrow-derived macrophage cells.**

To determine KUL01 surface expression, staining was with KUL01-FITC conjugate Ab (Southern Biotech), which was visible in the FL1 channel. To determine MHC class II surface expression, staining was with 2G11 Ab (Jim Kaufman, IAH) using a 2° FITC Ab (Molecular Probes), which was visible in the FL1 channel. Cell viability was determined by staining with Propidium Iodide (Sigma), which was visible in the FL2 channel. The isotype control used was the bovine antibody CC14 (Brenda Jones, IAH), which was visible in the FL1 channel.

	Mean %	S.D.
Gated	19.677	2.847
Gated KUL01	47.327	1.638
Gated MHC class II	33.713	0.271
Gated Propidium Iodide	15.053	1.466

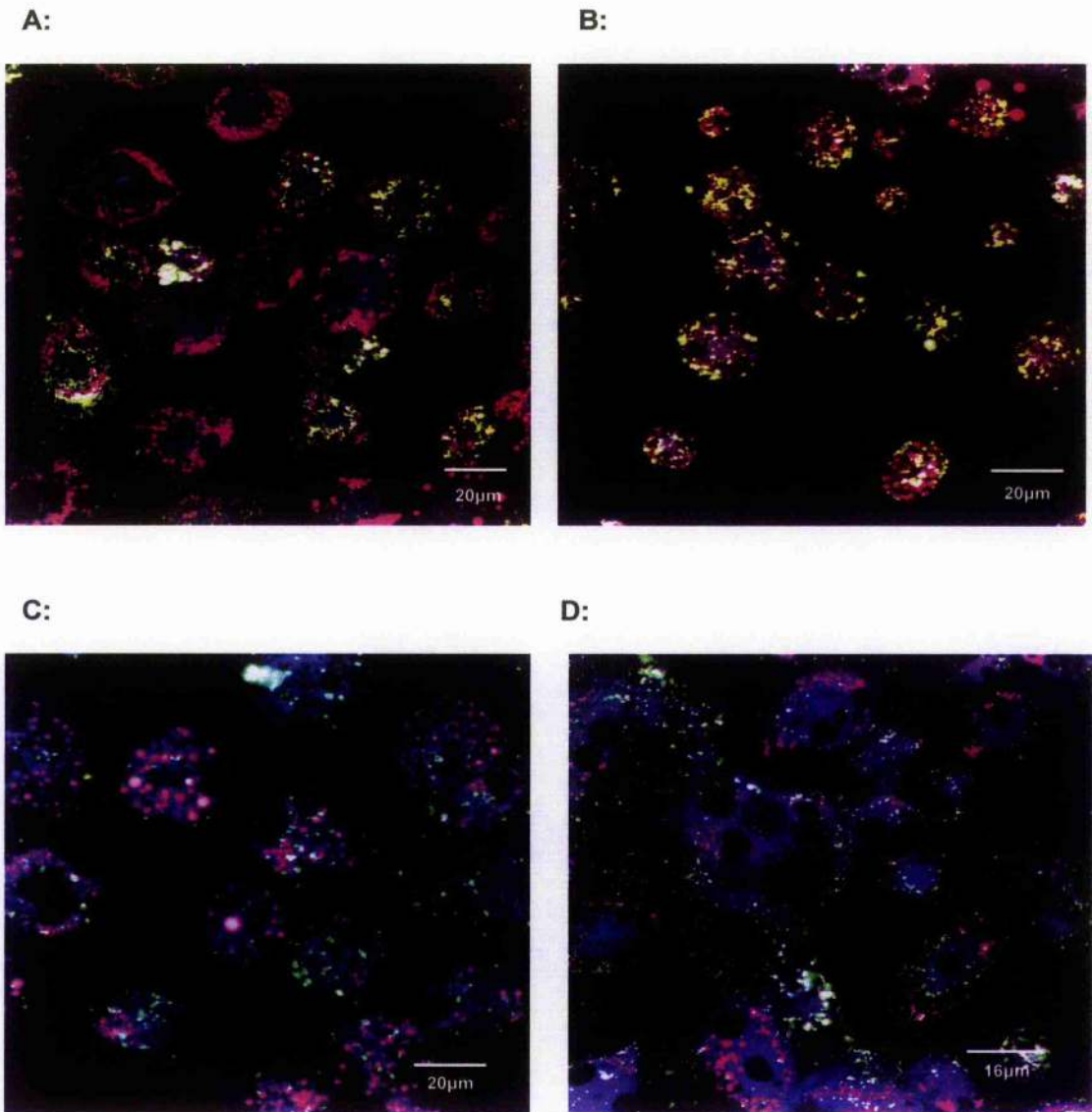
**Table 3.3.1: Flow cytometry results of bone marrow-derived macrophages stained with antibodies for KUL01 and MHC class II in the FL-1 channel and with propidium iodide in the FL2 channel.** To determine KUL01 surface expression, staining was with KUL01-FITC conjugate Ab (Southern Biotech), which was visible in the FL1 channel. To determine MHC class II surface expression, staining was with 2G11 Ab (Jim Kaufman, IAH) using a 2° FITC Ab (Molecular Probes), which was visible in the FL1 channel. Cell viability was determined by staining with Propidium Iodide (Sigma), which was visible in the FL2 channel.

scatter plots show the forward (FSC) and side scatter (SSC) profiles of the cells, reflecting both their cell surface area and their granularity/complexity (respectively). From this a population of cells thought to include the cells of interest (i.e. medium to high surface area and granularity) was selected for gating. The gated cell population is indicated by the red area in Figure 3.5A. A large area of cells was selected in order to encompass the mixed population of monocytes, macrophages and bone marrow progenitor cells likely to be included in the population. The cells selected in this gated area are shown in Figure 3.5B, which shows the un-stained cell profiles in the FL1 and FL2 channels. A small amount of autofluorescence is evident for the un-stained cells (10.15% in the assay shown). Figure 3.5C shows the gated population of the cells following staining with an IgG1 isotype control antibody (CC14), to show non-specific binding, as the antibodies used in the assay to check for KUL01 and MHC class II surface expression are IgG1. Figure 3.5D shows the gated population of the cells following staining with a FITC antibody as a control, visible in the FL1 channel. The KUL01 antibody used in the assay is a direct FITC conjugate and the MHC class II antibody uses a secondary FITC antibody, so the FITC control again shows non-specific binding (11.56% in the assay shown). Figure 3.5E shows the gated cell population following staining with the KUL01-FITC antibody. 47.21% of the cells are stained with KUL01-FITC and this is shown in the FL1 channel. Figure 3.5F shows the gated cell population following staining using the MHC class II antibody 2G11 and the secondary FITC antibody. 33.65% of the cells are positively stained with the 2G11 + FITC combination and this is visible in the FL1 channel. Viability of the cell population is shown by staining with propidium iodide in the FL2 channel. Dead and dying cells take up propidium iodide and so stain positive. The gated population shows only 1.13% of the cells to be dead or dying. Table 3.3.1 shows the mean percentages of differentially

stained cells from flow cytometry assays performed in triplicate. It shows that on average approximately 20% of the cell populations investigated were included in the gate specified. Approximately 47% of these were positive for KUL01 surface expression, approximately 34% for MHC class II expression and approximately 15% to be dead or dying.

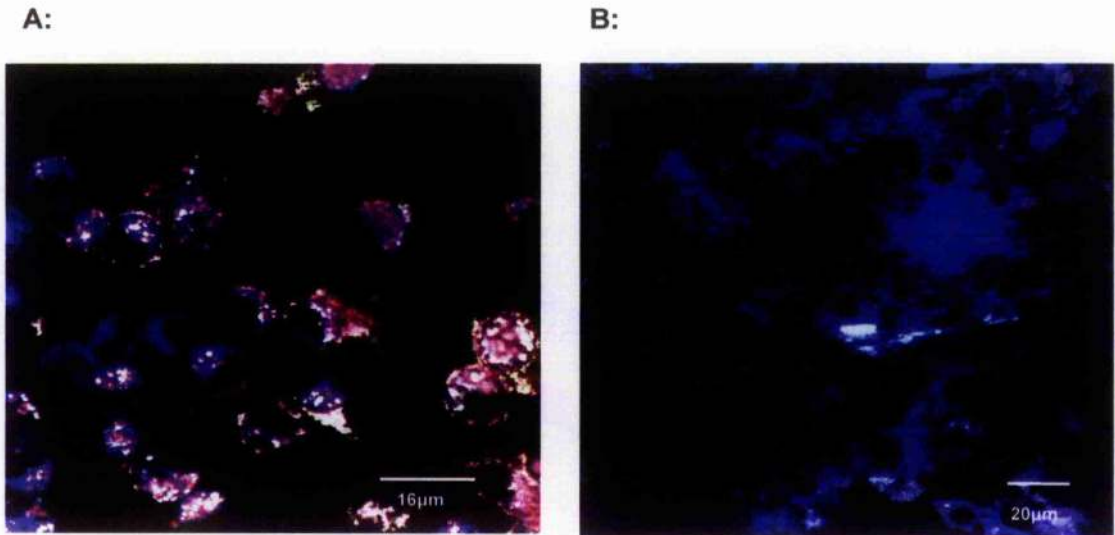
### 3.3.2.2 Confocal imaging

Figure 3.6 shows typical confocal images of bone marrow-derived macrophages following a phagocytosis assay using latex beads (shown in green on the image), immunofluorescence staining to show KUL01 surface expression using un-conjugated KUL01 antibody with a secondary TRITC antibody (shown in red on the image) and staining of the lipid bilayer of the cell using Nile Red (shown in blue on the image). Figure 3.6A shows bone marrow-derived macrophages cultured till day 5 *ex vivo* without rhGM-CSF. Figure 3.6B shows bone marrow-derived macrophages cultured till day 5 *ex vivo* in 1/100 rhGM-CSF. In both images, the cells have stained positive for KUL01 surface expression and readily phagocytosed latex beads. Figure 3.6C shows bone marrow-derived macrophages cultured till day 7 *ex vivo* without rhGM-CSF. Figure 3.6D shows bone marrow-derived macrophages cultured till day 7 *ex vivo* in 1/100 rhGM-CSF. Again, the cells shown in these images continued to stain positively for KUL01 surface expression and readily phagocytosed latex beads. The confocal images shown in Figure 3.7 comprise typical images of HD11 cells (Figure 3.7A) and CKC (Figure 3.7B) taken following a phagocytosis assay using latex beads (shown in green on the image), immunofluorescence staining to show KUL01 surface expression using un-conjugated KUL01 antibody with a secondary TRITC antibody (shown in red on the image) and staining of the lipid bilayer of the cell using Nile Red (shown in blue



**Figure 3.6: Typical confocal images of bone marrow-derived macrophages.** Assays were performed on cells grown till day 5 *ex vivo* without (A) and with rhGM-CSF (B) *ex vivo*, and on cells grown till day 7 *ex vivo* without (C) and with rhGM-CSF (D) *ex vivo*. KUL01 staining is shown in red (un-conjugated KUL01- Southern Biotech; 2° Ab TRITC-Molecular Probes), the lipid bilayer of the cell is shown in blue (Nile Red- Molecular Probes) and phagocytosed latex beads are shown in green (Fluoresbrite 0.5  $\mu\text{m}$  YG Carboxylate microspheres- Polysciences Inc.)





**Figure 3.7: Typical confocal images of HD11 cells (A) and CKC (B).** KUL01 staining is shown in red (un-conjugated KUL01- Southern Biotech; 2° Ab TRITC-Molecular Probes), the lipid bilayer of the cell is shown in blue (Nile Red- Molecular Probes) and phagocytosed latex beads are shown in green (Fluoresbrite 0.5  $\mu\text{m}$  YG Carboxylate microspheres- Polysciences Inc.)

on the image). Figure 3.7A shows that the HD11 cells stained positively for KUL01 surface expression and readily phagocytosed latex beads. The CKC shown in Figure 3.7B, though, did not stain positively for KUL01 surface expression and did not phagocytose latex beads.

### 3.3.3 Secretory products

#### 3.3.3.1 Cytokines and chemokines

Figure 3.8 shows pro-inflammatory cytokine mRNA expression, as determined by real-time qRT-PCR, by bone marrow-derived macrophages at 5 days *ex vivo* culture following stimulation for 24 h with either *E. coli* LPS, with rchIFN- $\gamma$ , with *E. coli* LPS + rchIFN- $\gamma$  or following no stimulation as described in Chapter 2. The mRNA expression profiles were compared with those of PBMC and HD11 cells treated in the same way. Figure 3.8A shows IL-1 $\beta$  mRNA expression for the differentially stimulated cells. The pattern of mRNA expression for the bone marrow-derived macrophages was similar to that for the PBMC and HD11 cells, but following stimulation up-regulation is not as marked. Cells cultured without rchGM-CSF *ex vivo* had significantly up-regulated IL-1 $\beta$  mRNA levels following priming with rchIFN- $\gamma$  (P=0.003), stimulation with LPS (P=0.0013) and stimulation with rchIFN- $\gamma$  + LPS (P=0.001) compared to levels in un-stimulated cells. Cells cultured in 1/100 rchGM-CSF *ex vivo* had significantly up-regulated IL-1 $\beta$  mRNA expression following stimulation with LPS (P=0.015) and stimulation with IFN- $\gamma$  + LPS (P=0.006). There was a significant difference, following rchIFN- $\gamma$  priming, between the IL-1 $\beta$  mRNA expression levels of cells cultured with and without rchGM-CSF *ex vivo* (P=0.003), with cells cultured without rchGM-CSF having significantly up-regulated IL-1 $\beta$  mRNA. Figure 3.8B shows IL-6 mRNA expression for the differentially stimulated cells. The pattern of

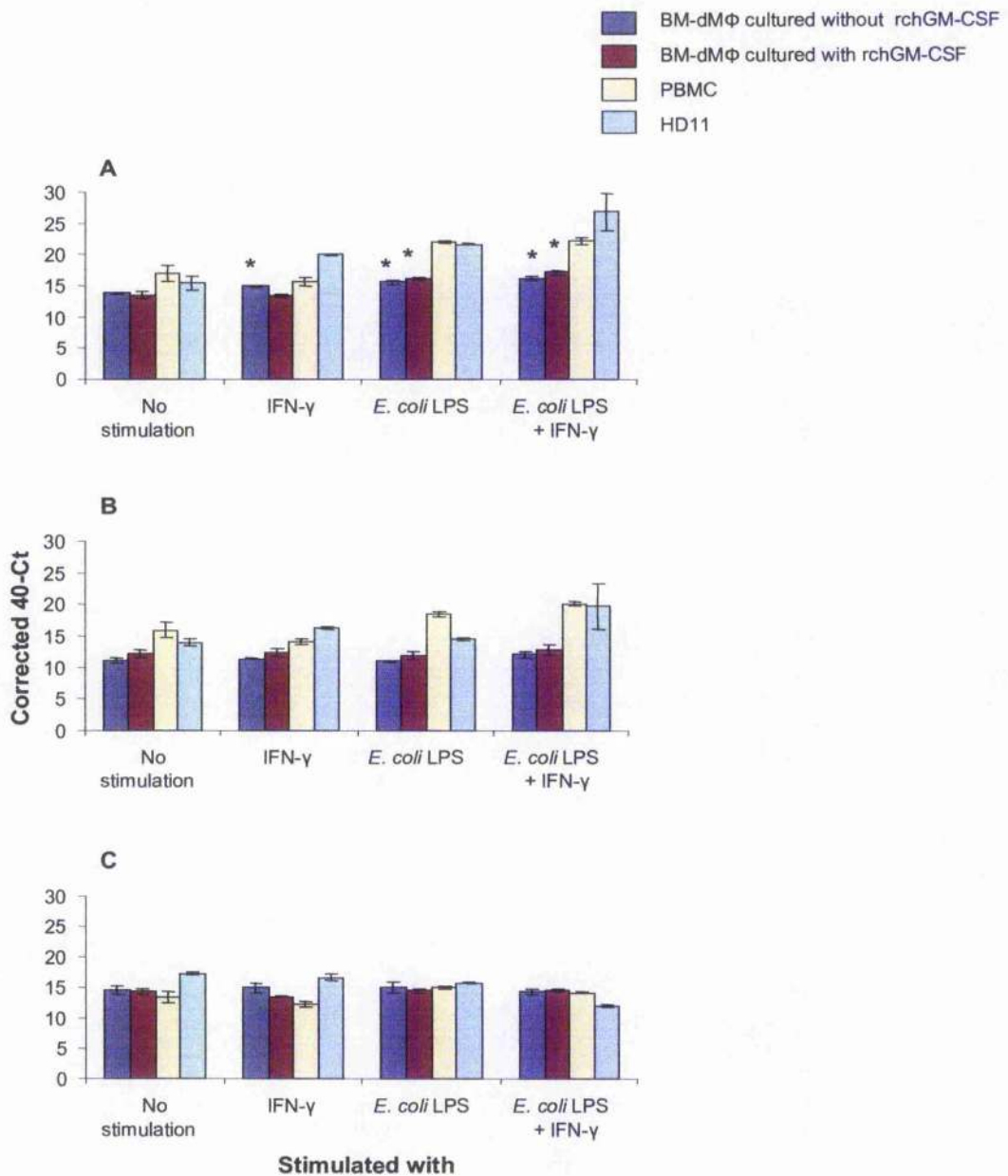


**Figure 3.8: IL-1 $\beta$  (A), IL-6 (B) and IL-18 (C) mRNA expression levels in bone marrow-derived macrophages 5 days *ex vivo* following stimulation with either rchIFN- $\gamma$ , *E. coli* LPS, *E. coli* LPS + rchIFN- $\gamma$  or no stimulation, compared with the mRNA expression profiles for PBMC and HD11 cells. mRNA levels are expressed as corrected 40-Ct values as obtained by real-time qRT-PCR. (n=3; SE $\pm$ 0.05). Statistical significance compared to unstimulated cells represented by \*.**

mRNA expression for the bone marrow-derived macrophages followed that measured for the PBMC and HD11 cells, but following stimulation up-regulation was not as marked. There were no significant differences measured between the un-stimulated cells and the stimulated bone marrow-derived macrophages. Figure 3.8C shows IL-18 mRNA expression for the differentially stimulated cells. The IL-18 mRNA expression profile for the bone marrow-derived macrophages followed that measured for the PBMC and HD11 cells, but up-regulation following stimulation was not as marked. Again, there were no significant differences measured in IL-18 mRNA expression levels between the un-stimulated and stimulated bone marrow-derived macrophages.

Figure 3.9 shows CXCLi1 and CXCLi2 chemokine mRNA expression levels as determined by real-time qRT-PCR in bone marrow-derived macrophages at 5 days *ex vivo* culture following stimulation with either *E. coli* LPS, with rhIFN- $\gamma$ , with *E. coli* LPS + rhIFN- $\gamma$  or following no stimulation. CXCLi1 and CXCLi2 mRNA expression levels were investigated as these two chemokines both have a similar homology and action to mammalian IL-8. The mRNA expression profiles were compared with those for PBMC and HD11 cells treated in the same way. Figure 3.9A shows CXCLi1 mRNA expression for the differentially stimulated cells. The pattern of mRNA expression for the bone marrow-derived macrophages was comparable to that measured for the PBMC, and was similar to that measured for the HD11 cells, but up-regulation was not as marked following stimulation. Bone marrow-derived macrophages cultured *ex vivo* without rhGM-CSF had significantly up-regulated CXCLi1 mRNA expression following stimulation with LPS compared to un-stimulated cells. Figure 3.9B shows CXCLi2 mRNA expression for the differentially stimulated cells. The pattern of CXCLi2 mRNA expression for the bone marrow-derived macrophages was similar to that measured for the PBMC and HD11 cells, but up-regulation following stimulation

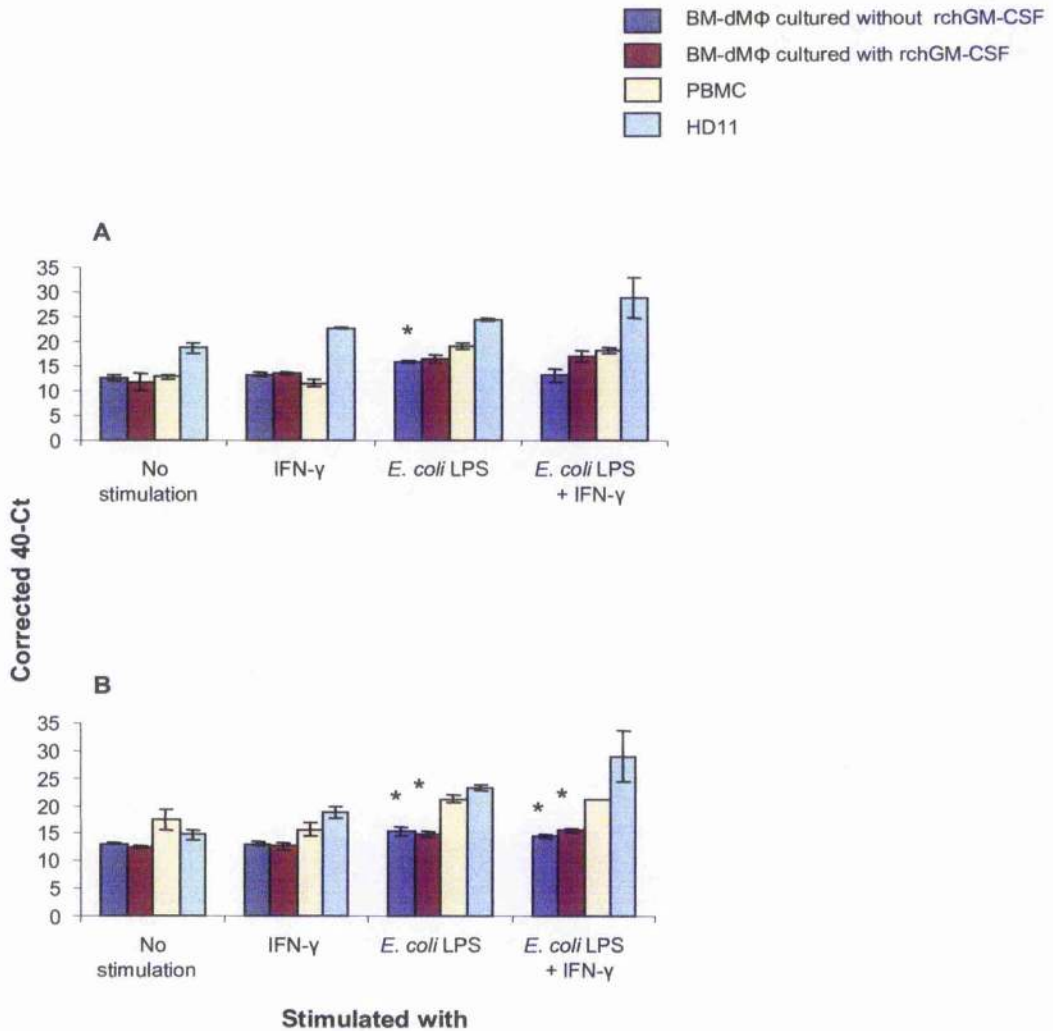


**Figure 3.9: CXCLi1 (A) and CXCLi2 (B) mRNA expression levels in bone marrow-derived macrophages 5 days *ex vivo* following stimulation with either rchIFN- $\gamma$ , *E. coli* LPS, *E. coli* LPS + rchIFN- $\gamma$  or no stimulation, compared with the mRNA expression profiles for PBMC and HD11 cells. mRNA levels are expressed as corrected 40-Ct values as obtained by real-time qRT-PCR. (n=3; SE $\pm$ 0.05). Statistical significance compared to unstimulated cells represented by \*.**

was to a lesser extent. Bone marrow-derived macrophages cultured without rhGM-CSF *ex vivo* had significantly up-regulated CXCLi2 mRNA expression compared to the control following stimulation with both LPS (P=0.036) and with rhIFN- $\gamma$  + LPS (P=0.039). Bone marrow-derived macrophages cultured in 1/100 rhGM-CSF *ex vivo* had significantly up-regulated CXCLi2 mRNA expression following stimulation with both LPS (P=0.013) and with rhIFN- $\gamma$  + LPS (P=0.004).

Figure 3.10 shows the cytokine mRNA expression as determined by real-time qRT-PCR for bone marrow-derived macrophages at 7 days *ex vivo* culture following stimulation with either *E. coli* LPS, with rhIFN- $\gamma$ , with *E. coli* LPS + rhIFN- $\gamma$  or following no stimulation. The mRNA expression profiles were compared with those for PBMC and HD11 cells treated in the same way. Figure 3.10A shows the IL-1 $\beta$  mRNA expression profile for the differentially stimulated cells. The pattern of IL-1 $\beta$  mRNA expression followed that measured for both PBMC and HD11 cells, but up-regulation following stimulation was to a lesser extent. Bone marrow-derived macrophages cultured *ex vivo* with and without rhGM-CSF had significantly up-regulated IL-1 $\beta$  mRNA expression following stimulation with rhIFN- $\gamma$  + LPS compared to the un-stimulated cells (P=0.008 and P=0.026 respectively). Figure 3.10B shows the IL-6 mRNA expression for the differentially infected cells. The mRNA expression profiles for the bone marrow-derived macrophages were comparable to that measured for both the PBMC and HD11 cells. Bone marrow-derived macrophages cultured with rhGM-CSF *ex vivo* had significantly up-regulated mRNA expression following rhIFN- $\gamma$  + LPS stimulation compared to the un-stimulated cells (P=0.022). Figure 3.10C shows the IL-18 mRNA expression profile for the differentially infected cells, and shows the pattern for PBMC and HD11 cell mRNA expression was comparable to the bone marrow-derived macrophages following stimulation. There was no significant

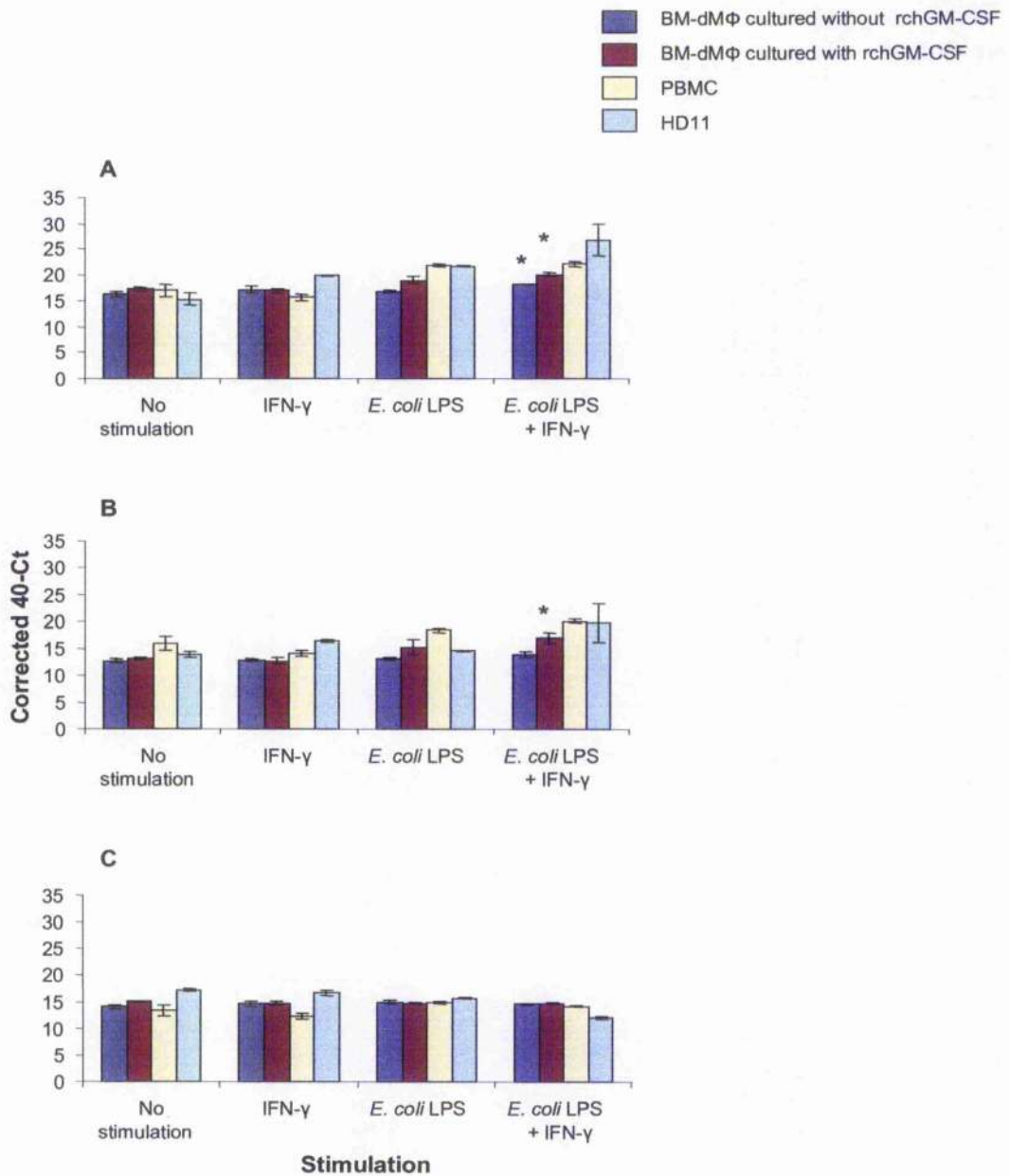


**Figure 3.10: IL-1 $\beta$  (A), IL-6 (B) and IL-18 (C) mRNA expression levels in bone marrow-derived macrophages 7 days *ex vivo* following stimulation with either rchIFN- $\gamma$ , *E. coli* LPS, *E. coli* LPS + rchIFN- $\gamma$  or no stimulation, compared with the mRNA expression profiles for PBMC and HD11 cells. mRNA levels are expressed as corrected 40-Ct values as obtained by real-time qRT-PCR. (n=3; SE $\pm$ 0.05). Statistical significance compared to unstimulated cells represented by \*.**

up-regulation of IL-18 mRNA expression following stimulation, but bone marrow-derived macrophages cultured *ex vivo* in rhGM-CSF had significantly higher levels of IL-18 mRNA expression compared to those cells cultured without rhGM-CSF *ex vivo* ( $P=0.033$ ).

Figure 3.11 shows the chemokine mRNA expression as determined by real-time qRT-PCR for bone marrow-derived macrophages at 7 days *ex vivo* culture following stimulation with either *E. coli* LPS, with rhIFN- $\gamma$ , with *E. coli* LPS + rhIFN- $\gamma$  or following no stimulation. The mRNA expression profiles were compared with those for PBMC and HD11 cells treated in the same way. Figure 3.11A shows the CXCLi1 mRNA expression profile which following stimulation formed a comparable pattern to that measured for PBMC and was similar to that measured for HD11 cells. Following rhIFN- $\gamma$  stimulation, cells cultured *ex vivo* without rhGM-CSF had significantly up-regulated CXCLi1 mRNA expression compared to un-stimulated cells ( $P=0.001$ ). Stimulating with rhIFN- $\gamma$  + LPS resulted in a significant up-regulation of CXCLi1 mRNA expression in cells cultured with and without rhGM-CSF *ex vivo* when compared to the un-stimulated cells ( $P=0.047$  and  $P=0.007$  respectively). Bone marrow-derived macrophage cells cultured with rhGM-CSF *ex vivo* had significantly up-regulated CXCLi1 mRNA expression levels when compared to cells cultured without rhGM-CSF *ex vivo* following stimulation with rhIFN- $\gamma$  ( $P=0.034$ ), with rhIFN- $\gamma$  + LPS ( $P=0.017$ ) and following no stimulation ( $P=0.001$ ). Figure 3.11B shows the CXCLi2 mRNA expression profile which following stimulation formed a similar pattern to that measured for both PBMC and HD11 cells. There was a significant up-regulation of CXCLi2 mRNA expression in bone marrow-derived macrophage cells cultured in rhGM-CSF *ex vivo* following stimulation with LPS ( $P=0.018$ ) and with



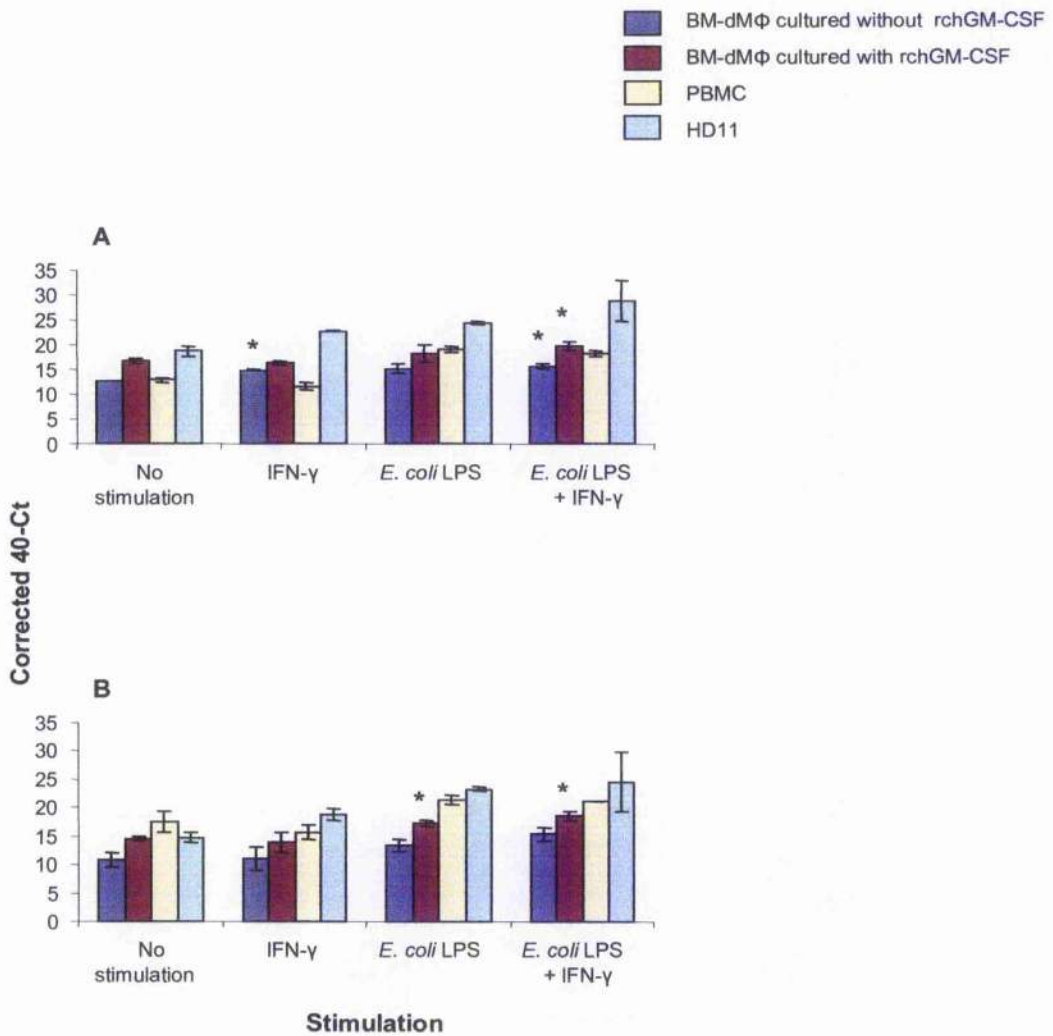


**Figure 3.11: CXCLi1 (A) and CXCLi2 (B) mRNA expression levels in bone marrow-derived macrophages 7 days *ex vivo* following stimulation with either rchIFN- $\gamma$ , *E. coli* LPS, *E. coli* LPS + rchIFN- $\gamma$  or no stimulation, compared with the mRNA expression profiles for PBMC and HD11 cells. mRNA levels are expressed as corrected 40-Ct values as obtained by real-time qRT-PCR. (n=3; SE $\pm$ 0.05). Statistical significance compared to unstimulated cells represented by \*.**

rchIFN- $\gamma$  + LPS ( $P=0.013$ ) compared to un-stimulated cells. The CXCLi2 mRNA expression measured in cells cultured with rchGM-CSF *ex vivo* was significantly greater than that measured in cells cultured without rchGM-CSF during both LPS stimulation of the culture ( $P=0.040$ ) and no stimulation ( $P=0.050$ ).

### 3.3.3.2 Metabolites

Figure 3.12 shows results from Griess assays performed on cell supernatants to determine nitric oxide production by bone marrow-derived macrophages cultured in different concentrations of rchGM-CSF ranging from 0 to 1/100. Cells were either stimulated with *E. coli* LPS, primed with rchIFN- $\gamma$  or primed with rchIFN- $\gamma$  and stimulated with *E. coli* LPS. Nitric oxide production during these conditions was compared to that from cells which had been left un-stimulated. The results shown are the average of three biological replicates. These values are shown in Table 3.3.2 and the P values for the significant differences of the differentially stimulated cells are shown in Table 3.3.3. Figure 3.12A shows cells grown till day 5 *ex vivo*, which were originally seeded at  $2.5 \times 10^6$  cells/ml. Cells which were un-stimulated produce a relatively similar level of nitrite for the different *ex vivo* rchGM-CSF culture concentrations. Stimulation with LPS significantly increased nitric oxide production, compared to the control, of cell populations which were cultured *ex vivo* in higher rchGM-CSF concentrations, but did not have any effect on nitric oxide production at lower concentrations. Priming with rchIFN- $\gamma$  significantly increased nitric oxide production above that measured for the control. Priming with rchIFN- $\gamma$  followed by stimulation with LPS significantly increased nitric oxide production above the control in a relatively stable manner. Priming with rchIFN- $\gamma$  followed by stimulation with LPS significantly increased the nitric oxide production of cells compared to stimulation with LPS or priming with

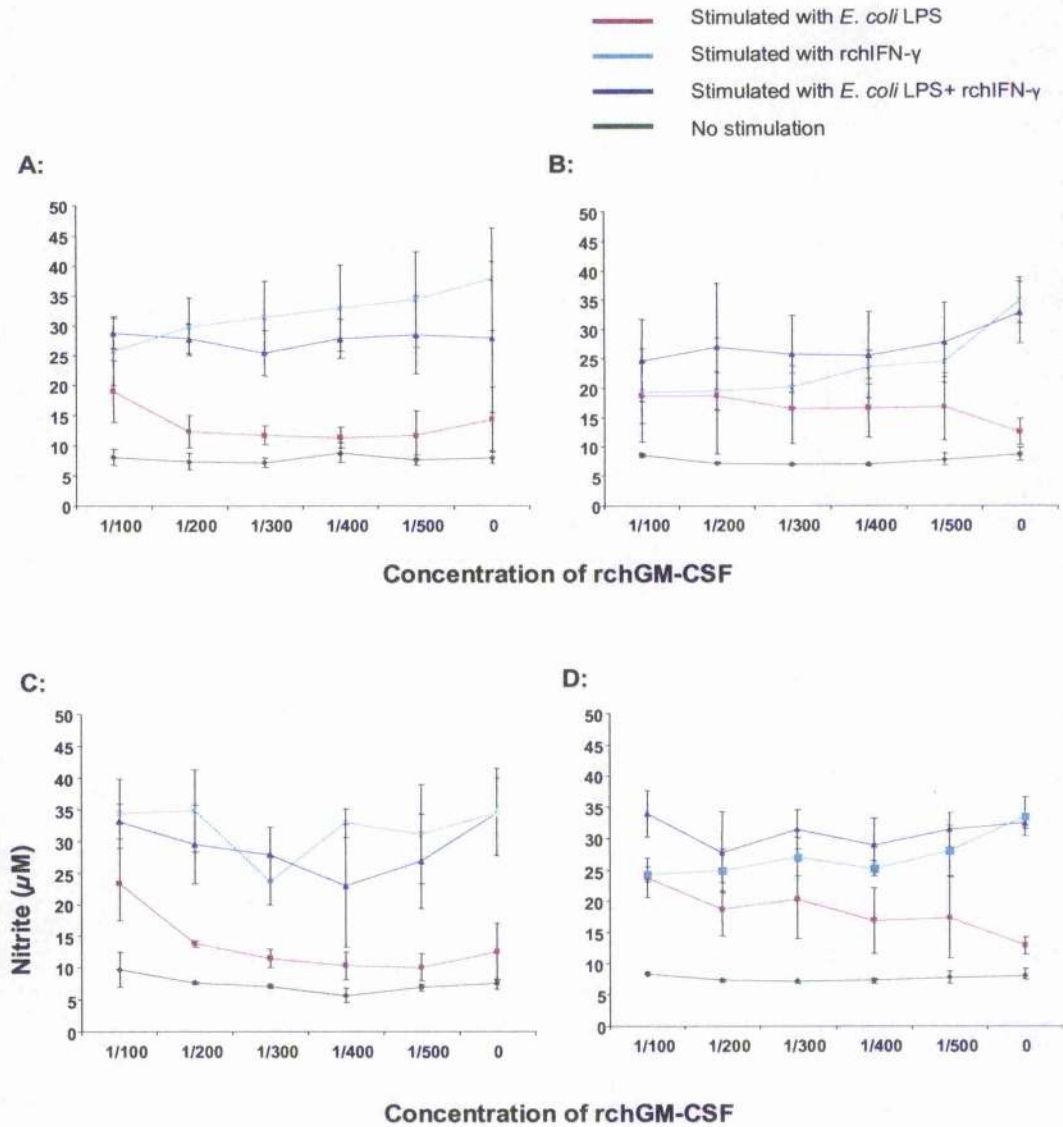


**Figure 3.12: Griess assay to determine Nitric Oxide production by bone marrow-derived macrophages during stimulation with either *E. coli* LPS, rchIFN- $\gamma$  or *E. coli* LPS+rchIFN- $\gamma$ .** Assays were performed on cells seeded at  $2.5 \times 10^6$  cells/ml then grown till day 5 (A) and day 7 (B) *ex vivo* and on cells seeded at  $5 \times 10^6$  cells/ml then grown till day 5 (C) and day 7 (D) *ex vivo*. Nitric Oxide production is determined by the amount of Nitrite present, measured by Griess assay performed on  $50 \mu\text{l}$  supernatants from stimulated and un-stimulated cells ( $n=3$ ;  $\text{SD} \pm 0.05$ ).

**A**

Concentration of rch GMCSF	Stimulation			
	No stimulation	LPS	LPS+IFN	IFN
1/100	8.10	19.13	28.73	25.76
1/200	7.37	12.34	27.85	29.81
1/300	7.18	11.68	25.42	31.43
1/400	8.83	11.37	27.80	32.98
1/500	7.63	11.74	28.42	34.34
0	8.00	14.39	28.02	37.74

**B**

Concentration of rch GMCSF	Stimulation			
	No stimulation	LPS	LPS+IFN	IFN
1/100	8.63	18.77	24.65	19.34
1/200	7.30	18.73	27.04	19.48
1/300	7.07	16.56	25.81	20.19
1/400	7.01	16.63	25.67	23.53
1/500	7.92	16.86	27.76	24.58
0	8.73	12.55	32.89	34.97

**C**

Concentration of rch GMCSF	Stimulation			
	No stimulation	LPS	LPS+IFN	IFN
1/100	9.72	23.23	33.10	34.40
1/200	7.63	13.80	29.50	34.82
1/300	7.03	11.46	27.92	23.78
1/400	5.63	10.39	22.98	32.88
1/500	6.86	10.09	26.84	31.16
0	7.48	12.52	34.43	34.55

**D**

Concentration of rch GMCSF	Stimulation			
	No stimulation	LPS	LPS+IFN	IFN
1/100	8.32	23.70	34.00	24.38
1/200	7.23	18.74	27.80	25.00
1/300	7.06	20.32	31.41	27.06
1/400	7.25	16.87	28.92	25.23
1/500	7.68	17.34	31.41	28.08
0	8.03	12.85	32.54	33.57

**Table 3.3.2: Nitrite concentrations ( $\mu\text{M}$ ) by bone marrow-derived macrophages determined by Griess assay following stimulation with either *E. coli* LPS, rchIFN- $\gamma$  or *E. coli* LPS+rchIFN- $\gamma$ . Assays were performed on cells seeded at  $2.5 \times 10^6$  cells/ml then grown till day 5 (A) and day 7 (B) *ex vivo* and on cells seeded at  $5 \times 10^6$  cells/ml then grown till day 5 (C) and day 7 (D) *ex vivo*. Data is that shown in Figure 3.12.**

A			
Compared to no stimulation			
Concentration of rchGMCSF	LPS Stimulation	IFN	LPS+IFN
1/400	0.023	0.007	0
1/200	0.049	0.002	0
1/300	0.012	0.002	0.001
1/400		0.005	0.081
1/800		0.004	0.006
0		0.004	0.051

B			
Compared to no stimulation			
Concentration of rchGMCSF	LPS Stimulation	IFN	LPS+IFN
1/400		0.026	0.017
1/200		0.003	0.035
1/300		0.051	0.008
1/400		0.029	0.012
1/800		0.054	0.006
0		0.055	0.001

C			
Compared to no stimulation			
Concentration of rchGMCSF	LPS Stimulation	IFN	LPS+IFN
1/400		0.021	0
1/200		0	0.004
1/300		0.007	0.001
1/400		0.029	0.038
1/800		0.006	0.009
0		0.002	0.001

D			
Compared to no stimulation			
Concentration of rchGMCSF	LPS Stimulation	IFN	LPS+IFN
1/400		0.001	0
1/200		0.01	0.005
1/300		0.023	0
1/400		0.033	0.001
1/800		0.001	0
0		0.005	0

A			
Compared to LPS+IFN			
LPS	IFN	LPS+IFN	
	0.045		
	0.002		0.006
	0.005		0.005
	0.002		0.097
	0.02		0.012
			0.016

B			
Compared to LPS			
LPS	IFN	LPS+IFN	
		0.045	
		0.002	
		0.005	
		0.002	
		0.002	
	0.001		0.003

C			
Compared to LPS			
LPS	IFN	LPS+IFN	
		0.052	
	0.005		0.012
	0.005		0.003
	0		
	0.011		0.019
	0.01		0.006

D			
Compared to LPS			
LPS	IFN	LPS+IFN	
		0.021	
			0.055
			0.037
	0.054		0.028
			0

D			
Compared to LPS+IFN			
LPS	IFN	LPS+IFN	
			0.013

**Table 3.3.3: P values for significantly different data from the experiment shown in Figure 3.12 and Table 3.3.2, comparing the nitrite concentrations of bone marrow-derived macrophages following stimulation with either *E. coli* LPS, rchIFN- $\gamma$  or *E. coli* LPS+rchIFN- $\gamma$ . Assays were performed on cells seeded at  $2.5 \times 10^6$  cells/ml then grown till day 5 (A) and day 7 (B) *ex vivo* and on cells seeded at  $5 \times 10^6$  cells/ml then grown till day 5 (C) and day 7 (D) *ex vivo*.**

rchIFN- $\gamma$  alone. Figure 3.12B shows cells grown till day 7 *ex vivo*, which were originally seeded at  $2.5 \times 10^6$  cells/ml. Stimulation with LPS significantly increased nitric oxide production, compared to the control, of cell populations following *ex vivo* culture in lower concentrations of rchGM-CSF but did not have any effect on nitric oxide production at 1/100 and 1/200 culture concentrations. Priming with rchIFN- $\gamma$  significantly increased nitric oxide production above that measured for the control. Priming with rchIFN- $\gamma$  followed by stimulation with LPS significantly increased nitric oxide production above the control in a relatively stable manner across the differing rchGM-CSF culture concentrations. Priming with rchIFN- $\gamma$  followed by stimulation with LPS significantly increased the nitric oxide production of cells compared to stimulation with LPS alone. Figure 3.12C shows cells grown till day 5 *ex vivo*, which were originally seeded at  $5 \times 10^6$  cells/ml. Cells which were un-stimulated produced a relatively similar level of nitrite during the different *ex vivo* rchGM-CSF culture concentrations. Stimulation with LPS significantly increased nitric oxide production, compared to the control at higher rchGM-CSF concentrations but did not have any effect on nitric oxide production at lower concentrations. Priming with rchIFN- $\gamma$  alone, and priming with rchIFN- $\gamma$  followed by stimulation with LPS, significantly increased nitric oxide production above that measured for the control across the range of rchGM-CSF culture concentrations. In addition, priming with rchIFN- $\gamma$  followed by stimulation with LPS significantly increased the nitric oxide production of cells compared to stimulating with LPS alone. Figure 3.12D shows cells originally seeded at  $5 \times 10^6$  cells/ml and grown till day 7 *ex vivo*. Cells which were un-stimulated produced a relatively similar level of nitrite for the different *ex vivo* rchGM-CSF culture concentrations. Stimulation with LPS significantly increased nitric oxide production, compared to the control, with a general trend of decrease in levels of nitrite coupled

with the decrease in rhGM-CSF culture concentrations, and priming with rhIFN- $\gamma$  significantly increased nitric oxide production above that measured for the control. Nitric oxide levels during priming with rhIFN- $\gamma$  were increased across the rhGM-CSF concentration spectrum, from levels similar to that measured during LPS stimulation at 1/100, to levels comparable to that measured during priming with rhIFN- $\gamma$  and stimulation with LPS, when no rhGM-CSF was added to the culture. Priming with rhIFN- $\gamma$  followed by stimulation with LPS significantly increased the nitric oxide production of cells compared to the control in a relatively stable manner following *ex vivo* culture. Priming with rhIFN- $\gamma$  followed by stimulating with LPS significantly increased the nitric oxide production of cells compared to stimulating with LPS alone or after priming with rhIFN- $\gamma$  alone following *ex vivo* culture in concentrations of 1/100 rhGM-CSF.

Figure 3.13 shows superoxide anion activity measured in the supernatants of bone marrow-derived macrophages following priming with rhIFN- $\gamma$ . The results shown are the average of three biological replicates. There are large error bars on the results for the differentially cultured cells and no clear patterns following priming with IFN- $\gamma$  are apparent. The results show that priming with IFN- $\gamma$  does not alter superoxide anion activity in the cells.

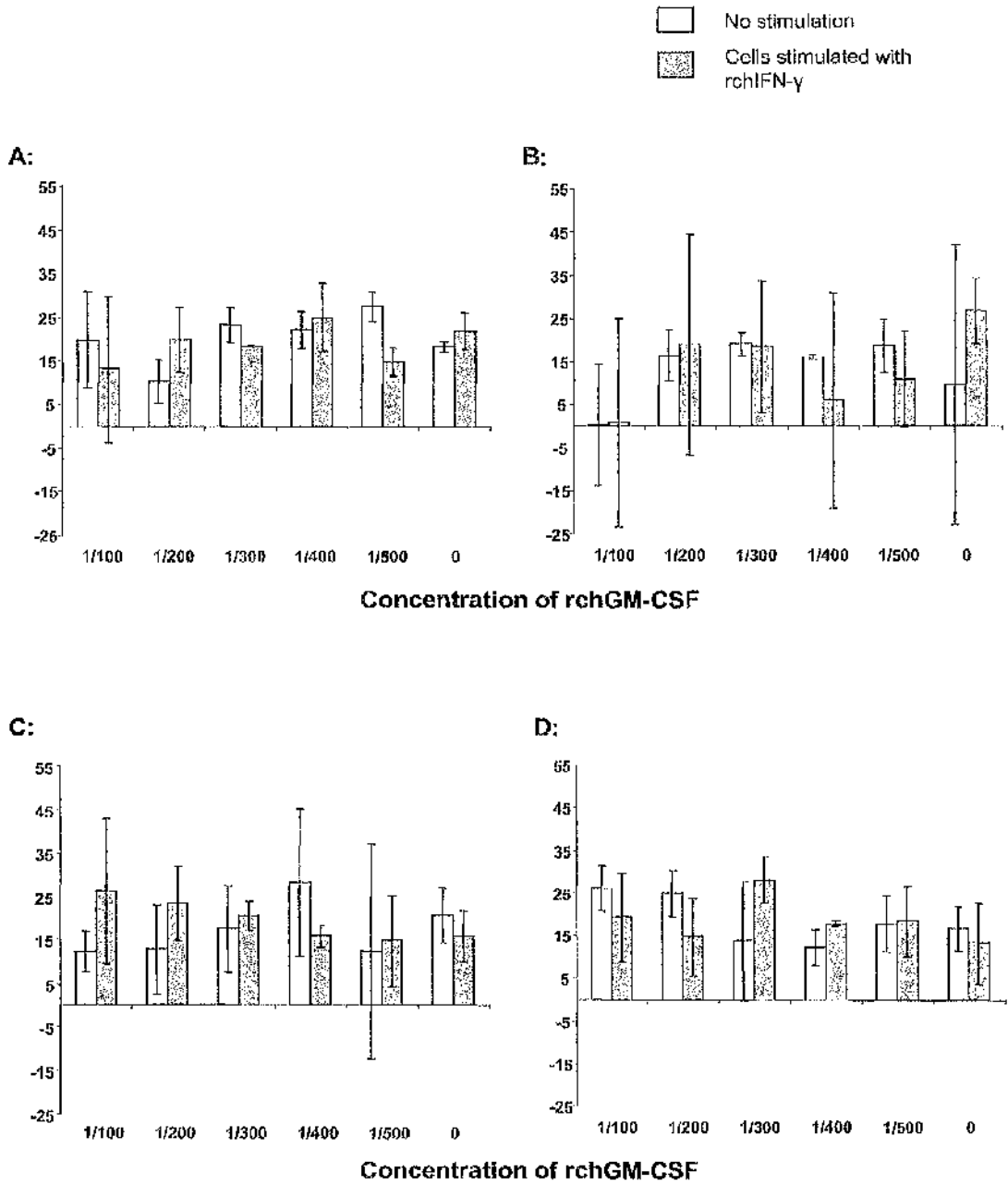


**Figure 3.13: Superoxide anion production by bone marrow-derived macrophages during stimulation with rhIFN- $\gamma$ .** Assays were performed on cells seeded at  $2.5 \times 10^6$  cells/ml then grown till day 5 (A) and day 7 (B) *ex vivo* and on cells seeded at  $5 \times 10^6$  cells/ml then grown till day 5 (C) and day 7 (D) *ex vivo*. Superoxide anion activity is determined by the nmol O<sub>2</sub><sup>-</sup> released, measured in 50  $\mu$ l supernatants from cells stimulated with 1/1000 rhIFN- $\gamma$  (n=3; SD $\pm$ 0.05).



### 3.4 Discussion

The highly reactive metabolite nitric oxide has long been known to be produced by activated macrophages to target bacteria. The production of nitric oxide by bone marrow-derived cells following priming and/or stimulation gives an indication of the types of cells and their stage of development within the population. Nitric oxide production in cells grown in various concentrations of rhGM-CSF *ex vivo* for two different time periods and at two different initial seeding rates was assessed to determine the optimal culture conditions for bone marrow-derived macrophages. Growth till day 7 *ex vivo* at an initial seeding rate of  $5 \times 10^6$  cells/ml and a culture concentration of 1/100 rhGM-CSF gave a population of cells, which after priming with rhIFN- $\gamma$  produced a level of nitric oxide equal to that produced following stimulation with *E. coli* LPS. The level of nitric oxide produced after LPS stimulation during these culture conditions was the highest for the whole experiment. There was also a large significant increase in nitric oxide production following priming and stimulation of the same cells with both rhIFN- $\gamma$  and LPS. Macrophages go through two stages of activation. The first stage changes the naïve cell from a "responsive" to a "primed" state, and inducing this *in vitro* requires addition of IFN- $\gamma$ . The second stage terminally activates the primed cells, and *in vitro* this requires LPS. Prolonged exposure to LPS actually abolishes this requirement for priming (Johnston *et al.*, 1987). This is not the case in the experiment described though, as the results show that the length of LPS stimulation time was not sufficient to prime naïve cells, as shown by the significant increases observed between the nitric oxide levels produced following stimulation with LPS + rhIFN- $\gamma$  compared to those measured following stimulation with LPS alone. Comparing the levels of nitric oxide production after priming with rhIFN- $\gamma$  and stimulating with LPS separately therefore gives an indication of the proportion of the

macrophage cell population that is naïve and the proportion that is already primed. Since these are primary cells, the population will always be mixed in terms of the state of differentiation and activation. The best conditions for culture, therefore, are those which result in a relatively equal amount of naïve and primed cells and a high level of production of nitric oxide following stimulation. The optimal culture conditions for the growth of the cells, hereafter referred to as bone marrow-derived macrophages, suggested by the data are therefore in media containing 1/100 rchGM-CSF till 7 days *ex vivo* with an initial seeding rate of  $5 \times 10^6$  cells/ml.

Superoxide anion is a reactive oxygen intermediate (ROI), and its activity was measured in cells grown using the same range of culture conditions as for the Griess assay in order to investigate the respiratory burst. Priming the cells with IFN- $\gamma$  did not increase superoxide anion activity in the cells. This suggests that the use of superoxide anion is not a significant bactericidal activity of the cells studied, as if it was then the priming with IFN- $\gamma$  should have been sufficient to stimulate a response. Interestingly, it has been suggested that ROI's may not in fact play a major role in bacterial killing by macrophages, but that the activities of reactive nitrogen intermediates, particularly nitric oxide, are actually much more important (Flesch and Kaufmann, 1991).

The pro-inflammatory cytokine mRNA expression profiles of bone marrow-derived cells grown till day 5 *ex vivo* with (at a concentration of 1/100) and without rchGM-CSF were determined through real-time qRT-PCR, and compared with those for both PBMC and the HD11 macrophage-like cell line. IL-1 $\beta$  mRNA expression levels for the bone marrow-derived cells were similar to those measured for both PBMC and HD11 cells. The PBMC and HD11 cells were more sensitive to stimulation with LPS alone and stimulation with LPS + IFN- $\gamma$ , displaying a greater up-regulation of IL-1 $\beta$  mRNA expression under these conditions. Stimulating with LPS and with LPS + IFN- $\gamma$

resulted in an up-regulation of IL-1 $\beta$  mRNA expression in bone marrow-derived cells cultured with and without rhGM-CSF. Although the mRNA expression profiles were comparable to those measured for PBMC and HD11 cells, there was no significant up-regulation of IL-6 or IL-18 following priming and stimulation with either IFN- $\gamma$ , with LPS or with LPS + IFN- $\gamma$ . The mRNA expression profiles of the chemokines CXCLi1 and CXCLi2 were also measured for the same cells. CXCLi1 and CXCLi2 mRNA expression levels in the bone marrow-derived cells, cultured with and without rhGM-CSF, were comparable with those in PBMC and HD11 cells. CXCLi2 mRNA expression levels in bone marrow-derived cells cultured with and without rhGM-CSF were up-regulated following priming and stimulation with either IFN- $\gamma$ , with LPS or with LPS + IFN- $\gamma$ .

The pro-inflammatory cytokine mRNA expression profile of bone marrow-derived cells grown till day 7 *ex vivo* was also assessed and compared to those for PBMC and HD11 cells. The mRNA expression profiles for the bone marrow-derived cells were similar to those seen for PBMC and HD11 cells and closer in pattern to them when also compared alongside the cells grown till day 5 *ex vivo*. Bone marrow-derived cells cultured with rhGM-CSF had significantly up-regulated levels of IL-1 $\beta$  and IL-6 mRNA following stimulation with LPS + IFN- $\gamma$ . Bone marrow-derived cells cultured without rhGM-CSF had significantly up-regulated levels of IL-1 $\beta$  following stimulation with LPS + IFN- $\gamma$ . The mRNA expression profiles for the chemokines CXCLi1 and CXCLi2 were also determined. The pattern of CXCLi1 mRNA expression for the bone marrow-derived cells was comparable to that measured for the PBMC, and although it followed the same pattern as that measured for the HD11 cells, the bone marrow-derived macrophages appeared more sensitive to stimulation, having a greater up-regulation of expression at these points. Both bone marrow-derived cells cultured

with and without rhGM-CSF were found to have significantly up-regulated CXCLi1 mRNA expression following stimulation with LPS + IFN- $\gamma$ . The CXCLi2 mRNA expression profile of bone marrow-derived cells was similar and comparable to that measured for PBMC and HD11 cells. Stimulating with LPS + IFN- $\gamma$  and with LPS alone caused a significant up-regulation of CXCLi2 in bone marrow-derived cells cultured with rhGM-CSF.

In summary, bone marrow-derived cells grown till day 5 *ex vivo* up-regulate IL-1 $\beta$  and CXCLi2 mRNA expression levels in response to stimulation with LPS + IFN- $\gamma$ . Cells grown till day 7 *ex vivo* up-regulate IL-1 $\beta$ , IL-6, CXCLi1 and CXCLi2 mRNA expression levels in response to stimulation with LPS + IFN- $\gamma$ . This up-regulation of pro-inflammatory cytokines and chemokines supports the evidence that bone marrow-derived cell populations grown till 7 days *ex vivo* behave like macrophages.

The flow cytometry analysis showed that approximately 47% of the gated cells stained positively with KUL01, and that approximately 34% stained positively for MHC class II surface expression. The reason that 100% of the cells were not, and would not be expected to, stain positively with both the KUL01 and MHC class II antibodies is that the cell population is mixed, containing cells at all stages of monocyte/macrophage differentiation. The cell surface marker recognised by KUL01 is not known, and it is therefore possible that it could be a marker that is expressed at later stages of differentiation. This would provide an explanation for the staining pattern, as just below 50% of the cells gated positive. MHC class II is expressed during the later stages of monocyte/macrophage differentiation, and its surface expression varies greatly even at these stages, becoming greatly up-regulated upon terminal activation, to enable effective presentation of internalised pathogen peptide following phagocytosis and processing by the cell. Again, since the bone marrow-derived cell population is mixed, this could

provide an explanation as to why MHC class II was detected on just over 33% of the cells.

The confocal images clearly show that the bone marrow-derived cells readily phagocytose opsonised latex beads and that these cells also stain positively with the mAb KUL01. Since just below 50% of the cells stained positive with the KUL01 antibody during the flow cytometry experiments, it may seem inconsistent that a much higher percentage of the cells stained positively with the antibody during confocal imaging. The cells used for confocal imaging were prepared in a slightly different way to those used for flow cytometry and this difference may explain the differential staining patterns. The flow cytometry method required the cells to be in suspension, so these cells were grown *ex vivo* on low-adherence plates and the cells were not permitted to form a monolayer. The cells used for confocal imaging were initially grown in suspension and then seeded onto a monolayer on glass coverslips 24 hours prior to use (in order to gain a cleaner preparation for the imaging and reduce background staining). This method resulted in a "purer" monocyte/macrophage cell population, whereas those cells grown in suspension for the duration of the *ex vivo* culture would have been more of a mixed cell population. Since the method of *ex vivo* culture used for subsequent invasion assays would be culture on a monolayer, the cells in the confocal images present a more realistic picture of the population obtained from the original protocol developed and suggested for the culture of bone marrow-derived macrophages.

Taken together, this evidence shows that the bone marrow-derived cells therefore appear to be macrophages. They produce NO following stimulation with *E. coli* LPS, up-regulate production of pro-inflammatory cytokines and chemokines such as IL-1 $\beta$ , IL-6, CXCLi1 and CXCLi2, readily phagocytose opsonised latex beads and stain positively for KUL01 and MHC class II.

Relatively little is known about the ultrastructure of chicken macrophages and so further confocal analysis was performed using antibodies for actin,  $\alpha$ -tubulin and endoplasmic reticulum. Actin is a key component of the cytoskeleton of cells and in the bone marrow-derived macrophages was located throughout the cell.  $\alpha$ -tubulin is a component of microtubules, which form part of the cytoskeleton of cells. Microtubules are important in the intracellular movement of materials and organelles and also in the formation of the mitotic and meiotic spindles. In the bone marrow-derived macrophages shown in the confocal images, the  $\alpha$ -tubulin was centrally located. Endoplasmic reticulum is an interconnecting network of tubules, vesicles and cisternae that extends through the cell and functions to transport and fold proteins. Indeed, endoplasmic reticulum means "little net within the cytoplasm" in Latin and this describes exactly how it appeared in the images within the bone marrow-derived macrophages.

Since confocal microscopy is dependent on the availability of specific antibodies for organelles, further analysis of the ultrastructure of the bone marrow-derived macrophages was done using the Transmission Electron Microscope (TEM). The TEM images clearly show that the macrophages do have a bifurcated nucleus (as suggested by the confocal imaging), and that the majority of the organelles are relatively centrally located. The pseudopodia of the cells are clearly visible, and the presence of these is characteristic of macrophages which use pseudopodia during motility and to aid in engulfing antigens during phagocytosis. The cells have a high proportion of vacuoles. Some of these vacuoles are possibly lysosomes, but it is very difficult to distinguish this without specific staining for lysozyme. Another organelle found within the macrophages was vesicles, which appear to contain granules (this was confirmed through discussions with Professor Inre Olah, Semmelweis University, Hungary, at the 9<sup>th</sup> Avian Immunology Research Group Meeting). Granule-containing vesicles are

organelles usually found in neutrophils (heterophils in avian species), and not what would be expected in macrophages. TEM images of PBMC also clearly show the presence of these vesicles, and in fact their prevalence is increased in these cells. This suggests that avian macrophages could function in a different way to mammalian macrophages. The concurrent evolution of avian and mammal orders from a common reptilian ancestor 300 million years ago has resulted in differences between the modern immune systems of both groups. It is quite possible that avian macrophages are in fact different to their mammalian counterparts. The presence of these granule-containing vesicles in all primary macrophage cells viewed in the course of this study under the TEM suggests the hypothesis that avian macrophages function as intermediate cells having properties similar to both mammalian macrophages and neutrophils. Since macrophages and neutrophils (heterophils) differentiate through the same stem cell lineage in the bone marrow, it is highly possible that the evolution of these cells has diverged from their function in their common ancestor. Interestingly there are differences in heterophil and neutrophil granule contents, with heterophils lacking at least one of the components found in neutrophil granules (Harmon, 1998).

HD11 cells do not contain these unusual organelles, though, and appear quite different in morphology compared to the primary cells. This is hardly surprising since HD11 cells are a virus-transformed macrophage-like cell line (Beug *et al.*, 1979). They appear much more densely packed with organelles compared to the primary macrophages, generally rounder in shape and with very few vacuoles. The differences in HD11 morphology compared with that of primary macrophages reiterates the fact that they are not particularly suitable substitutes for macrophages for studying bacterial infection *in vitro*.

In conclusion, the *ex vivo* culture of bone marrow-derived cells from chicken femurs in 1/100 rchGM-CSF for 7 days at an initial seeding rate of  $5 \times 10^6$  cells/ml results in a population of macrophages that produce IL-1 $\beta$ , IL-6, CXCLi1, CXCLi2 and NO upon stimulation with LPS, stain positively with KUL01 antibody, express MHC class II and readily phagocytose opsonised latex beads. The identification of vesicles which contain granules with chicken macrophages may mean that these cells function differently to mammalian macrophages and that avian macrophages are possibly an intermediate cell type preceding the mammalian evolution of macrophages and neutrophils.



## Chapter 4: Bacterial mutant construction

### 4.1 Introduction

SPI-1 and SPI-2 both encode a type-three secretion system that translocates effector proteins into the host cell cytoplasm. Therefore, attenuation of the TTSS associated with SPI-1 or SPI-2 essentially attenuates the SPI that it is associated with, as translocation of the related effector proteins is abrogated. Serovar Pullorum SPI-1 TTSS and SPI-2 TTSS mutants were already available at the start of this project. A serovar Pullorum strain containing a mutation in *spaS* (referred to as serovar Pullorum *spaS*) a structural component of the SPI-1 TTSS, was previously constructed by co-workers by conjugation of the suicide plasmid pSS1 into serovar Pullorum 449/87 Na<sup>r</sup> to make an insertion mutant (Jones *et al.*, 1998). Similarly a strain containing a mutation in *ssaU* (referred to as serovar Pullorum *ssaU*), a structural component of the SPI-2 TTSS, was also constructed by the conjugation of the suicide plasmid pSS2 into serovar Pullorum 449/87 Na<sup>r</sup> to make an insertion mutant (Jones *et al.*, 2001). An insertion mutant is constructed by the addition of an insert into the gene to disrupt it (usually an antibiotic resistance cassette), so the gene cannot be transcribed and is therefore inactive. These insertions are liable to revert over time back to the wild-type due to there being no biological or environmental advantage to the mutation due to selective pressure. There was some evidence for this in preliminary studies of poultry infections with serovar Pullorum (Wigley and Jones unpublished data). Insertion mutants are therefore useful in short term assays (i.e. for *in vitro* and short *in vivo* experiments), but are unstable for long-term assays (i.e. long *in vivo* assays).

#### 4.1.1 Molecular Koch's postulates

When identifying bacterial virulence genes and therefore candidates for mutagenesis, a molecular version of Koch's postulates can be adopted and considered (Falkow, 1988):

- 1) The gene should be present in bacteria which cause disease, but should be either absent, inactivated or not expressed in avirulent strains.
- 2) A mutation in the gene of interest should reduce virulence.
- 3) Complementation of the cloned gene should restore virulence to avirulent strains.

The first rule can be investigated by comparing bacterial genomes. When attempting to identify virulence genes in serovar Pullorum this is a problem, as large regions of the genome have not yet been sequenced. Much of the information about potential virulence genes arises from research on other *S. enterica* serovars and searching for those genes in the available serovar Pullorum sequence. This can be done using the *coli*BASE database which allows comparisons between the different *S. enterica* serovars (Chaudhuri *et al.*, 2004).

Attenuations in the gene of interest can be made by targeted mutagenesis, and the resulting mutations tested for virulence *in vitro* and *in vivo*. There are many different techniques for the targeted mutagenesis of bacteria, but they follow one of two principles. The first system works on the principle of disrupting the gene of interest using a suicide vector. This is the system by which the existing mutant constructs in serovar Pullorum were made. The second system disrupts the gene of interest using linear DNA. The method chosen for targeted mutagenesis of virulence genes in this study uses the second system and is known as the  $\lambda$  Red system. This system utilises a plasmid-encoded bacteriophage  $\lambda$  Red recombination system to promote the

recombination of linear dsDNA into the bacterial genome. Most bacteria do not respond to transformation with linear DNA due to the presence of intracellular exonucleases which readily degrade linear DNA (Lorenz and Wackernagel, 1994). Cosloy and Oishi (1973) found that bacterial mutants lacking exonuclease V (part of the RecBCD recombination complex) were transformable with linear DNA. Many bacteriophages encode their own homologous recombination systems (Smith, 1988), and the Red recombination system function of bacteriophage  $\lambda$  was shown by Murphy (1998) to promote a higher rate of recombination of linear DNA compared to that in bacteria lacking a functional exonuclease V. The Red recombination system of the bacteriophage  $\lambda$  constitutes three genes, *exo*, *bet* and *gam*, which are clustered in the  $P_L$  operon and are expressed early in the phage's transcriptional program (reviewed in Poteete, 2001). The gene *exo* encodes  $\lambda$  exonuclease, which degrades the 5'-ends of dsDNA (Little, 1967).  $\lambda$  exonuclease forms a ring-shaped trimer through which dsDNA can be housed at one end but only ssDNA will fit at the other (Kovall and Matthews, 1997). The second gene, *bet*, encodes  $\beta$  protein, which binds to ssDNA and functions to promote the renaturation of complementary strands (Li *et al.*, 1998). The products of these two genes combine to form a  $\beta$ -modulated  $\lambda$  exonuclease complex (reviewed in Poteete, 2001). RecBCD is the pathway through which host conjugational or transductional recombinations normally take place, and the *gam* gene product is a polypeptide which binds to and inhibits the activity of the host RecBCD exonuclease V (Murphy, 1991). This enables the  $\beta$ -modulated  $\lambda$  exonuclease to gain access to the ends of the DNA and promote recombination (Murphy, 1991). Murphy (1998) found that the plasmid-encoded Red system could be utilised to promote recombination events between the bacterial chromosome and PCR-generated linear dsDNA in *E. coli*. Building on this work, Datsenko and Wanner (2000) described a method using bacteriophage  $\lambda$  to promote

mutation of genes in *E. coli* that could be adapted for use in other bacterial species. The method uses linear dsDNA which is obtained through the PCR amplification of a plasmid encoding a selectable resistance marker, with primers containing long tails (approximately 40 bp) designed to the flanking regions of the bacterial gene of interest (Datsenko and Wanner, 2000). The linear DNA is then electroporated into bacteria carrying a plasmid containing the three  $\lambda$  bacteriophage genes that encode the Red system (Datsenko and Wanner, 2000). The plasmid used is pKD46, and it is a low copy number plasmid (Datsenko and Wanner, 2000), thereby reducing interference with recombination due to competitive inhibition, which is something that can occur with multicopy plasmids (Murphy, 1998). Upstream from the Red system, the plasmid contains a promoter, *P<sub>araB</sub>*, which is activated on addition of arabinose (Datsenko and Wanner, 2000). The plasmid then transcribes the three Red system genes, the proteins of which then incorporate the linear PCR-generated fragment into the genome of the bacteria, thus creating a disruption of the targeted gene (Datsenko and Wanner, 2000). The pKD46 vector is temperature-sensitive, and this allows it to be easily removed from the resulting mutants (Hashimoto-Gotoh *et al.*, 1981). These gene disruptions are thought to be very stable and the method is very efficient and fast (Datsenko and Wanner, 2000).

The method of trans-complementation of bacterial mutants has been used previously for mutant validation, but findings by Johnson *et al.* (2003) highlighted the importance of making this technique routine practice. Their study found a high frequency of secondary mutations following suicide-driven allelic exchange mutagenesis of *E. coli* (Johnson *et al.*, 2003). This suggests that, in the absence of trans-complementation, caution should be taken when ascribing phenotype to mutation in virulence genes. The serovar Pullorum strains with mutations in *spaS* and *ssaU* that are

already available have not been trans-complemented and so one of the aims of this study was to construct new mutants in these genes and then prove the position and presence of the single mutation. This would enable any observed phenotypic differences during infection to be more accurately attributed to the virulence gene, or in this case pathogenicity island, of interest. Datsenko and Wanner (2000) continually checked for additional chromosomal rearrangements resulting from recombination events following mutation using the  $\lambda$  Red system, but found none. This indicates that the occurrence of secondary mutations, in the form of unwanted chromosomal rearrangements, may be reduced using the  $\lambda$  Red system compared to other methods of bacterial mutant construction.

#### 4.1.2 Genes for $\lambda$ Red mutagenesis

Several gene candidates for mutagenesis using the  $\lambda$  Red system were initially considered for study and eventually five were decided upon. The intention was to use the  $\lambda$  Red system to construct mutants in these five genes (see below) then to create new stable constructs for *spaS*- and *ssaU*-.

The gene *avrA* (also known as STM2865) encodes an effector protein in serovar Typhimurium which is located in the SPI-1 region of the *Salmonella* genome, and is secreted by TTSS-1. The *avrA* gene is a *Salmonella* homologue of the *Yersinia pestis* gene *yopJ* which blocks the intracellular MAPK (mitogen activated protein kinase) kinases (MKKs) signalling pathway (Collier-Hyams *et al.*, 2002; McClelland *et al.*, 2001). Analysis using the *coli*BASE database shows predicted orthologues of *avrA* to be present in serovars Bongori, Enteritidis, Dublin and Gallinarum. An alignment of the section of the serovar Typhimurium LT2 genome containing *avrA* with the corresponding sections of the serovar Pullorum genome that have been sequenced was

performed using *coli*BASE and is shown in Figure 4.1. In serovar Typhimurium, *avrA* inhibits the pro-inflammatory, anti-apoptotic NF- $\kappa$ B signalling pathway during infection of human epithelial cells (Collier-Hyams *et al.*, 2002). Therefore it was interesting to study its function during infection with serovar Pullorum due to the lack of inflammatory pathology attributed to the disease.

In serovar Typhimurium, *sopE2* encodes an invasion-associated effector protein secreted by the SPI-1 TTSS but located on a different part of the chromosome to the SPI-1 TTSS itself (Miao *et al.*, 1999; McClelland *et al.*, 2001) and analysis using the *coli*BASE database shows it to be a pseudogene in serovar Typhi. Analysis using the *coli*BASE database shows predicted orthologues of *sopE2* to be present in serovars Pullorum (2112\_12\_19\_ORF\_1), Bongori, Enteritidis and Gallinarum. An alignment of the section of the serovar Typhimurium LT2 genome containing *sopE2* with the corresponding predicted orthologue for serovar Pullorum was performed using *coli*BASE and is shown in Figure 4.2. In serovar Typhimurium, *sopE2* mutants were defective in their colonisation of chicks (Morgan *et al.*, 2004). Furthermore, during mammalian infection with serovar Typhimurium, SopE2 activates RhoGTPase signalling pathways, which mimic eukaryotic G-nucleotide exchange factors (Schlumberger and Hardt, 2005). This makes it an interesting target for study in serovar Pullorum, which unlike serovar Typhimurium does not appear to colonise the gut (Henderson *et al.*, 1999).

The *mgtB* gene is part of the *mgtBC* operon in SPI-3, and has been identified in serovars Typhimurium (Snaveley *et al.*, 1991; McClelland *et al.*, 2001) and Typhi (Parkhill *et al.*, 2001). Analysis using the *coli*BASE database shows predicted orthologues of *mgtB*

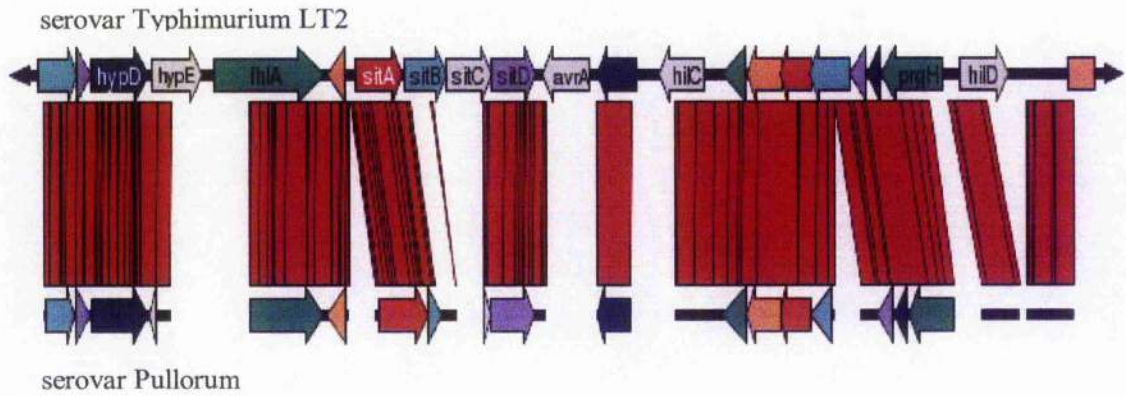


**Figure 4.1: *avrA* alignment viewer from coliBASE.** Region 3000353-3020352 of *Salmonella enterica* Typhimurium LT2, and the equivalent regions from serovar Pullorum (Contig 1371\_12\_19: 1-2406 [reversed]; Contig 1423\_12\_19: 27-1915 [reversed]; Contig 1075\_12\_19: 80-1628 [reversed]; Contig 355\_12\_19: 5-1193 [reversed]; Contig 593\_12\_19: 17-669 [reversed]; Contig 2030\_12\_19: 1-3046 [reversed]; Contig 1867\_12\_19: 1-1782; Contig 924\_12\_19: 1-732 [reversed]; Contig 740\_12\_19: 1-904 [reversed]), as determined using MUMmer (alignment viewer). The coloured arrows indicate annotated genes in the region. Putative orthologous genes (as determined in a mutual best hits analysis) are colour coded. Genes with no predicted orthologues are coloured grey. Red blocks indicate regions of close homology and darker shades within the red blocks indicate closer homology.

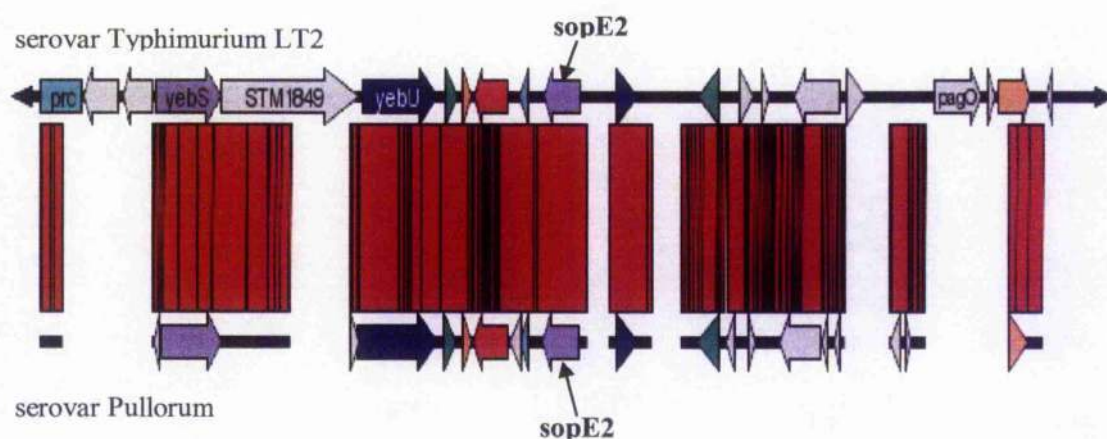


**Figure 4.2: *sopE2* alignment viewer from coliBASE.** Shown is a diagrammatic representation of the region 1942374-1962373 of *Salmonella enterica* serovar Typhimurium LT2, and the equivalent regions from serovar Pullorum (Contig 819\_12\_19: 1-446 [reversed]; Contig 1862\_12\_19: 1-2661 [reversed]; Contig 2112\_12\_19: 1-4540 [reversed]; Contig 366\_12\_19: 1-835; Contig 1835\_12\_19: 1-3148 [reversed]; Contig 241\_12\_19: 58-747; Contig 390\_12\_19: 2-661), as determined using MUMmer (alignment viewer). The coloured arrows indicate annotated genes in the region. Putative orthologous genes (as determined in a mutual best hits analysis) are colour coded. Genes with no predicted orthologues are coloured grey. Red blocks indicate regions of close homology and darker shades within the red blocks indicate closer homology.



to be present in serovars Pullorum (2135\_12\_19\_ORF\_1 and 2135\_12\_19\_ORF\_2), Bongori, Enteritidis, Dublin and Gallinarum. An alignment of the section of the serovar Typhimurium LT2 genome containing *mgtB* with the corresponding predicted orthologue for serovar Pullorum was performed using *coliBASE* and is shown in Figure 4.3. The *mgtB* gene mediates  $Mg^{2+}$  influx and is one of three  $Mg^{2+}$  transport systems that have been identified in the serovar Typhimurium genome (Snaveley *et al.*, 1991). MgtB, an ATPase enzyme, mediates the influx of the magnesium cation into the cytosol (Snaveley *et al.*, 1991). The *mgtBC* operon is regulated by PhoPQ and is important in intramacrophage survival as it is essential for bacterial growth in low  $Mg^{2+}$  environments (Amavisit *et al.*, 2003). It could therefore be hypothesised that *mgtB* is important for serovar Pullorum intramacrophage persistence.

The gene *siiE* (also known as STM4261) is a putative inner-membrane protein located in SPI-4 and has been identified in serovar Typhimurium (McClelland *et al.*, 2001). Analysis using the *coliBASE* database shows predicted orthologues of *siiE* to be present in serovars Pullorum (2179\_12\_19\_ORF\_2), Typhi, Bongori, Enteritidis, Dublin and Gallinarum. An alignment of the section of the serovar Typhimurium LT2 genome containing *siiE* with the corresponding predicted orthologue for serovar Pullorum was performed using *coliBASE* and is shown in Figure 4.4. The gene *siiF* (also known as STM4262) is a putative ABC-type exporter and has been identified in serovar Typhimurium (McClelland *et al.*, 2001). Analysis using the *coliBASE* database shows predicted orthologues of *siiF* to be present in serovars Pullorum (1761\_12\_19\_ORF\_4), Typhi, Bongori, Enteritidis, Dublin and Gallinarum. An alignment of the section of the serovar Typhimurium LT2 genome containing *siiF* with the corresponding glimmer predicted orthologue for serovar Pullorum was performed using *coliBASE* and is shown in Figure 4.5. Mutants in *siiE* and *siiF* are defective in

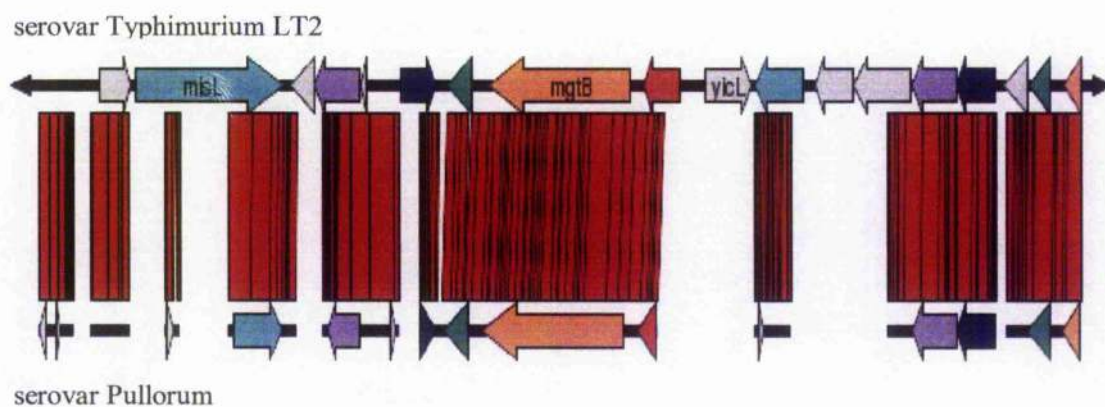


**Figure 4.3: *mgtB* alignment viewer from coliBASE.** Shown is a diagrammatic representation of the region 3952906-3972905 of *Salmonella enterica* serovar Typhimurium LT2, and the equivalent regions from serovar Pullorum (Contig 1965\_12\_19: 20-695 [reversed]; Contig 784\_12\_19: 1-757 [reversed]; Contig 293\_12\_19: 1-304; Contig 1302\_12\_19: 1-1319 [reversed]; Contig 1667\_12\_19: 75-1539; Contig 2135\_12\_19: 1-4568 [reversed]; Contig 3\_12\_19: 85-780 [reversed]; Contig 2150\_12\_19: 1-2088; Contig 1462\_12\_19: 1-1426), as determined using MUMmer (alignment viewer). The coloured arrows indicate annotated genes in the region. Putative orthologous genes (as determined in a mutual best hits analysis) are colour coded. Genes with no predicted orthologues are coloured grey. Red blocks indicate regions of close homology and darker shades within the red blocks indicate closer homology.

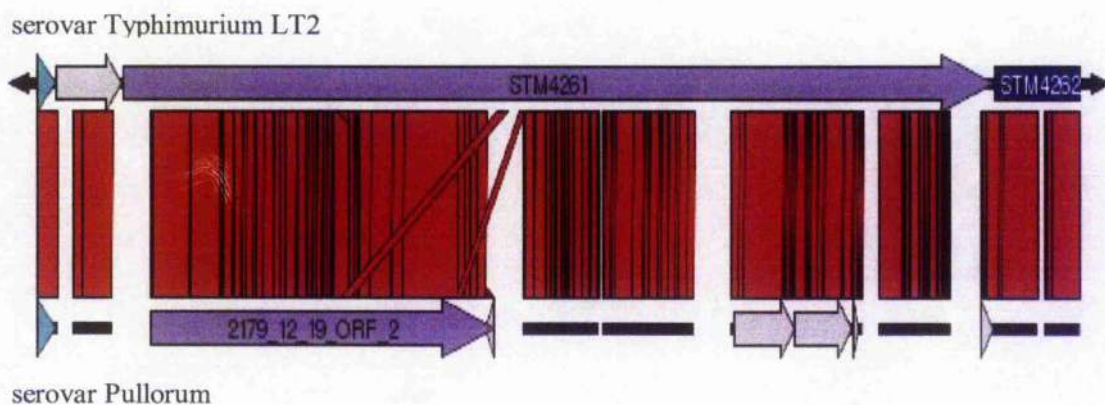


**Figure 4.4: *siiE* alignment viewer from coliBASE.** Shown is a diagrammatic representation of the region 4480814-4500813 of *Salmonella enterica* serovar Typhimurium LT2, and the equivalent regions from serovar Pullorum (Contig 268\_12\_19: 326-735; Contig 274\_12\_19: 1-756 [reversed]; Contig 2179\_12\_19: 17-6613 [reversed]; Contig 1230\_12\_19: 38-1495; Contig 1687\_12\_19: 1-1771 [reversed]; Contig 1569\_12\_19: 1-2525; Contig 681\_12\_19: 11-1387; Contig 821\_12\_19: 1-1091 [reversed]; Contig 490\_12\_19: 1-676 [reversed]), as determined using MUMmer (alignment viewer). The coloured arrows indicate annotated genes in the region. Putative orthologous genes (as determined in a mutual best hits analysis) are colour coded. Genes with no predicted orthologues are coloured grey. Red blocks indicate regions of close homology and darker shades within the red blocks indicate closer homology.

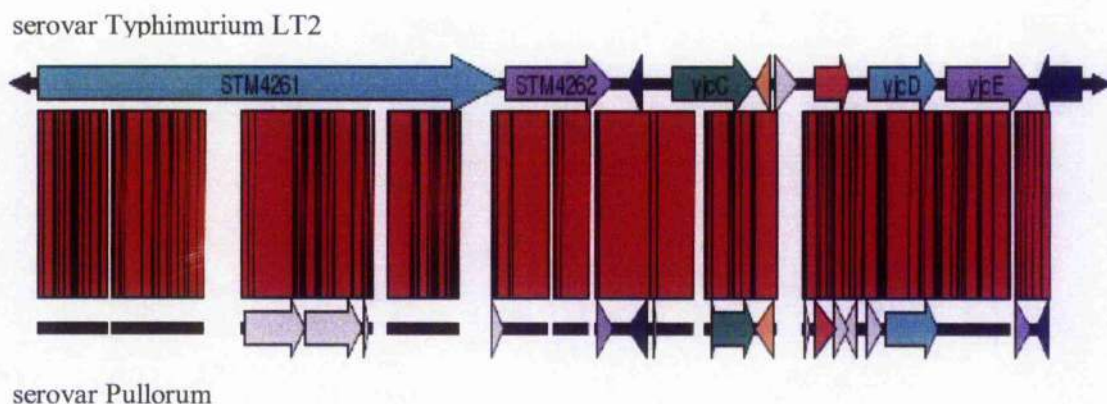


**Figure 4.5: *siiF* alignment viewer from coliBASE.** Shown is a diagrammatic representation of the region 4490227-4510226 of *Salmonella enterica* serovar Typhimurium LT2, and the equivalent regions from serovar Pullorum (Contig 1230\_12\_19: 143-1495; Contig 1687\_12\_19: 1-1771 [reversed]; Contig 1569\_12\_19: 1-2525; Contig 681\_12\_19: 11-1387; Contig 821\_12\_19: 1-1091 [reversed]; Contig 490\_12\_19: 1-676 [reversed]; Contig 1761\_12\_19: 1-1900 [reversed]; Contig 1571\_12\_19: 1-1396 [reversed]; Contig 2155\_12\_19: 30-4009 [reversed]; Contig 414\_12\_19: 1-666 [reversed]), as determined using MUMmer (alignment viewer). The coloured arrows indicate annotated genes in the region. Putative orthologous genes (as determined in a mutual best hits analysis) are colour coded. Genes with no predicted orthologues are coloured grey. Red blocks indicate regions of close homology and darker shades within the red blocks indicate closer homology.

intestinal colonisation but not systemic infection with serovar Typhimurium (Morgan *et al.*, 2004). These genes were therefore thought to be candidates for study in serovar Pullorum, which causes systemic infection but does not appear to colonise the intestine (Henderson *et al.*, 1999).

## 4.2 Methods

### 4.2.1 $\lambda$ -Red mutagenesis

This method is based on that developed and described by Datsenko and Wanner (2000), with modifications suggested by Professor Mark Roberts (University of Glasgow, U.K.). Forward and reverse primers were designed with a 40 bp homology to the gene of interest, approximately 6 bp upstream of the start codon and 6 bp downstream of the stop codon and including a priming site for pKD3/pKD4 (Sigma-Genosys). These primers are shown in Table 4.1. To obtain products containing the flanking regions of the gene of interest with an antibiotic resistance cassette, a PCR was performed (with 12 x 100  $\mu$ l reactions) using one of the template vectors pKD3(cm) or pKD4(Kan). A small amount of the PCR products was run on an agarose gel to check the product size. The PCR reactions were then pooled and PCR product purifications performed to clean up the reaction and isolate the DNA. Two QiaQuick PCR clean-up tubes (Qiagen) were used per gene as described in Chapter 2 with 600  $\mu$ l of PCR reaction passed through each tube. The DNA from the reaction was eluted with MQ water (75  $\mu$ l per column) and pooled (150  $\mu$ l total). The restriction enzyme *DpnI* (Invitrogen) (2  $\mu$ l) along with REact® 4 buffer (Invitrogen) (15  $\mu$ l) was added to the pooled DNA, and then this was incubated at 37°C for 3 h. The whole digest reaction was run on an agarose gel and the resulting digested bands excised from the gel. Purification of the gel product was then

Gene	Primer	Sequence
avrA *	Forward $\lambda$ primer: LamavrAF	5'-CAGCCTGACGTCAGCGGGGAGCTAAACACCGAAGCATTGAGTGTAGGCTGGAGCTGCTTC-3'
	Reverse $\lambda$ primer: LamavrAR	5'-AAATTTTACTAAGTTTCATAAAATTCAGAGCTGAAGTTTTTCCATATGAATATCCTCCTTA-3'
	Forward checking primer: checkavrAF	5'-AAACCCGTGGCTGCTACGTATG-3'
	Reverse checking primer: checkavrAR	5'-AGTTATTGCACCTGGTATTGC-3'
ngtS	Forward $\lambda$ primer: LamngtBF	5'-CCGGCGTCCAGAAAATGATAAGCAGCATAAAAAAGTATTCGGTAGGGCTGGAGCTGCTTC-3'
	Reverse $\lambda$ primer: LamngtBR	5'-ACTAAGAATTGACTGACTGATAAAGAGATGGCGCA CGCCCATATGAATATCCTCCTTA-3'
	Forward checking primer: checkngtBF	5'-CTGTAAATAAAGAAGATGAAAG-3'
	Reverse checking primer: checkngtBR	5'-ACCCGTCAGCCCTAAATTCAAC-3'
sopE2 *	Forward $\lambda$ primer: LamsopE2F	5'-ACTAACATAACACTATCCACCCAGCACTACAGAAATCATAGTGTAGGCTGGAGCTGCTTC-3'
	Reverse $\lambda$ primer: LamsopE2R	5'-GACAAAAGGATTCGCCCACTGGAGTAAATACGCA TATGAATATCCTCCTTA-3'
	Forward checking primer: checksope2F	5'-CTGATTTTCTCGTAGCGCG-3'
	Reverse checking primer: checksope2R	5'-GCAATAAAAATAAATGGCTG-3'
sifE *	Forward $\lambda$ primer: LamsifEF	5'-CTAACACAGACCGATGCTGAAAAAGTTCTTCCTCAACCTATGTAGGCTGGAGCTGCTTC-3'
	Reverse $\lambda$ primer: LamsifER	5'-CAGTTCCATCTTATCGACATCAAGGCTGGCAACCAGTTCATATGAATATCCTCCTTA-3'
	Forward checking primer: checksifEF	5'-GTTTTCTCTTCGGGGCCA GAC-3'
	Reverse checking primer: checksifER	5'-CGGCTTATTTACGTTGTCAG-3'
sifF *	Forward $\lambda$ primer: LamsifFF	5'-AGGGCTTCACCTGCGCCGAACTGTGGTTTTATCTTGCACGCTGAGGCTGGAGCTGCTTC-3'
	Reverse $\lambda$ primer: LamsifFR	5'-AACGGGATCGCGCGCCAGGGGTAGGCTCCGCCACCATCCATATGAATATCCTCCTTA-3'
	Forward checking primer: checksifFF	5'-ATCTGTCAATGTCTCTGGCCG-3'
	Reverse checking primer: checksifFR	5'-GTGTGGTTCTCTCCGGTGGC-3'

**Table 4.1: Primers for  $\lambda$  Red mutagenesis.** Where possible, primers were designed to serovar Pullorum sequence taken from *coliBase*. Otherwise, primers were designed using serovar Typhimurium LT2 sequence from *coliBase* (\*). Forward and reverse  $\lambda$  primers were designed within the gene of interest with the pKD3/4 priming site added to the tail (highlighted in blue). Checking primers were designed approximately 500 bp outside the gene, within the flanking regions.

performed using 2 QiaQuick gel clean-up columns (Qiagen). A 5 ml culture of serovar Pullorum carrying the vector pKD46 was set up in LB supplemented with 100  $\mu\text{g/ml}$  ampicillin, and grown at 30°C (as the plasmid is temperature-sensitive) overnight. The overnight culture was diluted 1/1000 in LB containing 100  $\mu\text{g/ml}$  ampicillin and 1 mM L-arabinose. The cells were grown to an OD of 0.6, and pelleted at 4°C, before washing twice in ice-cold sterile distilled water and once in sterile 10% glycerol. The final pellet was resuspended in 1 ml of 10% glycerol, and the cells kept on ice. The DNA (0, 2, 5, 10, 20 and 30  $\mu\text{l}$ ) was added to 100  $\mu\text{l}$  competent cells, then left on ice for 10 min. The reaction was electroporated in 2 mm cuvettes using standard *Salmonella* conditions (200 Ohms, 25  $\mu\text{F}$ , 1.75 kV). The cells were then recovered at 37°C in 5 ml of SOC medium or Lennox Broth and incubated for 2 h in an orbital shaker at 200 rpm. Following recovery, 100  $\mu\text{l}$  of the cells were plated aseptically onto LB-agar containing 25  $\mu\text{g/ml}$  or 30  $\mu\text{g/ml}$  of the desired antibiotic (i.e chloramphenicol for pKD3 or kanamycin for pKD4). The plates were then incubated overnight at 37°C and colonies containing the desired mutation were selected from the plate. Colonies not containing the desired mutation would not contain the antibiotic resistant cassette, which was transferred along with the mutation during electroporation, and therefore should not grow on the selective plates. An agglutination test and antigenic identification test were then carried out on the bacterial colonies selected. A slide agglutination test using acriflavin was carried out to determine if the LPS coat of each bacterial colony was intact (smooth) or was damaged (rough). This was based on a method described by Henry (1933), as described in Chapter 2. To then test the antigenic identification of the bacterial colony, a further slide agglutination test was used. The O antigenic group is used to determine *Salmonella* serotype and serovar Pullorum is in the same antigenic group as serovar Gallinarum, group O:O9. A droplet of *Salmonella* antisera O:O9 was added to the

suspension, and the bacterial serotype was identified as Pullorum if agglutination occurred. A negative control was used for comparison (e.g. O:O27). Bacterial colonies that had intact LPS and were of the correct antigenic group were then checked by PCR.

### 4.3 Results

Efforts to construct bacterial mutants in serovar Pullorum using the  $\lambda$  Red technique were unsuccessful. For the first nine attempts at mutagenesis, the plasmid pKD3 was used for the initial PCR. The first eight attempts failed to produce bacterial colonies on the selective plates post-electroporation. On the ninth attempt, a small number of bacterial colonies for each mutation were obtained post-electroporation (approximately 10 for each). Checking for the mutation by PCR revealed that these were in fact false positives. Modifications to the protocol were then made on the recommendation of Professor Mark Roberts (University of Glasgow). These included the use of the plasmid pKD4 rather than pKD3, recovering the electroporated bacteria in Lennox Broth rather than SOC medium and increasing the concentration of the antibiotic in the LB-agar plates (from 25  $\mu\text{g}/\text{ml}$  to 30  $\mu\text{g}/\text{ml}$ ) for selecting for the mutation. The method was then repeated a further eight times with these modifications. This resulted in a high yield of bacterial colonies post-electroporation, averaging approximately 100 bacterial colonies per electroporation. Subsequent screening using the acriflavin slide agglutination assay revealed all colonies were rough (i.e. with a damaged LPS structure).

### 4.4 Discussion

It is unclear why the desired mutations in serovar Pullorum were not generated using the  $\lambda$  Red system. The modifications made to the protocol on the recommendation



of Professor Mark Roberts (University of Glasgow) were sufficient to allow the successful construction of mutants in other *S. enterica* serotypes (Professor Mark Roberts, personal communication) but were not successful in serovar Pullorum.

In most *S. enterica* serotypes, LPS structures form a layer around the bacterium to give protection from the host immune system, as LPS interacts with both antibodies and with complement. Rough mutants lack this protective layer and activate complement by the alternative pathway. The membrane attack complex of complement is then able to kill the bacteria. Rough mutants are therefore avirulent, and so of no use in this study which was focussed on virulence. The structure of LPS can affect transfection of both *E. coli* (Taketo, 1972) and serovar Typhimurium (Bursztyn *et al.*, 1975), and it is generally accepted that DNA electroporates preferentially into rough bacteria as opposed to smooth. This may be due to the increased exposure of sites responsible for DNA binding (MacLachlan and Sanderson 1985).

The plasmid pKD46, which encodes the  $\lambda$  Red genes (*exo*, *bet* and *gam*), is a low-copy number plasmid (Datsenko and Wanner, 2000). Multicopy plasmids may act as competitive inhibitors to recombination, hence interfering with the process (Murphy, 1998). Although the  $\lambda$  Red system itself has a high frequency of recombination, when incorporated into a low copy number vector this is reduced to a relatively low frequency (Datsenko and Wanner, 2000). In some strains of *S. enterica* this may be reduced further or may not occur at all. For example attempts at using the technique to create mutations in serovar Enteritidis S1400 have been successful but attempts using serovar Enteritidis 125109 have not (Debra Clayton, personal communication). The factors that cause this reduction or non-occurrence of recombination are unknown, but could include the site of pKD46 insertion, which may be close to inhibitory factors on the genome. Another explanation could be that the gene of interest may be located near to

an essential gene. Thereby the disruption of the genome via the insertion of pKD46 could render the bacterium non-viable and unable to form colonies following electroporation. For example, the system has not worked with serovar Enteritidis 125109, but has been highly efficient in constructing mutants using other strains such as serovar Gallinarum (Debra Clayton, personal communication). Perhaps the method does not work in the serovar Pullorum strain used (447/89). A possible solution would be to try to create the mutation in another serovar Pullorum strain, and then conjugate the mutated strain with serovar Pullorum 447/89. Unfortunately, time did not allow for this and the potential unsuitability of some strains for this method did not become apparent until late in the project.

The  $\lambda$  Red system was initially chosen for the construction of mutants in serovar Pullorum due to its reputation for being able to create mutants more rapidly than by using a suicide vector and the fact that the mutations were thought to be relatively stable (Datsenko and Wanner, 2000). If time had permitted, other methods of mutant construction would have been investigated. For example the vector pDM4, which is maintained as a plasmid in  $\lambda$  pir *E. coli* strains as it integrates into the chromosome in other strains. Suicide vectors typically contain an antibiotic resistance cassette (for example, the vector pDM4 includes a chloramphenicol resistance cassette), which can be used as an indication of their integration into DNA of recipient strains or to disrupt the gene itself. To construct a genetic mutation via this method, the flanking regions of the gene of interest are amplified, and then linked by a second amplification thereby excluding the gene. The gene deletion is then cloned into the suicide plasmid and transformed (e.g. by electroporation or calcium chloride transformation) into an *E. coli*  $\lambda$  pir strain. A conjugation between the *E. coli*  $\lambda$  pir and the final recipient can be used to transfer the suicide plasmid containing the mutation into the desired strain.

Successful mutations can be selected by plating bacteria onto the appropriate selective media, and further checked via PCR. This is the method by which the existing two serovar Pullorum SPI mutant constructs were created (Jones *et al.*, 1998; 2001). Rather than being gene deletions though, these mutants were constructed by an insertion disruption of the gene, using an antibiotic resistance cassette. Problems occur when using insertion mutations during longer *in vivo* assays, as selection pressure may cause reversion of the mutation to the wild-type. Therefore, although *spaS*<sup>r</sup> and *ssaU* can be used for *in vitro* and short *in vivo* assays, they should not be used for long *in vivo* assays. However, Wigley *et al.* (2002) successfully used serovar Pullorum *ssaU* *in vivo* over a relatively long time-scale. This was successful as the mutant was completely attenuated in the establishment of a systemic infection and therefore selection pressure on the bacteria to revert to wild-type was not an issue. If there had not been complete attenuation in the establishment of systemic infection, it is likely that the bacteria *in vivo* would have reverted to wild-type, thus confounding the subsequent results.

As mutant construction using the  $\lambda$  Red system was not successful, this study concentrated on the role of the SPI-1 TTSS and the SPI-2 TTSS in early-stage serovar Pullorum infection using the bacterial mutants that were already available. The mutants were stable for use *in vitro* and for short *in vivo* experiments, so research was focused around the initial invasion event in the gut and the establishment of persistent infection in macrophages.

## Chapter 5: Modelling the role of the SPI-1 TTSS and the SPI-2 TTSS in infection with *Salmonella enterica* serovar Pullorum *in vitro*

### 5.1 Introduction

Modelling disease *in vitro* provides the opportunity to study the individual mechanisms taking place during an infection and to demonstrate the interactions between individual cell types in a controlled environment, something which is more problematic during *in vivo* investigations. For Pullorum Disease, it is useful to investigate the mechanisms of both the initial invasion event and the establishment of systemic infection. Systemic infection involves persistence and consequently understanding the mechanisms of, and the host immune response to, persistence are central to our understanding of the aetiology of the disease.

The SPI-1 TTSS plays a role in the initial invasion event during serovar Pullorum infection (Wigley *et al.*, 2002). Invasion during serovar Pullorum infection occurs through areas of organised lymphoid tissue associated with the gut (i.e. the GALT), and there is evidence to suggest the bursa of Fabricius is one of these invasion sites (Henderson *et al.*, 1999). It is difficult to accurately replicate these areas of GALT *in vitro*, and therefore intestinal epithelial cell models are used. Currently, there is no chicken intestinal epithelial cell line. Chick kidney cells (CKC) contain a high proportion of epithelial cells, relatively few phagocytic cells, and are readily invaded by a range of *S. enterica* serovars (Barrow and Lovell, 1989). They have been used in previous studies to model different aspects of the *Salmonella* invasion event, and consequently are now accepted as the best available model for gut epithelial cells (Wigley *et al.*, 2002; Kaiser *et al.*, 2000). Persistence during serovar Pullorum infection takes place preferentially within macrophages located in the spleen (Wigley *et al.*,

2001). A current model for this cell type is HD11, which are MC29 virus-transformed chicken haematopoietic cells that function in ways comparable to macrophages (Beug *et al.*, 1979). Although HD11 cells are a convenient model for the chicken macrophage, it is important to remember that they are only a chicken macrophage-like cell line. In addition, the use of a primary macrophage population *ex vivo* was considered, as this would provide a more realistic model for persistence and would highlight differences between the responses of the primary macrophage cell population and HD11 cells. Protocols for the isolation and differentiation of primary cells such as monocyte-derived macrophages from peripheral blood mononuclear cells (PBMC) (Wigley *et al.*, 2002) or from the spleen (Wigley *et al.*, 2001) yield relatively low quantities of cells which have a short lifespan *ex vivo*. The isolation and differentiation of chicken bone marrow-derived macrophages, as described in Chapter 3, overcomes these problems for modelling serovar Pullorum persistence.

The initial invasion event of serovar Pullorum in the gut is SPI-1 TTSS-mediated, but not dependent (Wigley *et al.* 2001). Serovar Pullorum is able to invade and establish an initial systemic infection without causing considerable pathology in the gut, unlike other related serovars. This poses the question as to whether there is any involvement of the SPI-1 TTSS in the modulation of the host immune response during serovar Pullorum infection. Even though the SPI-1 and SPI-2 TTSS are well conserved within *S. enterica* serovars (Oehman and Groisman 1996), there is increasing evidence to suggest differences in the range of effector proteins that are secreted by this machinery (Hardt and Galán, 1997; Mirold *et al.*, 1999; Amavisit *et al.*, 2003). Also, the translocation of SPI-1 TTSS effector proteins into host cells results in, amongst other things, the activation of various transcription factors (Suárez and Rüssmann, 1998), which may in turn have an effect on the immune response mounted by the host cell.

This highlights the need to study the specific effects of both the serovar Pullorum SPI-1 and SPI-2 TTSS on the avian host. Interestingly, Kaiser *et al.* (2000) reported that the cytokine profiles expressed by CKC in response to infection with either serovar Typhimurium, Enteritidis or Gallinarum were markedly different, and this could be directly related to differences in both the pathogenesis and progression of the different diseases caused by these agents. It was therefore an aim of the study to investigate the pro-inflammatory immune response of CKC cells to infection with serovar Pullorum, and to determine any involvement of the SPI-1 TTSS. The effects of the SPI-1 TTSS on bacterial invasion of the macrophage cell models is also of interest, to ascertain whether invasion into macrophage cells is mediated by the SPI-1 TTSS or by a different mechanism, compared to invasion into gut epithelial cells.

SPI-2 TTSS-mediated persistence within splenic macrophages during serovar Pullorum infection has been previously demonstrated *in vivo* by Wigley *et al.* (2001) and a functional SPI-2 TTSS was essential for both virulence and carriage (Wigley *et al.*, 2002). The SPI-2 TTSS is essential for virulence during serovar Gallinarum infection and this persistence has been successfully modelled *in vitro* using HD11 cells (Jones *et al.*, 2001). However, persistence due to the SPI-2 TTSS during serovar Pullorum infection has not yet been modelled *in vitro*. Attempts at using HD11 cells for this purpose have so far been unsuccessful (Paul Wigley, personal communication). Due to the previous lack of an effective cell model, studies into the mechanisms of and the consequent host cell responses to persistence have not been possible. Utilisation of the bone marrow-derived macrophage model for *Salmonella* persistence aims to address these issues.

## 5.2 Methods

### 5.2.1 Cells

CKC and HD11 cells were prepared as described in Chapter 2, section 2.3.1. Bone marrow-derived macrophages were isolated from line 7<sub>2</sub> White Leghorn chickens and cultured on a monolayer, as described in Chapter 3, using complete media and with a 1/100 dilution of rhGM-CSF for either 5 or 7 days *ex vivo*. Two hours prior to use the monolayer was washed to remove all traces of antibiotics and the cell culture media was replaced with RPMI 1640 containing 5% chick serum (Sigma).

### 5.2.2 Data Analysis

Experiments were performed on three separate occasions and for each experiment each parameter was repeated in triplicate. For real-time qRT-PCR, just one of the repeated parameters was taken from each experiment (giving  $n=3$ ) for the analysis. Differences were analysed using Analysis of Variance and the two-tailed t-test, and were carried out using Minitab for Windows version 14 statistical package (Minitab Ltd., Coventry, West Midlands, UK). Values of  $P \leq 0.05$  were taken as significant.

## 5.3 Results

### 5.3.1 The effect of SPI-1 TTSS on invasion of CKC with serovar Pullorum

Figure 5.1 shows intracellular bacterial counts as colony forming units (i.e. a count of the viable bacteria) per ml from CKC infected with either serovar Pullorum, serovar Pullorum *spaS* attenuated mutant or serovar Enteritidis over a 6 h time-course. Cells were also mock infected as a control. These cells were negative for intracellular bacterial counts for the duration of the time-course, demonstrating that the cells were not contaminated. At the early time-points of 2 and 3 h post-infection (hpi), the numbers

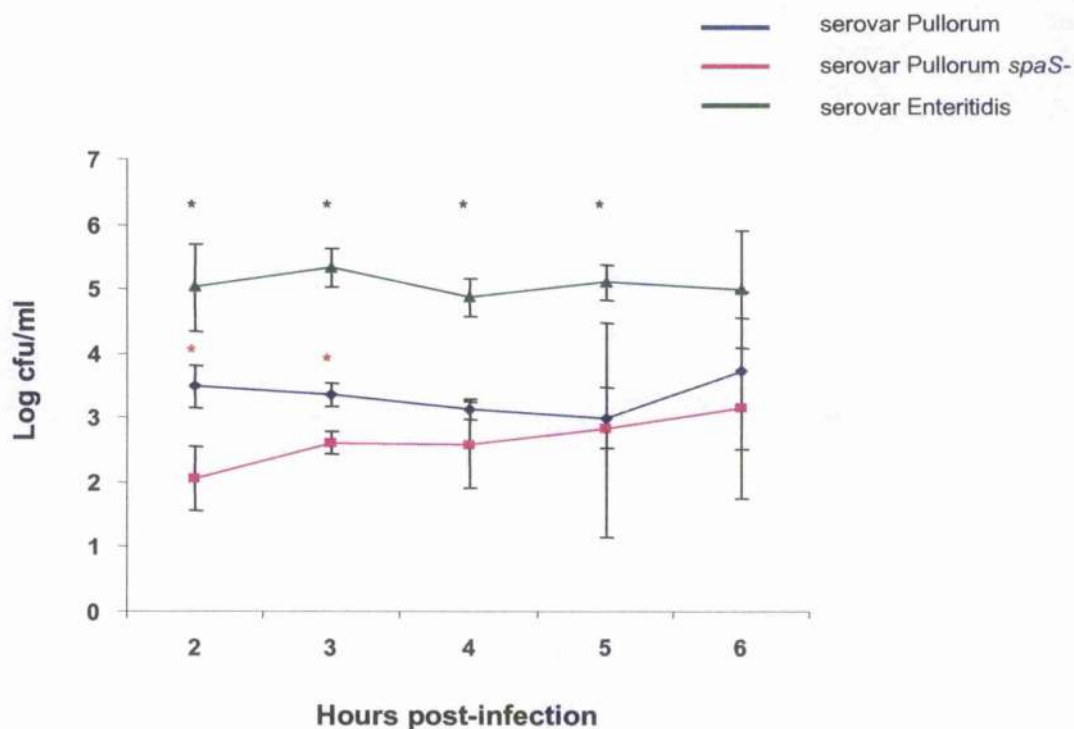


**Figure 5.1: Intracellular bacterial counts from CKC following infection with 100  $\mu$ l/ml of a late log phase  $10^8$  cfu/ml culture of either *Salmonella enterica* serovar Pullorum, serovar Pullorum *spaS*- or serovar Enteritidis.** Bacterial counts are expressed as log cfu/ml (n=9; SD $\pm$ 0.05). Statistical significance is represented by \*, or \* for significance that is SPI-1 TTSS-mediated.



of intracellular serovar Pullorum bacteria are statistically significantly higher ( $P=0.015$ ,  $P=0.021$  respectively) than numbers of the *spaS* attenuated mutant, by approximately 1.5 log at 2 hpi then 1 log at 3 hpi. By 4 hpi, there is no longer any significant difference between these groups. The numbers of serovar Enteritidis within the CKC over the time-course stay relatively constant at approximately 5 log/ml, and they are significantly higher at 2, 3, 4 and 5 hpi compared to numbers of serovar Pullorum ( $P=0.024$ ,  $P=0.001$ ,  $P=0.001$ ,  $P=0.003$  respectively) and at 2, 3 and 4 hpi when compared to numbers of the *spaS* attenuated mutant ( $P=0.004$ ,  $P=0.002$ ,  $P=0.006$  respectively).

Results of Griess assays to determine nitric oxide production were performed on the supernatants collected from the gentamicin protection assays and are shown in Figure 5.2. There was no significant difference between the amounts of nitrite measured in any of the supernatants across the time-course, after intracellular infection with either serovar Pullorum, serovar Pullorum *spaS*, serovar Enteritidis or from the control mock-infected CKC.

Figure 5.3 shows cytokine mRNA expression in the same CKC. Figure 5.3A shows the expression profile of IL-1 $\beta$  mRNA for the differentially infected cells across the time-course. At 2 hpi, IL-1 $\beta$  mRNA expression levels during serovar Enteritidis infection were significantly up-regulated compared to those seen during serovar Pullorum infection ( $P=0.019$ ), *spaS* ( $P=0.033$ ) and for the mock-infected control cells ( $P=0.006$ ). At 3 hpi, there were no significant differences for IL-1 $\beta$  mRNA expression from the differentially infected cells. At 4 hpi the mRNA expression levels following serovar Enteritidis infection were significantly up-regulated compared to those seen during infection with serovar Pullorum ( $P=0.026$ ), with *spaS* ( $P=0.041$ ) and for the mock-infected control ( $P=0.02$ ). At 5 hpi, IL-1 $\beta$  mRNA expression levels during

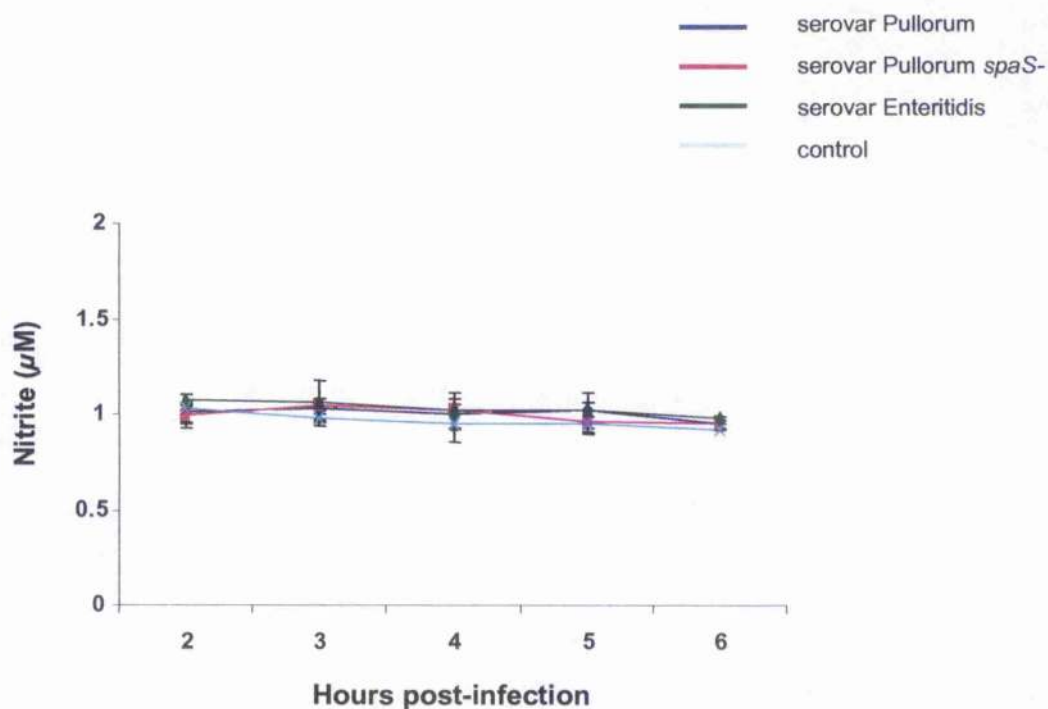


**Figure 5.2: Nitric oxide production by CKC following infection with 100 µl/ml of a late log phase  $10^8$  cfu/ml culture of either *Salmonella enterica* serovar Pullorum, serovar Pullorum *spaS*- or serovar Enteritidis.** Nitric oxide production is illustrated by the amount of nitrite present, measured by Griess assay on 50 µl of supernatants from gentamicin protection assays (n=3; SD±0.05).

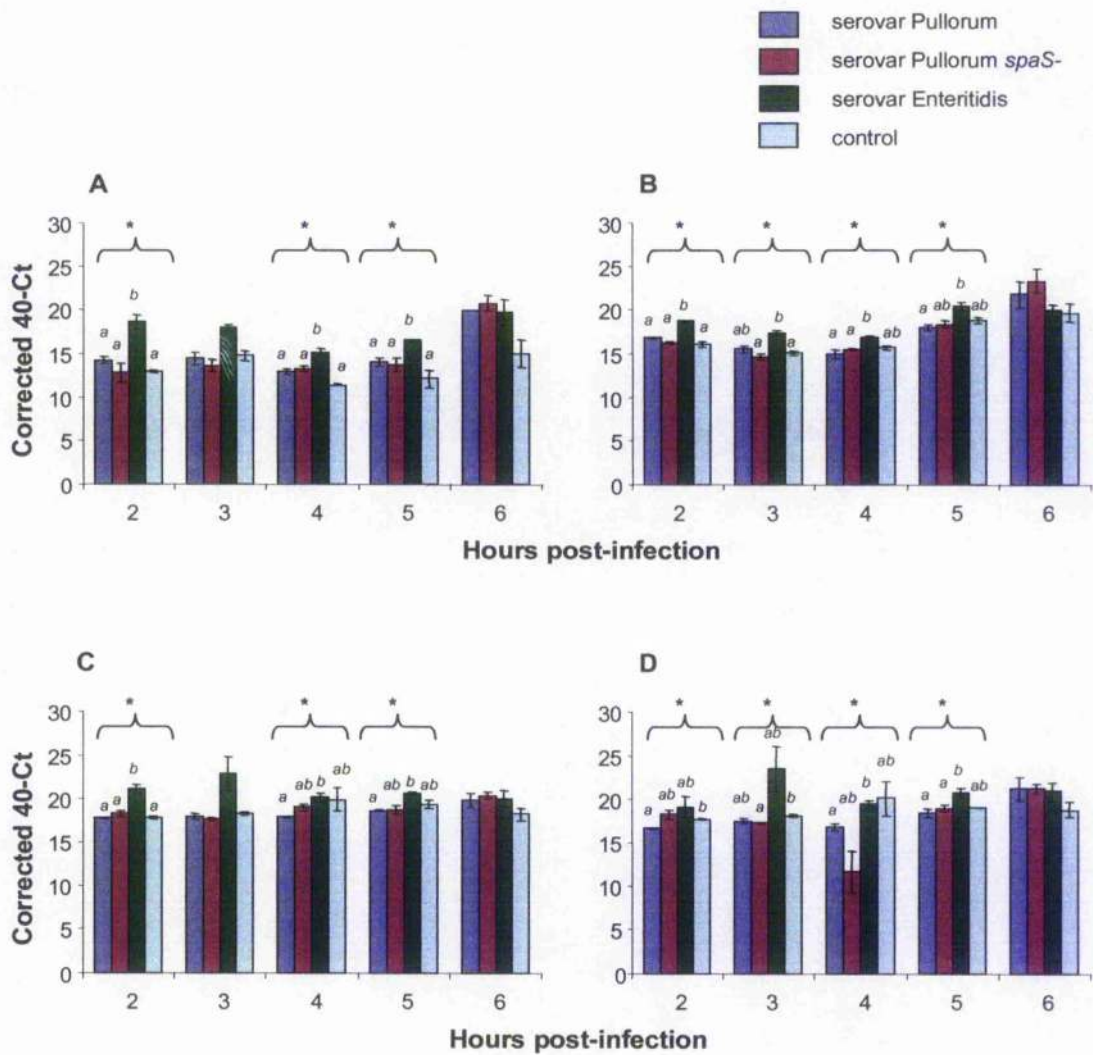


**Figure 5.3:** IL-1 $\beta$  (A), IL-6 (B), CXCLi1 (C) and CXCLi2 (D) mRNA expression levels in CKC following infection with 100  $\mu$ l/ml of a late log phase  $10^8$  cfu/ml culture of either *Salmonella enterica* serovar Pullorum, serovar Pullorum *spaS*-, serovar Enteritidis or mock-infected control. mRNA levels expressed as corrected 40-Ct values obtained by real-time qRT-PCR (n=3; SE $\pm$ 0.05). Statistical significance within a time point is represented by \*. Bars, within same time point for each cytokine, not sharing a letter (when letters are shown) are statistically significantly different.

serovar Enteritidis infection were significantly up-regulated compared to those during infection with serovar Pullorum ( $P=0.015$ ), with *spaS* ( $P=0.054$ ) and for the mock-infected control cells ( $P=0.0025$ ). There was no significant difference between IL-1 $\beta$  mRNA expression levels during serovar Pullorum and *spaS* infections across the time-course.

Figure 5.3B shows the expression profile of IL-6 mRNA for the differentially infected cells across the time-course. At 2 hpi, IL-6 mRNA expression was significantly up-regulated in serovar Enteritidis-infected cells compared to levels in serovar Pullorum-infected ( $P=0.001$ ), *spaS*-infected ( $P=0.001$ ) and in mock-infected control cells ( $P=0.003$ ). At 3 hpi, in serovar Enteritidis-infected cells there was a significant up-regulation of IL-6 mRNA levels compared to those in *spaS*-infected cells ( $P=0.016$ ) and in control cells ( $P=0.048$ ). At 4 hpi serovar Enteritidis-infected cells had significantly up-regulated IL-6 mRNA levels compared to serovar Pullorum-infected ( $P=0.046$ ) and *spaS*-infected cells ( $P=0.017$ ). By 5 hpi, this significant up-regulation was only evident when comparing serovar Enteritidis-infected cells to serovar Pullorum-infected cells ( $P=0.025$ ). There was no significant difference in IL-6 mRNA levels between the differentially infected cells at 6 hpi. There was no significant difference between IL-6 mRNA expression levels during serovar Pullorum and *spaS* infections across the time-course.

Figure 5.3C shows the mRNA expression profile for CXCL11 across the time-course. At 2 hpi, CXCL11 mRNA expression levels were significantly higher during serovar Enteritidis infection when compared to those measured during serovar Pullorum infection ( $P=0.005$ ), *spaS* infection ( $P=0.015$ ) and for the control cells ( $P=0.006$ ). At 4 and 5 hpi, levels of CXCL11 mRNA during serovar Enteritidis infection were significantly higher than those measured during serovar Pullorum infection ( $P=0.025$

and  $P=0.002$ ) and at 5 hpi during *spaS* infection ( $P=0.047$ ). There was no significant difference in CXCLi1 mRNA levels between the differentially infected cells at 6 hpi. There was no significant difference between CXCLi1 mRNA expression levels during serovar Pullorum and *spaS* infections across the time-course.

Figure 5.3D shows the CXCLi2 mRNA expression profile over the time-course of the experiment. There were significant differences between the levels of CXCLi2 mRNA expression for the groups of differentially-infected cells at 2, 3, 4 and 5 hpi. At 2 hpi, CXCLi2 mRNA expression by serovar Pullorum-infected cells was significantly down-regulated when compared to control cells ( $P=0.001$ ). At 3 hpi, the *spaS*-infected cells had significantly down-regulated CXCLi2 mRNA levels compared to those measured in the control cells ( $P=0.008$ ). At 4 and 5 hpi, CXCLi2 mRNA levels from serovar Enteritidis-infected cells were significantly up-regulated when compared to those measured in serovar Pullorum-infected cells ( $P=0.010$ ,  $P=0.030$  respectively). At 5 hpi, there was also significant up-regulation of CXCLi2 mRNA during serovar Enteritidis infection when compared to *spaS* infection ( $P=0.052$ ). There was no significant difference between CXCLi2 mRNA expression levels during serovar Pullorum and *spaS* infections across the time-course.

### 5.3.2 The effect of SPI-2 TTSS on invasion of CKC with serovar Pullorum

Intracellular bacterial counts from CKC over a time-course following infection with either serovar Pullorum, serovar Pullorum *ssaU* attenuated mutant or serovar Enteritidis are shown in Figure 5.4. The cells were also mock infected as a control, and these results were negative for the time course demonstrating that the cells were not contaminated during the experiment. Intracellular bacterial counts during serovar

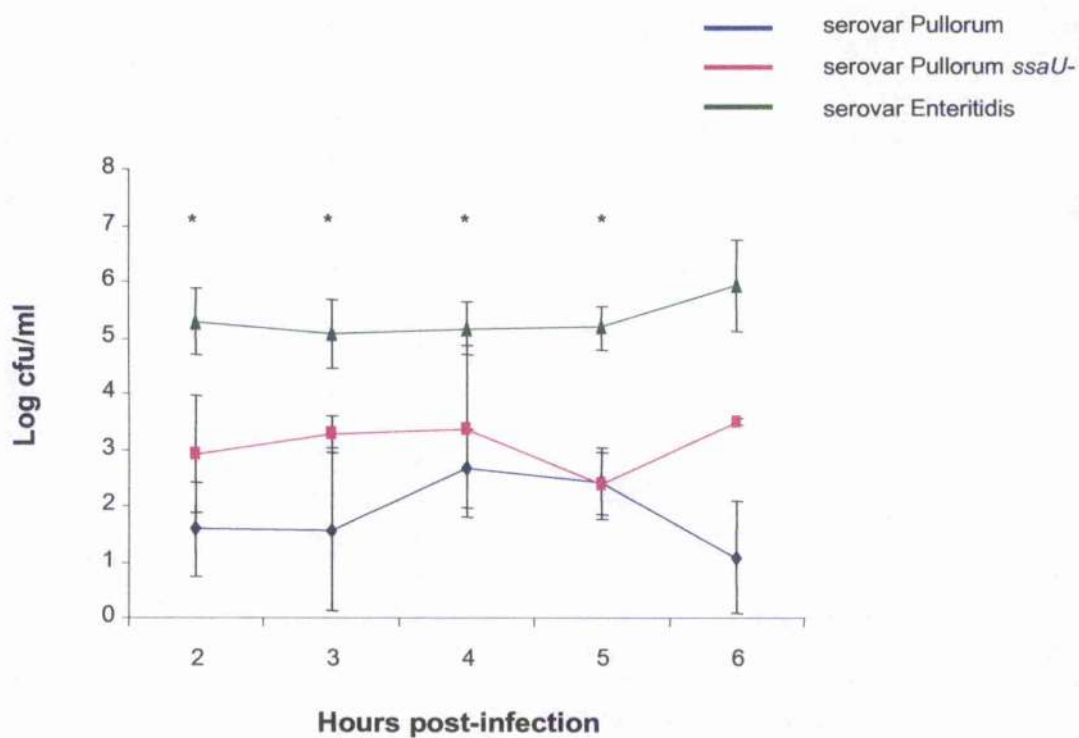
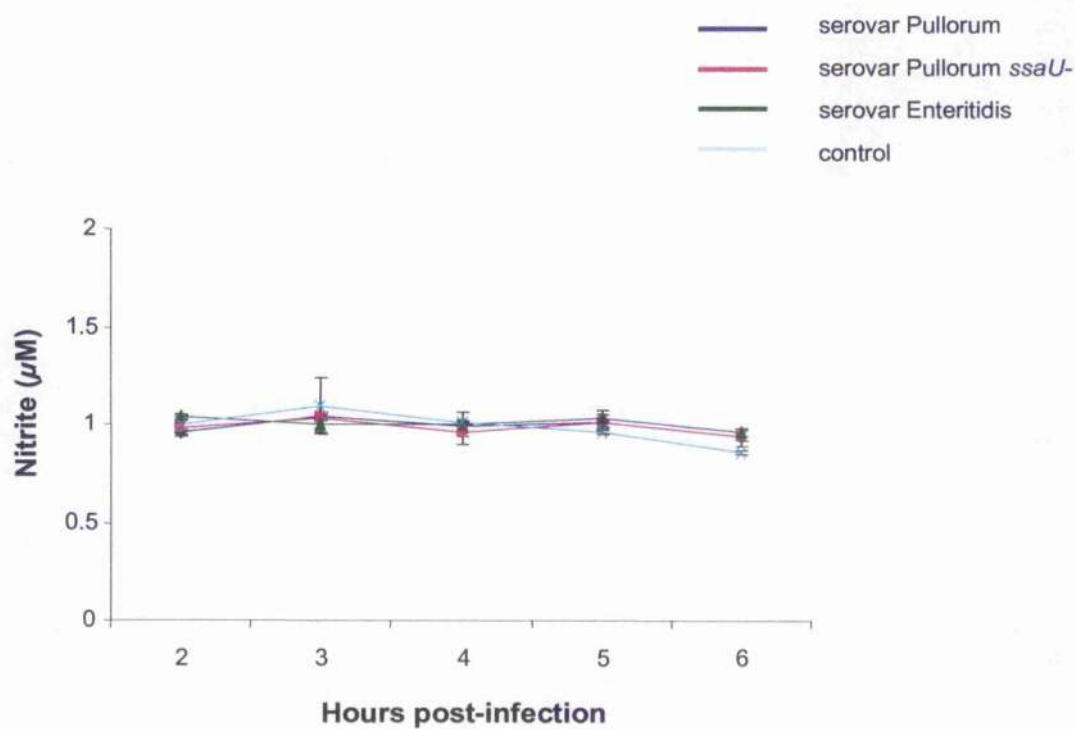


**Figure 5.4: Intracellular bacterial counts from CKC following infection with 100  $\mu$ l/ml of a late log phase  $10^8$  cfu/ml culture of either *Salmonella enterica* serovar Pullorum, serovar Pullorum ssaU- or serovar Enteritidis. Bacterial counts expressed as log cfu/ml (n=9; SD $\pm$ 0.05). Statistical significance represented by \*.**

Enteritidis infection were relatively stable over the time-course at between 5 and 6 log/ml, and significantly higher than those during serovar Pullorum infection at 2, 3, 4 and 5 hpi ( $P=0.003$ ,  $P=0.018$ ,  $P=0.007$  and  $P=0.003$  respectively) and during *ssaU* infection at 2, 3 and 5 hpi ( $P=0.026$ ,  $P=0.011$  and  $P=0.002$  respectively). There was no significant difference between numbers of intracellular serovar Pullorum and *ssaU* over the time-course.

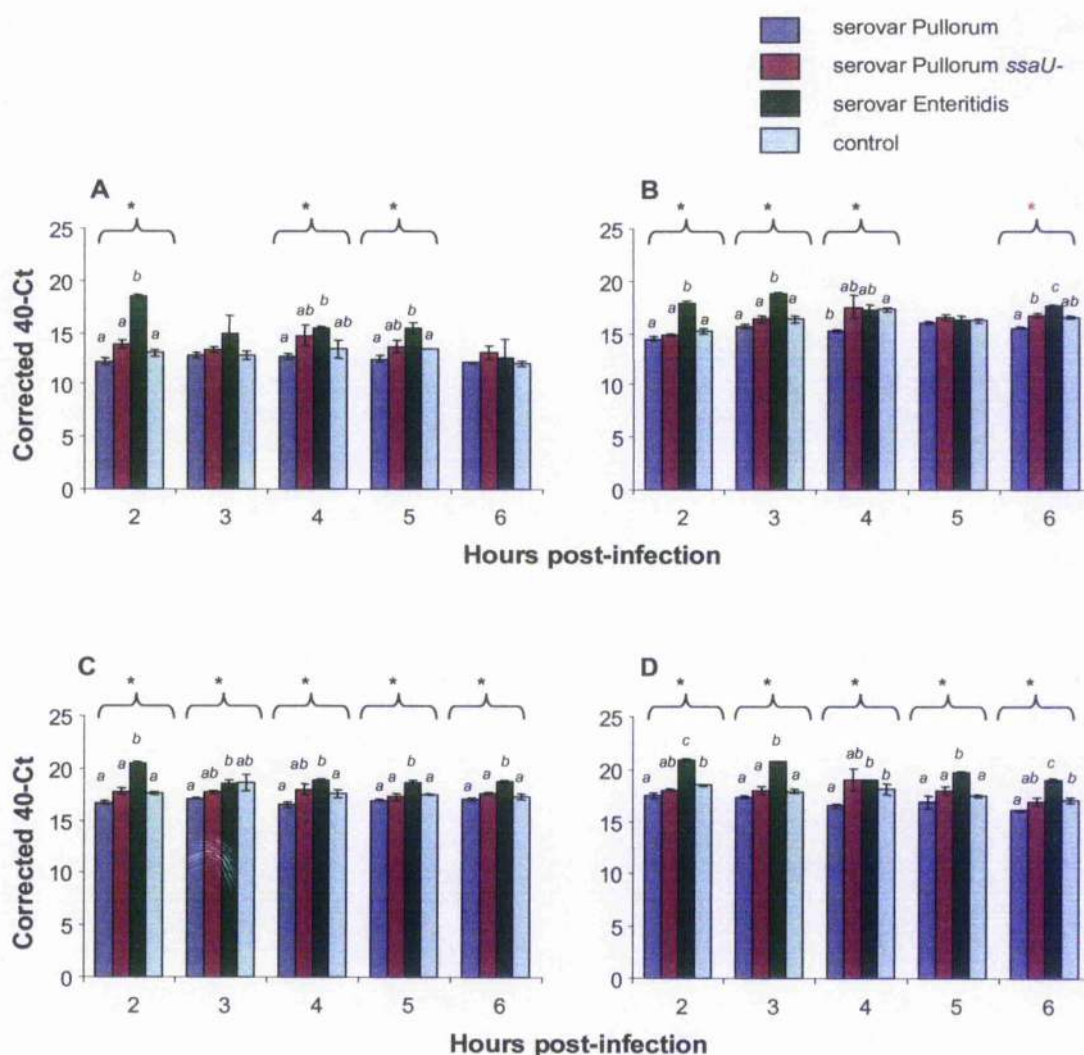
Griess assays performed on the supernatants collected from the gentamicin protection assay are shown in Figure 5.5. Across the time-course, there was no significant difference between nitrite levels measured during intracellular serovar Pullorum, *ssaU* or serovar Enteritidis infection, or for the control mock-infected CKC cells, with levels remaining at approximately 1  $\mu\text{M}$  nitrite for the duration of the experiment.

Figure 5.6 shows cytokine mRNA expression in the same CKC. IL-1 $\beta$  mRNA expression levels during the experiment are shown in Figure 5.6A. There was significant up-regulation of IL-1 $\beta$  mRNA expression levels at 2 hpi during infection with serovar Enteritidis compared to those during infection with serovar Pullorum ( $P=0.000$ ), with *ssaU* ( $P=0.001$ ) and in the control cells ( $P=0.000$ ). At 4 hpi, IL-1 $\beta$  mRNA expression levels during serovar Enteritidis infection were significantly up-regulated compared to those measured during serovar Pullorum infection ( $P=0.001$ ). At 5 hpi, there was significant up-regulation of IL-1 $\beta$  mRNA expression levels during serovar Enteritidis infection compared to those measured during serovar Pullorum infection ( $P=0.018$ ) and in the control cells ( $P=0.000$ ). There was no significant difference between IL-1 $\beta$  mRNA expression levels during serovar Pullorum and *spaS* infections across the time-course.



**Figure 5.5: Nitric oxide production by CKC following infection with 100 µl/ml of a late log phase 10<sup>8</sup> cfu/ml culture of either *Salmonella enterica* serovar Pullorum, serovar Pullorum ssaU- or serovar Enteritidis.** Nitric oxide production is illustrated by the amount of nitrite present, measured by Griess assay on 50 µl of supernatants from gentamicin protection assays (n=3; SD±0.05).





**Figure 5.6: IL-1 $\beta$  (A), IL-6 (B), CXCLi1 (C) and CXCLi2 (D) mRNA expression levels of CKC following infection with 100  $\mu$ l/ml of a late log phase  $10^8$  cfu/ml culture of either *Salmonella enterica* serovar Pullorum, serovar Pullorum *ssaU*-, serovar Enteritidis or mock-infected control. mRNA levels expressed as corrected 40-Ct values obtained by real-time qRT-PCR. (n=3; SE $\pm$ 0.05). Statistical significance within a group is represented by \*, or \* for significance that is SPI-2 TTSS-mediated. Bars, within same time point for each cytokine, not sharing a letter (when letters are shown) are statistically significantly different.**

IL-6 mRNA expression levels during the experiment are shown in Figure 5.6B. At 2 and 3 hpi, IL-6 mRNA expression during serovar Enteritidis infection was significantly up-regulated compared to those levels measured during serovar Pullorum infection ( $P=0.000$  and  $P=0.001$  respectively), *ssaU* infection ( $P=0.001$  and  $P=0.006$  respectively) and in the control cells ( $P=0.002$ ,  $P=0.007$ ). At 4 hpi, IL-6 mRNA expression levels during serovar Pullorum infection were significantly down-regulated when compared to the control ( $P=0.004$ ). At 6 hpi, IL-6 mRNA expression levels during serovar Enteritidis infection are significantly up-regulated when compared to those levels measured during serovar Pullorum infection ( $P=0.001$ ), *ssaU* infection ( $P=0.050$ ) or in the control cells ( $P=0.020$ ). At 6 hpi there was a significant up-regulation of IL-6 mRNA levels measured during *ssaU* infection compared to those measured during serovar Pullorum infection ( $P=0.015$ ). This was the only time point at which there was a significant difference between IL-6 mRNA expression levels during serovar Pullorum and *ssaU* infections.

CXCL11 mRNA expression levels during the experiment are shown in Figure 5.6C. There was significant up-regulation of CXCL11 mRNA expression levels during serovar Enteritidis infection compared to levels measured during serovar Pullorum infection at 2, 3, 4, 5 and 6 hpi ( $P=0.000$ ,  $P=0.040$ ,  $P=0.006$ ,  $P=0.018$  and  $P=0.002$  respectively). At 2 and 6 hpi, CXCL11 mRNA expression was significantly up-regulated during serovar Enteritidis infection compared to levels measured during *ssaU* infection ( $P=0.005$  and  $P=0.011$  respectively) and to those levels measured for the control cells at 2, 4 and 6 hpi ( $P=0.001$ ,  $P=0.039$  and  $P=0.022$  respectively). There was no significant difference between CXCL11 mRNA expression levels during serovar Pullorum and *ssaU* infections across the time-course.

CXCLi2 mRNA levels are shown in Figure 5.6D. Again, as for the CXCLi1 expression profile, CXCLi2 mRNA expression levels during serovar Enteritidis infection were significantly up-regulated at all time-points compared to those measured during serovar Pullorum infection ( $P=0.001$ ,  $P=0.001$ ,  $P=0.000$ ,  $P=0.0026$  and  $P=0.000$  respectively). There was up-regulation of CXCLi2 mRNA levels during serovar Enteritidis infection at 2, 3, 5 and 6 hpi compared to those measured during *ssaU* infection ( $P=0.000$ ,  $P=0.015$ ,  $P=0.050$  and  $P=0.015$  respectively) and in the control cells ( $P=0.000$ ,  $P=0.004$ ,  $P=0.002$  and  $P=0.008$  respectively). At 2, 4 and 6 hpi CXCLi2 mRNA levels measured during serovar Pullorum infection were significantly down-regulated compared to those measured in the control cells ( $P=0.039$ ,  $P=0.041$  and  $P=0.047$  respectively), and at 2 hpi were significantly down-regulated during *ssaU* infection compared to levels in the control cells ( $P=0.020$ ). There was no significant difference between CXCLi2 mRNA expression levels during serovar Pullorum and *ssaU* infections across the time-course.

### 5.3.3 The effect of SPI-1 TTSS on invasion of HD11 cells with serovar Pullorum

Intracellular bacterial counts from HD11 cells over a 24 h time-course following infection with either serovar Pullorum, *spaS* or serovar Enteritidis are shown in Figure 5.7. Cells were also mock-infected as a control. These cells were negative for intracellular bacterial counts for the duration of the time-course, demonstrating that the cells were not contaminated. At 2 hpi, intracellular serovar Enteritidis bacterial counts were significantly higher compared to those measured for serovar Pullorum ( $P=0.002$ ) and for the *spaS*-attenuated mutant ( $P=0.003$ ) by approximately 1 log. There was no

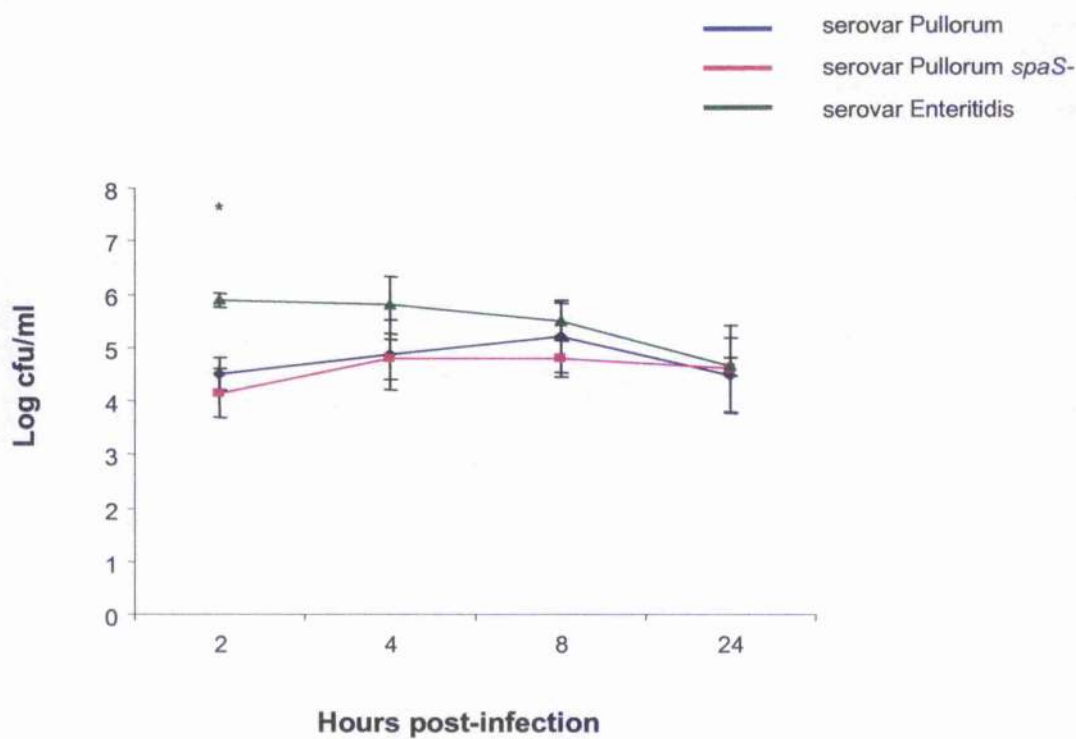


**Figure 5.7: Intracellular bacterial counts from HD11 cells following infection with 100  $\mu$ l/ml of a late log phase  $10^8$  cfu/ml culture of either *Salmonella enterica* serovar Pullorum, serovar Pullorum *spaS*- or serovar Enteritidis. Bacterial counts expressed as log cfu/ml (n=9; SD $\pm$ 0.05). Statistical significance represented by \*.**

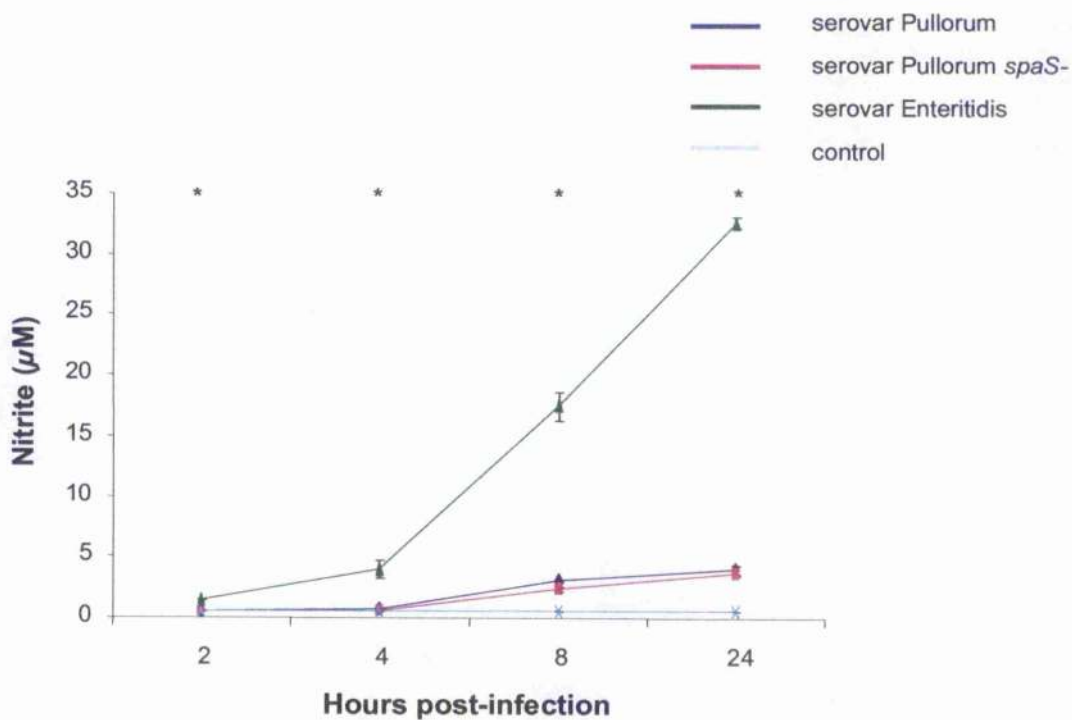


**Figure 5.8: Nitric oxide production of HD11 cells following infection with 100 µl/ml of a late log phase 10<sup>8</sup> cfu/ml culture of either *Salmonella enterica* serovar Pullorum, serovar Pullorum *spaS*- or serovar Enteritidis.** Nitric oxide production is illustrated by the amount of nitrite present, measured by Griess assay on 50 µl supernatants from gentamicin protection assays (n=3; SD±0.05). Statistical significance represented by \*.

significant difference between the bacterial numbers in any of the differentially infected cells at the other time-points.

Griess assays performed on the supernatants collected from the gentamicin protection assays are shown in Figure 5.8. The amounts of nitrite measured in the supernatants following serovar Enteritidis infection of the HD11 cells were significantly higher at 2, 4, 8 and 24 hpi compared to those produced following serovar Pullorum infection ( $P=0.001$ ,  $P=0.019$ ,  $P=0.008$  and  $P=0.000$  respectively), *spaS* infection ( $P=0.001$ ,  $P=0.016$ ,  $P=0.006$  and  $P=0.000$  respectively) and in the control cells ( $P=0.001$ ,  $P=0.015$ ,  $P=0.004$  and  $P=0.000$  respectively). The levels of nitrite produced following serovar Pullorum infection were significantly greater than those measured in the supernatants of control cells at 8 and 24 hpi ( $P=0.004$  and  $P=0.000$ ), and also significantly greater following *spaS* infection compared to those in the control cells at 8 and 24 hpi ( $P=0.001$  and  $P=0.005$  respectively). There were no significant differences between the levels of nitrite produced following serovar Pullorum infection compared to *spaS* infection for the time-course.

Figure 5.9 shows cytokine mRNA expression in the same HD11 cells. IL-1 $\beta$  mRNA expression levels during the experiment are shown in Figure 5.9A. At 2 hpi, IL-1 $\beta$  mRNA expression levels following serovar Enteritidis and *spaS* infection of HD11 cells were significantly up-regulated compared to those measured in control cells ( $P=0.003$  and  $P=0.001$  respectively). At 4 hpi, IL-1 $\beta$  mRNA levels following serovar Pullorum infection were significantly up-regulated when compared to those measured following infection with serovar Enteritidis ( $P=0.010$ ). IL-1 $\beta$  mRNA levels at 8 hpi during serovar Enteritidis, serovar Pullorum and *spaS* infection were significantly up-regulated compared to those in control cells ( $P=0.003$ ,  $P=0.001$  and  $P=0.001$

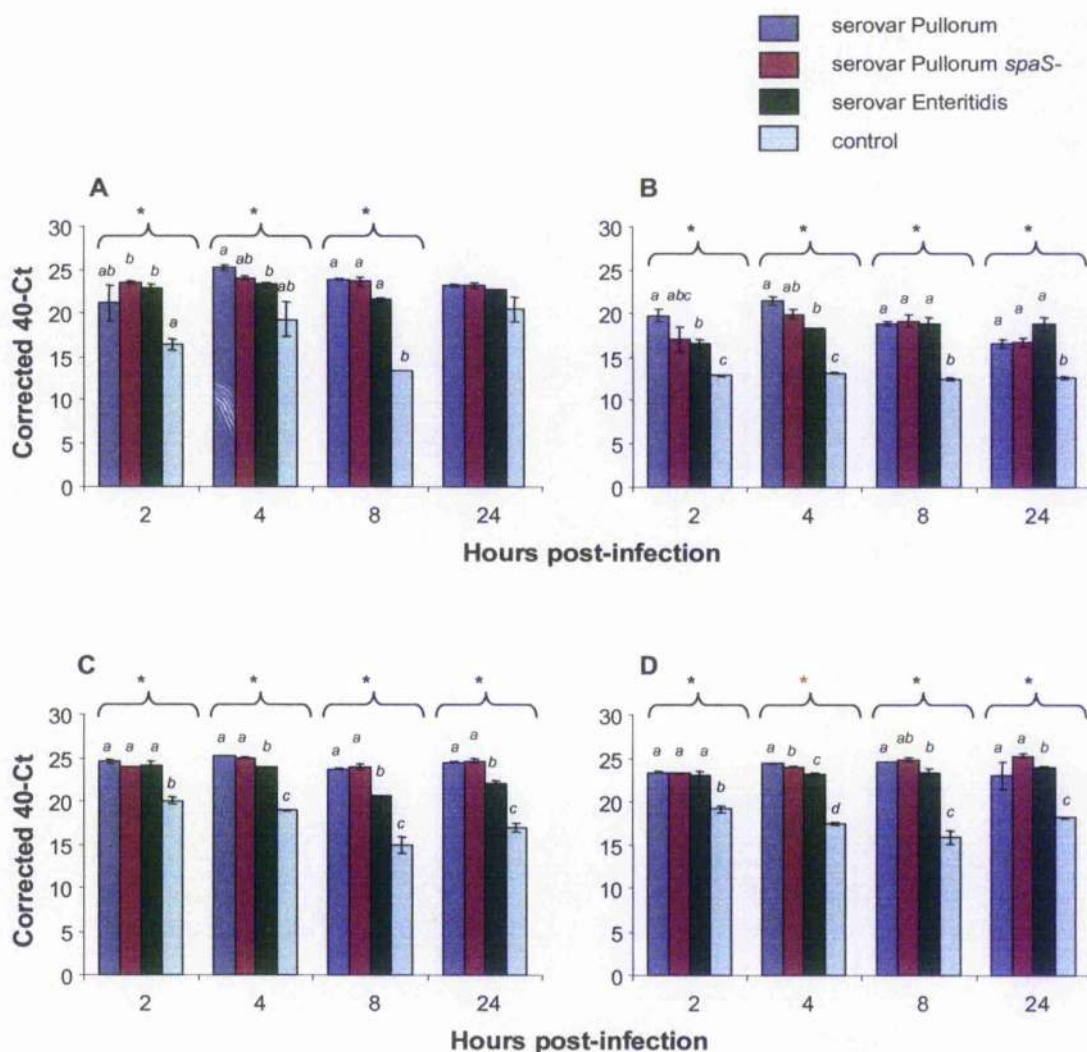


**Figure 5.9: IL-1 $\beta$  (A), IL-6 (B), CXCLi1 (C) and CXCLi2 (D) mRNA expression levels of HD11 cells following infection with 100  $\mu$ l/ml of a late log phase  $10^8$  cfu/ml culture of either *Salmonella enterica* serovar Pullorum, serovar Pullorum *spaS*-, serovar Enteritidis or mock-infected control. mRNA levels expressed as corrected 40-Ct values obtained by real-time qRT-PCR. (n=3; SE $\pm$ 0.05). Statistical significance within a group is represented by \*, or \* for significance that is SPI-1 TTSS-mediated. Bars, within same time point for each cytokine, not sharing a letter (when letters are shown) are statistically significantly different.**

respectively). There was no significant difference between IL-1 $\beta$  mRNA expression levels during serovar Pullorum and *spaS* infections across the time-course.

IL-6 mRNA expression levels during the experiment are shown in Figure 5.9B.

Following infection with serovar Pullorum, IL-6 mRNA expression levels were significantly higher compared to those measured in the control cells at 2, 4, 8 and 24 hpi (P=0.002, P=0.002, P=0.000 and P=0.011 respectively). IL-6 mRNA expression levels during serovar Enteritidis infection were also significantly higher across the time-course when compared to those measured in the control cells (P=0.002, P=0.000, P=0.005 and P=0.034 respectively). Following *spaS* infection at 4, 8 and 24 hpi, IL-6 mRNA expression levels were significantly up-regulated compared to those measured in the control cells (P=0.004, P=0.002 and P=0.006 respectively). At 2 and 4 hpi, IL-6 mRNA expression levels during serovar Pullorum infection were significantly up-regulated compared to those measured during serovar Enteritidis infection (P=0.041 and P=0.007 respectively). There was no significant difference between IL-6 mRNA expression levels during serovar Pullorum and *spaS* infections across the time-course.

CXCLi1 mRNA expression levels for the experiment are shown in Figure 5.9C.

Across the time-course, compared to those measured in the control cells, levels of CXCLi1 mRNA were significantly up-regulated following infection with serovar Pullorum (P=0.001, P=0.000, P=0.001 and P=0.001 respectively), with *spaS* (P=0.001, P=0.000, P=0.001 and P=0.001 respectively) with serovar Enteritidis (P=0.009, P=0.000, P=0.003 and P=0.024 respectively). At 4, 8 and 24 hpi, compared to those measured during infection with serovar Enteritidis, CXCLi1 mRNA expression levels were up-regulated during infection with serovar Pullorum (P=0.001, P=0.000 and P=0.004 respectively) and with *spaS* (P=0.004, P=0.002 and P=0.012 respectively).



There was no significant difference between CXCLi1 mRNA expression levels during serovar Pullorum and *spaS* infections across the time-course.

Figure 5.9D shows CXCLi2 mRNA expression levels for the experiment. At 2 hpi, compared to those measured in the control cells, mRNA expression levels were up-regulated following infection with serovar Pullorum ( $P=0.002$ ), with *spaS* ( $P=0.002$ ) and with serovar Enteritidis ( $P=0.011$ ). CXCLi2 mRNA expression levels at 4 hpi in serovar Pullorum-infected cells were up-regulated compared to in *spaS*-infected cells ( $P=0.044$ ), serovar Enteritidis-infected cells ( $P=0.011$ ), and compared to those measured in the control cells ( $P=0.025$ ). CXCLi2 mRNA expression levels during *spaS* infection were significantly up-regulated compared to those measured during serovar Enteritidis infection ( $P=0.029$ ) and in the control cells ( $P=0.031$ ) at 4 hpi. At 8 hpi, mRNA expression levels following serovar Pullorum infection were up-regulated compared to those measured following serovar Enteritidis infection ( $P=0.050$ ), and compared to those in control cells ( $P=0.000$ ). CXCLi2 mRNA expression levels measured during both serovar Enteritidis and *spaS* infection of HD11 cells were significantly higher compared to those measured in control cells at 8 hpi ( $P=0.001$  and  $P=0.000$  respectively) and at 24 hpi ( $P=0.004$  and  $P=0.000$  respectively). CXCLi2 mRNA expression levels were significantly up-regulated following *spaS* infection at 24 hpi compared to those measured during serovar Enteritidis infection ( $P=0.052$ ).

#### **5.3.4 The effect of SPI-2 TTSS on invasion of HD11 cells with serovar Pullorum**

Intracellular bacterial counts from HD11 cells infected with either serovar Pullorum, with serovar Pullorum *ssaU* attenuated mutant or with serovar Enteritidis over a 24 h time-course are shown in Figure 5.10. The cells were also mock infected as

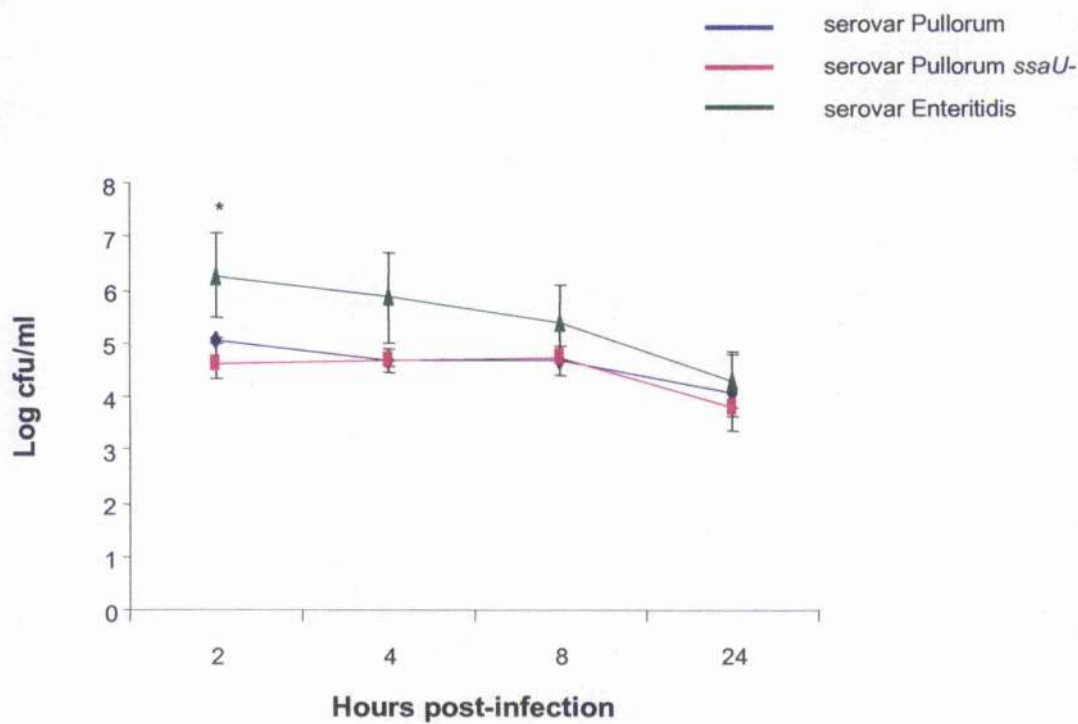


**Figure 5.10: Intracellular bacterial counts from HD11 cells following infection with 100  $\mu$ l/ml of a late log phase  $10^8$  cfu/ml culture of either *Salmonella enterica* serovar Pullorum, serovar Pullorum *ssaU*- or serovar Enteritidis. Bacterial counts expressed as log cfu/ml (n=9; SD $\pm$ 0.05). Statistical significance represented by \*.**

a control, and the results were negative for the time-course demonstrating that the cells were not contaminated. At 2 hpi, numbers of intracellular serovar Enteritidis were significantly higher compared to numbers of intracellular serovar Pullorum and *ssaU* ( $P=0.045$ ,  $P=0.026$ ) by approximately 1 log. There are no significant differences in the intracellular bacterial numbers of the differentially infected cells across the rest of the time-course and the numbers of all bacteria slightly decreased over time.

Griess assays performed on supernatants collected from the gentamicin protection assays are shown in Figure 5.11. Across the time-course, nitrite levels measured during intracellular serovar Enteritidis infection were significantly higher compared to those measured during serovar Pullorum infection ( $P=0.040$ ,  $P=0.015$ ,  $P=0.011$  and  $P=0.006$  respectively), *ssaU* infection ( $P=0.042$ ,  $P=0.015$ ,  $P=0.009$  and  $P=0.001$  respectively) and compared to those measured in control cells ( $P=0.041$ ,  $P=0.014$ ,  $P=0.004$  and  $P=0.000$  respectively). Nitrite levels increased across the time-course to a maximum of approximately 25  $\mu\text{M}$ . At 24 hpi, nitrite levels measured in the supernatants of serovar Pullorum-infected and *ssaU*-infected HD11 cells were significantly higher than those measured in the supernatants of control cells, at approximately 5  $\mu\text{M}$  compared to approximately 1  $\mu\text{M}$ .

Figure 5.12 shows cytokine mRNA expression in the same HD11 cells. IL-1 $\beta$  mRNA expression levels for the differentially infected HD11 cells across the time-course are shown in Figure 5.12A. At 2, 4, 8 and 24 hpi, compared to levels in control cells, there was significant up-regulation of IL-1 $\beta$  mRNA levels during serovar Pullorum infection ( $P=0.046$ ,  $P=0.002$ ,  $P=0.000$  and  $P=0.009$  respectively) and during *ssaU* infection ( $P=0.037$ ,  $P=0.001$ ,  $P=0.004$  and  $P=0.004$  respectively). IL-1 $\beta$  mRNA levels were up-regulated during serovar Enteritidis infection compared to those measured in the control cells at 4, 8 and 24 hpi ( $P=0.001$ ,  $P=0.000$  and  $P=0.009$  respectively).

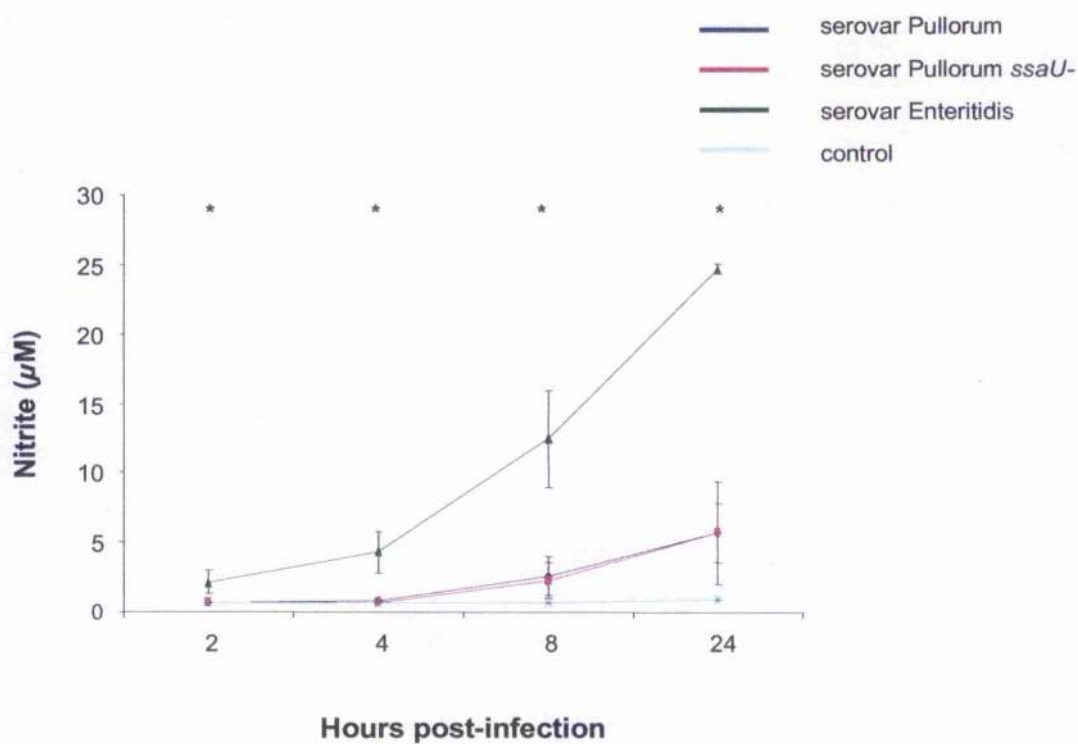


**Figure 5.11: Nitric oxide production by HD11 cells following infection with 100  $\mu\text{l/ml}$  of a late log phase  $10^8$  cfu/ml culture of either *Salmonella enterica* serovar Pullorum, serovar Pullorum *ssaU*- or serovar Enteritidis.** Nitric oxide production is illustrated by the amount of nitrite present, measured by Griess assay on 50  $\mu\text{l}$  of supernatants from gentamicin protection assays ( $n=3$ ;  $\text{SD}\pm 0.05$ ). Statistical significance represented by \*.

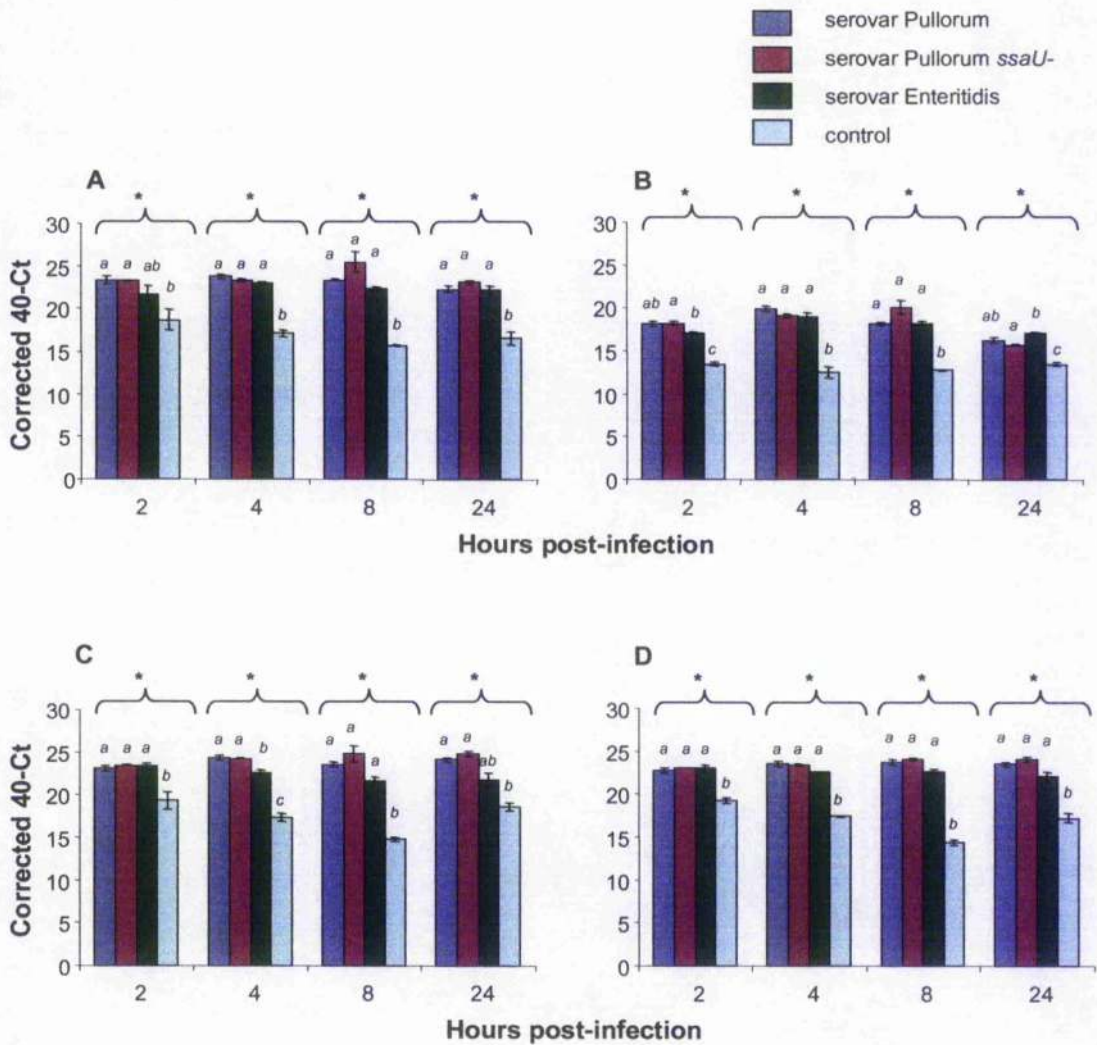


**Figure 5.12: IL-1 $\beta$  (A), IL-6 (B), CXCLi1 (C) and CXCLi2 (D) mRNA expression levels in HD11 cells following infection with 100  $\mu$ l/ml of a late log phase  $10^8$  cfu/ml culture of either *Salmonella enterica* serovar Pullorum, serovar Pullorum *ssaU*-, serovar Enteritidis or mock-infected control. mRNA levels expressed as corrected 40-Ct values obtained by real time qRT-PCR. (n=3; SE $\pm$ 0.05). Statistical significance within a group is represented by \*. Bars, within same time point for each cytokine, not sharing a letter (when letters are shown) are statistically significantly different.**

There was no significant difference between IL-1 $\beta$  mRNA expression levels during serovar Pullorum and *ssaU* infections across the time-course.

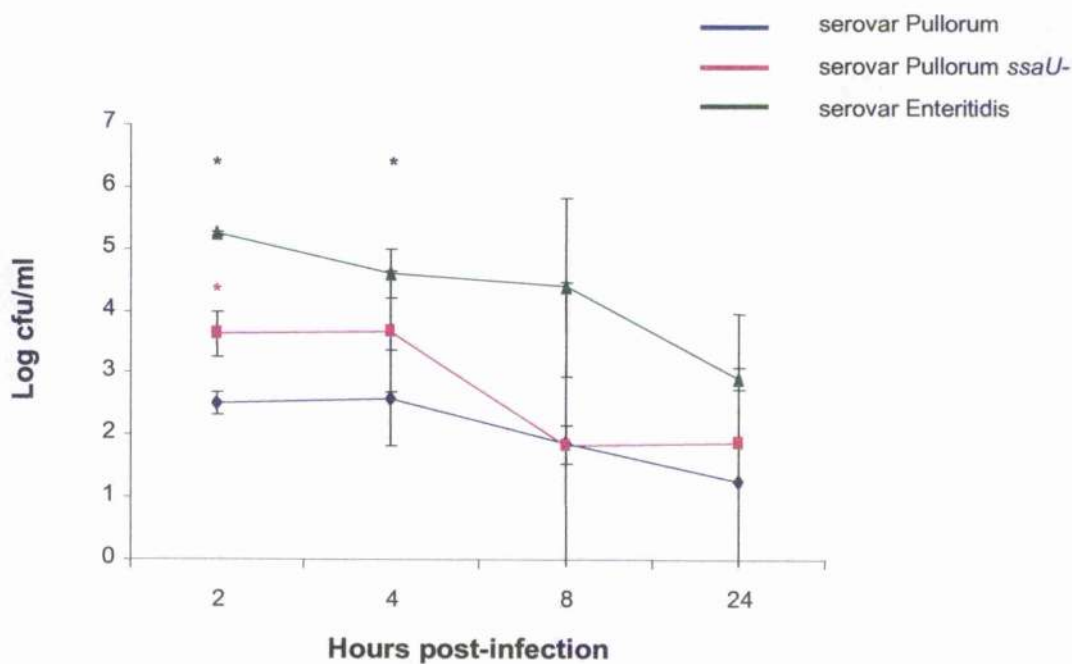
IL-6 mRNA expression levels during the experiment are shown in Figure 5.12B. Across the time course, compared to levels in control cells, there was significant up-regulation of IL-6 mRNA levels following infection with serovar Pullorum (P=0.001, P=0.004, P=0.000 and P=0.006 respectively), with *ssaU* (P=0.001, P=0.004, P=0.002 and P=0.008 respectively) and with serovar Enteritidis (P=0.002, P=0.006, P=0.000 and P=0.001 respectively). At 2 hpi, IL-6 mRNA expression levels in *ssaU*-infected cells were significantly up-regulated compared to those measured in serovar Enteritidis-infected cells (P=0.053), but by 24 hpi, levels were significantly down-regulated (P=0.052). There was no significant difference between IL-6 mRNA expression levels during serovar Pullorum and *ssaU* infections across the time-course.

Figure 5.12C shows expression levels of CXCLi1 mRNA during the experiment. There was significant up-regulation of CXCLi1 mRNA expression levels, compared to those measured for the control cells, at 2, 4, 8 and 24 hpi following infection with serovar Pullorum (P=0.054, P=0.003, P=0.000 and P=0.001 respectively) and *ssaU* (P=0.036, P=0.001, P=0.002 and P=0.001 respectively). Following serovar Enteritidis infection, there was significant up-regulation of CXCLi1 mRNA levels compared to those measured in control cells at 2, 4 and 8 hpi (P=0.048, P=0.005 and P=0.001 respectively). At 4 hpi, CXCLi1 mRNA expression levels of both serovar Pullorum-infected and *ssaU*-infected cells were significantly up-regulated compared to those measured for serovar Enteritidis-infected cells (P=0.035 and P=0.014 respectively). There was no significant difference between CXCLi1 mRNA expression levels during serovar Pullorum and *ssaU* infections across the time-course.

The CXCLi2 mRNA expression levels for the differentially infected HD11 cells across the time-course are shown in Figure 5.12D. There was significant up-regulation of CXCLi2 mRNA levels compared to those measured in control cells at 2, 4, 8 and 24 hpi following infection with serovar Pullorum (P=0.032, P=0.008, P=0.000 and P=0.000 respectively), with *ssaU* (P=0.021, P=0.007, P=0.000 and P=0.000 respectively) and with serovar Enteritidis (P=0.028, P=0.009, P=0.000 and P=0.003 respectively). There was no significant difference between CXCLi2 mRNA expression levels during serovar Pullorum and *ssaU* infections across the time-course.

### **5.3.5 The effect of SPI-2 TTSS on invasion of and persistence in bone marrow-derived macrophages with serovar Pullorum**

Intracellular bacterial counts from chicken bone marrow-derived macrophages (BM-dMΦ) infected on day 7 *ex vivo*, at 2, 4, 8 and 24 hpi following infection with serovar Pullorum, with serovar Pullorum *ssaU* attenuated mutant and with serovar Enteritidis are shown in Figure 5.13. The cells were also mock infected as a control, and the results were negative for the time-course demonstrating that the cells were not contaminated. At 2 hpi, numbers of intracellular *ssaU* were significantly higher (by approximately 1 log) compared to numbers of intracellular serovar Pullorum (P=0.008). Intracellular serovar Enteritidis bacterial numbers at 2 hpi were higher (by approximately 2.5 log) than those for serovar Pullorum (P=0.000), and (by approximately 1.5 log) than those for *ssaU* (P=0.001). At 4 hpi, serovar Enteritidis intracellular bacterial numbers were significantly higher compared to serovar Pullorum bacterial numbers (P=0.016). At 8 hpi, serovar Enteritidis intracellular bacterial numbers were significantly higher compared to *ssaU* bacterial numbers (P=0.041).



**Figure 5.13: Intracellular bacterial counts from chicken bone marrow-derived macrophages following infection with 100  $\mu$ l/ml of a late log phase  $10^8$  cfu/ml culture of either *Salmonella enterica* serovar Pullorum, serovar Pullorum *ssaU*- or serovar Enteritidis.** Gentamicin protection assays performed on day 7 of culture *ex vivo*. Bacterial counts expressed as log cfu/ml (n=9; SD $\pm$ 0.05). Statistical significance represented by \*, or \* for significance that is SPI-2 TTSS-mediated.



Griess assays performed on the supernatants collected from the gentamicin protection assays are shown in Figure 5.14. At 2, 4, 8 and 24 hpi, nitrite concentrations measured in the supernatants of serovar Enteritidis-infected cells were significantly higher than in serovar Pullorum-infected cells ( $P=0.009$ ,  $P=0.001$ ,  $P=0.000$  and  $P=0.000$  respectively), in *ssaU*-infected cells ( $P=0.009$ ,  $P=0.001$ ,  $P=0.000$  and  $P=0.000$  respectively) and when compared to those measured from control cells ( $P=0.009$ ,  $P=0.001$ ,  $P=0.000$  and  $P=0.000$  respectively). Nitrite levels following infection with serovar Enteritidis rose from approximately  $25 \mu\text{M}$  at 2 hpi to approximately  $45 \mu\text{M}$  at 24 hpi. Levels measured during serovar Pullorum infection, *ssaU* infection and in control cells did not rise above  $2.5 \mu\text{M}$  for the duration of the experiment.

Figure 5.15 shows cytokine mRNA expression levels in the same bone marrow-derived macrophages. The IL- $1\beta$  mRNA levels for the experiment are shown in Figure 5.15A. At 2 hpi, there were no significant differences between IL- $1\beta$  mRNA expression levels for the differentially infected cells. At 4, 8 and 24 hpi, compared to those measured for serovar Enteritidis-infected cells, IL- $1\beta$  mRNA expression levels were significantly up-regulated following serovar Pullorum infection ( $P=0.010$ ,  $P=0.001$  and  $P=0.004$  respectively) and following *ssaU* infection ( $P=0.050$ ,  $P=0.001$  and  $P=0.003$  respectively). IL- $1\beta$  mRNA levels were significantly up-regulated at 24 hpi, compared to those measured in control cells, during serovar Pullorum infection ( $P=0.044$ ) and during *ssaU* infection ( $P=0.041$ ). There was no significant difference between IL- $1\beta$  mRNA expression levels during serovar Pullorum and *ssaU* infections across the time-course.

The IL-6 mRNA expression levels for the experiment are shown in Figure 5.15B. Compared to levels in the control cells, there was significant up-

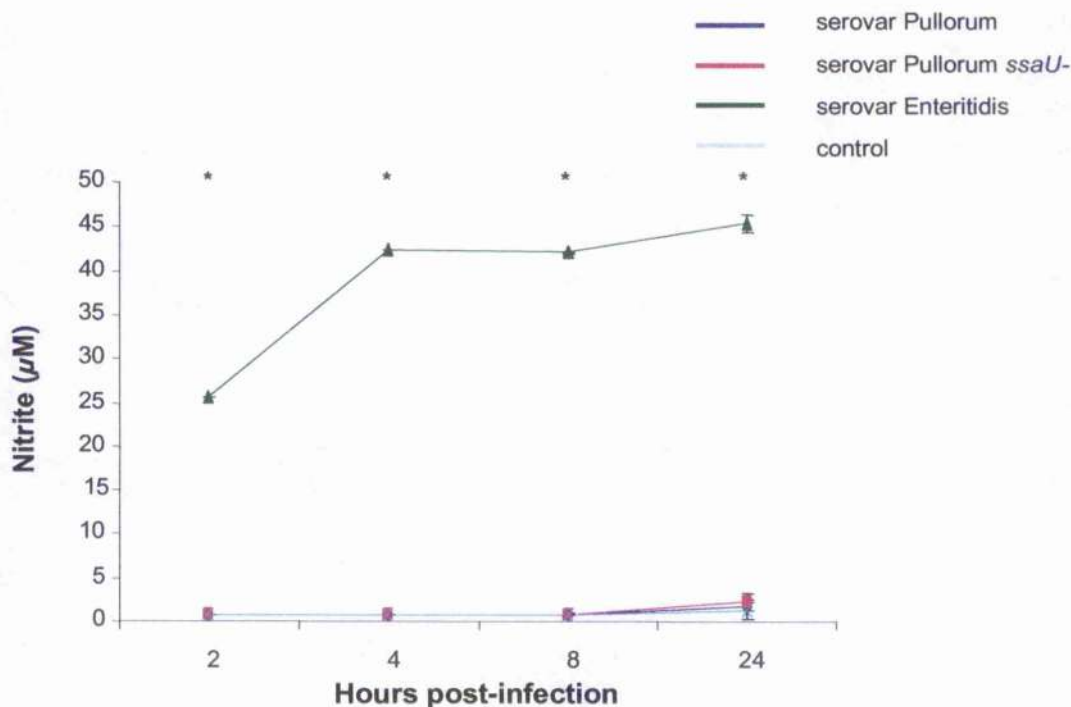


**Figure 5.14: Nitric oxide production by chicken bone marrow-derived macrophages following infection with 100 µl/ml of a late log phase 10<sup>8</sup> cfu/ml culture of either *Salmonella enterica* serovar Pullorum, serovar Pullorum ssaU- or serovar Enteritidis.**

Griess assay performed on supernatants from gentamicin protection assays performed on day 7 of culture *ex vivo*. Nitric oxide production is illustrated by the amount of nitrite present in 50 µl of supernatants from gentamicin protection assays (n=3; SD±0.05). Statistical significance represented by \*.

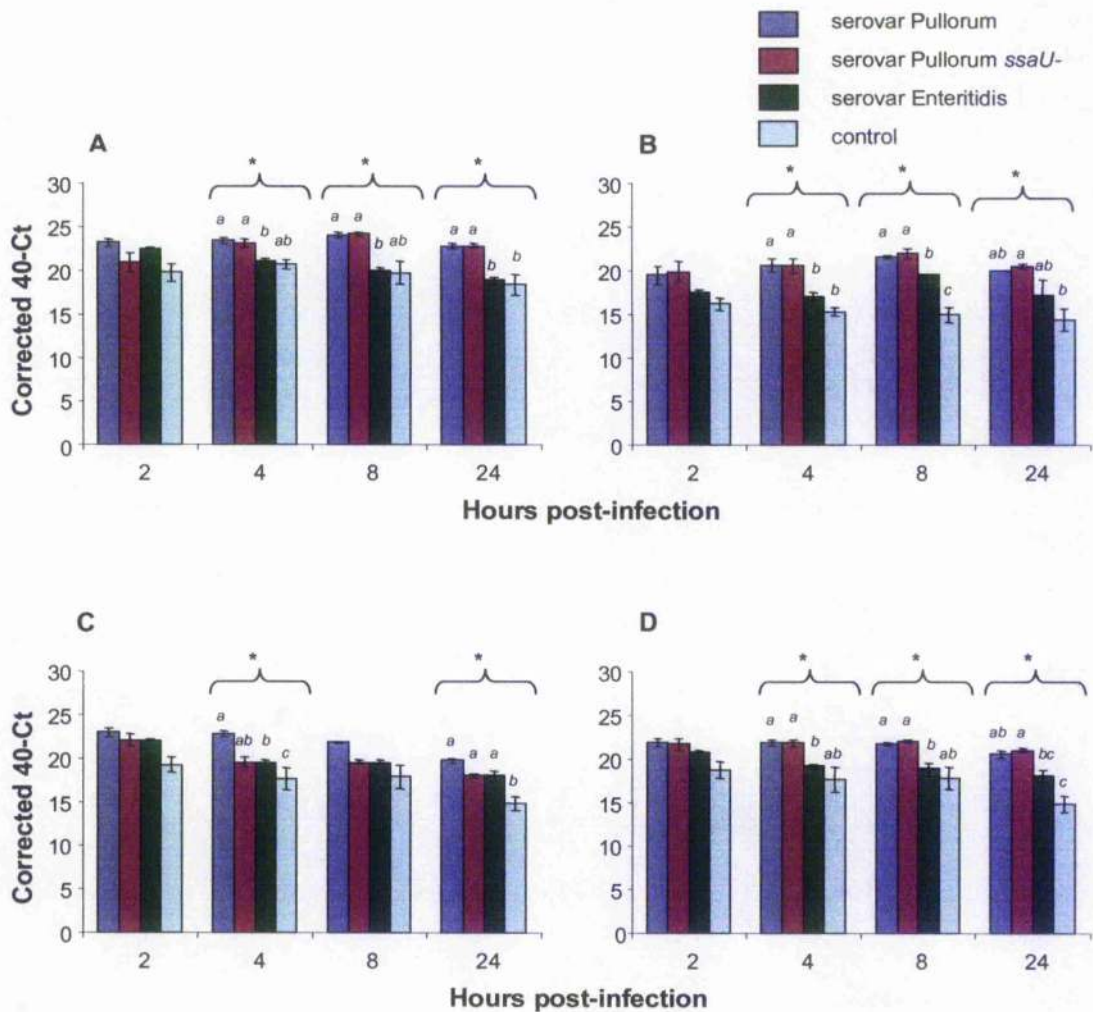


**Figure 5.15:** IL-1 $\beta$  (A), IL-6 (B), CXCLi1 (C) and CXCLi2 (D) mRNA expression levels in chicken bone marrow-derived macrophages following infection with 100  $\mu$ l/ml of a late log phase  $10^8$  cfu/ml culture of either *Salmonella enterica* serovar Pullorum, serovar Pullorum *ssaU*-, serovar Enteritidis or mock-infected control. mRNA levels expressed as corrected 40-Ct values obtained by real time qRT-PCR performed on mRNA isolated from day 7 of culture *ex vivo* (n=3; SE $\pm$ 0.05). Statistical significance within a group is represented by \*. Bars, within same time point for each cytokine, not sharing a letter (when letters are shown) are statistically significantly different.

regulation of IL-6 mRNA levels during infection with serovar Pullorum at 4 and 8 hpi (P=0.010 and P=0.003 respectively), with *ssaU* at 4, 8 and 24 hpi (P=0.016, P=0.005 and P=0.023 respectively) and with serovar Enteritidis at 8 hpi (P=0.012). There was significant up-regulation of IL-6 mRNA levels, compared to those measured following infection with serovar Enteritidis, at 4 and 8 hpi following infection with serovar Pullorum (P=0.029 and P=0.001 respectively) and with *ssaU* (P=0.047 and P=0.028 respectively). There was no significant difference between IL-6 mRNA expression levels during serovar Pullorum and *ssaU* infections across the time-course.

Expression levels of CXCLi1 mRNA are shown in Figure 5.15C. At 4 and 24 hpi, CXCLi1 mRNA expression levels were significantly up-regulated following serovar Pullorum infection compared to those in control cells (P=0.038 and P=0.009 respectively). Following *ssaU* infection this up-regulation of mRNA levels compared to serovar Enteritidis was significant at 4 hpi (P=0.021) and compared to the control was significant at 24 hpi (P=0.007). At 24 hpi, during serovar Enteritidis infection, there was significant up-regulation of CXCLi1 mRNA levels compared to those measured in control cells (P=0.053). There was significant up-regulation of CXCLi1 mRNA levels, compared to those measured during infection with serovar Enteritidis, at 4 hpi with serovar Pullorum (P=0.007). There was no significant difference between CXCLi1 mRNA expression levels during serovar Pullorum and *ssaU* infections across the time-course.

The CXCLi2 mRNA expression levels for the experiment are shown in Figure 5.15D. There was significant up-regulation of CXCLi2 mRNA levels at 4 and 8 hpi, compared to those measured following serovar Enteritidis infection, during serovar Pullorum infection (P=0.005 and P=0.041 respectively), also at 4, 8 and 24 hpi during *ssaU* infection (P=0.009, P=0.031 and P=0.038 respectively). At 24 hpi, compared to

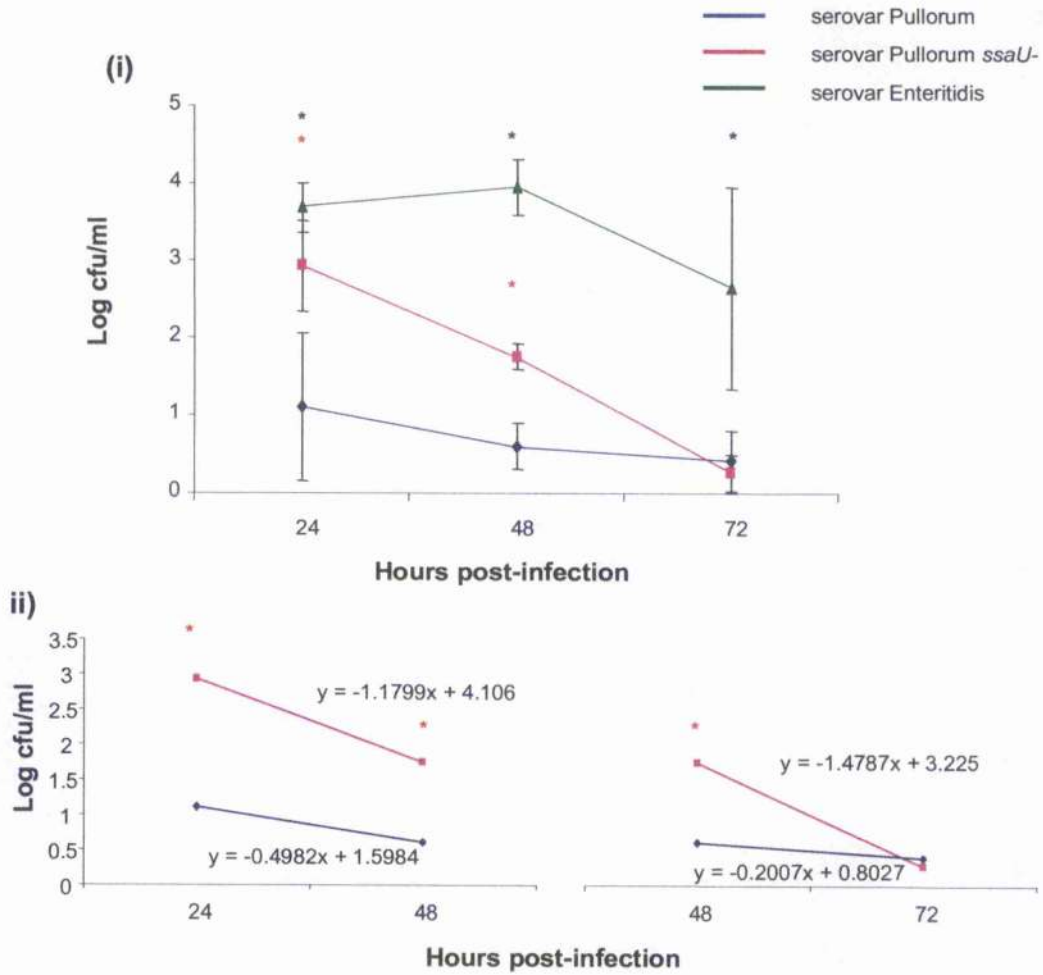


**Figure 5.16: Intracellular bacterial counts from chicken bone marrow-derived macrophages following infection with 100  $\mu$ l/ml of a late log phase  $10^8$  cfu/ml culture of (i) either *Salmonella enterica* serovar Pullorum, serovar Pullorum *ssaU*- or serovar Enteritidis, and (ii) comparison of the gradients of the time course for serovar Pullorum and serovar Pullorum *ssaU*- . Gentamicin protection assays performed on day 5 of culture *ex vivo*. Bacterial counts expressed as log cfu/ml (n=9; SD $\pm$ 0.05). Statistical significance represented by \*, or \* for significance that is SPI-2 TTSS-mediated.**

levels in control cells, there was significant up-regulation of CXCLi2 mRNA levels following serovar Pullorum infection ( $P=0.014$ ), and following *ssaU* infection ( $P=0.009$ ). There was no significant difference between CXCLi2 mRNA expression levels during serovar Pullorum and *ssaU* infections across the time-course.

Intracellular bacterial counts from BM-dMΦ infected on day 5 *ex vivo* with either serovar Pullorum, serovar Pullorum *ssaU* attenuated mutant or with serovar Enteritidis at 24, 48 and 72 hpi are shown in Figure 5.16. The cells were also mock infected as a control, and the results were negative for the time-course demonstrating that the cells were not contaminated. Intracellular bacterial numbers of *ssaU* were significantly higher compared to those measured for serovar Pullorum at 24 and 48 hpi ( $P=0.048$  and  $P=0.010$  respectively). The intracellular levels of *ssaU* were high (approximately log 3) at 24 hpi, but they then fell dramatically over the time-course to numbers similar to those measured following serovar Pullorum infection. Numbers of intracellular serovar Pullorum bacteria remained relatively stable over the time-course, with much lower gradients when plotted across the time-course, compared to those measured for *ssaU*. Numbers of intracellular serovar Enteritidis were significantly higher compared to those of serovar Pullorum at 24 and 48 hpi ( $P=0.011$  and  $P=0.009$  respectively), and significantly higher compared to those of *ssaU* at 48 and 72 hpi ( $P=0.002$  and  $P=0.044$  respectively).

Griess assays performed on supernatants from the experiment collected from the gentamicin protection assays are shown in Figure 5.17. At 24 hpi, there were no significant differences between the nitrite levels measured following serovar Pullorum and *ssaU* infection. By 48 hpi, though, the *ssaU*-infected BM-dMΦ cells produced significantly increased levels of nitrite compared to those measured from the serovar Pullorum infected cells ( $P=0.025$ ) and this significant increase continued to 72 hpi

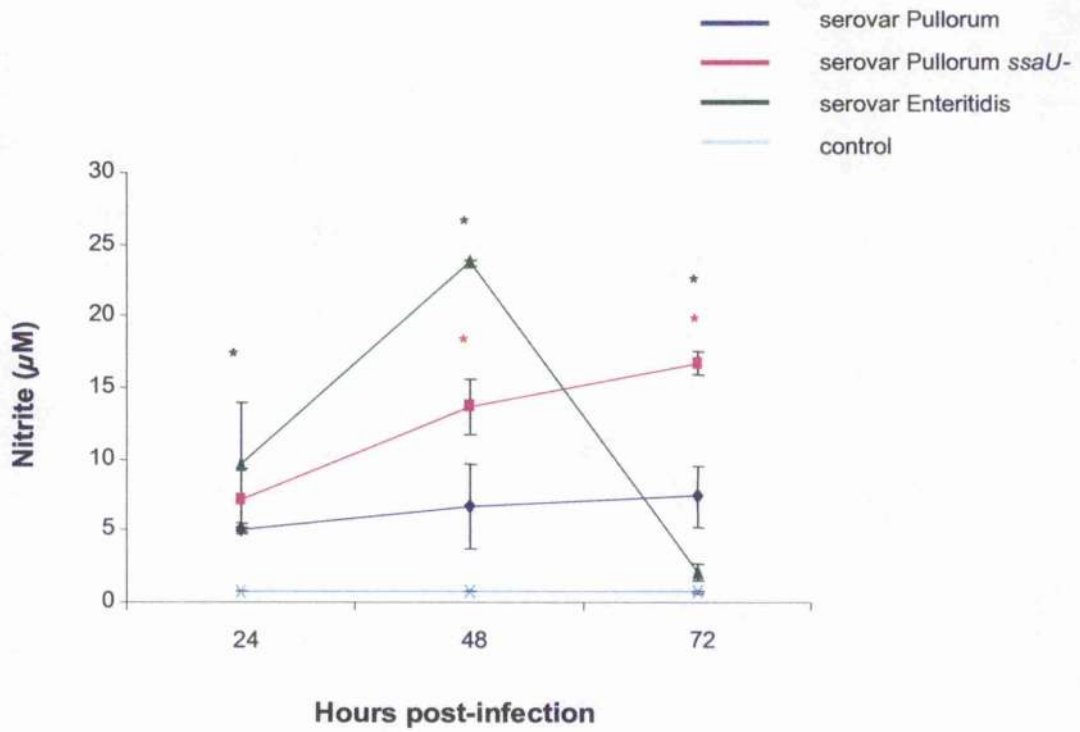


**Figure 5.17: Nitric oxide production by chicken bone marrow-derived macrophages following infection with 100  $\mu\text{l/ml}$  of a late log phase  $10^8$  cfu/ml culture of either *Salmonella enterica* serovar Pullorum, serovar Pullorum ssaU- or serovar Enteritidis.**

Griess assay performed on supernatants from gentamicin protection assays performed on day 5 of culture *ex vivo*. Nitric oxide production is illustrated by the amount of nitrite present in 50  $\mu\text{l}$  supernatants from gentamicin protection assays ( $n=3$ ;  $SD\pm 0.05$ ). Statistical significance represented by \*, or \* for significance that is SPI-2 TTSS-mediated.

( $P=0.011$ ). Nitrite levels were significantly higher compared to those in control cells across the time-course following serovar Pullorum infection ( $P=0.000$ ,  $P=0.024$  and  $P=0.006$  respectively) and following *ssaU* infection ( $P=0.012$ ,  $P=0.000$  and  $P=0.000$  respectively). During serovar Enteritidis infection, nitrite levels were significantly higher at 48 and 72 hpi compared to those measured during serovar Pullorum infection ( $P=0.004$  and  $P=0.015$  respectively), during *ssaU* infection ( $P=0.006$  and  $P=0.000$  respectively) and for control cells ( $P=0.000$  and  $P=0.014$  respectively).

The cytokine mRNA expression profiles for the experiment are shown in Figure 5.18. IL-1 $\beta$  mRNA expression levels are shown in Figure 5.18A. IL-1 $\beta$  mRNA levels were significantly up-regulated, compared to those measured in control cells, following infection with serovar Pullorum at 24 and 72 hpi ( $P=0.002$  and  $P=0.001$  respectively), with *ssaU* at 24 and 72 hpi ( $P=0.002$  and  $P=0.003$  respectively) and with serovar Enteritidis at 72 hpi ( $P=0.000$ ). Compared to levels during infection with serovar Enteritidis at 24 hpi, there was significant up-regulation of IL-1 $\beta$  mRNA levels measured during serovar Pullorum infection ( $P=0.014$ ) and *ssaU* infection ( $P=0.016$ ). There was no significant difference between IL-1 $\beta$  mRNA expression levels during serovar Pullorum and *ssaU* infections across the time-course.

IL-6 mRNA expression levels across the time course for the differentially infected cells are shown in Figure 5.18B. At 24, 48 and 72 hpi, IL-6 mRNA levels during *ssaU* infection were significantly up-regulated compared to those measured during serovar Pullorum infection ( $P=0.017$ ,  $P=0.013$  and  $P=0.015$  respectively). Compared to control cells, IL-6 mRNA levels were significantly up-regulated throughout the time-course during *ssaU* infection ( $P=0.000$ ,  $P=0.046$  and  $P=0.017$  respectively), but this difference was only seen at 24 hpi during serovar Pullorum infection ( $P=0.002$ ). At 24 and 48 hpi, compared to those measured for



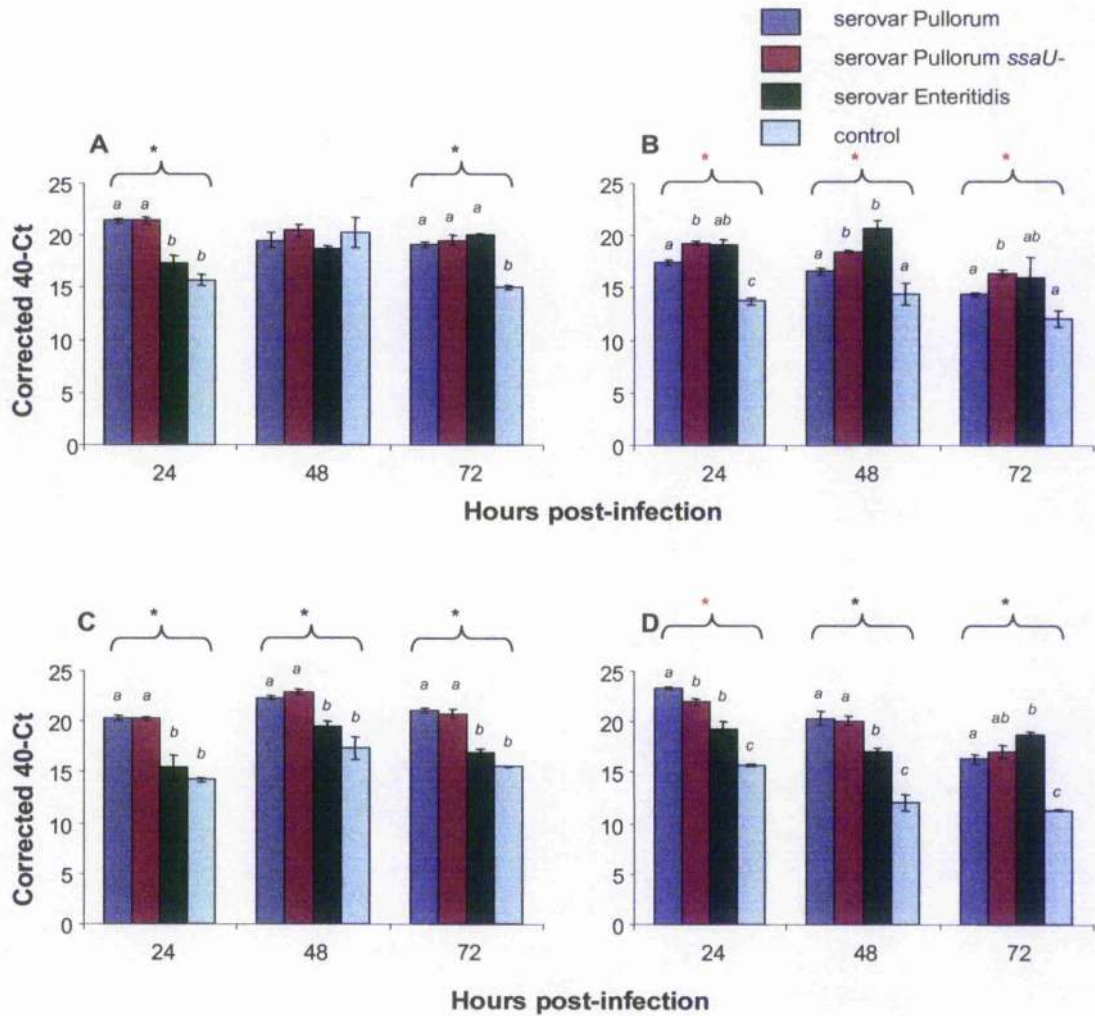


**Figure 5.18:** IL-1 $\beta$  (A), IL-6 (B), CXCLi1 (C) and CXCLi2 (D) mRNA expression levels in chicken bone marrow-derived macrophages following infection with 100  $\mu$ l/ml of a late log phase  $10^8$  cfu/ml culture of either *Salmonella enterica* serovar Pullorum, serovar Pullorum *ssaU*-, serovar Enteritidis or mock-infected control. mRNA levels expressed as corrected 40-Ct values obtained by real time qRT-PCR performed on mRNA isolated from day 5 of culture *ex vivo* (n=3; SE $\pm$ 0.05). Statistical significance within a group is represented by \*, or \* for there was significant up-regulation of IL-6 mRNA during infection with serovar Enteritidis (P=0.003 and P=0.039 respectively). IL-6 mRNA levels were significantly down-

control cells, regulated during infection with serovar Pullorum at 48 hpi when compared to those measured during serovar Enteritidis infection ( $P=0.021$ ).

The mRNA expression levels for CXCLi1 are shown in Figure 5.18C. Across the time-course, compared to levels in control cells, expression levels of CXCLi1 mRNA were significantly up-regulated during infection with serovar Pullorum significance that is SPI-2 TTSS-mediated. Bars, within same time point for each cytokine, not sharing a letter (when letters are shown) are statistically significantly different.

( $P=0.000$ ,  $P=0.034$  and  $P=0.002$  respectively) and during *ssaU* infection ( $P=0.000$ ,  $P=0.026$  and  $P=0.007$  respectively). There was also significant up-regulation of CXCLi1 mRNA levels across the time-course when compared to those measured following serovar Enteritidis infection, following infection with serovar Pullorum ( $P=0.036$ ,  $P=0.019$  and  $P=0.002$  respectively) and *ssaU* ( $P=0.036$ ,  $P=0.011$  and  $P=0.008$  respectively). There was no significant difference between CXCLi1 mRNA expression levels during serovar Pullorum and *ssaU* infections across the time-course.

The CXCLi2 mRNA expression levels for the experiment are shown in Figure 5.18D. CXCLi2 mRNA levels were significantly up-regulated when compared to those measured in control cells across the time-course during infection with serovar Pullorum ( $P=0.000$ ,  $P=0.013$  and  $P=0.001$  respectively), *ssaU* ( $P=0.000$ ,  $P=0.007$  and  $P=0.002$  respectively) and serovar Enteritidis ( $P=0.022$ ,  $P=0.018$  and  $P=0.000$  respectively). At 24 hpi, CXCLi2 mRNA expression levels following *ssaU* infection were significantly lower than those measured following serovar Pullorum infection ( $P=0.032$ ). CXCLi2 mRNA levels measured following serovar Pullorum infection were significantly higher and those measured following serovar Enteritidis infection at 24, and 48 hpi ( $P=0.016$  and  $P=0.034$  respectively). At 48 hpi, levels of mRNA expression during *ssaU* infection were significantly higher compared to those measured during serovar

Enteritidis infection ( $P=0.014$ ). Levels of CXCL12 mRNA expression were significantly higher during serovar Enteritidis infection compared to those measured during serovar Pullorum infection at 72 hpi ( $P=0.023$ ).

#### 5.4 Discussion

The data clearly show that the SPI-1 TTSS is involved in, but not essential for, the invasion of CKC by serovar Pullorum. There were significant differences between intracellular numbers of serovar Pullorum wild-type and the SPI-1 TTSS-attenuated mutant at early time-points post-infection. The serovar Pullorum wild-type bacteria invaded CKC faster than the SPI-1 TTSS-attenuated bacteria suggesting a role for this system in the invasion process. Attenuation of the SPI-1 TTSS does not, however, completely inhibit this process as intracellular bacteria were still found at the early time-points. These data support and build on those reported by Wigley *et al.* (2002), who investigated the effect of the SPI-1 TTSS on invasion of CKC at 2 hpi. Intracellular levels of serovar Pullorum within the CKC were constant throughout the experiment. The SPI-1 TTSS-attenuated mutant bacteria were present intracellularly in significantly lower numbers at the start of the assay, but their numbers quickly increased to be comparable to those seen during the serovar Pullorum wild-type infection. This was not due to continued invasion into the CKC over the time-course, as the addition of gentamicin at 1 hpi to the culture would have prevented invasion by the bacteria past this point. The increase in bacterial numbers over the time course must therefore be due to intracellular proliferation, and the SPI-1 TTSS did not appear to play a role in this process.

The intracellular survival of the bacteria did not induce nitric oxide production in the CKC. In general, in CKC, serovar Enteritidis induced increased pro-inflammatory

mRNA expression when compared to levels measured in non-infected cells and cells that were infected with either the serovar Pullorum wild-type or the SPI-1 TTSS-attenuated mutant. The extent of this up-regulation of expression decreased over the time-course to levels similar to those measured in control cells. There were no significant differences in IL-1 $\beta$ , IL-6, CXCL11 and CXCL12 mRNA expression during serovar Pullorum wild-type and SPI-1 TTSS-attenuated mutant infection, which indicates that although the SPI-1 TTSS is involved in the initial invasion event, it does not appear to have any affect on host pro-inflammatory cytokine production. Expression of the pro-inflammatory cytokines was significantly increased at early time-points during serovar Enteritidis infection, but not during serovar Pullorum infection. This could be due to either immune modulation by serovar Pullorum or due to the lower numbers of intracellular bacteria. Since the serovar Pullorum bacteria invaded and persisted in lower numbers than serovar Enteritidis this may just be a case of avoiding an immune response by maintaining a lower intracellular bacterial population. This would reduce the chance of detection by the immune system and lessen the need for active immune modulation.

Repetition of the assay using the SPI-2 TTSS-attenuated mutant did not show a role for the SPI-2 TTSS in the initial invasion of serovar Pullorum into CKC, which suggests that the SPI-2 TTSS does not play a role in the initial invasion event in the gut. This is in line with previous work (Wigley *et al.*, 2002). None of the bacteria induced nitric oxide production by CKC. The pro-inflammatory cytokine mRNA expression profiles were similar to those measured when evaluating the role of the SPI-1 TTSS in CKC, with expression being significantly up-regulated during serovar Enteritidis infection, but not during serovar Pullorum infection when compared to the control. It is of note, though, that at 6 hpi, IL-6 mRNA expression due to serovar Pullorum infection

appeared to be down-regulated in a SPI-2 TTSS-dependent manner. It has been suggested that the SPI-2 TTSS becomes functional in the course of intracellular persistence during *in vivo* infection due to a specific set of environmental signals (Diewick *et al.*, 1999), and the persistence of the bacteria within the CKC, could be the reason for this late difference in function and phenotype of the SPI-2 TTSS mutant during the experiment. The role of the SPI-2 TTSS in intracellular persistence and host immune modulation will be discussed further below.

The SPI-1 TTSS plays a role in invasion of CKC, suggesting that it functions in aiding the invasion event in the chicken gut, but interestingly, the results did not suggest that it had an effect on invasion into HD11 macrophage-like cells. This in itself suggests that the up-take of bacteria into the macrophage is via a different mechanism than that employed in invading the gut. In the gut, invasion of *S. enterica* bacteria involves, in some part, membrane-ruffling (Francis *et al.*, 1993), which involves processes mediated by the SPI-1 TTSS (Hayward and Koronakis, 1999; Gálan and Zhou, 2000; reviewed in Zhou and Gálan, 2001). Jepson *et al.* (2001) suggested that *S. enterica* entry into cells in the gut is not completely dependent on the process of membrane-ruffling though, and that other SPI-1 TTSS-mediated forms of invasion may also play a role. Uptake into macrophages, however, is likely to be through phagocytosis initiated by the host cell, therefore not requiring the SPI-1 TTSS.

Although serovar Enteritidis and serovar Pullorum bacteria were present in HD11 cells in relatively similar numbers throughout the time-course, intracellular infection with serovar Enteritidis induced significantly greater nitric oxide production when compared to that induced by serovar Pullorum infection. This could suggest that serovar Pullorum is perhaps modulating host cell nitric oxide induction, but the results do not suggest any involvement of the SPI-1 TTSS at this stage. The pro-inflammatory

mRNA expression profile during serovar Pullorum and serovar Enteritidis infection of HD11 cells showed a generalised significant up-regulation of IL-1 $\beta$ , IL-6, CXCLi1 and CXCLi2 mRNA levels compared to those measured in control cells. From the results, there was no suggestion of SPI-1 TTSS involvement in this induction of increased expression, as no significant differences were measured following infection with either serovar Pullorum wild-type or the SPI-1 TTSS-attenuated mutant. There is also no indication of immune modulation by serovar Pullorum as pro-inflammatory cytokine mRNA expression was of similar (sometimes significantly greater) levels to those measured during infection with serovar Enteritidis across the time-course.

There were no significant differences in the numbers of intracellular serovar Pullorum bacteria counted in HD11 cells infected with either the wild-type or the SPI-2 TTSS-attenuated mutant, suggesting that there was no SPI-2 TTSS-attenuated mutant involvement in bacterial persistence within the HD11 cells up to 24 hpi. There was no involvement of the SPI-2 TTSS in the induction of nitric oxide in HD11 cells, and nitrite levels in supernatants collected during invasion and persistence of serovar Pullorum and serovar Enteritidis were comparable to those measured when investigating the role of the SPI-2 TTSS. The cytokine mRNA expression profiles measured over the time-course for the differentially infected HD11 cells showed an up-regulation of IL-1 $\beta$ , IL-6, CXCLi1 and CXCLi2 mRNA during infection with serovar Pullorum and serovar Enteritidis when compared to levels in the control. There was no apparent role for the SPI-2 TTSS in modulation of cytokine mRNA expression measured during serovar Pullorum infection of HD11 cells up to 24 hpi, as no significant differences were observed between the mRNA expression profiles for the serovar Pullorum wild-type and the SPI-2 TTSS-attenuated mutant-infected cells.

Repetition in BM-dMΦ of the assays initially performed in HD11 cells to evaluate the role of the SPI-2 TTSS in serovar Pullorum infection showed that at 2 hpi there was a significant difference in the intracellular numbers of wild-type serovar Pullorum and the SPI-2 TTSS-attenuated mutant. The SPI-2 TTSS-attenuated mutant was present in significantly higher numbers within the BM-dMΦ than the serovar Pullorum wild-type, suggesting a possible role for the SPI-2 TTSS in infection of macrophages. Initially, it is slightly surprising that the SPI-2 TTSS-attenuated mutant appears to be more efficient at establishing an initial intracellular infection than the wild-type, but this may actually be advantageous to persistence. Actively restricting intracellular bacterial numbers could decrease the chance of detection and clearance from the cells by the host immune system, thereby increasing the chance of successful intracellular persistence. During serovar Typhimurium infection, SPI-2 TTSS gene expression is induced by environmental cues believed to be homologous to those encountered by the bacteria within the intra-macrophage phagosome, such as  $Mg^{2+}$  deprivation and phosphate starvation (Diewick *et al.*, 1999). Since the SPI-2 TTSS are thought to be conserved between *S. enterica* serovars (Ochman and Groisman 1996), environmental regulation of the SPI-2 TTSS gene expression (Diewick *et al.*, 1999) is also likely to be applicable during infections with serovar Pullorum. Therefore, this apparent difference in the ability to invade macrophages may in fact be an early restriction placed on intracellular proliferation, rather than due to differences in numbers of invading bacteria, as SPI-2 TTSS gene expression is unlikely to be "switched on" during the invasion process.

There was no apparent SPI-2 TTSS effect on nitric oxide production up to 24 hpi during serovar Pullorum infection, or on the pro-inflammatory cytokine mRNA expression profile. Generally, infection of BM-dMΦ with either serovar Pullorum or

serovar Enteritidis resulted in a significant up-regulation of IL-1 $\beta$ , IL-6, CXCLi1 and CXCLi2 mRNA, when compared to the control. In fact, serovar Pullorum infection in general resulted in increased up-regulation of the pro-inflammatory cytokines compared to levels measured during serovar Enteritidis infection across the time-course up to 24 hpi.

When modelling persistence, the duration of culture and infection should be considered. It would be interesting to investigate the role of SPI-2 TTSS over a time-course longer than 24 hours, to more realistically model *in vitro* the nature of the *in vivo* infection. To this end, the BM-dM $\Phi$  were used at 5 days *ex vivo*, as opposed to 7 days as previously, as it was thought that a younger culture could better sustain the bacterial infection for a longer period of time. Because the cell population used was of a different age, there are slight differences in the bacterial numbers and the cellular responses seen at 24 hpi when comparing cells used at 5 days or at 7 days *ex vivo*. During the longer time-course, numbers of the intracellular SPI-2 TTSS-attenuated mutant at 24 and 48 hpi were significantly higher than those measured during serovar Pullorum infection, but by 72 hpi there was no significant difference observed. Interestingly, intracellular numbers of serovar Pullorum bacteria remained relatively constant over the time-course from 24-72 hpi, and although intracellular numbers of the SPI-2 TTSS-attenuated mutant were significantly higher than those of the serovar Pullorum wild-type at 24 hpi, they dropped rapidly thereafter. This would suggest that the levels at which the SPI-2 TTSS-attenuated mutant initially proliferated within the BM-dM $\Phi$  are not sustainable during a persistent infection. SPI-2 TTSS-attenuated mutants were also measured in significantly higher numbers than the wild-type in BM-dM $\Phi$  at 2 hpi during the shorter time-course. This suggests that the SPI-2 TTSS probably plays a role in restricting intracellular bacterial proliferation, limiting it so as to persist and reduce the chance of



detection by the host's immune system and the host cell itself. In an earlier study, serovar Pullorum mutants defective in SPI-2 TTSS were fully attenuated for virulence (Wigley *et al.*, 2002). Interestingly, research by Hensel *et al.* (1998) suggested that, during infection of murine macrophages with serovar Typhimurium, one of the functions of the SPI-2 TTSS is to enable intracellular proliferation. This does not completely disprove the hypothesis recommended by the data in this study though, as serovar Typhimurium strains with mutations in SPI-2 genes were attenuated in virulence during infection of murine macrophages (Hensel *et al.*, 1998). The apparent SPI-2 TTSS-mediated limitation of serovar Pullorum proliferation found in this study may in fact allow for a more controlled intracellular growth. This would essentially agree with the suggestion by Hensel *et al.* (1998), that SPI-2 TTSS promote virulence by enabling effective sustainable intracellular growth. The levels of nitric oxide detected within the supernatants were significantly higher at 48 and 72 hpi during infection with the SPI-2 TTSS-attenuated mutant compared to levels measured during infection with the serovar Pullorum wild-type. This indicates that the SPI-2 TTSS also inhibits induction of nitric oxide synthesis by the cells. Nitric oxide synthesis is associated with antimicrobial mechanisms within the lysosome of macrophages. It is one of the components required for the generation of peroxynitrite, a potent antimicrobial effector of macrophages in mammalian species (Nathan and Shiloh, 2000). The effects of nitric oxide synthesis in avian species are generally accepted to be analogous to those described in mammalian species and the inhibition of this process is likely to be advantageous to the persistence of intracellular bacteria. Chakravorty *et al.* (2002) demonstrated by use of immunofluorescence microscopy that murine macrophages infected with serovar Typhimurium defective in SPI-2 TTSS were able to effectively co-localise nitric oxide within the *Salmonella*-containing vacuole (SCV), but that this

was not the case with wild-type bacteria. It was therefore suggested that a function of the SPI-2 TTSS was to exclude peroxynitrite from the SCV (Chakravorty *et al.*, 2002). The inhibition of nitric oxide synthesis by the SPI-2 TTSS during serovar Pullorum infection of BM-dM $\Phi$  is therefore likely to be a survival mechanism employed by the bacteria to enable intracellular persistence. It is also interesting to note the rapid decrease in nitrite levels measured in the supernatants of serovar Enteritidis-infected cells from 48-72 hpi. The reason behind this decrease is unknown, but may be due to nitric oxide being toxic to cells and tissues. If NO synthesis has no effect on reducing bacterial numbers, it is not advantageous for the cells to continue nitric oxide production. Another possibility could be that the SPI-2 TTSS of serovar Enteritidis takes longer to "switch on" compared to that of serovar Pullorum due to fundamental differences between the two serovars. Furthermore, as serovar Enteritidis causes disease in a range of hosts, including mammalian and avian species, there will be slight differences in the conditions encountered by the bacteria depending on the host. The SPI-2 TTSS may therefore require an extended period of activation by environmental factors in order to induce gene expression, to prevent expression at incorrect stages of the infection (e.g. expression during the initial invasion of gut epithelial cells).

IL-6 is a pleiotropic cytokine that plays a fundamental role in the inflammatory response. Interestingly, IL-6 mRNA expression was significantly up-regulated during SPI-2 TTSS-attenuated mutant infection of BM-dM $\Phi$  at 24, 48 and 72 hpi when compared to levels measured during serovar Pullorum infection. This suggests a role for the SPI-2 TTSS in inhibiting IL-6 mRNA expression during serovar Pullorum infection. The involvement of the SPI-2 TTSS in IL-6 mRNA expression regulation was first indicated during serovar Pullorum infection of CKC, when it was observed at 6 hpi. This could point to an attempt by the bacteria to inhibit the progression of the immune

response from innate to adaptive, to reduce the likelihood of bacterial clearance. There was also a significant difference in CXCLi2 mRNA expression levels during serovar Pullorum wild-type infection compared to those measured during the SPI-2 TTSS-attenuated mutant infection at 24 hpi, with expression during serovar Pullorum wild-type infection being significantly up-regulated. This SPI-2 TTSS-mediated up-regulation of CXCLi2 could be utilised to continue recruitment of monocytes to the site of infection in order to increase the number of target cells capable of being infected, as chCXCLi2 is chemotactic for monocytes (Barker *et al.*, 1994). By 48 hpi, though, this difference was no longer observed. Possibly any SPI-2 TTSS-mediated up-regulation is short-lived due to the host's need to restrict recruitment of naïve cells in an attempt to reduce disease pathology.

In conclusion, the data show that the SPI-1 TTSS is involved in, but not essential for, the initial invasion of serovar Pullorum in CKC, a model for endothelial cells. The SPI-2 TTSS is involved in intra-macrophage persistence, limiting bacterial proliferation within primary macrophages. The SPI-2 TTSS also plays a role in the modulation of nitric oxide synthesis, most likely in an attempt to reduce targeted macrophage killing of the bacteria within the SCV. Active SPI-2 TTSS-mediated suppression of IL-6 mRNA expression, a cytokine which the macrophage would normally produce in response to infection with an intracellular pathogen, during serovar Pullorum infection may help to prevent the progression from a localised pro-inflammatory innate immune response to a systemic adaptive immune response, enabling the bacteria to persist quietly within macrophages for long periods of time.

## Chapter 6: The role of the SPI-1 TTSS in early-stage infection with *Salmonella enterica* serovar Pullorum *in vivo*

### 6.1 Introduction

The main aim of these experiments was to determine the role of the serovar Pullorum SPI-1 TTSS in entry and the inflammatory immune response during infection of inbred chickens. Comparisons to infection with serovar Enteritidis were also made, as serovar Enteritidis causes a more severe gastrointestinal disease in the chicken and so was used as a positive control for inflammation.

Previous work (Wigley *et al.*, 2002) has not been able to establish a strong phenotype for the SPI-1 TTSS attenuated mutant used in this experiment, compared to infection with the wild-type. The SPI-1 TTSS was not essential for the virulence of serovar Pullorum, but it played a part in the disease process (Wigley *et al.*, 2002). The study investigated bacterial numbers and pathology in birds over a three week time-course, and so looked at bacterial persistence. To date, there have been no reports on the initial invasion stage of Pullorum Disease, the role that SPI-1 TTSS plays during the early establishment of the infection, the host immune response to the bacteria, and how the SPI-1 TTSS contributes to this.

Cytokine expression levels can indicate the immune response during infection and changes in their expression can indicate presence, movement, promotion of differentiation, and the proliferation of specific cell populations. It is difficult to directly measure levels of avian cytokines as few specific bioassays exist. However, cytokine mRNA expression levels can be measured in tissue samples from infected birds, giving an indication of changes in transcription levels.

Antimicrobial peptides provide a defence mechanism against a broad spectrum of micro-organisms including pathogenic Gram-negative and Gram-positive bacteria, fungi and yeast. As discussed in Chapter 1, the only antimicrobial peptides found in avian species are  $\beta$ -defensins. The exact mechanism of action of these peptides is unknown but they are thought to cause disruption in membrane integrity, resulting in cell death (Kagan *et al.*, 1990). Avian antimicrobial peptides were first described by both the terms “gallinacin” and “ $\beta$ -defensin” and due to inconsistency in nomenclature arising between different research groups, a new system has now been proposed and they are now known as avian  $\beta$ -defensins (abbreviated to AvBD) (Lynn *et al.*, 2007). To date 14 avian  $\beta$ -defensin molecules have been described in the literature and they are now numbered AvBD1-14 (Table 1.1) (Evans *et al.*, 1994; Harwig *et al.*, 1994; Zhao *et al.*, 2004; Lynn *et al.*, 2004; Xiao *et al.*, 2004, Lynn *et al.*, 2007).

The role of avian  $\beta$ -defensins during *Salmonella enterica* infection of the chicken is unknown, but transgenic mice expressing human enteric defensin 5 are completely protected against normally lethal doses of serovar Typhimurium (Salzman *et al.*, 2003). Also, mice deficient in matrilysin, the protein responsible for the activation of enteric defensins, are more susceptible to serovar Typhimurium infection (Wilson *et al.*, 1999). As little is known about avian  $\beta$ -defensin responses to enteric disease, I decided to investigate expression profiles of a selection of these peptides during serovar Pullorum infection of the chicken and the role of the SPI-1 TTSS in this. As there are no current bioassays for avian  $\beta$ -defensins, levels of mRNA were measured using real-time quantitative RT-PCR.

## 6.2 Methods

### 6.2.1 Animal Experiment

60 day-old line 7<sub>2</sub> White Leghorn chickens, from the Poultry Production Unit at the Institute for Animal Health (Compton, UK), were used in this experiment and they were housed in colony cages in the Experimental Animal House (EAH) at IAH for the length of the experiment. Upon arrival into the EAH, they were divided into four groups of 15 birds per group. The groups then received the following by oral inoculation using a sterile gavage needle:

Group 1 received 10<sup>8</sup> cfu of an overnight broth culture of a spontaneous nalidixic acid mutant of *Salmonella Pullorum* 449/87 in 0.1 ml of LB broth.

Group 2 received 10<sup>8</sup> cfu of an overnight broth culture of a *S. Pullorum* 449/87 *spaS* mutant (Jones et al, 1998) in 0.1 ml of LB broth.

Group 3 received 10<sup>8</sup> cfu of an overnight broth culture of a spontaneous nalidixic acid mutant of *S. Enteritidis* 125589 in 0.1 ml LB broth.

Group 4 contained control birds which were mock-infected with 0.1 ml LB broth.

After inoculation the birds were given access *ad libitum* to food and water.

### 6.2.2 Post Mortem analysis

Time-points for post-mortem sampling in this experiment were at 10, 24 and 48 hours post infection (hpi). At each time-point, five birds were sampled from each group. Samples were taken for bacteriology (liver, caecal contents) and RNA isolation (ileum, caecal tonsil, spleen). Observations of pathology were made at each of the time-points.

The liver and caecal contents were weighed and diluted 1/10 with sterile PBS. Dilutions of the caecal contents were then plated out onto selective Brilliant Green agar containing 20 µg/ml sodium nalidixate and 1 µg/ml novobiocin. The liver was manually

homogenised using a sterile Griffiths Tube and dilutions plated out onto selective Brilliant Green agar as per the caecal contents. The plates were incubated for 24 h at 37°C in 5% CO<sub>2</sub> and the resulting colonies counted.

Tissues removed for RNA isolation were placed directly into 500 µl RNeasy lysis buffer (Qiagen) in cryovials, and incubated at 4°C overnight for effective penetration of the tissue, before storing at -20°C until RNA isolation (see Methods chapter).

Real-time quantitative RT-PCR using TaqMan reagents (Eurogentec) was carried out as described in Chapter 2.

### 6.2.3 Data Analysis

Differences were analysed using Analysis of Variance and the two-tailed T-Test, and were carried out using the Minitab for Windows version 14 statistical package (Minitab Ltd., Coventry, West Midlands, UK). Values of  $P \leq 0.05$  were taken as significant.

## 6.3 Results

### 6.3.1 Bacteriology

The log bacterial counts measured as colony-forming units (which represent the viable bacteria) per ml of the caecal contents and liver collected post-mortem over the time-course of the experiment are shown in Figure 6.1. Figure 6.1A shows the bacterial counts measured in the caecal contents. At 10 hpi, there were significantly lower bacterial numbers counted in the caecal contents of serovar Pullorum-infected birds compared to those counted in the *spaS*-infected birds ( $P=0.038$ ), and in the serovar Enteritidis-infected birds ( $P=0.000$ ). The bacterial numbers counted in the *spaS*-infected birds were significantly lower compared to those counted in the serovar

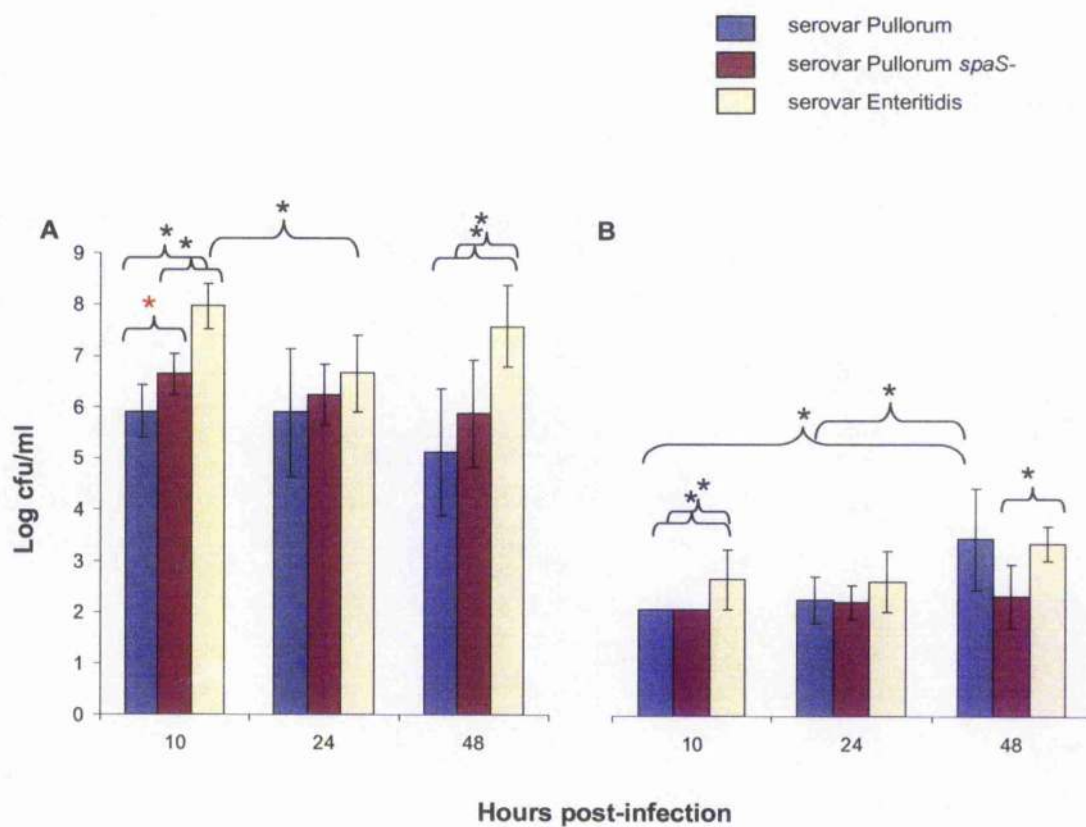


**Figure 6.1: Bacterial counts (expressed as log cfu/ml) from dilutions of caecal contents (A) and homogenised liver (B) obtained post-mortem from line 7<sub>2</sub> birds at 10, 24 and 48 hours post-infection with a 0.1ml broth culture of 10<sup>8</sup> cfu of either *Salmonella enterica* serovar Pullorum, serovar Pullorum *spaS*- or serovar Enteritidis. (n=5; SD±0.05). Statistical significance within a group is represented by \*, or \* for significance that is SPI-2 TTSS-mediated.**



Enteritidis-infected birds ( $P=0.002$ ) at 10 hpi. There were no significant differences between bacterial numbers counted in the differentially infected groups at 24 hpi. At 48 hpi, though, the numbers of bacteria counted in caecal contents of the birds infected with serovar Enteritidis were significantly higher compared to those measured in the birds infected with serovar Pullorum ( $P=0.023$ ) and with *spaS*<sup>-</sup> ( $P=0.054$ ). The bacterial counts from the birds infected with both serovar Pullorum and the *spaS*<sup>-</sup> mutant decreased slowly over the course of the infection, but this trend was not significant. When comparing the bacterial numbers counted in the serovar Enteritidis-infected birds, there was a significant decrease between 10 and 24 hpi ( $P=0.018$ ).

In Figure 6.1B, the bacterial numbers measured in the liver significantly increased during infection with serovar Pullorum between 10 and 48 hpi ( $P=0.014$ ) and also between 24 and 48 hpi ( $P=0.041$ ). Although there was an increase in bacterial numbers in the liver of *spaS*<sup>-</sup> infected birds over the time-course, this was not significant and numbers were almost undetectable at log 2 cfu/ml (which was used as the baseline). The bacterial counts from serovar Enteritidis-infected birds stayed relatively constant between 10 hpi and 24 hpi at a log of 2.5 cfu/ml, then rose slightly to a log of 3.2 cfu/ml by 48 hpi. At 10 hpi, bacterial counts in the serovar Enteritidis-infected birds were significantly higher than those measured in the serovar Pullorum-infected ( $P=0.051$ ) and the *spaS*<sup>-</sup>-infected birds ( $P=0.051$ ). By 24 hpi, there were no significant differences in bacterial numbers measured between the groups, but at 48hpi the bacterial numbers within serovar Enteritidis-infected birds had risen to be significantly higher than those measured in *spaS*<sup>-</sup>-infected birds ( $P=0.040$ ).

### 6.3.2 Pathological observations made post-mortem

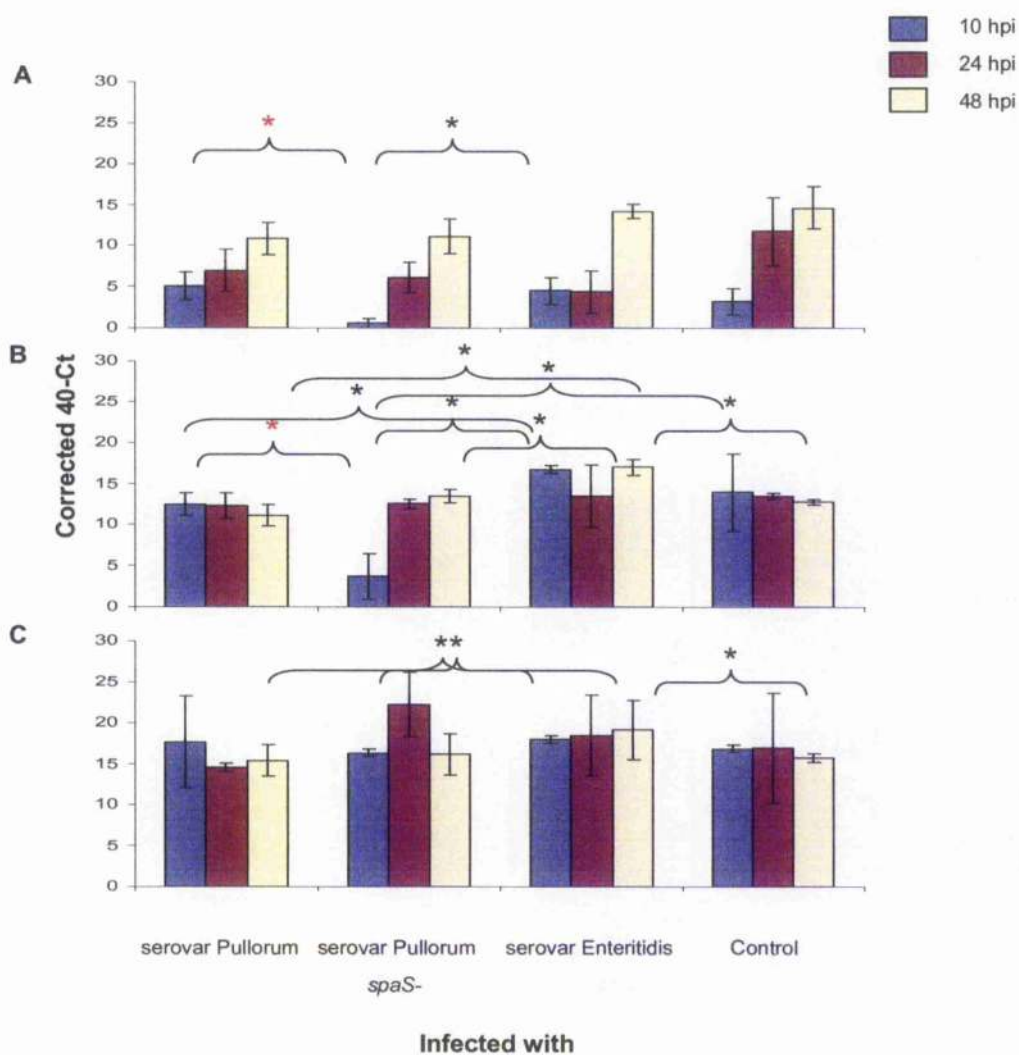
Observations of gross pathology made during the post mortem of the birds at all time-points were recorded. All the birds appeared healthy, and no abnormal pathology was recorded when post mortems were carried out at 10 hpi in any of the groups. At 24 hpi, no pathology was apparent in the serovar Pullorum-infected birds, whereas in the serovar Pullorum *spaS*- group, 3/5 of the birds killed had generalised ileal inflammation. The serovar Enteritidis-infected group had 4/5 birds with marked ileal inflammation. The remaining bird in the group had a hyperaemic gut. 4/5 of the group had evident hepatosplenomegaly with the spleen of the remaining bird appearing swollen. By 48 hpi, 5/5 of the serovar Pullorum-infected birds displayed signs of hepatosplenomegaly. Although there was little gut inflammation observed within this group, 3/5 of the birds had a generalised gut hyperaemia and 2/5 of the birds appeared to have a yolk-sac infection. In the group infected with *spaS*-, 5/5 of the birds displayed signs of hepatosplenomegaly and had slight, patchy gut inflammation. In 3/5 of these birds, mucosa was evident in the caecal contents. Two of the serovar Enteritidis-infected birds were found dead at 48 hpi so no tissues could be collected for RNA isolation from them. When examined during the post mortem, they both had severe yolk-sac infections, acute inflammation in the gut and substantial blood and mucosa was found in the caecal contents. Of the remaining three, all displayed evident hepatosplenomegaly and gut inflammation. 2/5 of these birds had suffered haemorrhaging in the ileum resulting in bloody ileal contents.

### 6.3.3 Pro-inflammatory cytokine mRNA expression

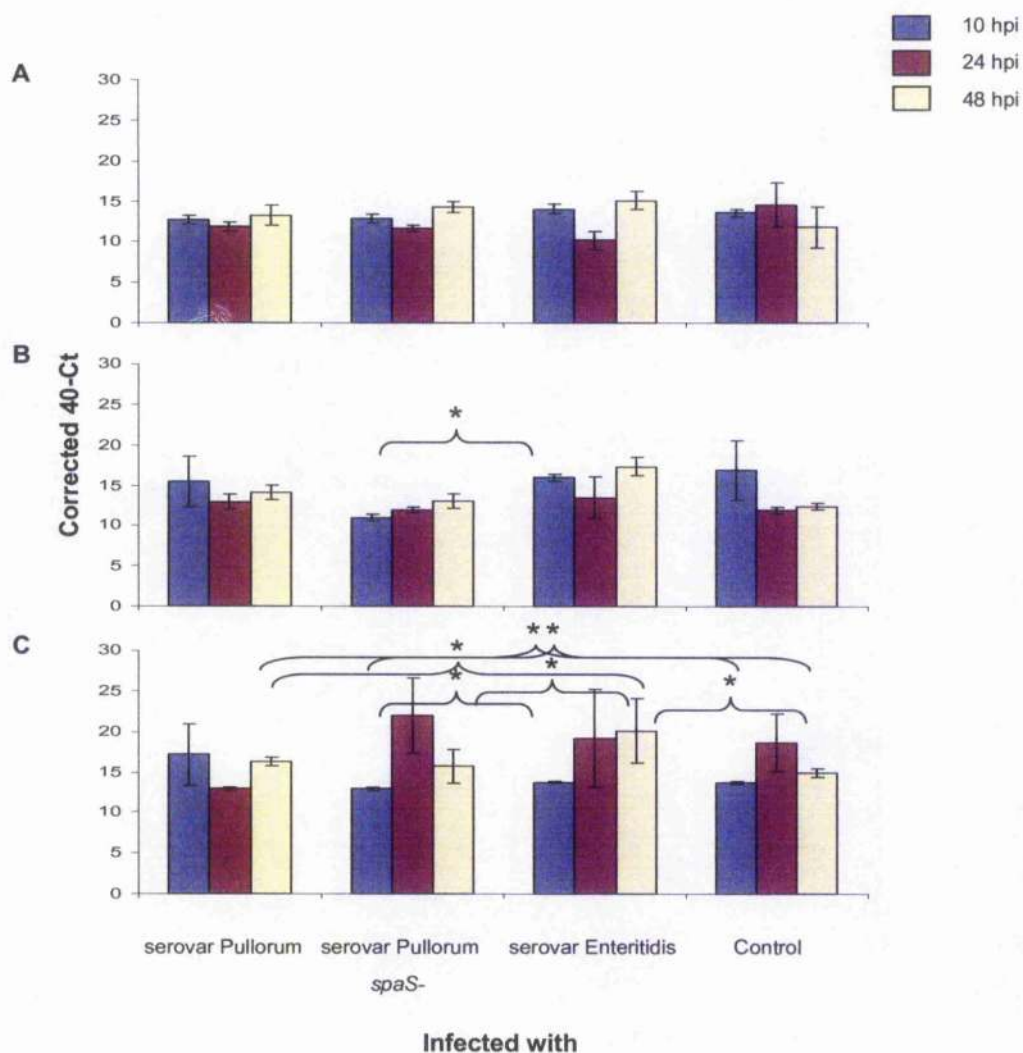
Levels of IL-1 $\beta$  mRNA isolated from the ileum, caecal tonsil and spleen of the differentially infected birds were measured by real-time qRT-PCR and are shown in

Figure 6.2. At 10 hpi, IL-1 $\beta$  mRNA expression levels measured in the ileum *spaS*-infected birds were significantly down-regulated compared to those from serovar Pullorum-infected birds (P=0.037), and from serovar Enteritidis-infected birds (P=0.053). In the caecal tonsil at 10 hpi, IL-1 $\beta$  mRNA levels during *spaS* infection were significantly down-regulated compared to those measured during serovar Pullorum-infection (P=0.022). A significant up-regulation of IL-1 $\beta$  mRNA levels was measured in the caecal tonsil at 10 hpi during serovar Enteritidis infection compared to those measured during serovar Pullorum infection (P=0.020) and during *spaS* infection (P=0.002). In the caecal tonsil at 48 hpi, IL-1 $\beta$  mRNA levels were significantly up-regulated during infection with serovar Enteritidis compared to those measured during infection with serovar Pullorum (P=0.022), with *spaS* (P=0.033) and for the control (P=0.003). The IL-1 $\beta$  mRNA levels measured in the spleen at 10 hpi were significantly up-regulated during serovar Enteritidis infection compared to those measured during *spaS* infection (P=0.023). Levels of IL-1 $\beta$  mRNA expression in the spleen were significantly higher following infection with serovar Enteritidis compared to those measured following infection with serovar Pullorum (P=0.048) and to the control (P=0.013).

IL-6 mRNA expression levels measured in the ileum, caecal tonsil and spleen during the experiment are shown in Figure 6.3. There were no significant differences in IL-6 mRNA expression levels measured in the ileum across the time-course for the differentially infected bird groups. At 10 hpi in the caecal tonsil, IL-6 mRNA levels were significantly higher during infection with serovar Enteritidis compared to those measured during infection with *spaS* (P=0.000). In the spleen at 10 hpi the IL-6 mRNA levels measured following infection with *spaS* were significantly lower compared to those measured following infection with serovar Enteritidis (P=0.004) and for the



**Figure 6.2: IL-1 $\beta$  mRNA levels of ileal (A), caecal tonsil (B) and splenic (C) tissues obtained post-mortem from line 7<sub>2</sub> birds 10, 24 and 48 hpi with a 0.1ml broth culture of 10<sup>8</sup> cfu of either *Salmonella enterica* serovar Pullorum, serovar Pullorum *spaS*- or serovar Enteritidis. mRNA levels expressed as corrected 40-Ct values obtained by real-time qRT-PCR. (n=5; SE $\pm$ 0.05). Statistical significance within a group is represented by \*, or \* for significance that is SPI-2 TTSS-mediated.**



**Figure 6.3: IL-6 mRNA levels of ileal (A), caecal tonsil (B) and splenic (C) tissues obtained post-mortem from line 7<sub>2</sub> birds 10, 24 and 48 hpi with a 0.1ml broth culture of 10<sup>8</sup> cfu of either *Salmonella enterica* serovar Pullorum, serovar Pullorum *spaS*- or serovar Enteritidis. mRNA levels expressed as corrected 40-Ct values obtained by real-time qRT-PCR. (n=5; SE±0.05). Statistical significance within a group is represented by \*.**

control ( $P=0.009$ ). At 48 hpi in the spleen following infection with serovar Enteritidis, IL-6 mRNA expression levels were significantly higher compared to those measured following infection with serovar Pullorum ( $P=0.006$ ), with *spaS* ( $P=0.017$ ) and for the control ( $P=0.000$ ). IL-6 mRNA levels were significantly up-regulated following infection with serovar Pullorum compared to those measured in the control birds ( $P=0.038$ ) at 48 hpi in the spleen.

#### 6.3.4 Pro-inflammatory chemokine mRNA expression

The mRNA expression levels for CXCLi1 for the experiment are shown in Figure 6.4. In the ileum at 10 hpi, CXCLi1 mRNA levels following infection with serovar Enteritidis were significantly up-regulated compared to those measured following infection with serovar Pullorum ( $P=0.031$ ) and *spaS* ( $P=0.016$ ). At 24 hpi in the ileum, CXCLi1 mRNA levels were significantly higher in the control birds compared to those infected with serovar Pullorum ( $P=0.014$ ). By 48 hpi, compared to those measured for the control birds, CXCLi1 mRNA levels were significantly higher in birds infected with serovar Pullorum ( $P=0.018$ ), with *spaS* ( $P=0.049$ ) and with serovar Enteritidis ( $P=0.003$ ). In the caecal tonsil, CXCLi1 mRNA expression levels were significantly lower during infection with *spaS* compared to those measured during infection with serovar Pullorum ( $P=0.043$ ) and with serovar Enteritidis ( $P=0.007$ ). There were no significant differences between CXCLi1 mRNA levels measured in the differentially infected birds at 24 hpi. At 48 hpi, compared to those measured for the control birds, CXCLi1 mRNA levels were significantly higher in birds infected with *spaS* ( $P=0.020$ ) and with serovar Enteritidis ( $P=0.003$ ). CXCLi1 mRNA levels were significantly lower following infection with *spaS* compared to those measured following serovar Enteritidis ( $P=0.046$ ). In the spleen at 10 hpi, CXCLi1 mRNA levels

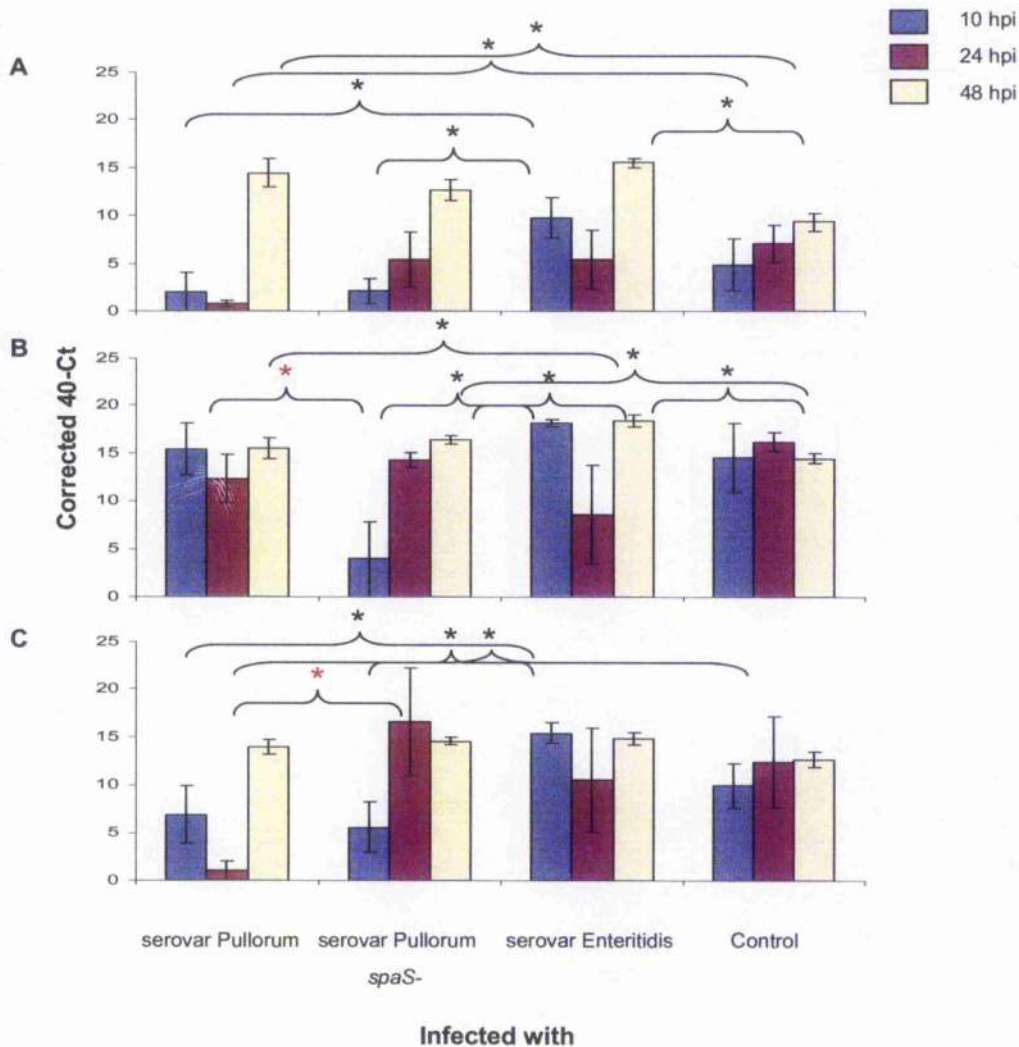


**Figure 6.4: CXCLi1 mRNA levels of ileal (A), caecal tonsil (B) and splenic (C) tissues obtained post-mortem from line 7<sub>2</sub> birds 10, 24 and 48 hpi with a 0.1ml broth culture of 10<sup>8</sup> cfu of either *Salmonella enterica* serovar Pullorum, serovar Pullorum *spaS*- or serovar Enteritidis.** mRNA levels expressed as corrected 40-Ct values obtained by real-time qRT-PCR. (n=5; SE±0.05). Statistical significance within a group is represented by \*, or \* for significance that is SPI-2 TTSS-mediated.

were significantly higher following infection with serovar Enteritidis compared to those measured following infection with both serovar Pullorum ( $P=0.029$ ) and *spaS* ( $P=0.009$ ). At 24 hpi, the CXCLi1 mRNA levels measured during serovar Pullorum infection were significantly lower when compared to those measured during infection with *spaS* ( $P=0.025$ ) and in the control birds ( $P=0.044$ ).

CXCLi2 mRNA expression levels measured in the ileum, caecal tonsil and spleen during the experiment are shown in Figure 6.5. There were no significant differences in the CXCLi2 mRNA expression levels in the ileum at 10 and 24 hpi. At 48 hpi, though, CXCLi2 mRNA levels were significantly up-regulated in birds infected with serovar Enteritidis compared to those measured in control birds ( $P=0.002$ ). In the caecal tonsil at 10 hpi, CXCLi2 mRNA levels were significantly higher following infection with serovar Enteritidis compared to those measured following infection with *spaS* ( $P=0.001$ ) and in the control birds ( $P=0.005$ ). There were no significant differences in CXCLi2 mRNA levels at 24 hpi, but at 48 hpi those levels measured during serovar Enteritidis infection were significantly higher compared to those measured during *spaS* infection ( $P=0.032$ ) and in the control birds ( $P=0.007$ ). In the spleen at 10hpi and 24 hpi, CXCLi2 mRNA expression levels were significantly up-regulated following infection with serovar Enteritidis compared to those measured following infection with *spaS* ( $P=0.033$  and  $P=0.049$ ). CXCLi2 mRNA levels were also higher at 24 hpi in the spleen following infection with serovar Enteritidis compared to those measured following infection with serovar Pullorum ( $P=0.013$ ).



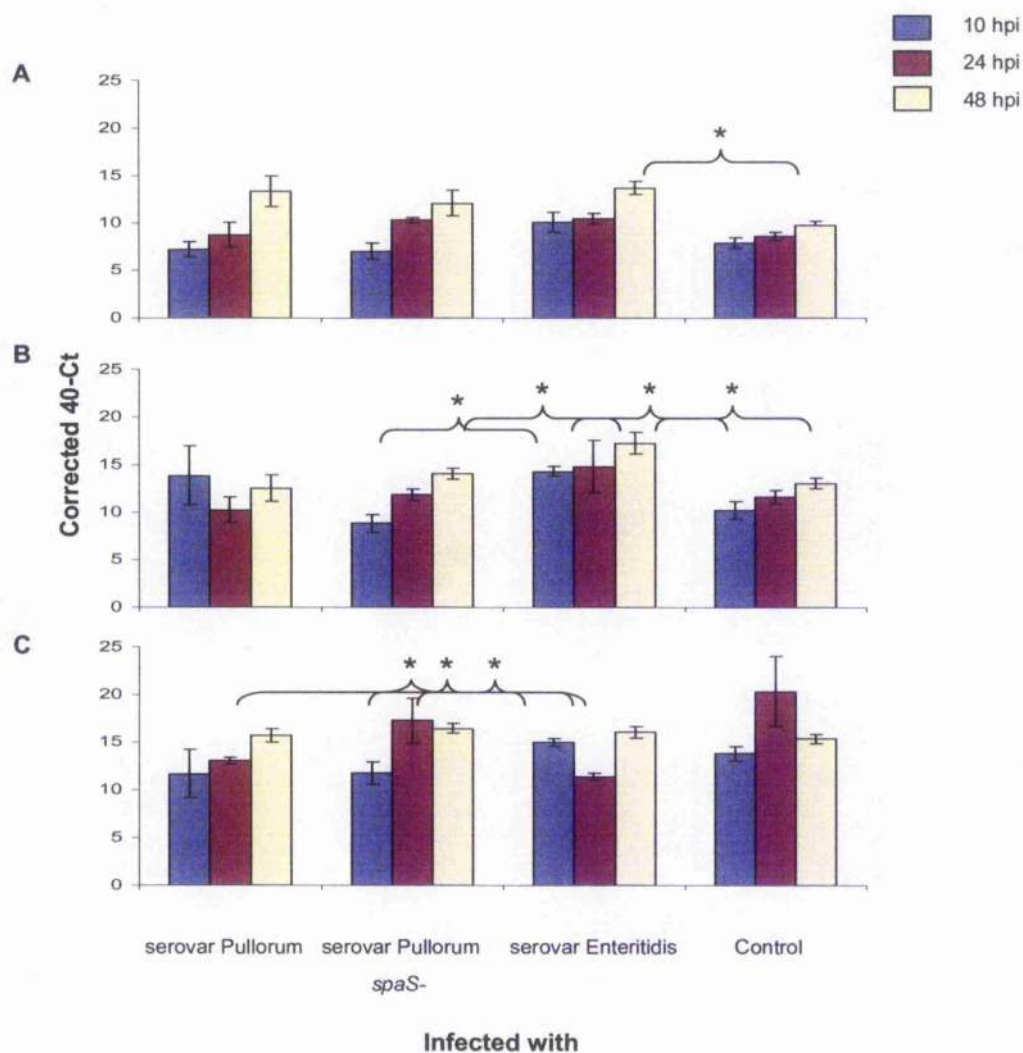


**Figure 6.5: CXCLi2 mRNA levels of ileal (A), caecal tonsil (B) and splenic (C) tissues obtained post-mortem from line 7<sub>2</sub> birds 10, 24 and 48 hpi with a 0.1ml broth culture of 10<sup>8</sup> cfu of either *Salmonella enterica* serovar Pullorum, serovar Pullorum *spaS*- or serovar Enteritidis. mRNA levels expressed as corrected 40-Ct values obtained by real-time qRT-PCR. (n=5; SE±0.05). Statistical significance within a group is represented by \*.**

### 6.3.5 Avian $\beta$ -defensin mRNA expression

The mRNA expression levels for AvBD1 for the experiment are shown in Figure 6.6. There were no significant differences between AvBD1 mRNA levels measured in the ileum at 10, 24 and 48 hpi. In the caecal tonsil at 10 hpi, AvBD1 mRNA levels were significantly lower following infection with *spaS*<sup>-</sup> compared to those measured in control birds ( $P=0.032$ ). At 24 hpi, AvBD1 mRNA levels were significantly down regulated following infection with serovar Enteritidis compared to those measured following infection with serovar Pullorum ( $P=0.042$ ) and *spaS*<sup>-</sup> ( $P=0.011$ ). There were no significant differences between the AvBD1 mRNA levels measured at 48 hpi in the caecal tonsil for the differentially infected birds. In the spleen at 10 and 24 hpi, there are no significant differences between the AvBD1 mRNA levels measured. AvBD1 mRNA levels at 48 hpi in the spleen were significantly up-regulated, when compared to infection with serovar Pullorum and also in control birds, following infection with *spaS*<sup>-</sup> ( $P=0.002$  and  $P=0.038$  respectively) and serovar Enteritidis ( $P=0.003$  and  $0.041$  respectively).

AvBD2 mRNA expression levels measured during the experiment are shown in Figure 6.7. In the ileum at 10 hpi, AvBD2 mRNA levels following infection with serovar Enteritidis were significantly higher compared to those measured following infection with serovar Pullorum ( $P=0.032$ ) and with *spaS*<sup>-</sup> ( $P=0.045$ ). Whilst there were no significant differences at 24 hpi, at 48 hpi AvBD2 mRNA levels were significantly down-regulated following infection with serovar Enteritidis compared to those measured following infection with serovar Pullorum ( $P=0.009$ ). Furthermore, at 48 hpi, AvBD2 mRNA levels were significantly lower in control birds compared to those measured in birds infected with serovar Pullorum ( $P=0.000$ ), with *spaS*<sup>-</sup> ( $P=0.004$ ) and with serovar Enteritidis ( $P=0.025$ ). There were no significant differences in AvBD2

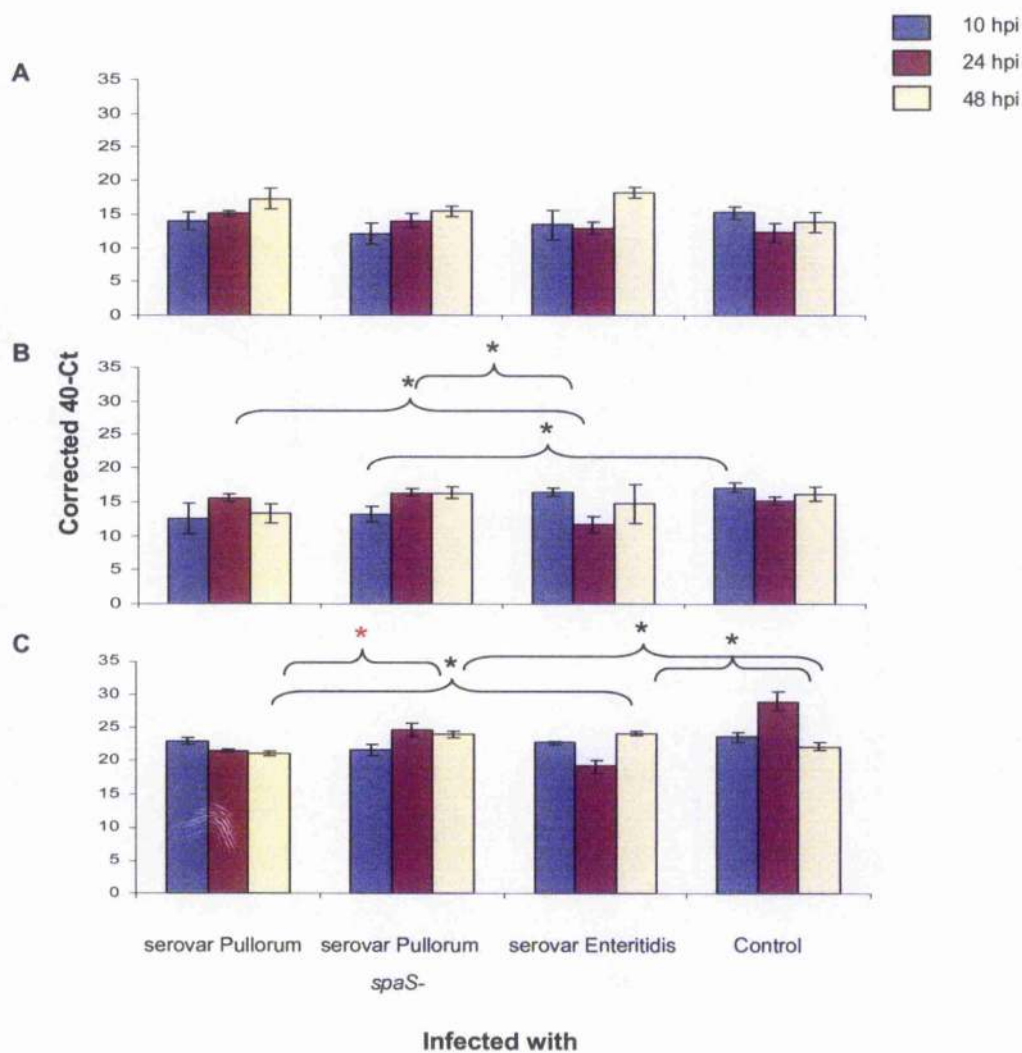


**Figure 6.6: AvBD1 mRNA levels of ileal (A), caecal tonsil (B) and splenic (C) tissues obtained post-mortem from line 7<sub>2</sub> birds 10, 24 and 48 hpi with a 0.1ml broth culture of 10<sup>8</sup> cfu of either *Salmonella enterica* serovar Pullorum, serovar Pullorum *spaS*- or serovar Enteritidis.** mRNA levels expressed as corrected 40-Ct values obtained by real-time qRT-PCR. (n=5; SE±0.05). Statistical significance within a group is represented by \*, or \* for significance that is SPI-2 TTSS-mediated.

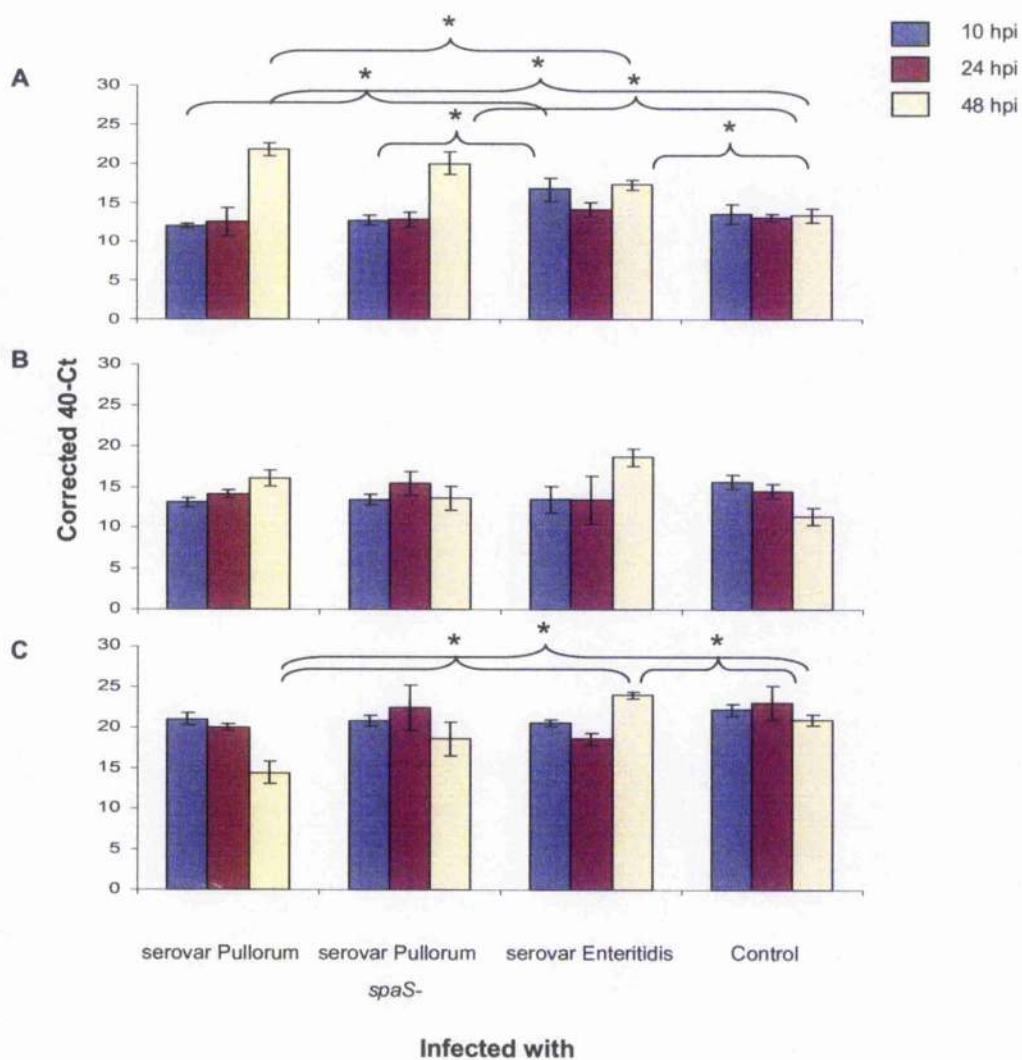


**Figure 6.7: AvBD2 mRNA levels of ileal (A), caecal tonsil (B) and splenic (C) tissues obtained post-mortem from line 7<sub>2</sub> birds 10, 24 and 48 hpi with a 0.1ml broth culture of 10<sup>8</sup> cfu of either *Salmonella enterica* serovar Pullorum, serovar Pullorum *spaS*- or serovar Enteritidis. mRNA levels expressed as corrected 40-Ct values obtained by real-time qRT-PCR. (n=5; SE±0.05). Statistical significance within a group is represented by \*.**

mRNA levels in the caecal tonsil over the time-course for the differentially-infected birds. In the spleen, there were no significant differences until 48 hpi, when AvBD2 mRNA levels measured following infection with serovar Pullorum were significantly down-regulated compared to those measured following infection with serovar Enteritidis ( $P=0.002$ ) and in the control birds ( $P=0.000$ ). AvBD2 mRNA levels following infection with serovar Enteritidis at 48 hpi in the spleen were significantly higher compared to those measured in control birds ( $P=0.025$ ).

The AvBD3 mRNA levels measured during the experiment are shown in Figure 6.8. At 24 hpi in the ileum AvBD3 mRNA levels following infection with serovar Enteritidis were significantly down-regulated compared to those measured in the control birds ( $P=0.045$ ). There were no significant differences in AvBD3 mRNA levels measured in the ileum at 10 and 48 hpi. In the caecal tonsil at 10 hpi there were no significant differences in AvBD3 mRNA levels for the differentially infected birds. At 24 hpi in the caecal tonsil, AvBD3 mRNA levels following infection with serovar Enteritidis were significantly down-regulated compared to those measured in the control birds ( $P=0.016$ ). AvBD3 mRNA levels at 48 hpi in the caecal tonsil were significantly lower following infection with serovar Pullorum compared to those measured following infection with *spaS* ( $P=0.000$ ) and with serovar Enteritidis ( $P=0.001$ ). Levels of AvBD3 mRNA following infection with *spaS* at 48 hpi in the spleen were significantly higher compared to those measured in the control birds ( $P=0.008$ ).

Figure 6.9 shows AvBD5 mRNA levels measured during the experiment. In the ileum, there were no significant differences between the AvBD5 mRNA levels measured for the differentially infected cells at 10 and 24 hpi. At 48 hpi though, AvBD5 mRNA levels following infection with serovar Enteritidis were significantly up-regulated compared to those measured following infection with *spaS* ( $P=0.006$ ). In the

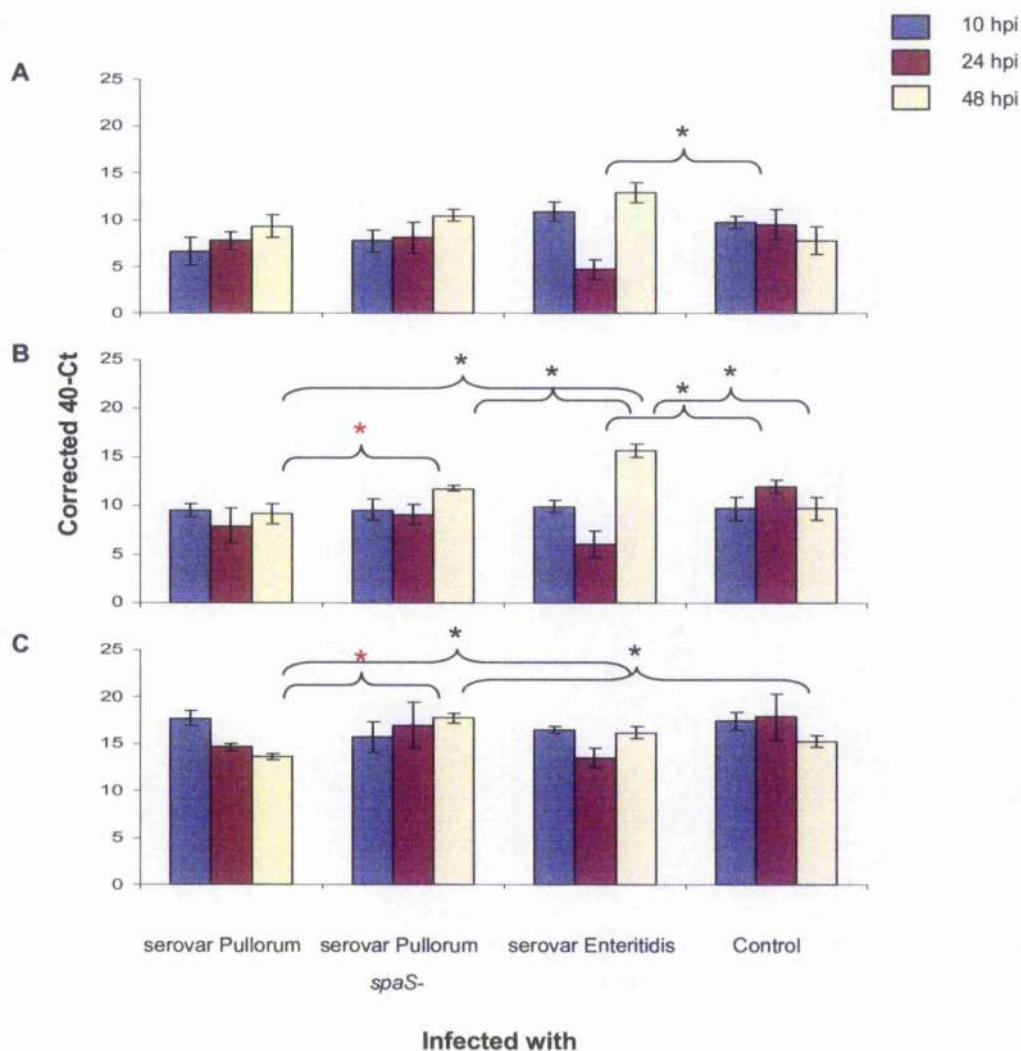


**Figure 6.8: AvBD3 mRNA levels of ileal (A), caecal tonsil (B) and splenic (C) tissues obtained post-mortem from line 7<sub>2</sub> birds 10, 24 and 48 hpi with a 0.1 ml broth culture of 10<sup>8</sup> cfu of either *Salmonella enterica* serovar Pullorum, serovar Pullorum *spaS*- or serovar Enteritidis.** mRNA levels expressed as corrected 40-Ct values obtained by real-time qRT-PCR. (n=5; SE±0.05). Statistical significance within a group is represented by \*, or \* for significance that is SPI-2 TTSS-mediated.

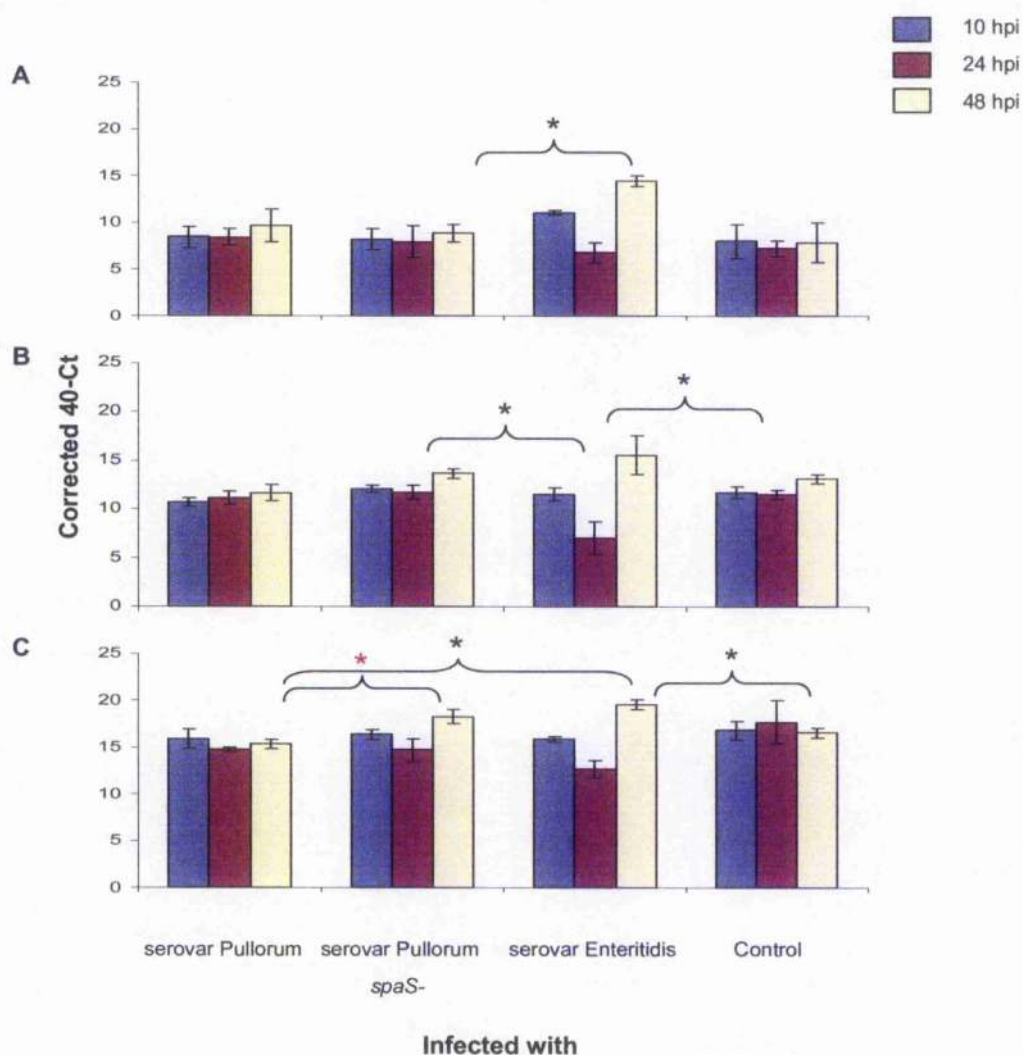


**Figure 6.9: AvBD5 mRNA levels of ileal (A), caecal tonsil (B) and splenic (C) tissues obtained post-mortem from line 7<sub>2</sub> birds 10, 24 and 48 hpi with a 0.1ml broth culture of 10<sup>8</sup> cfu of either *Salmonella enterica* serovar Pullorum, serovar Pullorum *spaS*- or serovar Enteritidis.** mRNA levels expressed as corrected 40-Ct values obtained by real-time qRT-PCR. (n=5; SE±0.05). Statistical significance within a group is represented by \*, or \* for significance that is SPI-2 TTSS-mediated.

caecal tonsil, AvBD5 mRNA levels at 24 hpi following infection with serovar Enteritidis were significantly lower compared to those measured following infection with *spaS* ( $P=0.039$ ) and measured in the control birds ( $P=0.039$ ). There were no significant differences in the caecal tonsil at 10 and 48 hpi in AvBD5 mRNA levels. In the spleen at 10 and 24 hpi, there are no significant differences in AvBD5 mRNA levels measured for the differentially infected birds. At 48 hpi though, AvBD5 mRNA levels following infection with serovar Enteritidis were significantly up-regulated compared to those measured following infection with serovar Pullorum ( $P=0.002$ ) and to the control birds ( $P=0.013$ ). AvBD5 mRNA levels were significantly higher at 48 hpi in the spleen following infection with *spaS* compared to those measured following infection with serovar Pullorum ( $P=0.009$ ).

AvBD14 mRNA levels measured in the spleen during the experiment are shown in Figure 6.10. At 10hpi, AvBD14 mRNA levels were significantly higher following infection with serovar Pullorum compared to those measured following infection with serovar Enteritidis ( $P=0.014$ ). AvBD14 mRNA levels measured at 24 hpi were significantly down-regulated following infection with serovar Enteritidis compared to those measured following infection with serovar Pullorum ( $P=0.001$ ) and with *spaS* ( $P=0.015$ ). At 48 hpi, AvBD14 mRNA levels were significantly higher following infection with serovar Enteritidis compared to those measured following infection with serovar Pullorum ( $P=0.009$ ).



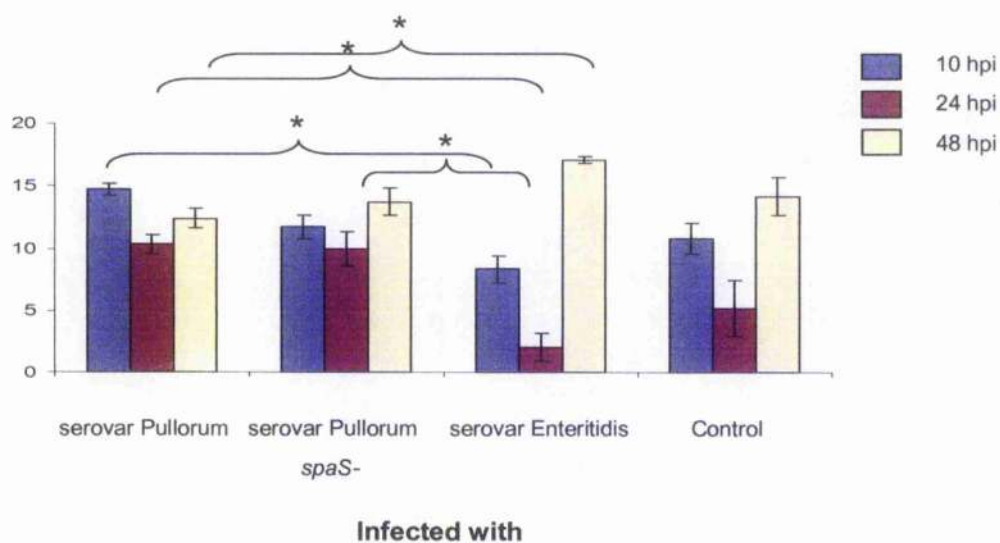


**Figure 6.10:** AvBD14 mRNA levels of splenic tissues obtained post-mortem from line 7<sub>2</sub> birds 10, 24 and 48 hpi with a 0.1ml broth culture of 10<sup>8</sup> cfu of either *Salmonella enterica* serovar Pullorum, serovar Pullorum *spaS*- or serovar Enteritidis. mRNA levels expressed as corrected 40-Ct values obtained by real-time qRT-PCR. (n=5; SE±0.05). Statistical significance within a group is represented by \*.

## 6.4 Discussion

Following oral inoculation, serovar Pullorum must exit the intestinal lumen to establish a systemic infection. There are several proposed routes of entry and one is thought to be through the caecal tonsil (Henderson *et al.*, 1999). The caeca provide an ideal environment for tissue invasion as they have a lower flow rate than the ileum, which gives time for the bacteria to attach and traverse the epithelial cells which line them. The caecal contents bacterial counts can therefore be used as an indication of the rate of invasion into the surrounding tissue. Therefore, the lower the bacterial count in the caecal contents, the higher the numbers of bacteria that have moved from the gut to more systemic sites. The caecal contents bacterial counts suggest that wild-type serovar Pullorum exit the caeca by invading the caecal walls at a faster rate compared to the SPI-1 TTSS attenuated mutant. Therefore although the SPI-1 TTSS is not essential for successful invasion of the caecal tissue by serovar Pullorum, invasion is SPI-1 TTSS-mediated. This is further supported by bacterial numbers counted in the liver, one of the systemic sites associated with persistence during serovar Pullorum infection. The SPI-1 TTSS mutant is barely detectable at 10 and 24 hpi with numbers only starting to rise by 48 hpi, compared to infection with the serovar Pullorum wild-type which shows a steady, statistically significant increase in bacterial numbers throughout the experiment. The SPI-1 TTSS, although not essential, does therefore appear to play a role in the rapid establishment of systemic serovar Pullorum infection.

The results suggest that serovar Pullorum promotes a generalised inhibition of the host pro-inflammatory immune response during infection. This is by an as yet unidentified constitutively expressed virulence factor which inhibits the host pro-inflammatory immune response during infection to levels below those seen in control birds. During the initial invasion event, the SPI-1 TTSS appears to be involved in

counteracting this, presumably to maintain normal levels of cellular recruitment to the site of infection. For the majority of the time, serovar Pullorum needs to keep a low profile in the host in order to persist for long periods and avoid discovery by the host immune system. During the initial invasion process, this profile of active down-regulation would not prove beneficial to the bacteria. As systemic infection of serovar Pullorum is reliant on intra-cellular survival of the bacterium in, and dissemination by, migrating phagocytes, it is not always of advantage to the bacteria to actively down-regulate the transcription of pro-inflammatory cytokines and chemokines which activate and attract macrophages to the site of infection. A temporary restoration of the levels of some specific pro-inflammatory cytokines/chemokines in the area around the site of infection is a way around this problem and this is what the results appear to suggest is happening.

The SPI-1 TTSS is involved in this restoration of the pro-inflammatory immune response during the early stage of serovar Pullorum infection (10 hpi) in the ileum and caecal tonsil by actively up-regulating IL-1 $\beta$  mRNA. Due to the dual constitutive inhibition and SPI-1 TTSS-mediated up-regulation of IL-1 $\beta$  by serovar Pullorum in the host, the net result is that IL-1 $\beta$  mRNA expression during infection are comparable to that in non-infected birds. This maintains migration of tissue macrophages through the GALT. IL-6 mRNA transcription was not highly up-regulated in the ileum, caecal tonsil or spleen during infection with either serovar Pullorum or serovar Enteritidis when compared to the control. Interestingly, serovar Typhimurium up-regulates IL-6 expression during invasion (Kaiser *et al.*, 2000). This suggests that both serovar Pullorum and serovar Enteritidis may actively inhibit transcription of this pro-inflammatory cytokine. This regulation was not mediated by the SPI-1 TTSS during serovar Pullorum infection. Immunomodulation during infection with serovar Pullorum

could reduce inflammation and damage in the intestines, which would increase the likelihood of the bacteria being able to establish a systemic infection. There has been contradictory evidence as to the role of SPI-1 in serovar *Gallinarum* infection (Jones *et al.*, 2001; Shah *et al.*, 2005). These differences could be due to the differences in the age and breed of chicken used for the experimental infections (Shah *et al.*, 2005). It is therefore most likely that although SPI-1 contributes to the virulence of serovar *Gallinarum* infection, the age and genetic makeup of the chicken may also contribute to any effect (Shah *et al.*, 2005). Interestingly invasion of a gut epithelial cell model with serovar *Gallinarum* has no effect on IL-6 expression (Kaiser *et al.*, 2000), a mechanism which appears to be SPI-1-mediated in other serovars.

ChCXCLi1 (K60) and chCXCLi2 (IL-8) share 48% and 50% homology with human CXCL8 (IL-8) respectively (Sick *et al.*, 2000; Kaiser *et al.*, 1999). CXCLi1 mainly chemoattracts heterophils (the avian equivalent of neutrophils) and CXCLi2 mainly chemoattracts monocytes (Poh, Pease, Young, Bumstead and Kaiser unpublished results). During serovar *Typhimurium* infection, which causes much damage to the intestinal epithelia, a SPI-1 TTSS-mediated increase in IL-8 production is observed in mammals (Hobbie *et al.*, 1997). From the observed pathology and the nature of the disease, it could be hypothesised that the converse is true during serovar *Pullorum* infection, and therefore there should be a decrease in CXCLi1 and CXCLi2. This is indeed the case, as there is a SPI-1 TTSS-mediated up-regulation of CXCLi1 during early-stage infection in the caecal tonsil to levels similar to those seen in the control. The SPI-1 TTSS does not seem to promote an up-regulation of CXCLi1 mRNA transcription in the ileum or spleen at this early time-point though, suggesting that the actions of SPI-1 TTSS must be highly targeted to specific organs/tissues. Conversely to the SPI-1 TTSS-mediated up-regulation of CXCLi1 mRNA in the caecal tonsil, there is

a down-regulation of transcription in the spleen at 24 hpi. This could be an attempt to reduce attraction and recruitment of immune cells to the site of persistence in the spleen in order to avoid a major inflammatory immune response. During a natural infection with serovar Pullorum, the main form of transmission within a group of chickens is vertical. For this to be effective, birds must first reach sexual maturity in order to transmit the pathogen vertically to their offspring. Therefore it does not benefit the bacteria to cause extensive pathology, which would ultimately reduce the health of the chicken host, and during the early stages of systemic infection this modulation of the immune response may in part be due to the SPI-1 TTSS. The expression profile of CXCLi2 suggests that any regulation of transcription of this chemokine is not SPI-1 TTSS-regulated in serovar Pullorum-infected birds, although immune modulation by the bacteria, in order to reduce up-regulation of chemokine transcription due to detection by the innate immune response, may be controlled by other virulence factors.

The mRNA levels of a selection of avian  $\beta$ -defensins were investigated as the defensins play a role in gram-negative bacterial infections in mammalian hosts (Sugiarto and Yu, 2004; Salzman *et al.*, 2003; Wilson *et al.*, 1999). AvBD1 mRNA is not transcribed above basal levels (those seen in control birds) in the ileum, but appears to be actively suppressed initially by serovar Pullorum (at 10 hpi) then subsequently by serovar Enteritidis (at 24 hpi) in the caecal tonsil which would suggest it functions in a localised manner. In the spleen at 48 hpi, AvBD1 mRNA levels in response to serovar Pullorum infection appear to be suppressed due to the SPI-1 TTSS, as the SPI-1 TTSS attenuated mutant has statistically significantly up-regulated mRNA levels compared to those observed in the wild-type-infected and control bird groups. The AvBD2 mRNA expression profile is different to that for AvBD1, and this  $\beta$ -defensin appears to be most important at later stages of the experiment (48 hpi). In the ileum, there is active up-

regulation of AvBD2 mRNA in response to serovar Pullorum infection, but in the spleen AvBD2 mRNA is down-regulated compared to the control. The differential regulation of AvBD2 mRNA does not appear to be due to the SPI-1 TTSS of serovar Pullorum, as the attenuated mutant-infected group does not have significantly different mRNA levels to the wild-type. The reason for the mRNA levels of AvBD2 in the ileum being at similar levels to those in control birds during serovar Pullorum infection at 10 and 24 hpi could be due to an active suppression by the bacteria to avoid detection and aid invasion. By 48 hpi, many of the bacteria will have escaped the caecal lumen and moved to systemic sites, so it becomes less important for serovar Pullorum to actively inhibit AvBD2 levels, which could explain the high increase in mRNA transcription at this time-point. The down-regulation by serovar Pullorum of AvBD2 levels in the spleen at 48 hpi could be an attempt to evade detection by the immune system and avoid the initiation of an inflammatory immune response.

AvBD3 mRNA levels in the ileum, the caecal tonsil and, to a lesser extent, in the spleen, demonstrate a similar expression pattern during serovar Enteritidis infection, with an active suppression at 24 hpi followed by an up-regulation at 48 hpi. AvBD3 mRNA levels in birds during infection with serovar Pullorum are unaltered compared to levels in birds within the control group up to 48 hpi in any of the tissues. Either serovar Pullorum does not stimulate AvBD3 mRNA transcription due to specific adaptation of the serovar, or there is an active inhibition of this  $\beta$ -defensin to maintain levels similar to that observed in control birds. If the latter is the case, then the inhibition is not SPI-1 TTSS-dependent, as infection with the SPI-1 TTSS-attenuated mutant does not affect the resulting mRNA levels. At 48 hpi, however, there does appear to be a SPI-1 TTSS-mediated active inhibition of AvBD3 transcription in both the spleen and caecal tonsil. The regulation of AvBD5 (Lynn *et al.*, 2004; Xiao *et al.*, 2004) mRNA in the spleen at

48 hpi by serovar Pullorum to levels similar to that seen in control birds is also SPI-1 TTSS-mediated. There is early up-regulation of AvBD14 in the spleen in response to serovar Pullorum infection which is not SPI-1 TTSS-dependent but, by 48 hpi, mRNA levels are not different to those found in mock-infected control birds. This early up-regulation precedes the physical presence of the bacteria systemically, as shown by the bacterial counts. Tissue expression profiles have found that AvBD14 is only expressed in the skin and the spleen (Annelise Soulier, unpublished results), but the early up-regulation of expression measured in the spleen indicates that transcription of this  $\beta$ -defensin may be triggered prior to invasion of the tissue itself. These data suggest a targeted response to serovar Pullorum infection by the host, in the spleen, by the production of AvBD14.

Although there has been some previous research into the role of mammalian  $\beta$ -defensins in *S. enterica* infection, to date the specific roles of the avian  $\beta$ -defensins are largely unknown. The actions of avian  $\beta$ -defensins during infection can be compared as a group to mammalian  $\beta$ -defensins, but they are not comparable individually (i.e. AvBD1 is not comparable to human  $\beta$ -defensin-1). It is important to study the role played by individual anti-microbial peptides during infection though, as  $\beta$ -defensins may each occupy a distinct functional niche important in intestinal mucosal defence (O'Neil *et al.*, 1999). An example of this is the differential expression of human  $\beta$ -defensin-1 and -2 in the colon. Human  $\beta$ -defensin-1 is expressed by the epithelium of normal human colon and small intestine, with a similar pattern of expression in the inflamed colon (O'Neil *et al.*, 1999). In contrast, there is little human  $\beta$ -defensin-2 expression by the epithelium of normal colon, but abundant human  $\beta$ -defensin-2 expression by the epithelium of inflamed colon (O'Neil *et al.*, 1999). Additionally, serovars Enteritidis, Typhimurium, Typhi and Dublin all induce human  $\beta$ -defensin-2

mRNA expression in human colon cells (Ogushi *et al.*, 2001). One avian  $\beta$ -defensin that has been studied with regard to the host response to *S. enterica* infection is AvBD9. There is a high, constitutive expression of AvBD9 in the proximal digestive tract and it has a broad antimicrobial activity against food-borne pathogens including serovar Typhimurium, which suggests that it plays an important role in chicken innate host defence (van Dijk *et al.*, 2007). Avian  $\beta$ -defensins may also play a role in reducing the transmission of *S. enterica* to subsequent generations. The expression of AvBD1, 2 and 3 in the cloacas of laying hens increases with age, and also decreases in the regressed oviduct during the non-laying phase (Yoshimura *et al.*, 2006). There is an increase in the synthesis of AvBD1, 2 and 3 in response to serovar Enteritidis infection in the cloacas of laying chickens, which may serve to reduce transmission of the bacteria from the egg (Yoshimura *et al.*, 2006). Avian  $\beta$ -defensins are involved in host resistance to *Salmonella* (Sadeyen *et al.*, 2006). There is an increased expression of avian  $\beta$ -defensin genes in chicken lines which are considered to be *Salmonella* resistant (Sadeyen *et al.*, 2006). The high expression of avian  $\beta$ -defensins in resistant lines is concurrent with lower serovar Enteritidis colonisation rates (Sadeyen *et al.*, 2006). Adult birds from a *Salmonella*-resistant line, have a high baseline level of expression for both AvBD1 and AvBD2 and in chickens exhibiting the most resistant *Salmonella* phenotype, these avian  $\beta$ -defensin genes have been found in levels approximately 10 times higher than those measured in a *Salmonella*-susceptible line (Sadeyen *et al.*, 2006).

In summary, there appears to be a generalised suppression of avian  $\beta$ -defensin mRNA expression in response to serovar Pullorum infection in the spleen at 48 hpi and this is SPI-1 TTSS-mediated for AvBD1, 3 and 5. The down-regulation observed for AvBD2 does not seem to be associated with the SPI-1 TTSS and therefore is probably due to another virulence factor. There is also a specific targeted up-regulation of



$\Delta$ vBD14 mRNA in the spleen during the early stages of the infection, which happens before the pathogen has disseminated in any real numbers to this systemic site. This up-regulation in levels of mRNA decreases as the bacteria are transported in greater numbers to the spleen. These results suggest a manipulation of avian  $\beta$ -defensin transcription in the chicken host during the first 48 hours following serovar Pullorum infection in order to suppress the antimicrobial actions of these molecules. This manipulation appears to be SPI-1 TTSS mediated, but is also clearly a result of other virulence factors utilised by serovar Pullorum to enhance the ability of the bacteria to cause a persistent systemic infection in the chicken.

The gross pathology observed during the post-mortem collection of tissues supports the hypothesis that the SPI-1 TTSS-attenuated mutant is slower to escape the caecal lumen than the wild-type serovar Pullorum bacteria. Birds infected with the serovar Pullorum SPI-1 TTSS-attenuated mutant presented with more severe gut-associated pathology than those infected with serovar Pullorum wild-type, and there was more localised damage to the caecal wall, with sloughing of the mucosa layer. Interestingly those birds infected with serovar Pullorum displayed more pronounced blood vessel growth around the gut than those infected with the SPI-1 TTSS-attenuated mutant. It is thought that serovar Pullorum translocates to systemic sites in the chicken transported inside phagocytes such as macrophages (Wigley *et al.*, 2001) and the increase in blood vessel provision around the site of infection would certainly aid in the process of cell recruitment. The gross pathology does indeed suggest that this process may be somewhat SPI-1-mediated. It is also interesting that the serovar Enteritidis-infected birds displayed more severe inflammation-related pathology than those infected with serovar Pullorum. This supports the hypothesis that serovar Pullorum actively evades and inhibits the chicken immune response to a greater extent than other *S.*

*enterica* serovars, in order to create a persistent low-level systemic infection until sexual maturity is reached (Shivaprasad, 2000).

In conclusion, the SPI-1 TTSS enables serovar Pullorum to invade the chicken host quickly without inducing a significant innate immune response. Although functionality of the SPI-1 TTSS is not vital for infection, it aids in the development of a more rapid systemic infection. This increases the chance of a successful persistent infection with minimum detection by the host immune system.

## Chapter 7: General Discussion

The relative contribution of SPI-1 and SPI-2 to the virulence of serovar Pullorum has previously been determined (Wigley *et al.*, 2002). Loss of SPI-1 function results in a reduction in virulence of serovar Pullorum, but not a complete attenuation (Wigley *et al.*, 2002). There has been contradictory evidence as to the role of SPI-1 in serovar Gallinarum infection (Jones *et al.*, 2001; Shah *et al.*, 2005). It appears that SPI-1 contributes to the virulence of serovar Gallinarum infection, but the age and genetic makeup of the chicken may also contribute to any effect (Shah *et al.*, 2005). SPI-2 is essential for the virulence of serovar Pullorum and its attenuation abrogates carriage in the chicken and the establishment of infection (Wigley *et al.*, 2002). The aetiology of disease resulting from infection with *S. enterica* can be directly related to the pathology caused by the host immune response reacting to the presence of the bacteria in the gut and at systemic sites. Pathology resulting from infection with serovar Pullorum is much reduced compared to that seen for other related serovars (Henderson *et al.*, 1999) and this was evident during comparisons with pathology in birds infected with serovar Enteritidis during this study. Previous research in this area has concentrated on the relative contribution of SPI-1 and SPI-2 to the success of infection with serovar Pullorum. Consequently, there has been limited research into the host immune response during infection or into the mechanisms used by the bacteria in order to evade this immune response. The primary aim of this study was to assess if these mechanisms may be in part as a result of virulence factors from the SPI-1 and the SPI-2. A range of *in vitro* and *in vivo* techniques were employed.

### 7.1 The initial invasion event during Pullorum Disease

The results collectively show that during infection with serovar Pullorum, invasion through the gut-associated lymphoid tissue (GALT) is in part SPI-1 mediated. The *in vivo* study described in Chapter six used counts of bacterial numbers in the caeca and at systemic sites over a time-course in order to establish rates of invasion. Invasion through the GALT is likely to be via the bursa and the caecal tonsil, as both sites have a high concentration of lymphoid tissue (Henderson *et al.*, 1999). The data showing the differences in the progression of the disease between the wild type and the mutant strains indicate that SPI-1 is important for the rapid systemic dissemination of serovar Pullorum in the chicken. This SPI-1 mediated rapid systemic spread could be as a direct result of the rapid initial invasion event. It is thought that this dissemination to systemic sites takes place via transport in macrophages (Wigley *et al.*, 2001).

The results show that during infection with serovar Pullorum, transcription of host pro-inflammatory cytokines and chemokines is in general similar to that measured in non-infected birds. This leads to the hypothesis that serovar Pullorum either promotes a generalised inhibition or does not elicit a host pro-inflammatory immune response during infection. If this is the case, then this stealth is achieved by an as yet unidentified, constitutively expressed, virulence factor. The result is an inhibition of the host pro-inflammatory immune response during infection, to transcription levels below those seen in control birds. It is likely that this would down-regulate normal levels of expression of pro-inflammatory mediators in the host such as IL-1 $\beta$ , and provide a favourable environment for the serovar Pullorum bacteria to persist in. During the initial invasion event, SPI-1 appears to be involved in counteracting this, which is presumably in order to maintain more normal levels of cellular recruitment to the site of infection (i.e. similar to those seen in non-infected hosts). For the majority of the time during the

infection, it is beneficial for serovar Pullorum to keep a low profile in the host, in order to persist for long periods and avoid discovery by the host immune system. Serovar Pullorum reduces the ability of the host to recognise the presence of the bacteria by down-regulating components of the host pro-inflammatory immune response, which would normally recognise the pathogen and mount an immune response against it. Establishment of systemic infection by serovar Pullorum is reliant on intra-cellular survival of the bacterium in, and dissemination by, migrating phagocytes (Wigley *et al.*, 2001). At this stage, it is not advantageous for the bacteria to actively down-regulate transcription of specific pro-inflammatory cytokines and chemokines which activate and attract macrophages to the site of infection. A temporary restoration of the levels of some specific pro-inflammatory cytokines/chemokines in the area around the site of infection is a way around this problem. The results suggest that this is in fact the case and is SPI-1 -mediated.

SPI-1 mediates an up-regulation of IL-1 $\beta$ , IL-6, CXCLi1 and CXCLi2 to levels comparable to those measured in the gastro-intestinal tract of control birds. These cytokines and chemokines can promote recruitment of phagocytes locally, to the site of infection. This up-regulation of expression will thus increase the likelihood that the bacteria will encounter macrophages. Infection of day-of-hatch birds with serovar Typhimurium leads to a significant up-regulation of CXCLi1, CXCLi2 and IL-1 $\beta$  expression in intestinal tissue which corresponds with the presence of inflammatory signs (Withanage *et al.*, 2004). CXCLi1 is a major chemotactic factor, which aids in mediating the serovar Enteritidis-induced recruitment of heterophils to the site of bacterial invasion (Kogut, 2002; Poh, Pease, Young, Bumstead and Kaiser unpublished results) and CXCLi2 is thought to aid recruitment of macrophages to the site of

infection (Poh, Pease, Young, Bumstead and Kaiser unpublished results). Thereby up-regulation of CXCLi1 and CXCLi2 expression may aid the systemic spread of infection.

## **7.2 Persistence within macrophages during Pullorum Disease**

Although SPI-1 is involved in the invasion of the gut epithelial cells, it does not play a role in the subsequent invasion of macrophages, which indicates that this event involves a different process. Entry into macrophages is likely to be via phagocytosis in most hosts. Avian macrophages are capable of engulfing both opsonised and unopsonised antigen, but phagocytosis is more efficient with opsonised antigens (Qureshi *et al.*, 1986; Powell, 1987). Once phagocytosed, the avian macrophage digests antigens with hydrolytic enzymes such as lysozymes and acid phosphatase (Fox and Soloman, 1981; Qureshi and Dietert, 1995). Avian macrophages, like their mammalian counterparts, also produce reactive oxygen intermediates (Golemboski *et al.*, 1990) and reactive nitrogen intermediates (Dietert *et al.*, 1991; Sung *et al.*, 1991; Qureshi *et al.*, 1993).

At this stage of infection, although uptake of serovar Pullorum is mediated by the macrophage, persistence of intracellular bacteria is SPI-2-mediated. The results suggest that SPI-2 may place a check on intracellular numbers in order to ensure persistence within the cell, as the cell is unlikely to be able to sustain large numbers of intracellular bacteria without detection by the immune system. SPI-2 therefore may promote controlled intracellular growth. The macrophage may be unable to sustain high numbers of intracellular bacteria and restrictions on proliferation would help. Serovar Pullorum bacteria lacking a functional SPI-2 were present in higher numbers compared to the wild-type early in the infection, but these numbers rapidly dropped over the time-course. Intracellular numbers of the wild-type bacteria remained at a low, sustained

level throughout the time-course. In addition to this, SPI-2 inhibits the induction of nitric oxide synthesis by the macrophage to control targeted antimicrobial activity. Interestingly, serovar Enteritidis also regulates intramacrophage numbers (Okamura *et al.*, 2005). Although invasion takes place at similar rates, numbers of intracellular serovar Enteritidis are significantly reduced when compared to serovar Typhimurium (Okamura *et al.*, 2005). Macrophages activated with IFN- $\gamma$  produce significantly less NO following treatment with serovar Enteritidis LPS compared to serovar Typhimurium LPS, and macrophage necrosis is significantly increased following infection with serovar Typhimurium (Okamura *et al.*, 2005). This may cause an increased inflammatory response during infections with serovar Typhimurium (Okamura *et al.*, 2005) which can be directly related to the aetiology of the disease. Therefore, limiting intracellular bacterial numbers may aid persistence of serovar Enteritidis in macrophages.

Serovar Pullorum inhibits IL-6 mRNA expression in macrophages in a SPI-2-dependent manner. This may play a role in masking the intracellular infection as the macrophage would normally produce IL-6 in response to infection with an intracellular pathogen. Strains with a functional SPI-2 also lead to increased levels of CXCLi2 expression in macrophages at early time-points compared to SPI-2 mutants. This would probably lead to increased monocyte recruitment to the site of infection and increase the chance of more phagocytic cells becoming infected, promoting the systemic spread of the bacteria. This increase in recruitment is short-lived though and is no longer apparent at later time-points.

### 7.3 Avian $\beta$ -defensins in Pullorum Disease

There are indications in mammals that the ability to resist the killing effect of host antimicrobial peptides is a virulence property of *Salmonella enterica* (Groisman *et al.*, 1992). In serovar Typhimurium this resistance has been associated with 8 separate genetic loci representing several virulence factors (Groisman *et al.*, 1992). The generalised suppression of avian  $\beta$ -defensin mRNA expression in the spleen at 48 hpi in response to infection with serovar Pullorum *in vivo* is SPI-1-mediated for AvBD1, 3 and 5. Milona *et al.* (2007) reported that infection with serovars Typhimurium and Enteritidis does not induce AvBD5 mRNA expression in the small intestine. Likewise, infection with serovar Pullorum did not induce AvBD5 mRNA expression in the ileum and caecal tonsil, with equivalent levels compared to mock-infected control birds. The down-regulation of AvBD2 mRNA expression during serovar Pullorum infection was not due to SPI-1. AvBD14 mRNA is up-regulated in spleen prior to bacterial infection in that tissue, but at 48 hpi the expression levels fall to be similar to those seen in control birds. This coincides with the systemic spread of the bacteria and at systemic sites avian  $\beta$ -defensin expression is, in general, reduced in a SPI-1-dependent mechanism.

### 7.4 Areas of future work

#### 7.4.1 Work involving primary macrophages

Large numbers of primary macrophages can be obtained from the chicken via culture of bone marrow-derived cells with rchGM-CSF using the method developed and described in Chapter three. Primary avian macrophages are required for the accurate study of macrophage function and, as demonstrated by the *in vitro* infection studies in this research, bacterial persistence assays. The effect of SPI-2 *in vivo* has been



demonstrated previously (Wigley *et al.* 2002), but the associated phenotype using macrophages *in vitro* had not been previously established (Paul Wigley, personal communication). This research described SPI-2-associated intracellular persistence using bone marrow-derived macrophages. This phenotype was only apparent when studying survival and response over a long time-course (up to 72 hpi) though, which is not practical using primary macrophages derived from other sources. The chicken bone marrow-derived macrophage model therefore provides a tool for potential future research into *Salmonella* persistence or that of other intracellular pathogens.

Granulocytic structures were seen in primary blood-derived macrophages and to a lesser extent in BM-dMΦ when images were taken using TEM. These structures are not found in mammalian macrophages, which may mean that avian macrophages are more different from their mammalian counterparts than first thought. The divergent evolution of avian and mammal orders from a common ancestor 300 million years ago has resulted in some differences between the modern immune systems of both groups. Avian macrophages may therefore have some different functions compared to mammalian macrophages, and may be involved in granulocytic activities. The heterophil inflammatory response in avian species more closely resembles the reptilian response than the mammalian neutrophil response (Montali, 1988). Further investigation into the nature of these granulocytic structures is needed.

#### **7.4.2 Determining the roles of virulence factors during infection with serovar Pullorum**

The contributions of virulence factors outwith the SPI-1 and SPI-2, and also of other SPIs, to the virulence of Pullorum Disease are important to establish and further research should address this. The unsuitability of serovar Pullorum 449/87 for the λ-Red

system means that any future work requiring mutagenesis of the serovar would need to either utilise a different serovar Pullorum strain or a different technique. Although considered to be a quick and easy method of mutant construction, widely used for other gram-negative bacteria, it is becoming more apparent that not all *S. enterica* strains lend themselves to mutagenesis via  $\lambda$ -Red.

#### **7.4.3 The mechanisms of infection of the reproductive tract and subsequent transovarian transmission of serovar Pullorum**

This research has concentrated on the establishment of systemic infection with serovar Pullorum in the chicken. Little work has been done to investigate the mechanisms behind the infection of the reproductive tract and subsequent transovarian transmission and the dissection of this could be one area of future work. During experimental infection, serovar Pullorum can persist for over 40 weeks at the systemic sites of the spleen and the reproductive tract (Wigley *et al.*, 2001). T cell responses to serovar Pullorum, and non-specific responses to mitogenic stimulation, reduce greatly in both infected and non-infected birds at the onset of lay (Wigley *et al.*, 2005). This fall in T cell responsiveness coincides with an increase in serovar Pullorum bacterial numbers in the spleen and the spread to the reproductive tract (Wigley *et al.*, 2005). Approximately three weeks following the onset of lay, T cell responsiveness is restored which coincides with a decline in bacterial numbers (Wigley *et al.*, 2005). This indicates a non-specific suppression of cell-mediated immunity occurs at the onset of lay, and that this plays a major role in the ability of serovar Pullorum to infect the reproductive tract (Wigley *et al.*, 2005). The bacterial mechanisms (if any) behind this are unknown, and future work could evaluate the contribution of the SPIs to this event. In the reproductive tract, serovar Pullorum colonises both the ovary and the oviduct of

hens, which leads to 6% of laid eggs being infected with the bacterium (Wigley *et al.*, 2001). Localised cell-mediated immunity may also be involved in the control of serovar Enteritidis infection of reproductive tissues, as there is a correlation between decreased bacterial survival with elevated lymphocyte and macrophage numbers in the ovary and oviduct (Withanage *et al.*, 2003). Therefore the loss of T cell activity at the point of lay may also aid serovar Enteritidis infection and transmission to eggs (Wigley *et al.*, 2005). This suggests that both serovar Pullorum and serovar Enteritidis may infect and colonise the reproductive tract using the same mechanisms, and the identification of the virulence factors which are involved in this process would be of interest.

## 7.5 Final conclusions

The results from this study suggest that *Salmonella enterica* serovar Pullorum does not promote the induction of a pro-inflammatory immune response in the gut, and that SPI-1 is responsible for up-regulating IL-1 $\beta$ , IL-6, CXCLi1 and CXCLi2 to recruit phagocytes to the site of infection. This is in contrast to the hypothesis that SPI-1 is responsible for dampening down the immune response. Although not required for full-virulence, SPI-1 enables a faster dissemination of serovar Pullorum to systemic sites. At systemic sites away from the gut, SPI-1 is responsible for a down-regulation of the antimicrobial peptides AvBD1, 3 and 5 and of CXCLi1. SPI-2 appears to play a role in maintaining sustainable intracellular numbers within macrophages. Methods by which it may do this include the inhibition of nitric oxide synthesis and down-regulation of IL-6 expression.

In conclusion, SPI-1 and SPI-2 both contribute to the virulence of serovar Pullorum, enabling the establishment of a more rapid and stealthy infection in the chicken.

## References

- ALPUCHE-ARANDA C. M., RACOOSIN E. L., SWANSON J. A., MILLER, S. I. 1994. *Salmonella* stimulate macrophage macropinocytosis and persist within spacious phagosomes. *Journal of Experimental Medicine*. **179** p.601-608
- AMAVISIT P., LIGHTFOOT D., BOWNING G.F., MARKHAM P. F. 2003. Variation between pathogenic serovars within *Salmonella* Pathogenicity Islands. *Journal of Bacteriological Sciences*. **185** p.2624-2635
- AVERY S., ROTHWELL L., DEGEN W.D., SCHIJNS V.E., YOUNG J., KAUFMAN J., KAISER P. 2004. Characterization of the first non-mammalian T2 cytokine gene cluster: the cluster contains functional single-copy genes for IL-3, IL-4, IL-13, and GM-CSF, a gene for IL-5 that appears to be a pseudogene, and a gene encoding another cytokine like transcript, KK34. *Journal of Interferon and Cytokine Research*. **24** p.600-610
- BARKER K. A., HAMPE A., STOECKLE, M. Y., HANAFUSA H. 1993. Transformation-associated cytokine 9E3/CEF4 is chemotactic for chicken peripheral blood mononuclear cells. *Journal of Virology*. **67** p.3528-3533
- BARROW P. A. 1991. Experimental infection of chickens with *Salmonella enteritidis*. *Avian Pathology*. **20** p.145-153
- BARROW P. A., LOVELL M. A. 1989. Invasion of Vero cells by *Salmonella* species. *Journal of Medical Microbiology*. **28** p.59-67
- BARROW P. A., LOVELL M. A. 1991. Experimental infection of egg-laying hens with *Salmonella enteritidis*. *Avian Pathology*. **20** p.339-352

- BARROW P. A., LOVELL M. A., BERCHIERI, A. 1991. The use of two live attenuated vaccines to immunize egg-laying hens against *Salmonella enteritidis* phage type 4. *Avian Pathology*. **20** p.681-692
- BARROW P. A., LOVELL M. A., STOCKER B. A. D. 2000. Protection against fowl typhoid by parental administration of live SL5828, an *aroA-serC* (aromatic dependent) mutant of wild-type *Salmonella Gallinarum* strain made lysogenic for P22 *sie*. *Avian Pathology*. **29** p.423-431
- BAUMLER A., TSOLIS R. M., FICHT T. A., ADAMS L. G. 1998. Evolution of host adaptation in *Salmonella enterica*. *Infection and Immunity*. **66** p.4579-4587
- BEAUDETTE F. R. 1930. Fowl typhoid and bacillary white diarrhea. 11<sup>th</sup> *International Veterinary Congress, London*. Baillière, Tindall and Cox, London. p.705-723
- BEAUDETTE F. R. 1936. Arthritis in a chick caused by *Salmonella pullorum*. *Journal of the American Veterinary Medicine Association*. **89** p.89-91
- BERCHIERI A., MURPHY C. K., MARSTON K., BARROW P. A. 2001  
Observations on the persistence and vertical transmission of *Salmonella enterica* serovars Pullorum and Gallinarum in chickens; effect of bacterial and host genetic background. *Avian Pathology*. **30** p.229-239
- BERCHIERI A., WIGLEY P., PAGE K., MURPHY C. K., BARROW P. A. 2001.  
Further studies on vertical transmission and persistence of *Salmonella enterica* serovar Enteritidis phage type 4 in chickens. *Avian Pathology*. **30** p.307-320
- BEUG H., VON KIRCHBACH A., DÖDERLEIN G., CONSCIENCE J.-F., GRAF T. 1979. Chicken hematopoietic cells transformed by seven strains of defective avian leukaemia viruses display three distinct phenotypes of differentiation. *Cell*. **18** p.375-390

- BEUZÓN C. R., BANKS G., DEIWICK J., HENSEL M., HOLDEN D. 1999. pH-dependent secretion of SseB, a product of the SPI-2 type III secretion system of *Salmonella typhimurium*. *Molecular Microbiology*. **33** p.806-816
- BREDT D. S., SNYDER S. H. 1994. Nitric oxide: A physiologic messenger molecule. *Annual Review of Biochemistry*. **63** p.175-195
- BUCKMEIER N. A., HEFFRON F. 1989. Intracellular survival of wild-type *Salmonella typhimurium* and macrophage-sensitive mutants in diverse populations of macrophages. *Infection and Immunity*. **57** p.1-7
- BURSZTYN H., SGARAMELLA V., CIFERRI O., LEDERBERG J. 1975. Transfectability of rough strains of *Salmonella typhimurium*. *Journal of Bacteriology*. **124** p.1630-1634
- CHAKRAVORTTY D., HANSEN-WESTER I., HENSEL M. 2002. *Salmonella* pathogenicity island 2 mediates protection of intracellular *Salmonella* from reactive nitrogen intermediates. *Journal of Experimental Medicine*. **195** p.1155-1166
- CHAUDHURI R.R., KHAN A. M., PALLEN M. J. 2004. coliBASE: an online database for *Escherichia coli*, *Shigella* and *Salmonella* comparative genomics. *Nucleic Acids Research*. **32**. Database issue D296-D299
- CHEMINAY C., SCHOEN M., HENSEL M., WANDERSEE-STEINHAUSER A., RITTER U., KÖRNER H., RÖLLINGHOFF M., HEIN J. 2002. Migration of *Salmonella typhimurium*-harboring bone marrow-derived dendritic cells towards the chemokines CCL19 and CCL21. *Microbial Pathogenesis*. **32** p.207-218
- CHOMARAT P., BANCHEREAU J., DAVOUST J., PALUCKA K.A. 2000. IL-6 switches the differentiation of monocytes from dendritic cells to macrophages. *Nature Immunology*. **1** p.510-514

- CIRILLO D., VALDIVIA R. H., MONACK D., FALKOW S. 1998. Macrophage-dependent induction of the *Salmonella* pathogenicity island 2 type III secretion system and its role in intracellular survival. *Molecular Microbiology*. **30** p.175-188
- COLLAZO C. M., GALÁN J. E. 1997. The invasion-associated type-III protein secretion system in *Salmonella* -- a review. *Gene*. **192** p.51-59
- COLLIER-HYAMS L. S., ZENG H., SUN J., TOMLINSON A. D., QIN BAO Z., CHEN H., MADARA J. L., ORTH K., NEISH A. S. 2002. Cutting Edge: *Salmonella* AvrA effector inhibits the key pro-inflammatory, anti-apoptotic NF- $\kappa$ B pathway. *The Journal of Immunology*. **169** p.2846-2850
- COSLOY S. D., OISHI M. 1973. Genetic transformation in *Escherichia coli* K12. *Proceedings of the National Academy of Sciences USA*. **70** p.84-87
- DAEFLER S. 1999. Type III secretion by *Salmonella typhimurium* does not require contact with a eukaryotic host. *Molecular Microbiology*. **31** p.45-51
- DANIELS J. J. D., AUTENREITH I. B., LUDWIG A., GOEBEL W. 1996. The gene *slyA* of *Salmonella typhimurium* is required for destruction of M cells and intracellular survival but not for invasion or colonization of the murine small intestine. *Infection and Immunity*. **64** p.5075-5084
- DATSENKO K. A., WANNER B. L. 2000. One-step inactivation of chromosomal genes in *Escherichia coli* K-12 using PCR products. *Proceedings of the National Academy of Sciences USA*. **97** p.6640-6645
- DAWSON T. M., DAWSON V. L. 1995. Nitric oxide: analysis and pathological role. *The Neuroscientist*. **1** p.7-18
- DEIWICK J., NIKOLAUS T., ERDOGAN S., HENSEL M. 1999. Environmental regulation of *Salmonella* pathogenicity island 2 gene expression. *Molecular Microbiology*. **31** p.1759-1773

- DIEHL S., ANGUITA J., HOFFMEYER A., ZAPTON T., IHLE J. N., FIKRIG E., RINCON M. 2000. Inhibition of Th1 differentiation by IL-6 is mediated by SOCS1. *Immunity*. **13** p.805-815
- DIETERT, R. R., GOLEMBOSKI K. A., BLOOM S. E., QURESHI M. A. 1991. The avian macrophages in cellular immunity. In *Avian Cellular Immunity*. J. M. Sharma, ed. CRC. Press, Boca Raton, FL. p.71-95
- ERBECK D. H., MCLAUGHLIN B. G., SINGH S. N. 1993. Pullorum disease with unusual signs in two backyard chicken flocks. *Avian Diseases*. **37** p.895-897
- EVANS E. W., BEACH G. G., WUNDERLICH J., HARMON B. G. 1994. Isolation of antimicrobial peptides from avian heterophils. *Journal of Leukocyte Biology*. **56** p.661-665
- EVANS W. M., BRUNER D. W., PECKHAM M. C. 1955. Blindness in chicks associated with salmonellosis. *Cornell Veterinarian*. **45** p.239-247
- FALKOW. 1988. Molecular Koch's postulates applied to microbial pathogenicity. *Review of Infectious Disease*. **10**(supplement 2) p.S274-S276
- FERGUSON A. E., CONNELL M. C. TRUSCOTT B. 1961. Isolation of *Salmonella pullorum* from the joints of broiler chicks. *Canadian Veterinary Journal*. **2** p.143-145
- FIELDS P.I., SWANSON R.V., HAIDARIS C.G., HEFFRON F. 1986. Mutants of *Salmonella typhimurium* that cannot survive within the macrophage are avirulent. *Proceedings of the National Academy of Sciences USA*. **30** p.5189-5193
- FLESCH, I. E. A., KAUFMANN S. H. E. 1991. Mechanisms involved in mycobacterial growth inhibition by gamma interferon-activated bone marrow macrophages: Role of reactive nitrogen intermediates. *Infection and Immunity*. **59** p.3213-3218



- FOX A. J., SOLOMON J. B. 1981. Chicken non-lymphoid leukocytes. In *Avian Immunology*. M. E. Rose, B. M. Freeman, and L. N. Payne, ed. British Poultry Science, Edinburgh, UK. p.135–201
- FRANCIS C. L., RYAN T. A., JONES B. D., SMITH S. J., FALKOW S. 1993. Ruffles induced by *Salmonella* and other stimuli direct macropinocytosis of bacteria. *Nature*. **364** p.639-642
- FU Y., GALÁN J. E. 1999. A *Salmonella* protein antagonizes Rac-1 and Cdc42 to mediate host-cell recovery after bacterial invasion. *Nature*. **401** p.293-297
- GALÁN J. E., CURTISS III R. 1989. Cloning and molecular characterisation of genes whose products allow *Salmonella typhimurium* to penetrate tissue culture cells. *Proceedings of the National Academy of Sciences USA*. **86** p.6383-6387
- GALÁN J. E., ZHOU D. 2000. Striking a balance: Modulation of the actin cytoskeleton by *Salmonella*. *Proceedings of the National Academy of Sciences USA*. **97** p.8754-8761
- GALLOIS A., KLEIN J. R., ALLEN L. H., JONES B. D., NAUSEEF W. M. 2001. *Salmonella* pathogenicity island 2-encoded type III secretion system mediates exclusion of NADPH oxidase assembly from the phagosomal membrane. *The Journal of Immunology*. **166** p.5741-5748
- GINOCCHIO C. G., OLMSTED S. B., WELLS C. L., GALÁN J. E. 1994. Contact with epithelial cells induces the formation of surface appendages on *Salmonella typhimurium*. *Cell*. **76** p.717-724
- GOLEMBOSKI K. A., WHELAN J., SHAW S., KINSELLA J. E., DIETERT R. R. 1990. Avian inflammatory macrophage functions: shifts in arachidonic acid metabolism, respiratory burst, and cell-surface phenotypes during the response to Sephadex. *Journal of Leukocyte Biology*. **48** p.495–501

- GRIESS P. 1879. Bemerkungen zu der abhandlung der H.H. Weselsky and Benedikt "Ueber einiger azoverbindungen". *Chemische Berichte*. **12** p.426-428
- GROISMAN K. H., OCHMAN H. 1997. How *Salmonella* became a pathogen. *Trends in Microbiology*. **5** p.343-349
- GROISMAN E. A., PARRA-LOPEZ C., SALCEDO M., LIPPS C. J., HEFFRON F. 1992. Resistance to host antimicrobial peptides is necessary for *Salmonella* virulence. *Proceedings of the National Academy of Sciences USA*. **89** p.11939-11943
- HALAVATKAR H., BARROW P.A. 1993. The role of a 54-kb plasmid in the virulence of strains of *Salmonella* Enteritidis of phage type 4 for chickens and mice. *Journal of Medical Microbiology*. **38** p.171-176
- HAMILTON, T. A., ADAMS D. O. 1987. Molecular mechanisms of signal transduction in macrophages. *Immunology Today*. **8** p.151-157
- HARDT, W.-D. GALAN J. E. 1997. A secreted *Salmonella* protein with homology to an avirulence determinant of plant-pathogenic bacteria. *Proceedings of the National Academy of Sciences USA*. **94** p.9887-9892
- HARMON B. G. 1998. Avian heterophils in inflammation and disease resistance. *Poultry Science*. **77** p.972-977
- HARWIG S. S., SWIDEREK K. M., KOKRYAKOV V. N., TAN L., LEE T. D., PANYUTICH E. A., ALESHINA G. M., SHAMOVA O. V., LEHRER R. I. 1994. Gallinacins: cysteine-rich antimicrobial peptides of chicken leukocytes. *Federation of European Biochemical Societies*. **342** p.281-285
- HASHIMOTO-GOTOH, T., FRANKLIN F. C. H., NORDHEIM A., TIMMIS K. N. 1981. Specific-purpose plasmid cloning vectors I. Low copy number, temperature-

- sensitive, mobilization-defective pSC101-derived containment vectors. *Gene*. **16** p.227-235
- HAYWARD R. D., KORONAKIS V. 1999. Direct nucleation and bundling of actin by SipC protein of invasive *Salmonella*. *The EMBO Journal*. **18** p.4926-4934
  - HENDERSON S. C., BOUNOUS D. I., LEE M. D. 1999. Early events in the pathogenesis of avian salmonellosis. *Infection and Immunity*. **67** p.3580-3586
  - HENRY B. S. 1933. Dissociation in the genus *Brucella*. *Journal of Infectious Diseases*. **52** p.374-402
  - HENSEL M., SHEA J. E., RAUPACH B., MONACH D., FALCOW S., GLEESON C., KUBO T., HOLDEN D. W. 1997a. Functional analysis of ssaJ and the ssaK/U operon, 13 genes encoding components of the type III secretion apparatus of *Salmonella* Pathogenicity Island 2. *Molecular Microbiology*. **24** p.155-167
  - HENSEL M., SHEA J.E., BÄUMLER A.J., GLEESON C., HOLDEN D.W. 1997b. Analysis of the boundaries of *Salmonella* pathogenicity island 2 and the corresponding chromosomal region of *Escherichia coli* K-12. *Journal of Bacteriology*. **30** p.1105-1111
  - HENSEL M., SHEA J. E., WATERMAN S. R., MUNDY R., NIKOLAUS T., BANKS G., VAZQUEZ-TORRES A., GLEESON C., FANG F. C., HOLDEN D. W. 1998. Genes encoding putative effector proteins of the type III secretion system of *Salmonella* pathogenicity island 2 are required for bacterial virulence and proliferation in macrophages. *Molecular Microbiology* **30** p.163-174
  - HENSEL M. 2000. *Salmonella* Pathogenicity Island 2. *Molecular Microbiology*. **36** p.1015-1023
  - HERSCH D., MONACK D. M., SMITH M. R., GHORI N., FALKOW S., ZYCHLINSKY A. 1999. The *Salmonella* invasin SipB induces macrophage

- apoptosis by binding to caspase-1. *Proceedings of the National Academy of Sciences USA*. **96** p.2396-2401
- HOBBIIE S., CHEN L. M., DAVIS R. J., GALAN J. E. 1997. Involvement of mitogen-activated protein kinase pathways in the nuclear responses and cytokine production induced by *Salmonella typhimurium* in cultured intestinal epithelial cells. *The Journal of Immunology*. **159** p.5550-5559
  - HUGHS D. A., FRASER I. P., GORDON S. 1995. Murine macrophage scavenger receptor: in vivo expression and function as receptor for macrophage adhesion in lymphoid and non-lymphoid organs. *European Journal of Immunology*. **25** p.466-473
  - JANAKIRAMAN A., SLAUCH J. M. 2000. The putative iron transport system SitABCD encoded on SPI1 is required for full virulence of *Salmonella typhimurium*. *Molecular Microbiology*. **35** p.1146-1155
  - JANTSCH J., CHEMINAY C., CHAKRAVORTTY D., LINDIG T., HEIN J., HENSEL M. 2003. Intracellular activities of *Salmonella enterica* in murine dendritic cells. *Cellular Microbiology*. **5** p.933-945
  - JEPSON M. A., CLARK M. A. 2001. The role of M cells in *Salmonella* infection. *Microbes and Infection*. **3** p.1183-1190
  - JEPSON M. A., KENNY B., LEARD A. D. 2001. Role of *sipA* in the early stages of *Salmonella typhimurium* entry into epithelial cells. *Cellular Microbiology*. **3** p.417-426
  - JOHNSON D. C., DAVID M., GOLDSMITH S. 1992. Epizootiological investigation of an outbreak of Pullorum Disease in an integrated broiler operation. *Avian Diseases*. **36** p.770-775

- JOHNSON, J. R., LOCKMAN H. A., OWENS K., JELACIC S., TARR P. I. 2003. High-frequency secondary mutations after suicide-driven allelic exchange mutagenesis in extraintestinal pathogenic *Escherichia coli*. *Journal of Bacteriology*. **185** p.5301-5305
- JOHNSTON, P.A., SOMERS, S. D., HAMILTON T. A. 1987. Expression of a 120 kilodalton protein during tumoricidal activation in murine peritoneal macrophages. *Journal of Immunology*. **138** p.2739-2744
- JONES M. A., HULME S. D., BARROW P. A., WIGLEY P. 2007. The *Salmonella* pathogenicity island 1 and *Salmonella* pathogenicity island 2 type III secretion systems play a major role in pathogenesis of systemic disease and gastrointestinal tract colonization of *Salmonella enterica* serovar Typhimurium in the chicken. *Avian Pathology*. **36** p.199-203
- JONES M. A., WOOD M. W., MULLAN P. B., WATSON P. R., WALLIS T. S., GALYOV E. E. 1998. Secreted effector proteins of *Salmonella* Dublin act in concert to induce enteritis. *Infection and Immunity*. **66** p.5799-5804
- JONES M. A., WIGLEY P., PAGE K., HULME S. D., BARROW P. A. 2001. *Salmonella enterica* serovar Gallinarum Requires the *Salmonella* pathogenicity island 2 type III secretion system but not the *Salmonella* pathogenicity island 1 type III secretion system for virulence in chicken. *Infection and Immunity*. **69** p.5471-5476
- KAGAN B. L., SFI,STEAD M. E., GANZ T., LEHRER R. I. 1990. Antimicrobial defence peptides form voltage-dependent ion-permeable channels in planar lipid bilayer membranes. *Proceedings of the National Academy of Sciences USA*. **87** p.210-214

- KAISER M. G., CHEESEMAN J. H., KAISER P., LAMONT S. J. 2006. Cytokine expression in chicken peripheral blood mononuclear cells after in vitro exposure to *Salmonella enterica* serovar Enteritidis. *Poultry Science*. **85** p.1907-1911
- KAISER P., HUGHES S., BUMSTEAD N. 1999. The chicken 9E3/CEF4 CXC chemokine is the avian orthologue of IL8 and maps to chicken chromosome 4 syntenic with genes flanking the mammalian chemokine cluster. *Immunogenetics*. **49** p.673-684
- KAISER P., ROTHWELL L., GALYOV E. E., BARROW P. A., BURNSIDE J., WIGLEY P. 2000. Differential cytokine expression in avian cells in response to invasion by *Salmonella typhimurium*, *Salmonella enteritidis* and *Salmonella gallinarum*. *Microbiology*. **146** p.3217-3226
- KAISER P., POH T. Y., ROTHWELL L., AVERY S., BALU S., PATHANIA U. S., HUGHES S., GOODCHILD M., MORRELL S., WATSON M., BUMSTEAD N., KAUFMAN J., YOUNG J. R. 2005. A genomic analysis of chicken cytokines and chemokines. *Journal of Interferon and Cytokine Research*. **25** p.467-484
- KISHIMOTO T., AKIRA S., NARAZAKI M., TAGA T. 1995. Interleukin-6 family of cytokines and gp130. *Blood*. **86** p.1243-1254
- KOGUT M. H. 2002. Dynamics of a protective avian inflammatory response: the role of an IL-8-like cytokine in the recruitment of heterophils to the site of organ invasion by *Salmonella enteritidis*. *Comparative Immunology, Microbiology and Infectious Diseases*. **25** p.159-172
- KOPF M., BAUMANN H., FREER G., FREUDENBERG M., LAMERS M., KISHIMOTO T., ZINKERNAGEL, R., BLUETHMANN H., KOHLER G. 1994. Impaired immune and acute-phase responses in interleukin-6-deficient mice. *Nature*. **368** p.339-342

- KOVALL R., MATTHEWS B. W. 1997. Toroidal structure of the lambda-exonuclease. *Science*. **277** p.1824-1827
- KRAAL G. 1992. Cells in the marginal zone of the spleen. *International Review of Cytology*. **132** p.31-74
- LEE C. A., SILVA M., SIBER A. M., KELLY A. J., GALYOV E., MCCORMICK B. A. 2000. A secreted *Salmonella* protein induces a pro-inflammatory response in epithelial cells, which promotes neutrophil migration. *Proceedings of the National Academy of Sciences USA*. **97** p.12283-12288
- LEUNG K.Y., FINLAY B.B. 1991. Intracellular replication is essential for the virulence of *Salmonella typhimurium*. *Proceedings of the National Academy of Sciences USA*. **30** p.11470-11474
- LIBBY S. J., GOEBEL W., LUDWIG A., BUCHMEIER N., BOWE F., FANG F. C., GUINEY D. G., SONGER J. G., HEFFRON F. 1994. A cytolysin encoded by *Salmonella* is required for survival within macrophages. *Proceedings of the National Academy of Sciences USA*. **91** p.489-493
- LITTLE, J. W. 1967. An exonuclease induced by bacteriophage  $\lambda$ . II. Nature of the enzymatic reaction. *Journal of Biological Chemistry*. **242** p.679-686
- LIU D., VERMA N. K., ROMANA L. K., REEVES P. R. 1991. Relationships among the *rfb* regions of *Salmonella* serovars A, B, and D. *Journal of Bacteriology*. **173** p.4814-4819
- LI Z., KARAKOUSIS G., CHIU S. K., REDDY G., RADDING C. M. 1998. The beta protein of phage lambda promotes strand exchange. *Journal of Molecular Biology*. **276** p.733-744
- LORENZ M. G., WACKERNAGEL W. 1994. Bacterial gene transfer by natural genetic transformation in the environment. *Microbiological Reviews*. **58** p.563-602

- LOSTROH C. P., LEE C. A. 2001. The *Salmonella* pathogenicity island-1 type III secretion system. *Microbes and Infection*. **3** p.1281-1291
- LOWRY V. K., TELLEZ G. I., NISBET D. J., GARCIA G., URQUIZA O., STANKER L. H., KOGUT M. H. 1999. Efficacy of *Salmonella enteritidis*- immune lymphokines on horizontal transmission of *S. arizonae* in turkeys and *S. gallinarum* in chickens. *International Journal of Food Microbiology*. **48** p.139-148
- LYNN D. J., HIGGS R., GAINES S., TIERNEY J., JAMES T., LLOYD A. T., FARES M. A., MULCAHY G., O'FARRELLY C. O. 2004. Bioinformatic discovery and initial characterisation of nine novel antimicrobial peptide genes in the chicken. *Immunogenetics*. **56** p.170-177
- LYNN D. J., HIGGS R., LLOYD A. T., O'FARRELLY C., HERVÉ-GRÉPINET V., NYS Y., BRINKMAN F., YU P-L., SOULIER A., KAISER P., ZHANG G., LEHRER R. I. 2007. Avian beta-defensin nomenclature: A community proposed update. *Immunology Letters*. **110** p.86-89
- MACLACHLAN P. R., SANDERSON K. E. 1985. Transformation of *Salmonella typhimurium* with plasmid DNA: Differences between rough and smooth strains. *Journal of Bacteriology*. **161** p.442-445
- MAST J., GODDEERIS B.M., PEETERS K., VANDESANDE F., BERGHMAN L.R. 1999. Characterisation of chicken monocytes, macrophages and interdigitating cells by the monoclonal antibody KUL01. *Veterinary Immunology and Immunopathology*. **61** p.343-357
- MAYAHI M., SHARMA R. N., MAKTABI S. 1995. An outbreak of blindness in chicks associated with *Salmonella pullorum* infection. *Indian Veterinary Journal*. **72** p.922-925



- MCCLELLAND M., SANDERSON K.E., SPIETH J., CLIFTON S.W., LATREILLE P., COURTNEY L., PORWOLLIK S., ALI J., DANTE M., DU F., HOU S., LAYMAN D., LEONARD S., NGUYEN C., SCOTT K., HOLMES A., GREWAL N., MULVANEY F., RYAN E., SUN H., FLOREA L., MILLER W., STONEKING T., NHAN M., WATERSTON R., WILSON R. 2001. Complete genome sequence of *Salmonella enterica* serovar Typhimurium LT2. *Nature*. **413** p.852-856
- MCCORMICK B. A., COLGAN S. P., DELP-ARCHER C., MILLER S. I., MADARA J. L. 1993. *Salmonella typhimurium* attachment to human intestinal epithelial monolayers: transcellular signalling to subepithelial neutrophils. *Journal of Cell Biology*. **123** p.895-907
- MCCORMICK B. A., MILLER S. I., CARNES D. K., MADARA J. L. 1995. Transepithelial signalling to neutrophils by *Salmonellae*: a novel virulence mechanism for gastroenteritis. *Infection and Immunity*. **63** p.2302-2309
- MACHUGH N. D., BENSALD A., DAVIS W. C., HOWARD C. J., PARSONS K. R., JONES B., KAUSHAL A. 1988. Characterization of a bovine thymic differentiation antigen analogous to CD1 in the human. *Scandinavian Journal of Immunology*. **27** p. 541-547
- MCGHIE E. J., HAYWARD R. D., KORONAKIS V. 2001. Cooperation between actin-binding proteins of invasive *Salmonella*: SipA potentiates SipC nucleation and bundling of actin. *The EMBO Journal*. **20** p.2131-2139
- MIAO E. A., SCHERER C.A., TSOLIS R.M., KINGSLEY R.A., ADAMS L.G., BÄUMLER A.J., MILLER S.I. 1999. *Salmonella typhimurium* leucine-rich repeat proteins are targeted to the SPI1 and SPI2 type III secretion systems. *Molecular Microbiology*. **34** p.850-864

- MILONA P., TOWNES C. L., BEVAN R. M., HALL J. 2007. The chicken host peptides, gallinacins 4, 7, and 9 have antimicrobial activity against *Salmonella* serovars. *Biochemical and Biophysical Research Communications*. **356** p.169-174
- MIROLD, S., RABSCH W., ROHDE, M., STENDER, S., TSCHÄPE, H., RÜSSMANN H., IGWE, E., HARDT W.-D. 1999. Isolation of a temperate bacteriophage encoding the type III effector protein SopE from an epidemic *Salmonella typhimurium* strain. *Proceedings of the National Academy of Sciences USA*. **96** p.9845-9850
- MITTRUCKER H. W., KAUFFMAN S. H. E. 2000. Immune response to infection with *Salmonella typhimurium* infection in mice. *Journal of Leukocyte Biology*. **67** p.457-463
- MONACK D. M., HERSH D., GHORI N., BOULEY D., ZYCHLINSKY A., FALKOW S. 2000. *Salmonella* exploits caspase-1 to colonize peyer's patches in a murine typhoid model. *Journal of Experimental Medicine*. **192** p.249-258
- MONACK D. M., DETWELLER C. S., FALKOW S. 2001. *Salmonella* pathogenicity island 2-dependent macrophage death is mediated in part by the host cysteine protease caspase-1. *Cellular Microbiology*. **3** p.825-837
- MONTALI R. J. 1988. Comparative pathology of inflammation in the higher vertebrates (reptiles, birds and mammals). *Journal of comparative Pathology*. **99** p.1-20
- MOODY A., SELLERS S., BUMSTEAD N. 2000. Measuring infectious bursal disease virus RNA in blood by multiplex real-time quantitative RT-PCR. *Journal of Virological Methods*. **85** p.55-64
- MORGAN E., CAMPBELL J.D., ROWE S.C., BISPHAM J., STEVENS M.P., BOWEN A.J., BARROW P.A., MASKELL D.J., WALLIS T.S. 2004. Identification

of host-specific colonization factors of *Salmonella enterica* serovar Typhimurium. *Molecular Microbiology*. **54** p.994-1010

- MUKAIDA N., MAHE Y., MATSUSHIMA K. 1990. Cooperative interaction of nuclear factor- $\kappa$ B and cis-regulatory enhancer binding protein-like factor binding elements in activating the interleukin-8 gene by pro-inflammatory cytokines. *Journal of Biological Chemistry*. **265** p.128-133
- MURPHY K. C. 1991.  $\lambda$  gam protein inhibits the helicase and  $\chi$ -stimulated recombination activities of *Escherichia coli* RecBCD enzyme. *Journal of Bacteriology*. **173** p.5808-5821
- MURPHY K. C. 1998. Use of bacteriophage  $\lambda$  recombination functions to promote gene replacement in *Escherichia coli*. *Journal of Bacteriology*. **180** p.2063-2071
- NATHAN, C., SHILOH, M. U. 2000. Reactive oxygen and nitrogen intermediates and the relationship between mammalian hosts and microbial pathogens. *Proceedings of the National Academy of Sciences USA*. **97** p.8841-8848
- OCHMAN H., GROISMAN E.A. 1996. Distribution of pathogenicity islands in *Salmonella* spp. *Infection and Immunity*. **64** p.5410-5412
- OCHMAN H., SONCINI F. C., SOLOMON F., GROISMAN E. A. 1996. Identification of a pathogenicity island required for *Salmonella* survival in host cells. *Proceedings of the National Academy of Sciences USA*. **93** p.7800-7804
- OGUSHI K., WADA A., NIIDOME T., MORI N., OISHI K., NAGATAKE T., TAKAHASHI A., ASAKURA H., MAKINO S., HOJO H., NAKAHARA Y., OHSAKI M., HATAKEYAMA T., AOYAGI H., KURAZONO H., MOSS J., IIRAYAMA T. 2001. *Salmonella enteritidis* FliC (flagella filament protein) induces human beta-defensin-2 mRNA production by Caco-2 cells. *The Journal of Biological Chemistry*. **276** p.30521-30526

- OKAMURA M., LILLEHOJ H. S., RAYBOURNE R. B., BABU U.S., HECKERT R. A., TANI H., SASAI K., BABA E., LILLEHOJ E. P. 2005. Differential responses of macrophages to *Salmonella enterica* serovars Enteritidis and Typhimurium. *Veterinary Immunology and Immunopathology*. **107** p.327-335
- OLSEN J. F., SKOV M. N., CHRISTENSEN J. P., BISGAARD M. 1996. Genomic lineage of *Salmonella enterica* serotype Gallinarum. *Journal of Medical Microbiology*. **45** p.413-418
- O'NEIL D.A., PORTER E.M., ELEWANT D., ANDERSON G.M., ECKMANN L., GANZ T., KAGNOFF M.F. 1999. Expression and regulation of the human beta-defensins hBD-1 and hBD-2 in intestinal epithelium. *Journal of Immunology*. **163** p.6718-6724
- PARKHILL J., DOUGAN G., JAMES K. D., THOMSON N. R., PICKARD D., WAIN J., CHURCHER C., MUNGALL K. L., BENTLEY S. D., HOLDEN M. T., SEBAIHIA M., BAKER S., BASHAM D., BROOKS K., CHILLINGWORTH T., CONNERTON P., CRONIN A., DAVIS P., DAVIES R. M., DOWD L., WHITE N., FARRAR J., FELTWELL T., HAMLIN N., HAQUE A., HIEN T. T., HOLROYD S., JAGELS K., KROGH A., LARSEN T. S., LEATHER S., MOULE S., O'GAORA P., PARRY C., QUAIL M., RUTHERFORD K., SIMMONDS M., SKELTON J., STEVENS K., WHITEHEAD S., BARRELL B. G. 2001. Complete genome sequence of a multiple drug resistant *Salmonella enterica* serovar Typhi CT18. *Nature*. **413** p.848-852
- PATEL J. C., GALÁN J. E. 2005. Manipulation of the host actin cytoskeleton by *Salmonella*- all in the name of entry. *Current Opinion in Microbiology*. **8** p.10-15
- PECK, R., MURTHY K. K., VANIO O. 1982. Expression of B-L (Ia-like) antigens on macrophages from chicken lymphoid organs. *Journal of Immunology*. **129** p.4-5

- POTEETE A. R. 2001. What makes the bacteriophage  $\lambda$  Red system useful for genetic engineering: molecular mechanism and biological function. *FIEMS Microbiology Letters*. **201** p.9-14
- POWELL P. C. 1987. Macrophages and other nonlymphoid cells contributing to immunity. In *Avian Immunology: Basis and Practice*. Vol. I. A. Toivanen and P. Toivanen, ed. CRC Press, Boca Raton, FL. p.195–212
- QURESHI M. A., DIETERT R. R., BACON L. D. 1986. Genetic variation in the recruitment and activation of chicken peritoneal macrophages. *Proceedings of the Society of Experimental Biological Medicine*. **181** p.560–566
- QURESHI M. A., DIETERT R. R. 1995. Bacterial uptake and killing by macrophage. In *Modern Methods in Immunotoxicology*. Vol. II. G. R. Burleson, J. Dean, and A. Munson ed., John Wiley and Sons, Inc., New York, NY. p.119–131
- QURESHI M. A., PETITTE J. N., LASTER S. M., DIETERT R. R. 1993. Avian macrophages: contribution to cellular microenvironment and changes in effector functions following activation. *Poultry Science*. **72** p.1280–1284
- RESCIGNO M., URBANO M., VALZASINA B., FRANCOLINI M., ROTTA G., BONASIO R., GRANUCCI F., KRAEHENBUHL J. P., RICCIARDI-CASTAGNOLI P. 2001. Dendritic cells express tight junction proteins and penetrate gut epithelial monolayers to sample bacteria. *Nature Immunology*. **2** p.361–367
- RICHTER-DAHLFORS A., BUCHAN A. M. J. 1997. Murine salmonellosis studied by confocal microscopy: *Salmonella typhimurium* resides intracellularly inside macrophages and exerts a cytotoxic effect on phagocytes *in vivo*. *Journal of Experimental Medicine*. **186** p.569-580

- ROSE M. E., HESKETH P. 1974. Fowl peritoneal exudate, collection and use for the macrophage migration inhibition test. *Avian Pathology*. **3** p.297-302
- SADEYEN J-R., TROTIEREAU J., PROTAIS J., BEAUMONT C., SELIER N., SALVAT G., VELGE P., LALMANACH A-C. 2006. *Salmonella* carrier-state in hens: study of host resistance by a gene expression approach. *Microbes and Infection*. **8** p.1308-1314
- SALCEDO S. P., NOURSADEGHI M., COHEN J., HOLDEN D. W. 2001. Intracellular replication of *Salmonella typhimurium* strains in specific subsets of splenic macrophages *in vivo*. *Cellular Microbiology*. **3** p.587-597
- SALEM M., ODOR E. M., POPE C. 1992. Pullorum disease on Delaware roasters. *Avian Diseases*. **36** p.1076-1080
- SALZMAN N. H., GHOSH D., HUTTNER K. M., PATTERSON Y., BEVINS C. L. 2003. Protection against enteric salmonellosis in transgenic mice expressing a human intestinal defensin. *Nature*. **422** p.522-526
- SCHLUMBERGER M.C., HARDT W.D. 2005. Triggered phagocytosis by *Salmonella*: bacterial molecular mimicry of RhoGTPase activation/deactivation. *Current Topics in Microbiological Immunology*. **291** p.29-42
- SCHNEIDER K., KLAAS R., KASPERS B., STAEHELI P. 2001. Chicken interleukin-6. cDNA structure and biological properties. *European Journal of Biochemistry*. **268** p.4200-4206
- SCHNEIDER K., PUEHLER F., BAEUERLE D., ELVERS S., STAEHELI P., KASPERS B., WEINING K. C. 2000. cDNA cloning of biologically active chicken interleukin-18. *Journal of Interferon and Cytokine Research*. **20** p.879-883

- SHABO Y., LOTEM J., RUBINSTEIN M., REVEL M., CLARK S. C., WOLF S. F., KAMEN R., SACHS L. 1988. The myeloid blood cell differentiation-inducing protein MGI-2A is interleukin-6. *Blood*. **72** p.2070-2073
- SHAI D. H., LEE M.-J., PARK J.-H., LEE J.-H., EO S.-K., KWON J.-T., CHAE J.-S. 2005. Identification of *Salmonella gallinarum* virulence genes in a chicken infection model using PCR-based signature-tagged mutagenesis. *Microbiology*. **151** p. 3957-3968
- SHEA J. E., HENSEL M., GLEESON C., HOLDEN D. W. 1996. Identification of a virulence locus encoding a second type III secretion system in *Salmonella typhimurium*. *Proceedings of the National Academy of Sciences USA*. **93** p.2593-2597
- SHIVAPRASAD H. L. 2000. Fowl typhoid and pullorum disease. *Scientific and Technical Review*. **19** p.405-424
- SICK, C., SCHNEIDER, K., STAEBELI, P., WEINING, K.C. 2000. Novel chicken CXC and CC chemokines. *Cytokine*. **12** p.181-186
- SMITH G. R. 1998. Homologous recombination in prokaryotes. *Microbiological Reviews*. **52** p.1-28
- SNAVLEY M.D., MILLER C.G., MAGUIRE M.E. 1991. The *mgtB* Mg<sup>2+</sup> transport locus of *Salmonella typhimurium* encodes a P-type ATP-ase. *The Journal of Biological Chemistry*. **266** p.815-823
- SNOEYENBOS G. H. 1991. Pullorum Disease. *In Diseases of poultry, 9<sup>th</sup> Ed.* (Calneck B. W., Barnes II. J., Beard C. W., Reed W. M., Yoder Jr H. W., eds). Iowa State University Press, Ames. p.73-86
- STEELE-MORTIMER O., BRUMELL J. H., KNODLER L. A., MÉRESSE S., LOPEZ A., FINLAY B. B. 2002. The invasion-associated type III secretion system

- of *Salmonella enterica* serovar Typhimurium is necessary for intracellular proliferation and vacuole biogenesis in epithelial cells. *Cellular Microbiology*. 4 p.43-54
- SUÁREZ M., RÜSSMANN H. 1998. Molecular mechanisms of *Salmonella* invasion: the type III secretion system of the pathogenicity island 1. *International Microbiology*. 1 p.197-204
  - SUGIARTO H., YU P. 2004. Avian antimicrobial peptides: the defence role of  $\beta$ -defensins. *Biochemical and Biophysical Research Communications*. 323 p.721-727
  - SUNG Y.-J., HOTCHKISS H., AUSTIC R. E., DIETERT R. R. 1991. Larginine-dependent production of a reactive nitrogen intermediate by macrophages of a uricotelic species. *Journal of Leukocyte Biology*. 51 p.49-56
  - SVENSSON M., JOHANSSON C., WICK M. J. 2001. *Salmonella typhimurium*-induced cytokine production and surface molecule expression by murine macrophages. *Microbial Pathogenesis*. 31 p.91-102
  - TAKETO A. 1972. Sensitivity of *Escherichia coli* to viral nucleic acid. V. Competence of calcium-treated cells. *Journal of Biochemistry*. 72 p.973-979
  - TANNENBAUM C. S., KOERNER, T. J., JANSEN, M. M., HAMILTON T. A. 1988. Characterisation of lipopolysaccharide-induced macrophage gene expression. *Journal of Immunology*. 140 p.3640-3645
  - VALDIVIA R. H., FALKOW S. 1997. Florescence-based isolation of bacterial genes expressed within host cells. *Science*. 277 p.2007-2011
  - VAN BUSKIRK M. A. 1987. A pullorum disease outbreak in a pullorum-free state. In *Proceedings of the 59<sup>th</sup> North Eastern Conference on Avian Diseases, Atlantic City, New Jersey*. p.40-42



- VANCOTT J. L., CHATFIELD S. N., ROBERTS M., HONE D. M., HOHMANN E. L., PASCUAL D. W., YAMAMOTO M., KIYONO H., MCGHEE J. R. 1998. Regulation of host immune responses by modification of *Salmonella* virulence genes. *Nature Medicine*. **4** p.1247-1252
- VAN DER VELDEN A. W. M., LINDGREN S. W., WORLEY M. J., HEFFRON F. 2000. *Salmonella* pathogenicity island 1-independent induction of apoptosis in infected macrophages by *Salmonella enterica* serotype Typhimurium. *Infection and Immunity*. **68** p.5702-5709
- VAN DER VELDEN A.W., VELASQUEZ M., STARNBACH M. N. 2003. *Salmonella* rapidly kill dendritic cells via a caspase-1-dependent mechanism. *Journal of Immunology*. **171** p.6742–6749
- VAN DIJK A., VELDHIJZEN E. J., KALKHOVE S. I., TJEERDSMA-VAN BOKHOVEN J. L., ROMIJN R. A., IIAAGSMAN H. P. 2007. The beta-defensin gallinacin-6 is expressed in the chicken digestive tract and has antimicrobial activity against food-borne pathogens. *Antimicrobial Agents and Chemotherapy*. **51** p.912-922
- VANIO, O., PECK, R., KOCH, C., TOIVANEN, A. 1983. Origin of peripheral blood macrophages in bursa-cell-reconstituted chickens. *Scandinavian Journal of Immunology*. **17** p.193
- VAZQUEZ-TORRES A., JONES-CARSON J., BÄUMLER A. J., FALKOW S., VALDIVIA R., BROWN W., LE M., BERGGREN R., PARKS W. T., FANG F. C. 1999. Extraintestinal dissemination of *Salmonella* by CD18-expressing phagocytes. *Nature*. **401** p.804-808
- VAZQUEZ-TORRES A., XU, Y., JONES-CARSON J., HOLDEN D. W., LUCIA S. M., DINAUER M. C., MASTROENI P., FANG F. C. 2000. *Salmonella*

Pathogenicity Island 2-Dependent Evasion of the Phagocyte NADPH Oxidase.

*Science*. **287** p.1655-1658

- WALLIS T., GALYOV E. E. 2000. Molecular basis of *Salmonella*-induced enteritis. *Molecular Microbiology*. **36** p.997-1005
- WATERMAN S. R., HOLDEN D. W. 2003. Functions and effectors of the *Salmonella* pathogenicity island 2 type III secretion system. *Cellular Microbiology*. **5** p.501-511
- WEINING K. C., SICK C., KASPERS B., STAEHELI P. 1998. A chicken homolog of mammalian interleukin-1 $\beta$ : cDNA cloning and purification of active recombinant protein. *European Journal of Biochemistry*. **258** p.994-1000
- WEINSTEIN D. L., O'NEILL B. L., HONE D. M., METCALF E. S. 1998. Differential Early interactions between *Salmonella enterica* serovar Typhi and two other pathogenic *Salmonella* serovars with intestinal epithelial cells. *Infection and Immunity*. **66** p.2310-2318
- WIGLEY P., BERCHIERI J. A., PAGE K. L., SMITH A. L., BARROW P. A. 2001. *Salmonella enterica* serovar Pullorum persists in splenic macrophages and in the reproductive tract during persistent disease-free carriage in chickens. *Infection and Immunity*. **69** p.7873-7879
- WIGLEY P., JONES M. A., BARROW P. A. 2002. *Salmonella enterica* serovar Pullorum requires the *Salmonella* pathogenicity island 2 type III secretion system for virulence and carriage in the chicken. *Avian Pathology*. **31** p.501-506
- WIGLEY P., HULME S.D., BUMSTEAD N., BARROW P.A. 2002. *In vivo* and *in vitro* studies of genetic resistance to systemic salmonellosis in the chicken encoded by the SAL1 locus. *Microbes and Infection*. **4** p.1111-1120

- WIGLEY P., HULME S. D., POWERS C., BEAL R. K., BERCHIERI A. JR., SMITH A., BARROW P. 2005. Infection of the reproductive tract and eggs with *Salmonella enterica* serovar Pullorum in the chicken is associated with suppression of cellular immunity at sexual maturity. *Infection and Immunity*. **73**(5) p.2986-2990
- WILSON C. L., OUELLETTE A. J., SATCHELL. D. P., AYABE, T., LOPEZ-BOADO Y. S., STRATMAN J. L., HULTGREN S. J., MATRISIAN L. M., PARKS W. C. 1999. Regulation of intestinal alpha-defensin activation by the metalloproteinase matrilysin in innate host defence. *Science*. **286** p.113-117
- WITHANAGE G. S., SASAI K., FUKATA T., MIYAMOTO T., LILLEHOJ H. S., BABA E. 2003. Increased lymphocyte subpopulations and macrophages in the ovaries and oviducts of laying hens infected with *Salmonella enterica* serovar Enteritidis. *Avian Pathology*. **32** p.583-590
- WITHANAGE G. S., KAISER P., WIGLEY P., POWERS C., MASTROENI P., BROOKS H., BARROW P., SMITH A., MASKELL D., MCCONNELL I. 2004. Rapid expression of chemokines and pro-inflammatory cytokines in newly hatched chickens infected with *Salmonella enterica* serovar Typhimurium. *Infection and Immunity*. **72** p.2152-2159
- XIAO Y., HUGHES A. L., ANDO J., MATSUDA Y., CHENG J., SKINNER-NOBLE D., ZHANG G. 2004. A genome-wide screen identifies a single  $\beta$ -defensin gene cluster in the chicken: implications for the origin and evolution of mammalian defensins. *BMC Genomics*. **5** p.56-67
- YOSHIMURA Y., OHASHI H., SUBEDI K., NISHIBORI M., ISOBE N. 2006. Effects of age, egg-laying activity, and *Salmonella*-inoculation on the expressions of gallinacin mRNA in the vagina of the hen oviduct. *The Journal of Reproduction and Development*. **52** p.211-218

- ZHAO C., NGUYEN T., LIU L., SACCO R. E., BROGDEN K. A., LEHRER R. I. 2001. Gallinacin-3, an inducible epithelial  $\beta$ -defensin in the chicken. *Infection and Immunity*. **69** p.2684-2691
- ZHOU D., GALÁN, J. 2001. *Salmonella* entry into host cells: the work in concert of type III secreted effector proteins. *Microbes and Infection*. **3** p.1293-1298
- ZHOU D., HARDT W-D., GALÁN J. E. 1999. *Salmonella typhimurium* encodes a putative iron transport system within the centisome 63 pathogenicity island. *Infection and Immunity*. **67** p.1974-1981

